A MULTI-FACETED APPROACH TO UNDERSTANDING THE EFFECTS OF FATIGUE ON MUSCLE AND KINEMATIC VARIABILITY

Matthew S. Russell

A DISSERTATION SUBMITTED TO THE FACULTY OF GRADUATE STUDIES
IN PARTIAL FULFILMENT OF THE REQUIREMENTS
FOR THE DEGREE OF DOCTOR OF PHILOSOPHY

GRADUATE PROGRAM IN KINESIOLOGY AND HEALTH SCIENCE
YORK UNIVERSITY
TORONTO, ONTARIO

February 2025

Abstract

An *in vivo* human model of muscular and kinematic indeterminacy, the shoulder joint offers potential insight on how the central nervous system optimizes several competing biophysical variables. Muscle fatigue is a condition that impacts several such biophysical variables and can instigate load-sharing; centrally mediated muscle control changes utilized to manage several optimality variables like effort, metabolic cost, and joint load. However, considerable variability in fatigue-mediated shoulder kinematic and muscle activity changes has challenged the ability to make clear inferences on fatigue-mediated shoulder control changes.

The goal of this dissertation was to quantify fatigue-mediated shoulder control changes from a multifaceted perspective, in hopes that comprehensive analyses and novel methodologies would further our understanding of the mechanisms that drive centrally mediated shoulder control. Of specific interest was the intent to identify factors which may explain some of the fatigue-mediated shoulder variability that remains unclear.

Chapter 3 of this dissertation used coactivation ratios of the scapular stabilizers to describe muscle control changes following a shoulder fatigue task. Shoulder kinematic and coactivation responses to fatigue were variable, yet results indicated that 20-40% of individuals may increase their risk of subacromial impingement syndrome due to fatigue.

Chapter 4 of this dissertation investigated how individuals adapt their fatigue-mediated muscular and kinematic responses when completing the same fatigue task from chapter 3 a second time. Participants demonstrated more aggregate kinematics on day 2, while consolidating a more mechanically efficient posture that may minimize serratus anterior fatigue exposure.

Chapter 5 harnessed an optimal control biomechanical shoulder model to predict shoulder kinematics changes associated with isolated scapular stabilizer muscle weakness. This study identified a key role of serratus anterior for stabilizing arm elevation, and identified shoulder muscle synergies which may compensate for serratus anterior weakness.

Chapter 6 sought to identify how fatigue-mediated changes in muscle elastic modulus may affect muscle control strategies. However, muscle stiffness

appeared to be sensitive to the type of exercise/fatigue stimulus which was unforeseen and may be an important consideration for fatigue-related variability.

This dissertation concludes by summarizing the integrated findings of chapters 3-6 and proposing new considerations for fatigue-mediated shoulder muscle control.

Keywords: shoulder, scapula, muscle fatigue, optimization, variability.

Lay Overview

The many muscles which contribute to shoulder movement overlap. Therefore, for many shoulder movements, people can recruit different muscles to achieve the same movement. This phenomenon introduces variability in human movement, and this variability makes it challenging to predict exactly how a human will move. Further, muscle fatigue promotes movement changes. Yet muscle fatigue is highly complex and may not be yet fully understood, further challenging our ability to predict human movement. Thus, this dissertation explored how shoulder movement would be affected by muscle fatigue,

Chapter 2 of this dissertation reviews some of the commonly understood ways in which fatigue alters muscle performance, and current research methods for probing these phenomena.

Chapter 3 of this dissertation explored how the balance of activity across key shoulder muscles may help explain some of the variation we observe. This study found new evidence that humans may have less variable movement when their arm is fully outstretched, and that humans may be able to sustain difficult or fatiguing upper limb tasks longer when their arm is located closer to their body.

Chapter 4 of this dissertation had participants complete the same overhead work task a second time; 7 days later. Findings suggest that the various arm postures displayed on day 2 were more similar than on day 1 (chapter 3). These findings could indicate that participants 'learned' across days to find a small range of postures that required the least effort.

Chapter 5 of this dissertation attempted to use a computer simulation to look at how changes in muscle strength can alter our shoulder movement, as muscle strength decreases are associated with fatigue. Our simulations predicted that two muscles – lower trapezius and serratus anterior – would alter shoulder movement patterns if weakened. Importantly, tasks where the arm is located at the side of the body may be less tiring/fatiguing than tasks located in front of the body.

Chapter 6 investigated how muscle stiffness changes with fatigue, and if stiffness changes can explain some of the movement changes we observe with fatigue.

However, we primarily found evidence that movement patterns were affected by the firing rate of muscle nerves (motoneurons), as this rate decreases with fatigue.

Overall, this dissertation presents new evidence for several variables that may alter our movement. Those highlighted in this document include: fatigue, task experience, where the task is located, and how much movement is allowed when completing a task. Motoneuron firing rate may be an important variable for updating how we move. Finally, while substantial variability in movement patterns was apparent in our data, postures which position the placement of the hand closer to the shoulder and in greater abduction may be beneficial for minimizing fatigue.

...

Nikki,

Thank you for helping me through all the tough days, and for celebrating all my little successes. I could not have persevered without your patience, support, and the love I get from you and Mika. Thank you for being my partner.

...

Acknowledgements

During my time at York, I have been surrounded with an incredibly considerate and supportive group of colleagues and mentors; I would like to take this moment to thank them.

Jackie, as my primary supervisor, there is unlikely to ever be anyone more pivotal in my professional development. Despite the challenge of setting up a research program in the middle of Covid, you have always prioritized setting myself and your other students up for success and giving us every opportunity. Thank you for all you have done to make my experience at York enjoyable and to support me. I hope that as your inaugural doctoral student I have done all I can to show my appreciation and admiration. I look forward to seeing all that I know you are going to achieve, and I am so glad that I could be involved in a small part of that journey.

To my other co-supervisor Janessa, as I am sure you know, you have imparted me with many valuable life lessons both within and outside the context of academia. You have always been in my corner, offering keen wisdom that I'm not sure I could get from another supervisor; wisdom that has helped me navigate so many challenges in academia. A particularly fond memory is the week spent navigating Fukuoka and spending time with your family! I will also miss the occasionally chaotic but real topics that came up in morning lab meetings, and your ability to always attract great people. I have come to learn that the selection of supervisor is really the most important decision of any Ph.D. student, so having had two wonderful supervisors I feel truly grateful.

Heather O'Reilly, thank you for taking me under your wing from day 1. Although we only crossed paths for less than a year at York, the example you set has been my goalpost for the last four years. You have been such a tremendous friend and mentor through both of our ups and downs. Your affinity to connect and care about people is more impactful than I'm sure you realize.

Nikki Richardson, thank you for always sharing your resources, being an open book, supporting my development as an aspiring lecturer and academic, and most importantly for being so patient with me as a sessional lecturer. You have helped fuel my enjoyment and passion for teaching and also helped me discover my pedagogical outlook and my identity as a teacher.

There are many other faculty who have supported me in important ways at some point at York, including my committee members Dr. George Mochizuki and Dr. Heather Edgell who have contributed much time and care to my development, Dr. Taylor Cleworth who has always made time to catch up with me, Dr. Lauren Sergio who lets me bother her students and use her coveted espresso machine, Dr. Chris Perry who has been such a supportive mentor with the Muscle Health Research Centre, and certainly Dr. Jen Kuk who has shared much of her time and lab space to help me succeed. I will miss being surrounded by such friendly and supportive faculty.

My brilliant and exceptionally patient collaborators Dr. Mulla, Dr. Keir, Dr. Chadwick, and Dr. Blana, thank you for bringing me into the exciting work you do and letting me be apart of a small piece of it. Working with such a prestigious team was a little scary at the outset, but you always supported my learning and shared the love of what you do, which I am incredibly grateful for.

I am glad to know that I am leaving the Sherman building in the hands of an incredible and exciting group of young masters and doctoral students. Sam, Dan, other Dan, Emily, and Alex, I am indebted you for all the hard work and late nights at the lab, and for being great friends. Stephen and Dominic, I have much excitement to see all that you will both achieve with Jackie now that I am out of your hair! Sara and Nicole, I'm so glad we had the chance to become friends – too bad it took 3 years.

Thank you, Dad, for putting your children before everything, including yourself. Thank you, Mom for always planning family time amidst our busy lives. Nate. And thank you Castillo's for treating me like a member of your family all these years. Love you all.

Co-Authorship Statement

The manuscripts enclosed in chapters 3 and 4 of this dissertation were co-authored with **Sam S. Vasilounis, Emily Lefebvre.** Chapter 5 describes a collaborative project with partners **Dr. Daanish M. Mulla** and **Dr. Peter J. Keir** from McMaster University, and **Dr. Edward K. Chadwick** and **Dr. Dimitra Blana** from the University of Aberdeen who are all co-authored. All research manuscripts (chapters 3-6) are additionally co-authored by **Dr. Janessa D.M. Drake** and **Dr. Jaclyn N. Chopp-Hurley**.

Sam S. Vasilounis and **Emily Lefebvre** contributed to the data collection process for chapters 3-4. **Dr. Daanish M. Mulla**, **Dr. Peter J. Keir**, **Dr. Edward K. Chadwick**, **and Dr. Dimitra Blana** consulted and advised on the application of optimal control methods in chapter 5. **Dr. Janessa D.M. Drake** and **Dr. Jaclyn N. Chopp-Hurley** acted as co-supervisors on all works presented and were primarily involved in study conception and design, data analysis, and interpretation. All coauthors have provided feedback on manuscript drafts for which they are coauthored. At the time of submission, chapter 3 has been published in **Applied Ergonomics**, and chapter 4 has been published in **Human Movement Science**; both having undergone extensive peer review.

I, **Matthew S. Russell**, was the primary contributor to all aspects of these works, including study conception and design, data collection, data analysis, and manuscript preparation.

Table of Contents

List of Tables

List of Figures

List of Equations

List of Abbreviations and Symbols

ANOVA	Analysis of Variance
CNS	Central Nervous System
COM	Center of Mass
COV	Coefficient of Variance
DASH	Disability of Arm, Shoulder, and Hand Questionnaire
DOF	Degree(s) of Freedom
DSEM	Delft Shoulder and Elbow Model
EMG	Electromyography
$_{i}$EMG	Intramuscular Electromyography
$_{S}$EMG	Surface Electromyography
FABq	Fear Avoidance Believes Questionnaire
ISB	International Society of Biomechanics
LCS	Local Coordinate System
MdAD	Median Absolute Deviation; Equation 4.1.
MPF	Mean Power Frequency
MRE	Maximal Reference Exertion
MU	Motor Unit
MVE	Maximal Voluntary Exertion
MVIC	Maximal Voluntary Isometric Contraction
NLP	Non-Linear Programming
ODE	Ordinary Differential Equation
PDE	Partial Differential Equation
POE	Plane of Elevation
RC	Rotator Cuff
ROM	Range of Motion
RMS	Root-Mean-Square
RPE	Rating of Perceived Exertion
SAIS	Subacromial Impingement Syndrome
SAS	Subacromial Space
SRE	Submaximal Reference Exertion
SVE	Submaximal Voluntary Exertion
SVIC	Submaximal Voluntary Isometric Contraction
SWV	Shear Wave Velocity
TSK	Tampa Scale for Kinesiophobia

$_{i}$IS	Infraspinatus; intramuscular electromyography recording
$_{s}$IS	Intramuscular; surface electromyography recording
LT	Lower Trapezius; coactivation ratio coefficient
MD	Middle Deltoid; coactivation ratio coefficient
MT	Middle Trapezius; coactivation ratio coefficient
SA	Serratus Anterior; coactivation ratio coefficient
$_{i}$SS	Supraspinatus; intramuscular electromyography recording
$_{s}$SS	Supraspinatus; surface electromyography recording
UT	Upper Trapezius; coactivation ratio coefficient

cm	Centimeter
Hz	Hertz
m	Meter
min	Minute
mm	Millimeter
n	Number/number of
N	Newton
Nm	Newton meters
sec	Second
kg	Kilogram
Pa	Pascals

c	time-delay constant of neuromuscular activation/deactivation
$C(q,\dot{q})$	Coriolis force vector
F_O^{MT}	Vector of maximal musculotendon forces, subject to length and velocity coefficients, multiplied by a vector containing muscle activations
$G(q)$	Generalized force of gravity
i	Time points for direct collocation
$J^T\tau_{end}$	Torque exposure at end effector
N	Nodes for direct collocation
$M(q)$	Inertial mass matrix
p	Muscle Density Coefficient: assumed 1,000 $kg \cdot m^{-3}$
q	Vector of generalized system coordinates
$\dot{q}$	Vector of generalized system velocities
$\ddot{q}$	Vector of generalized system accelerations
$R(q)$	Matrix of moment arms; joint x muscle
u	Control state; nervous excitation
V_s	Velocity

τ	Tau: vector of joint moments
μ	Mu: muscle elastic modulus

α_{GT}	Thoracic flexion/extension in the global coordinate system
β_{GT}	Lateral thoracic flexion in the global coordinate system
γ_{GT}	Axial thoracic rotation in the global coordinate system
α_{SC}	Sternoclavicular axial rotation
β_{SC}	Sternoclavicular depression
γ_{SC}	Sternoclavicular protraction
α_{AC}	Acromioclavicular tilt
β_{AC}	Acromioclavicular medial rotation
γ_{AC}	Acromioclavicular protraction
α_{S}	Scapulothoracic tilt
β_{S}	Scapulothoracic medial rotation
γ_{S}	Scapulothoracic protraction
γ_{GH}	Glenohumeral plane of elevation
β_{GH}	Glenohumeral depression
γ_{GH}^{2}	Glenohumeral axial Rotation
γ_{h}	Thoracohumeral plane of elevation
β_{h}	Thoracohumeral depression
γ_{h}^{2}	Thoracohumeral axial rotation
α_{HF}	Elbow flexion
β_{HF}	Elbow carrying angle (rarely analyzed)
γ_{HF}	Elbow pronation

1.1. Overview

The shoulder complex permits some of the greatest mobility observed between articulating segments of the human body [Dvir and Berme, 1978; Bechtol, 1980; Levin, 1997; Halder, Itoi, and An, 2000; Prescher, 2000; Barnes, Van Steyn, and Fischer, 2001; Veeger and Van Der Helm, 2007; Ludewig, et al., 2009; Johnston and Drake, 2021]. This mobility affords each arm the capacity to reach anywhere within a reach envelope that spans approximately one-third the area of a spherical projection about our shoulder [Selvan and Sen, 2020]. Such mobility arises from the 9 degrees of freedom (DOF) expressed about the 3 anatomical joints of the shoulder and the many muscles that manipulate any one of these joints [Bechtol, 1980; Halder, Itoi, and An, 2000; Prescher, 2000; Veeger and Van Der Helm, 2007].

The abundance of muscles and DOF presents many feasible solutions to achieve a targeted arm motion, yet muscular and kinematic strategies elicited in humans only appear to utilize a small subset of all the available solutions [Sohn and Ting, 2018; Mulla and Keir, 2023]. Still, among the subset of shoulder kinematic and motor strategies elicited in humans, much variability has been reported both between and within individuals [Groot, 1998; Janwantanakul, et al., 2001; Chopp-Hurley, et al., 2016; Mulla, McDonald, and Keir, 2018; Sohn and Ting, 2018]. This variability is thought to be a product of the central nervous system's (CNS) attempt to address many competing control criteria that might define an ‘optimal’ movement [Schouten, et al., 2001; Todorov, 2004; Van Den Bogert, Blana, and Heinrich, 2011; Hirashima and Oya, 2016; Kelly, 2017; Baker, et al., 2018; Bassani and Galbusera, 2018]. Frequently hypothesized criteria include muscle stress [Buchanan, et al., 2004; Erdemir, et al., 2007; Blana, et al., 2008], joint torque [Buchanan, et al., 2004], postural stability [Sohn and Ting, 2018], attention [Terrier and Forestier, 2009], effort [Sohn and Ting, 2018], cognitive demand [Terrier and Forestier, 2009], oxygen consumption [Praagman, et al., 2006], and metabolic cost [Praagman, et al., 2006], however many other criteria have been proposed. Further, the criteria that would define an ‘optimal’ motion for a single task is presumably influenced by different tasks, joints, exposure and training history, health, sex, and many other factors that would explain the observed range interindividual and intraindividual variability [Latash, Scholz, and Schöner, 2002; Hirashima and Oya, 2016; Metwali, 2019; Raviv, Lupyan, and Green, 2022].

Muscle fatigue ostensibly influences kinematic and muscular patterns and associated variability [Sparto, et al., 1997; Forestier and Nougier, 1998; McQuade, Dawson, and Smidt, 1998; Myers, et al., 1999; Enoka and Duchateau, 2008; Gates and Dingwell, 2008; Gates and Dingwell, 2011; Chopp-Hurley and Dickerson, 2015; Chopp-Hurley, et al., 2016; Tse, McDonald, and Keir, 2016; Mulla, McDonald, and Keir, 2018; Umehara, et al., 2018; Dupuis, et al., 2021]. Muscle fatigue is a complex, and transient state defined as a reduced force-generating capacity and/or fatigue resistance which can arise due to numerous neurophysiological factors [Bigland-Ritchie, et al., 1986; Enoka and Stuart, 1992; Enoka, 1995; Vøllestad, 1997; Allen, Lamb, and Westerblad, 2008; Enoka and Duchateau, 2008]. Truly, fatigue-related kinematic changes are a direct result of fatigue-related muscular changes, as the body employs load-sharing changes to maintain several CNS control criteria among a shifting landscape of muscular capacity [Dul, et al., 1984; Sparto, et al., 1997; Zhang, et al., 2003; Bouillard, et al., 2012; Bouillard, et al., 2014; Mulla and Keir, 2023]. However, muscular and kinematic fatigue responses between and within individuals also vary considerably even when presented with identical task conditions [de Groot, 1997; Chopp-Hurley, et al., 2016; Mulla, McDonald, and Keir, 2018; Metwali, 2019], challenging the ability to understand and clearly define principal fatigue-related control strategies.

Further, evidence suggests that some adaptive muscular and kinematic responses to shoulder muscle fatigue may promote mechanical risk factors for the most prevalent shoulder injuries which include subacromial impingement syndrome (SAIS), rotator cuff (RC) tear, labrum tear, long-head biceps strain, and potentially others [Reddy, et al., 2000; Michener, McClure, and Karduna, 2003; Lewis, Green, and Wright, 2005; Phadke, Camargo, and Ludewig, 2009; Chopp, Fischer, and Dickerson, 2011; Noguchi, et al., 2013; de Witte, et al., 2014; Chopp-Hurley and Dickerson, 2015; Michener, et al., 2015]. Such findings could suggest that fatigue-related central control strategies are associated with chronic injury risk, however other evidence suggests that fatigue-related muscular adaptations may protect against mechanical risk factors of shoulder injury [McQuade, Wei, and Smidt, 1995; McQuade, Dawson, and Smidt, 1998; Ebaugh, McClure, and Karduna, 2006; Chopp, Fischer, and Dickerson, 2011; Chopp-Hurley and Dickerson, 2015]. Chiefly, much of the variability associated with shoulder muscle control and shoulder muscular and kinematic responses to fatigue have shrouded our understanding of these potential risks and related insights on chronic injury mechanics, injury prevention, and rehabilitation. Such insights are also highly valuable in the pursuit of more accurate neuromuscular control models for highly redundant systems, for which the shoulder is exemplar.

1.2. Purpose and Objectives

The overarching purpose of this dissertation is to explore fatigue-related changes in shoulder muscle activity and kinematics and the variability therein, to glean insights on central control scheme adaptations in a highly redundant muscular system. Secondary goals of this dissertation are listed:

- Determine fatigue-related factors associated with chronic shoulder joint injury.
- Explore how familiarity to a muscle-fatigue inducing task adjusts kinematic and muscular control strategies.

- Investigate whether fatigue-related viscoelastic muscle changes influence neuromechanical and kinematic adaptation strategies.

Pursuant to these goals, a brief narrative recount of kinematic and muscular affects of fatigue is provided in chapter 2 before chapters 3-6 address the following specific research objectives:

Chapter 3

Muscle coactivation changes following a fatiguing overhead drilling task: implications for subacromial impingement syndrome.

3.1. Examine whether changes in shoulder muscle coactivation and associated upper limb kinematics changes following and occupationally relevant overhead muscle fatigue task targeting the shoulder, upper limb, and trunk, would reflect altered patterns previously shown in those with SAIS and RC tears.

3.2. Determine whether fatigue-induced changes in scapular stabilizer muscles coactivation explain variance in scapulothoracic kinematics.

3.3. Whether an overhead fatiguing task yielded reductions in force-generating capacity in muscle-specific myoelectric responses indicative of fatigue.

Chapter 4

Variability in musculoskeletal fatigue responses associated with repeated exposure to an occupational overhead drilling task completed on successive days.

4.1. Whether upper limb kinematics and static shoulder moments at baseline were different between repeated exposures to the same occupationally relevant overhead shoulder fatigue task.

4.2. Whether fatigue-related changes in upper limb muscle activity, kinematics, and kinetics were different between repeated exposures to the same occupationally relevant overhead shoulder fatigue task.

4.3. Whether kinematic and kinetic variability were different between repeated exposures to the same occupationally relevant overhead shoulder fatigue task.

Chapter 5

Shoulder kinematic and muscle activity compensations to scapular stabilizer weakness: An optimal control framework.

1.1. Use a computational musculoskeletal model of the shoulder to predict scapulothoracic kinematics changes associated with isolated reduced force-generating capacity of the scapular stabilizer muscles.

1.2. Determine the model-predicted scapular stabilizer muscle activity compensations associated with isolated reductions in force-generating capacity of the scapular stabilizer muscles.

Chapter 6

Fatigue-mediated shear wave velocity, force, electromyography, and kinematics at the scapular stabilizer muscles.

6.1. Determine whether fatigue-mediated changes in muscle stiffness are present following a targeted fatigue task of the scapular stabilizer muscles.

6.2. Whether fatigue-related changes in passive muscle element stiffness contribute significant predictive variance in determining fatigue state and subsequent kinematic changes.

Concluding the dissertation will be a general discussion in chapter 7. Consistent with a traditional ‘manuscript style’ dissertation a comprehensive reference list covering all chapters is included at the end of this document, and research methods will be reported as they are pertinent to each chapter in lieu of a common methodology section.

Chapter 2. Shoulder Muscle Control, Fatigue, and Injury: A Narrative Review.

Matthew S. Russell, Janessa D.M. Drake, Jaclyn N. Chopp-Hurley

School of Kinesiology and Health Science, York University, Toronto, Canada

Declarations of Interest: None

Funding Sources: This work was supported by the Natural Science and Engineering Council (NSERC) Discovery Grant program (J.N. Chopp-Hurley & J.D.M. Drake), and the NSERC Post-Graduate Scholarship program (M.S. Russell).

2.1. Shoulder Muscles

2.1.1. Anatomy

Considerable shoulder range of motion (ROM) is afforded by the three anatomical joints which comprise the shoulder complex [Dvir and Berme, 1978; Bechtol, 1980; Prescher, 2000; De Groot and Brand, 2001; Veeger and Van Der Helm, 2007; Ludewig, et al., 2009]. These joints are the glenohumeral joint between the humerus and scapula, the acromioclavicular joint between the scapula and clavicle, and the sternoclavicular joint between the sternum of the thorax and the clavicle. The sternoclavicular and acromioclavicular joints are each reinforced with 3 ligaments, however the bulk of the scapula which glides over the posterior surface of the thorax is not directly stabilized by any ligaments [Kibler, 1998; Reinold, Escamilla, and Wilk, 2009; Kibler, et al., 2013]. Most joints of the human body transmit bone-on-bone forces during loading and motion in order to provide stability, and muscular resistance can be applied to generate a secondary source of active stability [Nordin and Frankel, 2001]. Rather, scapular position about the thorax which is termed the scapulothoracic (SCT) 'joint' despite not being an anatomical joint, is governed primarily by the scapular stabilizer muscles [Levin, 1997; Veeger and Van Der Helm, 2007; McQuade, Borstad, and de Oliveira, 2016]. This lack of stability does in turn afford the SCT joint with improved mobility - an important trait for the dextrous upper limb [Veeger and Van Der Helm, 2007; Sohn and Ting, 2018].

2.1.1.1. Scapular Stabilizer Muscles

The scapular stabilizer muscles consist of the trapezius and serratus anterior muscles [Johnson, et al., 1994; Cools, et al., 2002; Ludewig, et al., 2004; Ekstrom, Soderberg, and Donatelli, 2005; Webb, Blemker, and Delp, 2014]. Trapezius is often partitioned into three subregions: upper trapezius, middle trapezius, and lower trapezius [Ludewig, et al., 2004]. This partitioning helps isolate unique actions of the trapezius as all partitions can retract the scapula, yet upper trapezius can also elevate the scapula and lower trapezius can depress the scapula [Dvir and Berme, 1978; Phadke, Camargo, and Ludewig, 2009]. Serratus anterior primarily opposes trapezius, acting to protract the scapula [Dvir and Berme, 1978; Ekstrom, et al., 2004]. Literature also identifies scapular depression as another key function of serratus anterior [Ekstrom, et al., 2004; Ludewig, et al., 2004]. Together, the upper and lower partitions of trapezius and serratus anterior are hypothesized to provide a triad of force vectors which can collectively manipulate scapular position about the thorax [Ludewig, et al., 2004; Michener, et al., 2016]. Static equilibrium across this triad of vectors has been evidenced to suggest that they stabilize the scapula's position, for which they have been termed 'scapular stabilizer muscles'. Serratus anterior also acts as a primary agonist for upward or lateral scapular rotation [Dvir and Berme, 1978; Ekstrom, et al., 2004; Phadke, Camargo, and Ludewig, 2009]. The ellipsoid shape of the thorax and the gliding of the scapula along this plane also changes muscle moment arms depending on scapular orientation, as well as humeral position.

For this reason, trapezius muscle appears to be more active during frontal plane arm elevation, while serratus anterior is more active in scapular and sagittal plane elevation [Inman, Saunders, and Abbott, 1944; Wiedenbauer and Mortensen, 1952].

2.1.1.2. Rotator Cuff (RC) Muscles

The RC muscles comprise supraspinatus, infraspinatus, subscapularis, and teres minor. As their name implies, a primary function of these muscles is to perform humeral rotation. Supraspinatus, infraspinatus, and teres minor all contribute to external rotation, varying in their relative contribution depending on the arms position, while subscapularis is considered the primary internal humeral rotator [Phadke, Camargo, and Ludewig, 2009; Allen, et al., 2013; Sangwan, Green, and Taylor, 2015]. However, these muscles achieve another vital shoulder function in maintaining stability of the humeral head within the center of the glenoid fossa [Cools, et al., 2004; Phadke, Camargo, and Ludewig, 2009; Ackland and Pandy, 2011; Cudlip and Dickerson, 2018]. Research suggests that the deeper partitions of the RC muscles may primarily act to counter shear joint forces supplied by the deltoid specifically [Cudlip and Dickerson, 2018].

2.1.1.3. Other Periscapular Muscles

Other muscles which manipulate the scapula but are not as involved in dynamic scapular stability include levator scapulae, and rhomboid major and minor [Bradley and Tibone, 1991; Ackland, et al., 2008; Escamilla and Andrews, 2009;

Ackland and Pandy, 2011; Webb, Blemker, and Delp, 2014; Mulla, et al., 2019]. These muscles assist with retraction and downward rotation of the scapula; a key characteristic to offset the scapular stabilizers which all contribute to upward rotation [Inman, Saunders, and Abbott, 1944; Phadke, Camargo, and Ludewig, 2009].

Muscles which join the humerus to the ribs, clavicle, or vertebrae generate biarticular or even triarticular moments [Ackland, et al., 2008; Hik and Ackland, 2019; Hoffmann, et al., 2020]. Key muscles under this definition include the deltoid, pectoralis major, and latissimus dorsi. These muscles can manipulate the humeral position relative to the thorax, or relative to the clavicle (anterior deltoid), bypassing more than one anatomical shoulder joint [Veeger and Van Der Helm, 2007; Ackland, et al., 2008]. The multi-joint articulation of these muscles makes their mechanical leverage (moment arm) highly sensitive to the arm's position [Ackland, et al., 2008; Hik and Ackland, 2019; Mulla, et al., 2019; Hoffmann, et al., 2020]. Further, cocontraction of other shoulder muscles may dictate the relative position of the scapula and clavicle [Levin, 1997; Levin, 2005; Amasay and Karduna, 2009].

2.2. Fatigue Affects in Muscle

2.2.1. Contractile Muscle Elements and Fatigue

The intra-muscular contractile elements (or neuromuscular elements) are affected by peripheral processes which include metabolite buildup due to blood flow occlusion, mechanical sarcomere damage, and declining finite muscle glycogen availability [Enoka, 1995; Allen, Lamb, and Westerblad, 2008; Enoka and Duchateau, 2008]. These factors all transiently reduce the strength and endurance of muscle through the phenomenon of peripheral muscle fatigue [Enoka, 1995; Vøllestad, 1997; Enoka and Duchateau, 2008; Potvin and Fuglevand, 2017; Pethick and Tallent, 2022]. However, fatigue-related control changes are not directly controlled by peripheral fatigue factors. Rather, control changes are governed by supraspinal synergistic muscular control that preferentially selects available motor units (MU's) that are best suited to the strength and endurance demands of the current task and will be discussed first [Adam and De Luca, 2003; Amann, 2011; Carroll, Taylor, and Gandevia, 2017], followed by a discussion on the non-contractile elements of muscle fatigue. Throughout fatigue progression, the initial MU selection by the CNS that is thought to be based on the most appropriate selection of force-generating capacity and fatigability characteristics will eventually reach failure [Enoka, 1995; Contessa, De Luca, and Kline, 2016; Potvin and Fuglevand, 2017]. Thus, less applicable MU's may be progressively recruited until all MU's are no longer viable [Enoka, 1995; Gandevia, et al., 1996; Zhang, et al., 2003; Amann, 2011]. However, during a task with multiple kinematic DOF, different muscles can also be preferentially recruited in order to further stall the rate of MU failure [Dul, et al., 1984; Duchateau and Baudry, 2014]. This describes the principle of load-sharing synergies, which are muscle synergies that determine the contribution of multiple muscles towards a demand or task [Bernstein, 1966; Dul, et al., 1984; Sparto, et al., 1997; Zhang, et al., 2003; Bouillard, et al., 2012; Bouillard, et al., 2014; Duchateau and Baudry, 2014]. Load-sharing muscle synergies are likely to change throughout the progression of fatigue to incorporate many or all of the DOF's within the specified bounds of the task [Dul, et al., 1984; Scholz and Schöner, 1999; Latash, Scholz, and Schöner, 2002; Inouye and Valero-Cuevas, 2016]. However, the incorporation of accessory muscular DOF's causes a shift in muscle activation which in turn influences a change in down-chain kinematics [Sparto, et al., 1997; Forestier and Nougier, 1998; Monjo, Terrier, and Forestier, 2015]. Load-sharing changes are often progressive, rather than abrupt, thus it can be expected that kinematics changes will be observed slowly over the course of fatigue build-up, and this rate of postural shift will be related to the strength and endurance of the load-sharing agonist muscles [Madeleine, 2010; Bouillard, et al., 2012; Duchateau and Baudry, 2014].

Similar to load-sharing synergies which determine agonist activity allocations during a task are coactivation synergies, which determine antagonist activity during a task [Latash, Scholz, and Schöner, 2007; Duchateau and Baudry, 2014; Latash, 2018]. Muscle coactivation activity is often elicited at a small fraction of the activity in the agonist muscles; approximately 5-15% in most cases [Baratta, et al., 1988]. However, this activity is essentially always non-zero, excluding specific muscle-quieting reflexes [Angel, Eppler, and Iannone, 1965]. Muscle coactivation supplies an increased control to our movements and is an example of muscles stabilizing a joint [Humphrey, Reed, and Desmedt, 1983]. Typically joints with less boney approximation and stability supplement this insufficiency with higher coactivation [Frey-Law and Avin, 2013]. During SCT joint motion and loading, coactivation among the opposing scapular stabilizers is observed in order to improve task control and joint stability [Mottram, 1997; Phadke, Camargo, and Ludewig, 2009].

The excess of kinematic DOF's available at the shoulder and upper limb, combined with the substantial amount of strength, endurance, and morphological differences between individuals may in part contribute to a high degree of inter-individual variability in shoulder control [Chopp-Hurley, et al., 2016; McDonald, Tse, and Keir, 2016; Tse, McDonald, and Keir, 2016; Mulla, McDonald, and Keir, 2018]. Further, the excess of DOF's at the shoulder and scapula provide a redundancy of available compensation patterns during fatigue, generating a great degree of inter-individual variability and potential intra-individual variability as well [Ludewig and Cook, 2000]. This is thought to be one of the primary reasons for why injury risk is so variable across populations [Chopp-Hurley, et al., 2016]. Since such variability is likely a product of human movement redundancy it may reflect that the available landscape of feasibly solutions are so abundant and competitive (in terms of optimality) that small changes in our subconscious perception of optimal control may permit the substantial intraindividual variability that is observed. Conversely, motor synergies, engrams which are postulated to arise from learned experience can be updated by current somatosensory feedback, thus proposing a hypothetical framework for how learned experiences can also inform movement variability (Macpherson 1991, Ting and McKay 2007, Inouye and Valero-Cuevas 2016). Overall, these hypotheses on the supraspinal origin of movement variation point towards it being a purposeful, or at least advantageous neuromotor feature in primates, yet making it potentially difficult to quantify.

2.2.1.1. Electromyography for Evaluating Neuromuscular Fatigue

While muscle control and fatigue-compensation synergies descend from a supraspinal origin, their effects can be measured and assessed through the muscle activity and kinematics changes they enact [Gandevia, et al., 1996; Vøllestad, 1997; Cairns, et al., 2005; Amann, 2011; Carroll, Taylor, and Gandevia, 2017]. Elaboration on supraspinal muscle control is provided in section 2.2.3.

Current gold-standard techniques in the evaluation of muscle activity include electromyography (EMG) analysis such as mean-power frequency (MPF) and median-power frequency (MnPF) [van Boxtel and Schomaker, 1984; Arendt-Nielsen and Mills, 1985; Öberg, Sandsjö, and Kadefors, 1990; Öberg, Sandsjö, and Kadefors, 1994; Christensen, et al., 1995], amplitude root-mean-square (RMS) [Merletti and Farina, 2009; Besomi, et al., 2020] or linear enveloping (rectify and low-pass filter) [Farina, Merletti, and Enoka, 2004; Merletti and Farina, 2009; Besomi, et al., 2020], and simple muscle on-off determination [Hodges and Bui, 1996]. Muscle fatigue is known to produce progressive decrements in MPF and MnPF (temporal shift), and a progressive increment in RMS (spatial shift) as a result of neuromuscular fatigue, which can make frequency and amplitude analysis difficult to compare [McDonald, et al., 2018]. Both spectral and amplitude changes to muscle activity and EMG are identified to arise from alterations in muscle fiber conduction velocity [Lindstrom and Magnusson, 1977; Stulen and De Luca, 1981; Arendt-Nielsen and Mills, 1985]. As lower motor neuron (LMN) activity is sustained, intracellular potassium is pumped into the extracellular space to maintain ion gradients necessary for action potentials [Vatner and Pagani, 1976; Arendt-Nielsen and Mills, 1985]. Without sufficient rest, this process temporarily alters the electrochemical gradient across the neuron cell membrane which impairs depolarization [Arendt-Nielsen and Mills, 1985; Bigland-Ritchie, et al., 1986]. Sustained contraction can also reduce ATP availability and promote metabolite accumulation; both factors which can slow the sodium-potassium pumps activity necessary to rebalance ion concentrations [Enoka and Stuart, 1992; Enoka, 1995; Bortolotto, et al., 2000; Allen, Lamb, and Westerblad, 2008; Enoka and Duchateau, 2008]. Collectively, these mechanisms slow the velocity of propagating of action potentials, which is reflected in the frequency of EMG signal [Stulen and De Luca, 1981]. The temporal delay in action potential propagation has also been identified to reduce the summated action potential amplitude as different action potentials are more likely to overlap and cancel each other out [van Boxtel and Schomaker, 1984; Arendt-Nielsen and Mills, 1985; Farina, Merletti, and Enoka, 2004]. This etiology suggests that fatigue-mediated amplitude increases commonly observed are not a product of impaired conduction velocity and point towards supraspinal modulation which amplifies descending neural drive to boost MU recruitment [Vøllestad, 1997; Contessa, De Luca, and Kline, 2016]. The many intersecting processes that alter MU activity have long challenged the ability to compare EMG signal properties throughout the time-course of fatigue. Fortunately, recent work by McDonald and colleagues validated the application of a new technique which uses a cubic spline to normalize amplitude changes across the progression of neuromuscular fatigue [McQuade, Borstad, and de Oliveira, 2016; McDonald, et al., 2018]. The recent validation of this technique offers new ways to compare fatigue-related changes in muscle activity that are hypothetically a result of muscle synergy and control changes by parsing out the neuromuscular effects of fatigue.

2.2.2. Non-Contractile Muscle Elements and Fatigue

Typically, the muscle fatigue state has been evaluated as a reduction in the contractile ability of the muscle [Vøllestad, 1997; Cairns, et al., 2005], or a change in the neuromuscular activity as discussed [Stulen and De Luca, 1981; van Boxtel and Schomaker, 1984; Öberg, Sandsjö, and Kadefors, 1994; Pethick and Tallent, 2022]. However, these criteria of muscle fatigue largely neglect the passive force generating capacity of muscle, which derives from the non-contractile or elastic components of muscle [Herzog, 2019]. Non-contractile force contributions can be observed throughout the lengthened state of muscle, where kinetic energy is stored in the elastic muscle components when muscle is stretched near their end range [Koo, et al., 2013; Herzog, 2019]. When the stretching force is removed, some of the stored potential energy is released as force, while some energy is also lost due to viscoelastic hysteresis [Collinsworth, et al., 2002; Lynch, Ramos, and Jones, 2017]. Muscle force evaluation for fatigue determination likely demonstrates combined force generating capacity changes from both contractile and non-contractile components, however EMG specific measurement and analyses only capture neuromuscular changes.

At a molecular level, it has been proposed that most of the passive force in skeletal muscle is generated by the giant protein Titin, which behaves viscoelastically and allows for force transmission between the Z-line and the I-band [Minajeva, et al., 2001; Tskhovrebova and Trinick, 2003]. However, fascia and elastin also respond viscoelastically to stress and deformation [Herzog, 2019]. As a property of viscoelastic tissue, creep describes the capacity for said tissue to temporarily lengthen when subjected to sustained or recurrent strain, causing a decrease in the stiffness of the tissue or a reduction in the muscle's elastic modulus [Caler and Carter, 1989; Wren, et al., 2003]. This transient change to the muscle length and stiffness reduces the amount of energy that can be stored elastically, and also alters the ROM under which the muscle is strongest, termed the force-length curve [Saldana and Smith, 1991]. Such changes may hypothetically affect muscle control and kinematics, although this interaction is not yet clear and requires investigation [Howarth, et al., 2013; Guo, et al., 2020].

2.2.2.1. Shear-Wave Velocity for Evaluating Muscle Stiffness

Recent work has validated the use of shear-wave velocity (SWV) application to muscle tissue to assess muscle elastic modulus during passive muscle rest, isometric contraction, or passive muscle lengthening [Kubo, et al., 2001; Koo, et al., 2013; Yoshitake, et al., 2014; Eby, et al., 2015; Ewertsen, et al., 2018; Siracusa, et al., 2019]. SWV is applied by a piezoelectric ultrasound transducer which generates a high intensity, low-frequency shear wavelength between 50-400 Hz that propagates the longitudinal axis of the muscle towards the musculotendinous end points [Eby, et al., 2015; Andonian, et al., 2016]. The SWV wavelength propagates the muscles at approximately 1-50 m/sec, and this velocity can be measured by the ultrasound transducer [Brandenburg, et al., 2014; Eby, et al., 2015]. The velocity of the waveform can quickly be related to Young's modulus of elasticity using equation 2.1. below [Davis, et al., 2019]. As discussed, fatigue will induce transient viscoelastic reductions in muscle stiffness and the elastic modulus, such that we may measure these changes to non-contractile muscle element stiffness throughout the progression of fatigue using SWV [Siracusa, et al., 2019].

Equation 2.1. **Young's Elastic Modulus.**

$$\mu = p \ \cdot V_s^2$$

Where,

μ is the muscle elastic modulus in Pascals (Pa),

p is the muscle density, assumed to be 1,000 kg·m^{-3},

and V_s is the SWV (m/s).

2.2.3. Central Fatigue

Thus far, section 2.2. has reviewed factors of peripheral fatigue etiology which includes neuromuscular and non-contractile element changes. The review of peripheral factors is not fully comprehensive, and does not discuss many chemical and metabolic pathways associated with fatigue [Vatner and Pagani, 1976; Enoka and Stuart, 1992; Bortolotto, et al., 2000; Allen, Lamb, and Westerblad, 2008; Amann, 2011; Eby, et al., 2015], but reviews those which are most contextual to the studies contained in this dissertation. While not directly quantified in the following studies, central fatigue will be reviewed as it has many implications on neuromuscular fatigue compensations.

Like peripheral fatigue, central fatigue is a transient neurological condition, yet otherwise these two processes are distinct. Central fatigue arises due to transient changes in efferent signalling modulated by the upper motor neurons in the brain and spinal cord [Amann, 2011; Carroll, Taylor, and Gandevia, 2017]. Upper motor neuron activity is signalled by neurotransmitters which offer two pathways associated with central fatigue. First, excitatory and signalling of upper motor neuron activity may decreases if availability of these neurotransmitter is depleted, which is often associated with a feeling of general lethargy and fatigue [Gandevia, et al., 1996; Carroll, Taylor, and Gandevia, 2017]. These central fatigue mechanisms also have implications for mental capacity, as depletion of the same excitatory neurotransmitters is shown to reduce attentional and cognitive processing, which is hypothesized to motivate volitional task failure. Second, increased release of inhibitory neurotransmitters may down-regulate descending motor drive as a centrally mediated response thought to protect muscles from the potential consequences of over exertion like injury [Gandevia, et al., 1996; Pethick and Tallent, 2022]. This process is mediated by afferent muscle feedback, linking peripheral and central fatigue pathways [Gandevia, 1998; Amann, 2012]. Importantly, the inhibitory central mechanisms can promote load sharing changes by down-regulating the activity of more fatigued muscles and up-regulating the activity of less fatigued options [Bernstein, 1966; Dul, et al., 1984; Baratta, et al., 1988; Sparto, et al., 1997; Zhang, et al., 2003; Bouillard, et al., 2014]. This acts as a potential strategy to manage peripheral fatigue, but also may be helpful in reducing the descending motor drive instigating temporal and spatial activation of lower motor neurons [Humphrey, Reed, and Desmedt, 1983; Farina, et al., 2004; Giszter, Patil, and Hart, 2007; Rathelot and Strick, 2009]. These considerations may be especially important for a highly redundant muscular system, where many alternative motor strategies are available. The shoulder complex offers an excellent in vivo human model of kinematic and muscular redundancy to potentially unveil what factors the CNS considers in the deployment of motor strategies among competing variables like fatigue and mechanical efficiency [De Groote, et al., 2016; Hirashima and Oya, 2016; Sohn and Ting, 2018].

2.2.3.1. Modelling Centrally Mediated Shoulder Control

Optimal control methods are a class of mathematical formulations for solving indeterminant problems; those where the number of variables is greater than the number of constraints, presenting multiple feasible solutions [Van Den Bogert, Blana, and Heinrich, 2011; De Groote, et al., 2016; Andersson, et al., 2019]. Such methods offer an approach to probe centrally mediated control conditions that result in empirically accurate muscle activity and kinematics patterns at the shoulder, and may help to identify how these control variables are weighted by the CNS to identify an 'optimal' solution amidst redundancy.

Traditional optimal control problems for biomechanics problems harness explicit ordinary differential equations (ODE) with Runge-Kutta or Euler methods to map control vectors to state vectors which can be solved with nonlinear programming (NLP) methods like gradient descent [Chen, Ballance, and Gawthrop, 2003; Menegaldo, de Toledo Fleury, and Weber, 2003]. The explicit formulation harnessed in these traditional methods benefitted from a relatively fast solutions when solving optimal gait control problems or upper limb formulations that treated the shoulder as single ball and socket joint (neglecting the clavicle and scapula) due to the relatively low numerical stiffness [Menegaldo, de Toledo Fleury, and Weber, 2003; Van Den Bogert, Blana, and Heinrich, 2011; Maas, 2014]. Often, these formulations treated stiff elements with high stiffness as a hard constraint, bypassing the need to inflate timesteps to maintain accuracy [Van den Bogert and Schamhardt, 1993]. However, replacing stiff elements with hard constraints is not always desirable. In the case of simulating scapulothoracic motion, the low mass of the scapula and clavicle relative to the stiff ligaments and tendons acting on them means that methods for handling stiffness become necessary. Advancements in optimal control have recently published new methods which harness implicit partial differential equations (PDE) that are more stable than ODE's for handling stiff differential equations over large timesteps [Van Den Bogert, Blana, and Heinrich, 2011]. This has made the simulation of scapular optimal control more viable, now achieving solutions in hours for problems that may have previously taken days [Van den Bogert and Schamhardt, 1993; Anderson and Pandy, 2001; Van Den Bogert, Blana, and Heinrich, 2011].

2.3. Scapular Stabilizer Equilibrium

Fatigue of the Lower Trapezius and Serratus Anterior muscles has been associated with increases in Upper Trapezius activation, which subsequently narrows the subacromial space (SAS) and is associated with SAIS [Cools, et al., 2004; Ludewig, et al., 2004; Szucs, Navalgund, and Borstad, 2009; Cooper and Karduna, 2022]. While upper trapezius contributes to elevation and upward rotation of the scapula, the alteration in functional SAS associated with dominance is thought to occur due to an imbalanced force couple with serratus anterior and lower trapezius [Cools, et al., 2004; Ludewig, et al., 2004; Szucs, Navalgund, and Borstad, 2009; Cooper and Karduna, 2022]. This imbalance causes excess elevation and stiffness of upper trapezius which resists motion and alters the axis of scapulothoracic rotation to be closer to the acromion [Bagg and Forrest, 1986; Page, 2011]. The effect of altering this rotation axis is that the moment arm to the acromion is shortened, thereby reducing the clearance of the acromion normally provided from upward rotation. Importantly, this mechanical rationale for increased upper trapezius activity and SAIS risk has been speculated but not yet verified [Bagg and Forrest, 1986; Page, 2011].

Historically, SAIS and scapular dyskinesis rehab interventions have focused on strengthening the Lower Trapezius and Serratus Anterior in an attempt to mitigate the effects of muscle weakness due to fatigue [Ludewig, et al., 2004; Szucs, Navalgund, and Borstad, 2009]. Yet recent literature may now suggest that scapular stabilizer strength is less important than scapular stabilizer control for the purpose of minimizing injury [Bang and Deyle, 2000; Ludewig, et al., 2004; Szucs, Navalgund, and Borstad, 2009; De Groote, et al., 2016; Michener, et al., 2016] . To discretize the semantic differences between scapular strength and scapular control: scapular strength training typically reinforces the force-generating capacity and fatigue resistance of Lower Trapezius and Serratus Anterior across a few select motions that generate preferential activation of these muscles [Bang and Deyle, 2000; Cools, et al., 2007]. Conversely, scapular control training focuses on maintaining an equitable activation of all three scapular stabilizers across the full range of scapular motion, thereby minimizing the dominance of Upper Trapezius that could lead to dyskinesis [Michener, McClure, and Karduna, 2003; Cools, et al., 2007; Michener, et al., 2016]. Good scapular control may afford more viable muscular DOF's towards shoulder tasks, as the scapular muscles are available to contribute over a broader ROM. The availability of more DOF's may in turn be vital for limiting the risk of dyskinesis and subsequent SAIS during shoulder fatigue, as this provides a greater selection of load sharing strategies and coactivation muscle synergies. Conversely, training scapular muscle strength rather than scapular control may be less likely to generate more DOF's, but simply reinforce existing muscle synergies and focalize the fatigue across fewer muscles.

Recently, a critical perspective on scapular stabilizer coactivation ratios has also arisen [McQuade, Borstad, and de Oliveira, 2016]. This perspective highlights the substantial anatomical variability in scapular shape and scapular stabilizer muscle morphology due to factors like sex, age, and genetics [Prescher, 2000; Graichen, et al., 2001]. For these reasons, relative activity among the scapular stabilizers is not universally proportional to the balance of force vectors acting on the scapula. Further, the scapular stabilizer muscles impart moments on the scapular which is a product of the muscle force and the moment arm length. Thus, for actions which rotate scapular position, the length of opposing muscle moment arms plays a big factor in determine the relative balance of the system, and this is not considered in coactivation ratio metrics [Cools, et al., 2004; McQuade, Borstad, and de Oliveira, 2016]. Thus, despite evidence linking coactivation ratio magnitudes to populations with SAIS and RC tear, a clear injury mechanism may be elusive and require more research.

2.4. Injury Mechanics

Shoulder muscle fatigue, particularly during suprapostural tasks, is associated with a heightened risk of SAIS and RC impingement and injury [Herberts, et al., 1984; Huisstede, et al., 2006; Bey, et al., 2007; Grieve and Dickerson, 2008; Van Rijn, et al., 2010; Chopp-Hurley, et al., 2016]. SAIS and RC tears account for 30-45% of all clinically presented shoulder conditions [Van der Windt, et al., 1995; Huisstede, et al., 2006]. The risk for SAIS and RC impingement is associated with scapular and RC muscle weakness and scapular muscle dyskinesis [Szucs, Navalgund, and Borstad, 2009; Chopp-Hurley and Dickerson, 2015; Chopp-Hurley, et al., 2016], the latter of which is defined as sub-optimal scapular motion patterns that may arise from poor control and coordination [Giuseppe, et al., 2020]. During suprapostural or overhead postures, the scapular and RC muscles elicit particularly elevated levels of muscle activity, which more rapidly induces fatigue of these muscle groups [Grieve and Dickerson, 2008; Chopp, Fischer, and Dickerson, 2011; Chopp-Hurley and Dickerson, 2015; Chopp-Hurley, et al., 2016]. These overhead postures are also shown to reduce the SAS by approximately 35-45 mm [Chopp, et al., 2010; Chopp and Dickerson, 2012; Chopp-Hurley, Langenderfer, and Dickerson, 2016], increasing the risk for RC tendon compression and subsequent injury. This reduction in SAS width can be considerable relative to an average healthy width of 9-10 mm, which can be significantly reduced to 7-8 mm in females [Graichen, et al., 2001; Bey, et al., 2007]. SAS width can be impeded by downward rotation or anterior tilting of the scapula, while scapular protraction can also be a factor but is less widely reported [Lewis, Green, and Wright, 2005; Chopp and Dickerson, 2012; Noguchi, et al., 2013; Chopp-Hurley and Dickerson, 2015; Chopp-Hurley, et al., 2016; Michener, et al., 2016]. These postures permit depression of the acromion, which provides the superior limit of the SAS. Thus, depression of the acromion reduces SAS width from the superior aspect and may even interpose the subacromial tissues including the RC tendons, the long-head biceps tendon, and the subacromial bursa.

Alternatively, the subacromial tissues and space can also be interposed by elevation of the humeral head which makes up the inferior limit of the SAS [Steenbrink, et al., 2006; Chopp and Dickerson, 2012; de Witte, et al., 2014; Overbeek, et al., 2018]. The humeral head position is stabilized compressively into the glenoid fossa by the RC muscles [Steenbrink, et al., 2006; Chopp and Dickerson, 2012; de Witte, et al., 2014; Overbeek, et al., 2018]. However, fatigue or weakness of the RC muscles may decrease their force-generating capacity and the resulting compressive force [Lewis, Green, and Wright, 2005; Steenbrink, et al., 2006; Myers, et al., 2009; de Witte, et al., 2014; Overbeek, et al., 2018]. Research has identified that the deltoid muscle exhibits large anterior shear forces on the glenohumeral joint, particularly at low levels of arm elevation as the resultant force vector of the deltoid pulls almost entirely vertical [Steenbrink, et al., 2006; de Witte, et al., 2014; Overbeek, et al., 2018]. As the arm elevates, the moment arm of the deltoid becomes more efficient and the superior shearing force on the glenohumeral joint may diminish [de Witte, et al., 2014]. However, static poses of arm elevation will maintain a consistent shearing force opposing the compressive force of the RC muscles, and research has indicated that these static postures provide a potent fatigue stimulus for the RC muscles [Sood, Nussbaum, and Hager, 2007; Grieve and Dickerson, 2008; McDonald, Tse, and

Keir, 2016; Sood, et al., 2017; Fewster and Dickerson, 2021]. Thus, static elevated arm postures pose a risk for promoting both mechanisms of SAS width reduction due to muscle fatigue, which may have important implications for many overhead occupational tasks.

2.5. Motivation for Dissertation

Neuromuscular fatigue-related variability of scapular kinematics have been extensively reported. A thorough understanding of factors that preclude this variability may reveal insights on shoulder muscle control that would permit inferences on neuromuscular fatigue compensation mechanisms, kinematic shoulder patterns that are determinant of shoulder muscle activity patterns, and associated injury mechanics.

To address these aims, the following chapters describe a transdisciplinary compendium of research studies blending gold-standard motion capture and EMG methodologies with novel techniques in signal processing, biomechanical modelling, and ultrasonography to target current gaps in literature.

Chapter 3 will use new methods in EMG signal processing designed to control for fatigue-related changes in EMG RMS amplitude which are expected to be unpredictable in a redundant system like the shoulder. These methods will permit an investigation into shoulder muscle coactivation patterns associated with a fatigue-workplace task to identify occupational risk factors for SAIS and RC tear. This will also set a foundation for chapter 4, which will feature participants returning to complete the same occupational fatigue task. This chapter will investigate how fatigue exposures drive a consolidation or 'learning' of task parameters to achieve more efficiency, and how variability may influence the ability to learn a task.

Chapter 5 reports on the validation and application of a new optimal control formulation harnessed with a comprehensive computational mechanistic shoulder model to identify muscle compensation mechanisms associated with muscle weakness or fatigue. Due to the variability in shoulder fatigue responses, many studies report challenges in isolating fatigue of a single scapular muscle [Chopp-Hurley, et al., 2016; Chopp-Hurley and Dickerson, 2015; Ebata 2012; Ebaugh, McClure, and Karduna, 2006; Emery and Cote, 2012; Fuller, et al., 2009; Metwali 2019]. Modelling methods allow the user to simulate isolated muscle weakness and probe the deterministic effects on kinematics.

Chapter 6 concludes this dissertation by exploring the ability of SWV to predict fatigue state. Ultrasonographic SWV methods are relatively novel and methods for quantifying fatigue have only been reported in a few studies [Agten, et al., 2017; Andonia, et al., 2016; Siracusa, et al., 2019; Vatovec, Ziga, and Voglar, 2022; Vanhaezebrouck 2021] . This chapter represents the first comprehensive scapular stabilizer fatigue analysis using SWV, and investigates how SWV measures may be important for future studies quantifying muscle fatigue in a redundant muscular system.

Chapter 3. Muscle Coactivation Changes Following a Fatiguing Overhead Task: Implications for Subacromial Impingement Syndrome.

Matthew S. Russell, Sam S. Vasilounis, Emily Lefebvre, Janessa D.M. Drake, Jaclyn N. Chopp-Hurley

School of Kinesiology and Health Science, York University, Toronto, Canada

Corresponding Author:
Jaclyn Hurley, PhD
School of Kinesiology and Health Science
York University
4700 Keele Street, Toronto, Ontario, CA, M3J 1P3
Phone: (416) 736-2100 x 22137
Email: jnhurley@yorku.ca

Declarations of Interest: None

Funding Sources: This work was supported by the Centre of Research Expertise for the Prevention of Musculoskeletal Disorders (CRE MSD) seed grant program (J.N. Chopp-Hurley) and the Ontario Graduate Scholarship program (M.S. Russell).

3.1. Introduction

Shoulder motion and stability is achieved through the coordination of multiple joints. Individuals with SAIS of the shoulder display distinct kinematic differences, and muscle control and coordination imbalances compared to healthy populations [Ludewig and Cook, 2000; Ludewig and Cook, 2002; Cools, et al., 2007; Michener, et al., 2016]. The RC muscles are key contributors to glenohumeral joint stability; acting to compress the humerus into the glenoid cavity in effort to reduce the upward shearing force of the deltoid [Poppen and Walker, 1978; Graichen, et al., 2000; Michener, McClure, and Karduna, 2003]. Reduced force generating capacity of the RC muscles due to fatigue or injury demonstrably leads to superior translation of the humeral head and subsequent narrowing of the SAS and potential impingement of the interposed tissues. The trapezius and serratus anterior have been implicated as key stabilizer muscles of the scapulothoracic joint [Mottram, 1997; Kibler, 1998]. Disrupted balance of co-contraction among the scapular stabilizer muscles, rather than muscle weakness, has been implicated in dyskinesis [Cools, et al., 2007; Szucs, Navalgund, and Borstad, 2009; Kibler, et al., 2013]. Specifically, pathological scapular muscle coactivity demonstrates a dominance in upper trapezius EMG amplitude relative to the middle trapezius, lower trapezius, and serratus anterior muscles [Ludewig, et al., 2004; Cools, et al., 2007; Szucs, Navalgund, and Borstad, 2009]. Thus, this relative imbalance in scapular muscle activity may lead to damaging kinematics in the context of SAIS risk [Ebaugh, McClure, and Karduna, 2006; Cools, et al., 2007; Szucs, Navalgund, and Borstad, 2009], such that the scapula displays more downward rotation, anterior tilting, and internal rotation [Ludewig and Cook, 2000; Ebaugh, McClure, and Karduna, 2006; Kibler, et al., 2013]. These scapular kinematics reduce the SAS, posing risk for SAIS and RC tears [Chopp, Fischer, and Dickerson, 2011; Chopp-Hurley and Dickerson, 2015; Giuseppe, et al., 2020]. While SAIS and RC tears have been associated with scapular dyskinesis, the effect of muscle fatigue on scapular kinematics is less clear, with previous research reporting extensive interpersonal variability [Chopp, Fischer, and Dickerson, 2011; Chopp-Hurley and Dickerson, 2015; Chopp-Hurley, et al., 2016; Mulla, McDonald, and Keir, 2018].

Some research has suggested that fatigue of the scapular and shoulder muscles in healthy individuals with no history of clinical shoulder conditions can induce transient alterations to scapular coactivation which are indicative of SAIS. One study previously reported an increase in upper trapezius and a decrease in lower trapezius and serratus anterior normalized EMG amplitude following fatigue; thus demonstrating that healthy, fatigued participants can exhibit a comparable increased dominance in upper trapezius to individuals with SAIS and RC tear [Szucs, Navalgund, and Borstad, 2009]. Contradictory to these findings, however, other studies investigating global upper limb fatigue tasks have shown fatigue-induced scapular orientation changes that act to widen the SAS (upward rotation, posterior tilt, external rotation), thereby reducing the risk of SAIS and RC tear [McQuade, Dawson, and Smidt, 1998; Ebaugh, McClure, and Karduna, 2006; Giuseppe, et al., 2020]. Emergent evidence now suggests that therapeutic attempts to resolve symptoms of scapular dyskinesis, SAIS, and/or RC tears should include exercises that promote balanced scapular muscle activity throughout the ROM [Cools, et al., 2002; Cools, et al., 2007; McClure, Greenberg, and Kareha, 2012]. Specifically, exercises which target an increased recruitment of lower trapezius and serratus anterior may be a more effective intervention strategy for reducing SAIS and RC tear risk and symptoms rather than targeting an improvement in global scapular muscle force-generating capacity or fatigue-resistance [Ludewig, et al., 2004; Lewis, Green, and Wright, 2005; Cools, et al., 2007; Michener, et al., 2016].

Overhead tasks (>90° arm elevation) are common in laborious occupations and produce increased shoulder muscle activity (quantified with EMG), increased shoulder and elbow joint moments, and increases in the resulting joint forces of the shoulder and arm, subsequently hastening the time-course for localized muscle fatigue development [Herberts, Kadefors, and Broman, 1980; Punnett, et al., 2000; Anton, et al., 2001; Grieve and Dickerson, 2008]. These postures have been highly studied in the context of understanding upper limb fatigue and consequent injury risk [Grieve and Dickerson, 2008; Dickerson, McDonald, and Chopp-Hurley, 2020]. Overhead postures often elicit elevated levels of scapular and RC muscle EMG amplitude, which leads to fatigue of these muscle groups [Sood, Nussbaum, and Hager, 2007; Grieve and Dickerson, 2008; Myers, et al., 2009; Chopp, Fischer, and Dickerson, 2010; Maciukiewicz, et al., 2016; Sood, et al., 2017]. Neuromuscular and kinematic alterations, consequent to overhead postures and related muscle fatigue, can be associated with an increased risk of SAIS [Chopp-Hurley, et al., 2016; Maciukiewicz, et al., 2016]. The variability of muscle control and kinematics related to upper limb fatigue, and the evidence surrounding the importance of scapular and glenohumeral muscle balance, warrants investigating the effects of fatigue on muscle synergies in the shoulder.

The objectives of this study were to (1) examine whether changes in shoulder muscle coactivation and associated upper limb kinematics changes following an occupationally relevant overhead muscle fatigue task targeting the shoulder, upper limb, and trunk, would reflect the altered patterns previously shown in those with SAIS and RC tears, and (2) determine whether fatigue-induced changes in scapular stabilizer muscle coactivation explain variance in scapulothoracic kinematics. This study also evaluated (3) whether an overhead fatiguing task yielded reductions in force-generating capacity and muscle-specific myoelectric responses indicative of fatigue. It was hypothesized that muscle coactivation ratios and upper limb kinematics following fatigue would be comparable to those demonstrated by clinical SAIS and RC tear populations, whereby muscle coactivation ratios will indicate an increase in upper trapezius dominance, and scapulothoracic kinematics will show increased anterior tilt, downward rotation, and internal rotation [Ludewig, et al., 2004; Steenbrink, et al., 2006; Cools, et al., 2007; Myers, et al., 2009; Szucs, Navalgund, and Borstad, 2009; de Witte, et al., 2012; de Witte, et al., 2014; Michener, et al., 2016]. Further, it was expected that the ratio of normalized upper trapezius EMG amplitude relative to the middle trapezius, lower trapezius, and serratus anterior would explain variance in scapulothoracic kinematics, such that an increase in coactivation would be related to a reduction in scapulothoracic upward rotation, posterior tilt, and external rotation.

3.2. Methods

This chapter reports data collected over a single 3-hour testing session. Ancillary to this study, 30 of the original 34 participants (15 male, 14 female) returned for a second identical follow-up collection, exactly 7 days after their first collection. Data comparing day-to-day changes in fatigue-related kinematic, kinetic, and muscle responses and variability within, and between successive days of the identical overhead drilling task will be presented in chapter 4.

3.2.1. Participant Demographics

34 right-handed participants (17 male, 17 female) were initially recruited for a single 3-hour long collection. Due to technical issues, the data from one female participant was unable to be analyzed, thus the final participant population

included 17 males (24.9yr ± 4.3, 24.4kg/m2 ± 2.9) and 16 females (23.2 ± 3.8 yr, 22.0 ± 2.8 kg/m2). A two-tailed t-test (α=0.05) using previously reported scapular stabilizer co-activity ratios of overhead athletes with and without shoulder pain [Cools, et al., 2007] determined that ≤ 25 participants were needed to achieve 80% power for analysis of scapular muscle coactivity changes . Participants were excluded if they reported working in an occupation with frequent overhead work demands (within the past year), had pain or lifestyle factors indicative of arm or trunk disability, or psychological factors that reflect an avoidance of movement, exertion, or discomfort. Pain and lifestyle factors were assessed using the Disabilities of the Arm, Shoulder, and Hand (DASH) questionnaire and the Oswestry Low Back Pain Disability questionnaire with inclusion cutoff scores of 25 and 20, respectively [Alcántara-Bumbiedro, et al., 2006]. Psychological factors were assessed using the Fear Avoidance Beliefs questionnaire subscales for physical activity and work with inclusion cutoffs of 11 and 18 respectively [Williamson, 2006], as well as the Tampa Scale for Kinesiophobia (TSK) with an inclusion cutoff of 22 [Chimenti, et al., 2021]. Participants were also excluded if they reported discomfort with needles, blood clotting disorders or currently taking blood thinning medications, HIV, Hepatitis B or C, diabetes, or respiratory conditions (Asthma, COPD, etc), allergies to isopropyl alcohol, betadine, latex, or nickel, or were pregnant. This study received ethics approval from the York University Office of Research Ethics (#e2021-395). All participants provided written informed consent.

3.2.2 Data Acquisition

3.2.2.1 Electromyography

Muscle activity recorded from 7 muscles of the shoulder using surface electromyography (sEMG) were included in the analysis of this study: supraspinatus, infraspinatus, upper trapezius, middle trapezius, lower trapezius, serratus anterior, and middle deltoid. While previous research has observed significant, moderate strength linear relationships between surface and intramuscular EMG amplitude from the RC muscles, limitations exist in the confidence of current RC muscle sEMG placements when the arm is oriented overhead and when the RC muscles are not the primary agonists [Allen, et al., 2013; Cudlip and Dickerson, 2018; Cudlip, Kim, and Dickerson, 2020]. Thus, an additional 2 channels of intramuscular EMG (iEMG) were collected from the supraspinatus and infraspinatus. EMG was collected using a Delsys Trigno system (Delsys Inc., 23 Strathmore Rd, Natick, MA, USA). To collect sEMG, Trigno Avanti sensors were placed over the muscle belly of the muscle of interest using published guidelines [Stegeman, et al., 2000; Waite, Brookham, and Dickerson, 2010], with 10 mm spaced silver (99.99%) bar electrodes oriented in the direction of the muscle fibers. For muscles monitored using both sEMG and iEMG (supraspinatus, infraspinus), two Ambu® Bluesensor N single use surface electrodes (Kego Corporation, London, ON) were affixed to the skin bilaterally of the iEMG insertion site, oriented in the direction of the muscle fibers, and connected to Trigno Snap-Lead adapters. Ambu® Bluesensor N single use surface electrodes provided the ability to more accurately orient the bipolar electrode pair on either side of the intramuscular insertion point. sEMG was sampled at 2148 Hz, with a 20-450 Hz bandwidth. Intramuscular insertions were localized to the muscle belly of interest following published guidelines [Geiringer, 1999; Perotto, 2011]. For each muscle, a 30 mm, 44-gauge stainless surgical steel hypodermic needle housing two barbed 304 series stainless steel wires (0.051 mm diameter, 200 mm length, nylon coating) (Motion Lab Systems Inc., 15045 Old Hammond Way, Baton Rouge, LA, USA) was administered. Intramuscular fine-wires were connected to a Delsys Trigno Spring Contact sensor, with iEMG sampled at 4370 Hz with a 10-2000 Hz pass band.

3.2.2.2 Kinematics

Kinematics of the thorax, right scapula, and right upper limb were collected using a 7-MX40+ camera Vicon system (Vicon Motion Systems Ltd., 7388 S. Revere Pkwy, CO, USA) at 100 Hz sampling rate. 19mm diameters reflective Vicon pearl markers were affixed to 14 bony landmarks of the upper limb (trunk, upper arm, lower arm, hand) following International Society of Biomechanics recommendations (Wu, Van der Helm et al. 2005). Rigid clusters were affixed to the forearm and upper arm, and a scapular tracking cluster was placed at the junction of the acromion and the lateral aspect of the scapular spine (Shaheen, Alexander et al. 2011).

3.2.2.3 Muscle Reference Testing

A series of 5-second shoulder and upper limb exertion tests [Boettcher, Ginn, and Cathers, 2008; Ginn, Halaki, and Cathers, 2011; McDonald, Sonne, and Keir, 2017] were used to examine muscle activity changes and normalize muscle activity [McDonald, et al., 2018] (table 3.1.). All exertions were manually resisted by a research assistant and force recorded using an ErgoFET push-pull force gauge (Hoggan Scientific, Salt Lake City, UT, USA). Prior to beginning the overhead drilling shoulder fatigue protocol, participants performed two repetitions of a series of maximal voluntary exertions (MVE) in a random order (three of these tests were used in the analysis of the current research) (table 3.1.) [McDonald, Sonne, and Keir, 2017]. The participants also performed one set of the MVE tests at 30% submaximal intensity (SVE) of the peak muscle test force, prior to beginning the overhead drilling shoulder fatigue protocol and after every 15 cycles of the fatigue protocol. This permitted the implementation of a time-varying normalization technique of EMG data to enable comparisons of RMS activity throughout the accumulation of fatigue while controlling for the fatigue-related effects on the EMG signal [McDonald, et al., 2018]. MVE trials were only used to scale SVE trials to 30% of their maximal voluntary exertion, and SVE trials were used to calculate muscle-specific EMG MPF and to enable time-varying EMG amplitude normalization (Section 2.4.2).

Two repetitions of maximal shoulder abduction and adduction exertions (MRE) were performed at 90° shoulder elevation and 90° internal rotation in the scapular plane. MREs were performed before and immediately after the overhead drilling shoulder fatigue protocol and presented in random order. As well, submaximal exertions at 15% of the peak maximal abduction and adduction forces (SRE) were performed in the scapular plane at 30°, 60°, 90°, and 120° shoulder elevation before beginning the fatigue protocol, and after every 5 cycles (5 minutes) of the fatiguing protocol (table 3.1). MRE trials were used to scale SRE trials to 15% of their maximal reference exertion and to test for significant changes in maximal abduction and adduction force following fatigue. SRE trials were used to calculate scapular muscle coactivation ratios (Section 2.4.2).

Table 3.1. **Definition and application of manual muscle tests. Electromyography and force were captured for each exertion.**

Muscle Test	Definition	Purpose
Maximal Voluntary Exertion (MVE)	Muscle tests performed with maximum voluntary effort: empty can, external rotation, flexion 125, Two sets of each test were performed.	MVE tests were used to determine each participants' maximal force for each multi-muscle test (for SVEs). 30% of the peak force output across two sets of MVE tests was used to determine SVE target forces.

		MRE tests were not explicitly used for any statistical tests.
Submaximal Voluntary Exertion (SVE)	MVE exertions performed at 30% submaximal force. One set of each test was performed after every 15 cycles (15 minutes) of the fatigue protocol.	SVE tests were used to determine the time-varying change in EMG RMS associated with fatigue. Linear enveloped EMG was normalized to a maximal RMS voltage calculated from the percent increase in SVE tests throughout the fatigue protocol. During cycles where SVEs were not sampled, a cubic spline was used to interpolate RMS increase from baseline [McDonald et al., 2013]. SVE tests were also used to assess muscle-specific fatigue changes in MPF based on the muscle-test associations by McDonald et al. [2018] and Boettcher et al. [2008]. SVE tests were used to compare muscle-specific EMG MPF at pre-fatigue and post-fatigue (Objective #3).
Maximal Reference Exertion (MRE)	Shoulder abduction and adduction performed at maximal effort in the scapular plane (γ_h = 30°) at 90° shoulder elevation ($-\beta_h$) and 90° internal rotation ($\gamma^2{}_h$). Two sets of each test were performed both pre- and post-fatigue.	MRE tests were used to determine the change in maximal shoulder abduction and adduction force from pre-fatigue to post fatigue. 15% of the peak force output across two sets of MVE tests was used to determine SRE target forces. MRE tests were used to compare pre-fatigue and post-fatigue abduction and adduction force (Objective #3).
Submaximal Reference	MRE exertions performed at 15% submaximal force.	SRE tests were used to compare muscle activity and coactivity changes at different shoulder

Exertion (SRE)	Submaximal abduction and adduction exertions were performed in the scapular plane (γ_h = 30°) and 90° internal rotation (γ^2_h), at 30°, 60°, 90°, and 120° shoulder elevation ($-\beta_h$). One set of each test was performed after every 5 cycles (5 minutes) of the fatigue protocol.	elevation angles between the pre- and post-fatigue states, using the time-varying normalized SVE magnitudes from the same cycle (Objective #1). SRE tests were also used to compare the fatigue-related change in scapular muscle coactivation with scapulothoracic kinematics changes (Objective #2)

3.2.2.4 Subjective Rating of Global Fatigue

Subjective ratings of fatigue were assessed using the 10-point Rating of Perceived Exertion (RPE) scale [Borg, 1982]. Participants were asked to provide a number between 1-10 on the RPE scale after successfully completing every 5th round of the overhead drilling task. RPE ratings were acceptable at half-decimal (0.5) intervals.

3.2.3 Protocol

Following EMG instrumentation, participants completed a resting trial, two repetitions of each MVE test presented in random order, and then two repetitions of each MRE test presented in random order. Following maximal exertions, participants were instrumented with motion capture markers and performed static kinematic calibration trials. Participants then began the fatiguing task (Figure 3.1.).

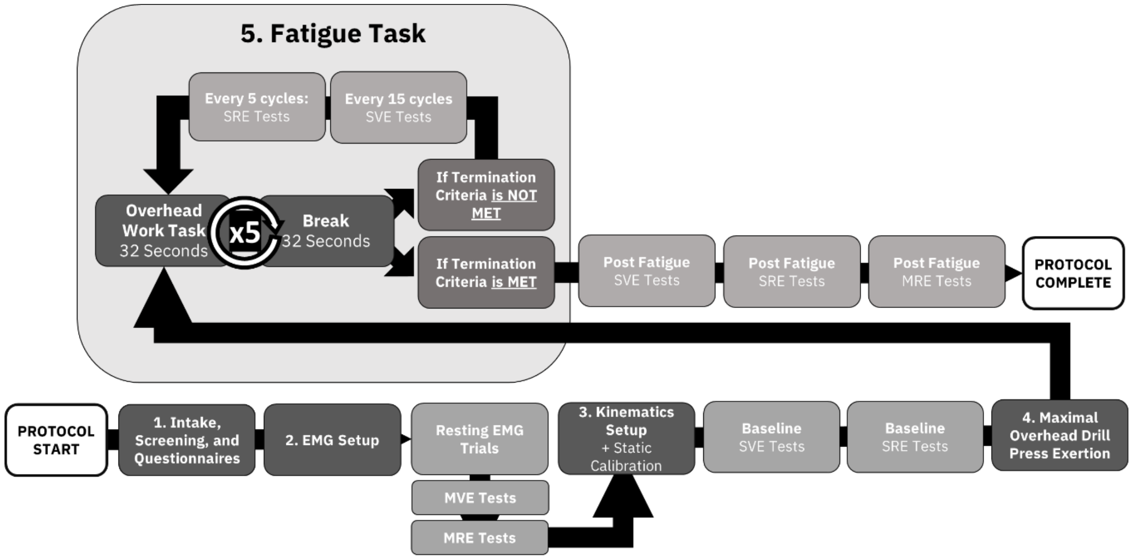

Figure 3.1. **Timeline of study protocol.**

The fatiguing task was a simulated, overhead drilling task designed based on a previously described protocol for inducing symptoms of occupational overhead fatigue [Sood, Nussbaum, and Hager, 2007; Maciukiewicz, et al., 2016; Sood, et al., 2017]. The overhead drilling task involved approximating the tip of a 2 kg drill to four overhead targets (table 3.2.; figure 3.2.). Targets were presented for 4 seconds, in a pseudorandom order such that each target was presented twice, for a total exertion time of 32 seconds. Prior to beginning the task, participants completed two maximal overhead exertions where they pressed a drill vertically in an arm posture of 90° elevation, 90° plane of elevation about the shoulder, and 90° flexion about the elbow to determine their maximum drill force. Participants were instructed to scale the force applied to the targets during the fatiguing task to 50% of their maximal overhead drill force (average of the peak force between two repetitions), as this force output threshold was shown to fatigue participants in 45 minutes on average [Sood, Nussbaum, and Hager, 2007; Maciukiewicz, et al., 2016; Sood, et al., 2017], and previous literature has determined that occupational fatigue tasks of similar or lower intensity precipitated decrements in strength and EMG MPF [Sood, Nussbaum, and Hager, 2007; Ebata, 2012; Metwali, 2019]. This force level was achieved using visual feedback provided by a live force-time trace shown on a 40-inch television, located 8 feet in front of the participant. Following the completion of a 32-second task (2 repetitions x 4 targets), the participant was given a 32-second rest period to achieve a 50% duty cycle. After every 5 cycles of overhead drilling, participants stopped the task and completed the SRE exertions (approximately 2 minutes to complete). Additionally, after completing 15 cycles of the overhead drilling task, participants completed both the SRE exertions and SVE exertions (approximately 5 minutes to complete). These breaks reduced the true duty cycle of the overhead drilling task to approximately 25-30%. Participants cycled between the overhead target task and the SRE/SVE testing until one of three completion criteria were met: 1) the participant reached RPE ≥ 9 and indicated they were unable to continue maintaining the 50% maximal overhead force level, 2) they were unable to generate 50% of their maximal overhead force in any of the target directions within the same cycle, 3) they completed 60 rounds of the overhead drilling task and maintained a stable RPE that was not increasing. Once a participant reached any of the completion criteria, they performed the SRE and SVE tests.

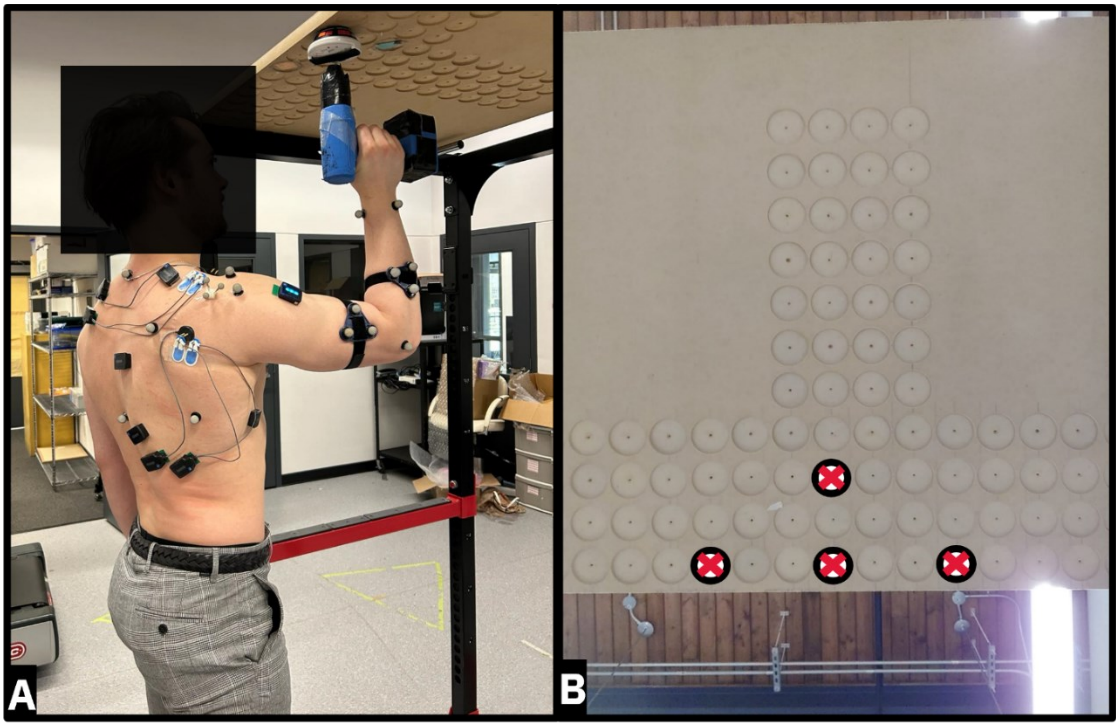

Figure 3.2. **Overhead drilling shoulder fatigue protocol target setup with kinematic markers**. **A:** parasagittal view. **B:** view of overhead targets.

Table 3.2. **Overhead drilling shoulder fatigue protocol target locations.**

Overhead Target Location	**Description**
Centre	70% distance from the greater trochanter to maximum overhead reach with 90° elbow flexion and 90° thoracohumeral plane of elevation
Far	70% distance from the greater trochanter to maximum overhead reach with 45° elbow flexion
Left	Shoulder plane of elevation increased to 125° from *centre* position
Right	Shoulder plane of elevation reduced to 45° from *centre* position

3.2.4 Data Analysis

3.2.4.1 Fatigue Confirmation

Peak MRE forces captured before (pre-fatigue) and immediately after completion of the overhead drilling task (post-fatigue) were compared to assess signs of global shoulder fatigue. Pre-fatigue and post-fatigue EMG data from SVE trials were dual-high-pass Butterworth filtered at 30Hz to remove ECG contamination, and then dual-low-pass Butterworth filtered at 500 Hz (sEMG) and 1000 Hz (iEMG) [Stulen and De Luca, 1981; Öberg, 1995; Hendrix, et al., 2010]. MPF was calculated from each 0.5-second epoch for the first 3 seconds of the 5-second SVE trial using a discrete Fourier transform with a rectangular window for each epoch, from which an overall mean was calculated [Hendrix, et al., 2010]. For each muscle, the MPF was analyzed for the SVE recommended for that particular muscle (empty can: supraspinatus; external rotation: infraspinatus; high flexion: upper trapezius, middle trapezius, lower trapezius, serratus anterior, anterior deltoid, middle deltoid) [Boettcher, Ginn, and Cathers, 2008; Ginn, Halaki, and Cathers, 2011; McDonald, Sonne, and Keir, 2017]. Consistent with previous literature [Öberg, 1995; Drake and Callaghan, 2006; Chopp, Fischer, and Dickerson, 2010; McDonald, Tse, and Keir, 2016], a ≥8% decrease in the average MPF of each muscle, as averaged across the study participant sample, was determined as a threshold for indicating groupwise muscle-specific fatigue.

3.2.4.2 Muscle Co-activation

Raw EMG were first decontaminated of ECG superimposition using a high-pass filter with 30 Hz cut off [Drake and Callaghan, 2006]. Surface and intramuscular signals were then full wave rectified and dual low-pass filtered with a 4 Hz cut-off. To permit time-varying EMG amplitude normalization, the average linear envelope amplitude from the middle 2 seconds (1.5-3.5 seconds) of each 5-second SVE trial were used as inputs into a least square cubic spline model to estimate changes in participant MVE RMS throughout the duration of the overhead drilling task [McDonald, et al., 2018]. The time-varying normalization of each muscle was used to adjust the SRE amplitude to enable comparisons of SRE trials at different stages of the muscle fatigue task without confounding outcomes with fatigue-related amplitude artifact. Normalized average SRE amplitude within a middle 2-second window of the 5-second contractions was then used to calculate coactivation ratios of the scapular stabilizer muscles (upper trapezius, middle trapezius, lower trapezius, serratus anterior) (equation 3.1.a) [Ludewig, et al., 2004; Cools, et al., 2007; Szucs, Navalgund, and Borstad, 2009; Michener, et al., 2016], and between the middle deltoid and RC muscles (supraspinatus and infraspinatus) (Equation 1b) [Myers, et al., 2009]. Coactivation ratios have been previously published to evaluate upper trapezius or middle deltoid muscle dominance relative to surrounding synergist muscles, whereby upper trapezius and middle deltoid dominance has been determined as clinically relevant for increased risk of SAIS due to abnormal scapular motion [Ludewig, et al., 2004; Cools, et al., 2007; Szucs, Navalgund, and Borstad, 2009; Michener, et al., 2016], or superior humeral head translation [Myers, et al., 2009]. Scapular stabilizer and middle deltoid:RC muscle coactivation ratios were calculated at both pre- and post-fatigue using published guidelines. Regarding EMG data of muscle coactivity, pre-fatigue was defined as the baseline submaximal SRE and SVE test taken before participants began the overhead drilling task. Post-fatigue was defined as the SRE and SVE tests taken immediately after completion of the overhead drilling task.

a. $i\colon\ UT\colon MT = UT/MT * 100$

$ii\colon\ UT\colon LT = UT/LT * 100$

$iii.\ UT\colon SA = UT/SA * 100$

b. $i\colon\ MD\colon sSS = MD/sSS * 100$

$ii\colon MD\colon iSS = MD/iSS * 100$

$iii\colon MD\colon sIS = MD/sIS * 100$

$iv\colon MD\colon iIS = MD/iIS * 100$

Equation 3.1. **Muscle Coactivation Calculations.** 1a. scapular stabilizer coactivation equations. Equations compared coactivity between the upper trapezius (UT) and each of middle trapezius (MT), lower trapezius (LT), and serratus anterior (SA). 1b. rotator cuff vs deltoid coactivation equations. Normalized supraspinatus (SS) and infraspinatus (IS) amplitude using both surface (sSS, sIS) and intramuscular (iSS, iIS) electrodes were compared to middle deltoid (MD) activity.

3.2.4.3 Upper Limb Kinematics

Upper limb joint position was assessed by comparing the scapulothoracic, thoracohumeral, elbow, and radiocarpal joint angles while the participant was approximating each of the four overhead targets (table 3.2.) during the pre-fatigue and post-fatigue states. Kinematics were captured during each 32-second cycle of the fatiguing task immediately preceding the SRE tests; that being the fifth overhead working cycle presented within each 5-cycle block. For the purposes of analyzing upper limb kinematics, pre-fatigue joint angles were characterized from the fifth 32-second working cycle presented in the fatigue protocol, to provide all participants with 4 working cycles of task familiarization. Post-fatigue joint angles were characterized as the very final 32-second cycle that participants completed before failure. Post-fatigue cycles were often the fifth and final 32-second work cycle presented within a 5-cycle work block for participants who reached termination criteria 1 (volitional fatigue: RPE ≥ 9 and unable to continue), or the fourth 32-second cycle within a back-to-back cycle of 5 working cycles for participants who reached termination criteria 2 (vertical drill force unable to achieve 50% MVE). For each joint angle assessment, three-dimensional local coordinate systems (LCS) were defined for the thorax, scapula, humerus, forearm, and hand based on coordinate definitions outlined by the International Society of Biomechanics [Wu and Cavanagh, 1995; Wu, et al., 2005]. LCS were also defined for each of the rigid clusters and the scapula tracking cluster. Relative rotation matrices were created between the clusters and anatomical markers. Euler angles were calculated from reconstructed virtual landmarks using the recommended joint angle decomposition sequences [Shaheen, Alexander, and Bull, 2011].

3.2.5 Statistical Analysis

Outliers two standard deviations above or below the mean were removed from both EMG and kinematic data. Due to the repeated measures design, if a data point was removed, the associated pairwise score was removed as well [Miller, 1991]. To evaluate changes in muscle coactivation following an overhead drilling task to failure (Objective #1), two-way repeated measures analysis of variance (ANOVA) models were used to assess the effects of fatigue (pre-fatigue, post-fatigue) and shoulder elevation (30, 60, 90, and 120 degrees elevation in the scapular plane) on (1) average normalized muscle coactivation coefficients for scapular coactivation ratios (UT:MT, UT:LT, and UT:SA) (Equation 3. 1.a), and (2) middle deltoid:rotator cuff coactivation ratios (MD:sSS, MD:iSS, MD:sIS, and MD:iIS) (Equation 1b), calculated from SRE tests (table 3.1.). Separate ANOVA models were calculated for both abduction and adduction isometric exertion directions. Further, to evaluate changes in scapulothoracic and upper limb kinematics associated with completing an overhead drilling task until failure (Objective #1), two-way repeated measures ANOVAs were used to determine the effect of fatigue (pre-fatigue, post-fatigue) and target location (close, far, right, left) on scapulothoracic (anterior/posterior tilt, upward rotation/downward rotation, internal/external rotation), thoracohumeral (plane of elevation, elevation, axial rotation), elbow (flexion/extension, axial rotation, carrying angle), wrist (flexion/extension, ulnar/radial deviation, pronation/supination) joint angles. Pairwise comparisons for all repeated measures ANOVA models used Sidak adjustment for multiple comparisons.

Multivariate linear regression models were used to determine whether fatigue-induced changes in scapular muscle co-activation ratios (post – pre co-activation) explained a significant amount of variance in scapulothoracic joint angles (post – pre joint angles) (Objective #2). The difference between pre- and post-fatigue scapular coactivation coefficient (UT:MT, UT:LT, and UT:SA), calculated from the SRE tests (equation 3.1.a.; table 3.1.) were predictor variables (e.g. post-fatigue UT:MT minus pre-fatigue UT:MT), and scapulothoracic joint angle changes from pre-fatigue to post-fatigue at each target location were the dependent variables. Twelve separate regression models were created for each scapulothoracic joint angle (anterior/posterior tilt, upward rotation/downward rotation, internal/external rotation) for each target location respectively (close, far, right, left) with all three predictor variables.

To evaluate whether the overhead drilling fatigue protocol elicited global and muscle-specific fatigue among our sample of participants (Objective #3), (1) paired two-sided T tests were used to compare pre- and post-fatigue shoulder abduction and adduction MRE forces [McDonald, Tse, and Keir, 2016; Tse, McDonald, and Keir, 2016; McDonald, et al., 2018], and (2) reduction of 8% or more in EMG MPF of each muscle from pre- to post-fatigue SVE was used as the criterion to confirm that the overhead drilling protocol induced muscle-specific fatigue [Stulen and De Luca, 1981; Öberg, 1995; Zabihhosseinian, Holmes, and Murphy, 2015; Zabihhosseinian, et al., 2019]. Previous overhead drilling studies have used similar methods to determine the presence of global and muscle-specific fatigue [Stulen and De Luca, 1981; McDonald, Tse, and Keir, 2016; Tse, McDonald, and Keir, 2016; McDonald, et al., 2018]. All EMG and kinematic data processing was performed using custom Matlab software (Mathworks, Natick, MA). All statistical analyses were performed using the Statistical Package for the Social Sciences (SPSS), version 28.0 (IBM Corp. Armonk, NY, USA).

3.3. Results

3.3.1. Fatigue Verification

The mean number of cycles to fatigue protocol termination was 27.5 cycles (male = 30 cycles/ ~28 min, female = 25 cycles/ ~24 min), with a range of 15-50 cycles to fatigue (16-53 minutes) for males, and 15-60 cycles to fatigue (16 to 64 minutes) for females. The most common protocol termination criterion was an RPE ≥ 9, while verbally indicating that they could no longer continue the task (n = 19). Most of the remaining participants reached protocol termination when they were unable to maintain the 50% target force output for at least one target within a cycle (n =13). Two participants reached the termination criteria by completing 60 cycles of the task with the desired force output while displaying an RPE < 9 (table 3.3.).

Participants exhibited a significant 13.3% decrease in MRE abduction force from pre-fatigue (106.1 (35.3) N) to post-fatigue (91.9 (33) N) ($t_{(32)} = 4.91$, $p < 0.0001$). MRE adduction force was not significantly different between fatigue states ($t_{(32)}$ = -0.94, p = 0.36). A decrease in average supraspinatus iEMG MPF of 8.3% was observed from 144.6 (28.8) Hz to 132.1 (26.9) Hz. No other EMG channels displayed mean decrease in MPF > 8%. However, participants demonstrated considerable interindividual (between participant) variability in which muscles showed myoelectric signs of fatigue (table 3.4.).

Table 3.3. **Distribution of termination criteria (subdivided by sex) that were met to complete the fatigue protocol.** *Termination criteria as follows:* RPE[1] - participant reached RPE ≥ 9 and indicated they were unable to continue maintain 50% max upward force, Force[2] - participant unable to generate 50% of their maximal overhead force in any of the target directions within the same cycle, Max[3] - participant completed 60 rounds of the fatigue protocol while maintaining a stable RPE.

Termination Criteria	**RPE[1]**	**Force[2]**	**Max[3]**
Males	10/17 (58.8%)	6/17 (35.3%)	1/17 (5.9%)
Females	9/17 (52.9%)	7/17 (41.1%)	1/17 (5.9%)

Table 3.4. **Number of participants showing a reduction in mean power frequency (MPF) from the pre-fatigue to post-fatigue state, and the interindividual range of MPF differences for each muscle.**

Muscle	Number (n) and percentage of participants (%) with ≥8% reduction in MPF	Range of interindividual MPF increase to interindividual MPF decrease
Supraspinatus (surface)	n= 2 (6%)	18.7% to -19.0 %
Supraspinatus (wire)	n= 8 (24%)	15.5% to -30.7%
Infraspinatus (surface)	n= 7 (21%)	22.3% to -22.7%
Infraspinatus (wire)	n= 6 (18%)	62% to -35.2%
Upper trapezius	n= 6 (18%)	30.7% to -20.3%
Middle trapezius	n= 2 (6%)	35.2% to -20.8%
Lower trapezius	n= 6 (18%)	18.5% to -24.4%
Serratus anterior	n= 10 (29%)	38.9% to -33.6%
Middle deltoid	n= 6 (18%)	22.7% to -21.6%

3.3.2. Muscle co-activation

No interaction effects between fatigue and arm elevation were revealed for any of the co-activation ratios examined. For scapular coactivation, no fatigue main effect was shown for any of the co-activation ratios (UT:MT, UT:LT, and

UT:SA) for either abduction or adduction. The UT:LT ANOVA model found a significant main effect of shoulder elevation angle on muscle coactivation during adduction ($F_{(3\ 81)} = 9.08$, $p > 0.001$), with co-activity increasing with elevation angle (figure 3.3.).

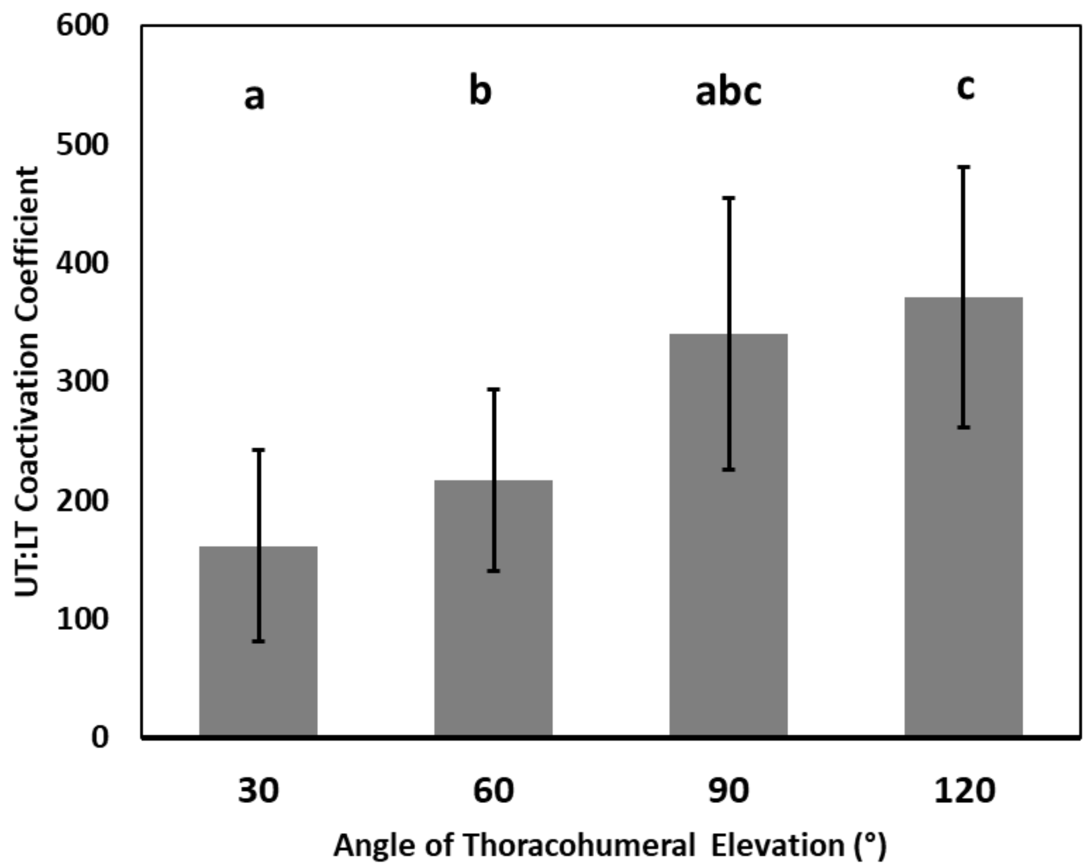

Figure 3.3. **UT:LT coactivation coefficient during adduction at different elevation angles.** Group means with the same letter indicate no significant difference at $p \leq 0.05$.

A significant main effect of angle was present for MD:sSS coactivation ($F_{(3,75)} = 5.66$, $p = 0.002$) during shoulder adduction (figure 3.4.A). A significant main effect of both angle ($F_{(3,84)} = 4.58$, $p = 0.020$; figure 3.4.C) and fatigue ($F_{(1,28)} = 6.44$, $p = 0.017$; figure 3.4.C) was present for MD:sIS coactivation during shoulder adduction. Similar findings were shown for iSS and iIS data, however these models did not reach significance.

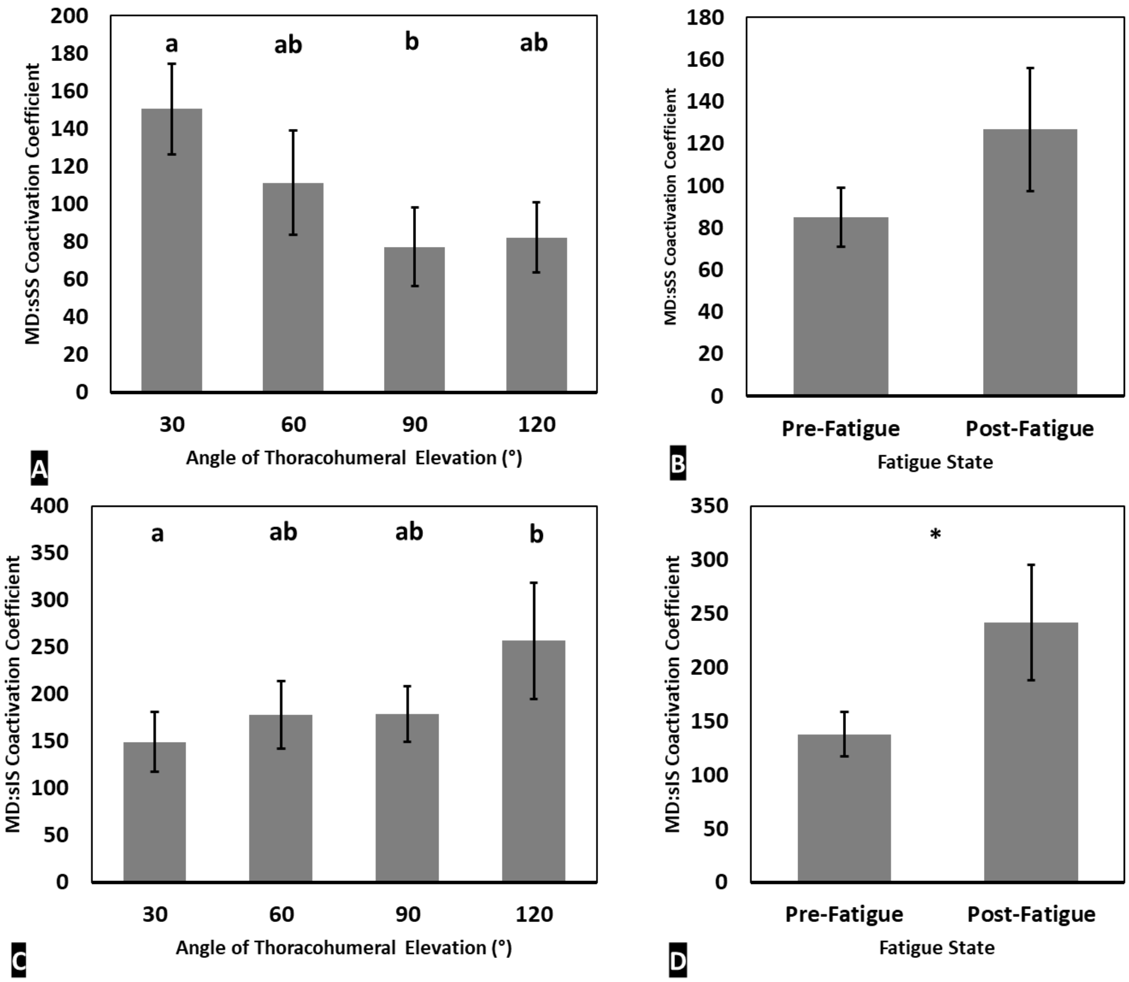

Figure 3.4. **Middle deltoid:supraspinatus (A and B) and middle deltoid:infraspinatus (C and D) (sEMG) coactivation coefficients.** Asterisks indicate significance at $p \leq 0.05$. Group means with the same letter indicate no significant difference at $p \leq 0.05$.

3.3.3. Upper Limb Kinematics

No interaction effects between fatigue and overhead target location were observed to affect upper limb kinematics. Significant fatigue effects were present for scapulothoracic, thoracohumeral plane of elevation, thoracohumeral elevation and elbow flexion when approximating certain targets (figure 3.5.). No significant effects were observed for the wrist kinematic joint angles.

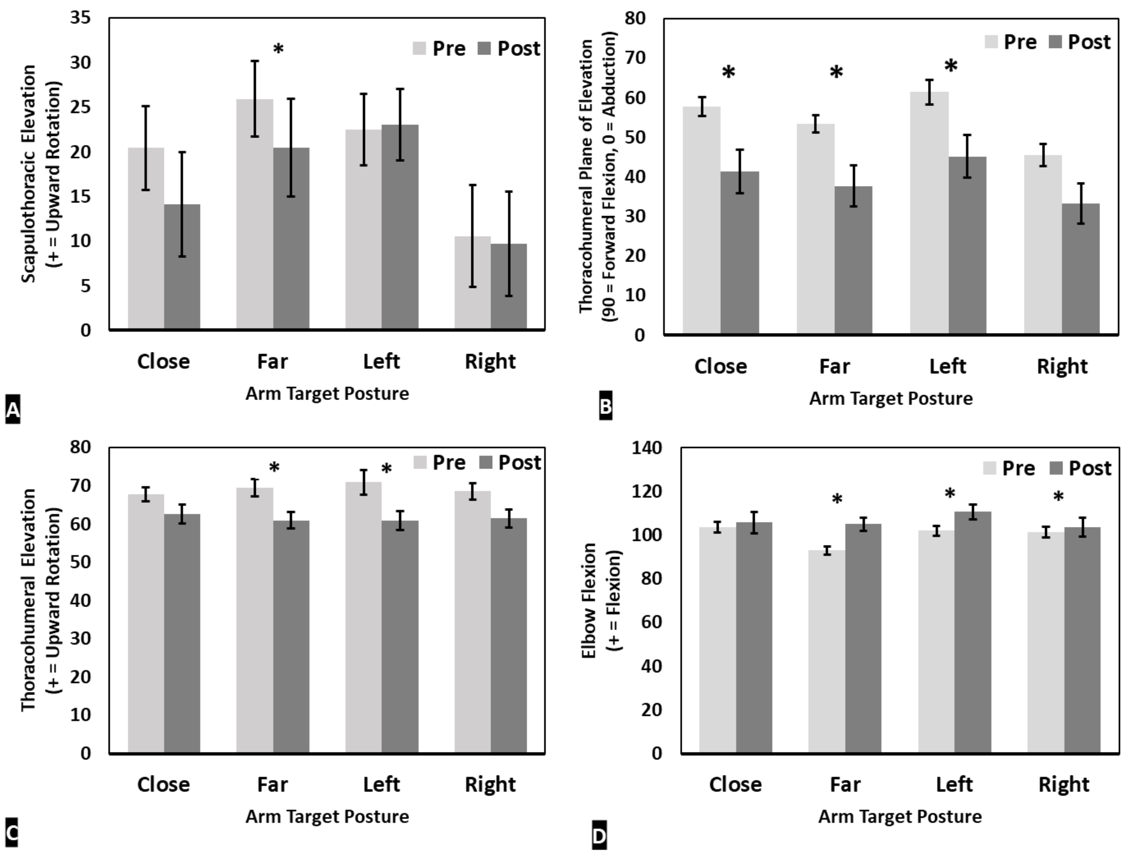

Figure 3.5. **Joint angle changes during overhead drilling task at all four target postures**. **A.** Scapulothoracic downward rotation (βs) **B.** Thoracohumeral plane of elevation (γ_h) **C.** Thoracohumeral negative elevation (β_h), **D.** Elbow flexion (α_{HF}). Asterisks indicate significance at $p \leq 0.05$.

3.3.4. Relationship between Scapular Coactivation and Scapular Kinematics

The fatigue-mediated change in UT:LT coactivation was also shown to be a significant predictor of scapulothoracic upward/downward rotation when approximating the *far* overhead target ($R_2 = 0.25$, $F_{(3,25)} = 3.56$, $p = 0.002$). Specifically, an increase in UT:LT coactivation was related to a fatigue-related increase in downward scapular rotation ($\beta = 0.068$) (figure 3.6.A). Further, the model for scapulothoracic internal rotation was significant when approximating the *left* overhead target ($R^2 = 0.29$, $F_{(3,21)} = 2.88$, $p = 0.009$), with a fatigue-induced increase in UT:SA shown to be a significant predictor of increased internal scapular rotation ($\beta = 0.033$) (figure 3.6.B).

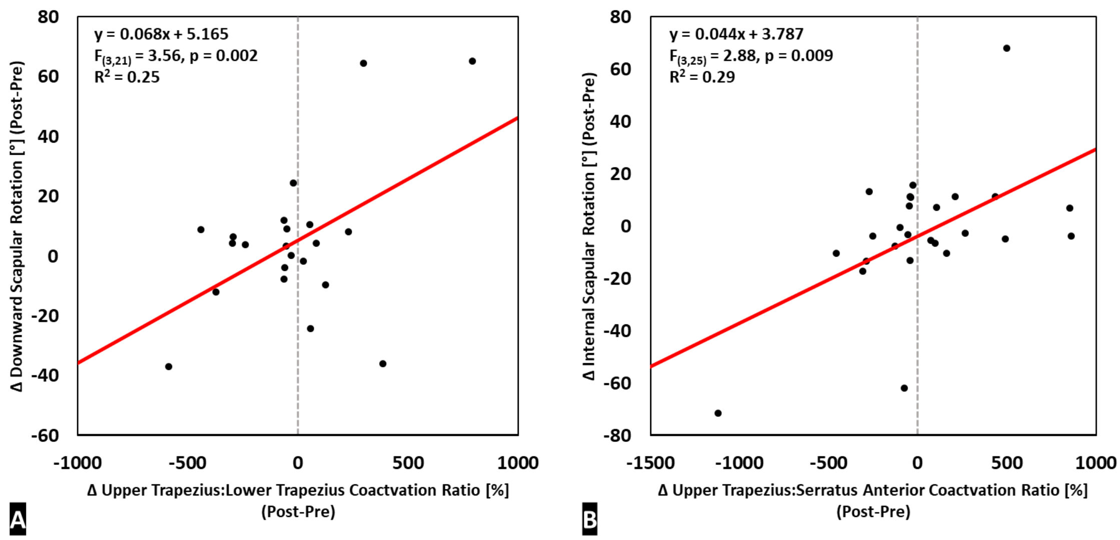

Figure 3.6. **Significant bivariate linear regressions between the fatigue-mediated change in scapular kinematics and the fatigue mediated change in the scapular stabilizer coactivation coefficients (equation 3.1.b.).**

3.3.5. Variability Among Measures of Muscle Coactivation and Kinematics

Participant-specific changes in co-activity were calculated to assess the proportion of participants displaying changes in scapular co-activity (increased UT:MT, UT:LT, UT:SA) and scapulothoracic kinematics (increased downward rotation, anterior tilt, internal rotation) which characterize SAIS risk. This post hoc analysis revealed that approximately half of participants displayed fatigue-mediated changes in scapular co-activation for all three ratios which could be considered disadvantageous for SAS width and SAIS risk (figure 3.7.). Similar findings were shown for scapulothoracic kinematics with a large proportion of participants showing potentially disadvantageous fatigue-induced changes that would narrow the SAS by rotating the acromion inferiorly (Watson, Balster et al. 2005, Ebaugh, McClure et al. 2006, McClure, Greenberg et al. 2012). Specifically, approximately half of participants displayed fatigue-induced scapular downward rotation and anterior tilting, while approximately 20-40% displayed scapular internal rotation (figure 3.8.). This analysis revealed that many of the potentially disadvantageous changes in kinematics could be considered clinically meaningful ($\Delta > 5°$) [Ebaugh et al., 2005; Watson et al., 2005; McClure et al., 2012].

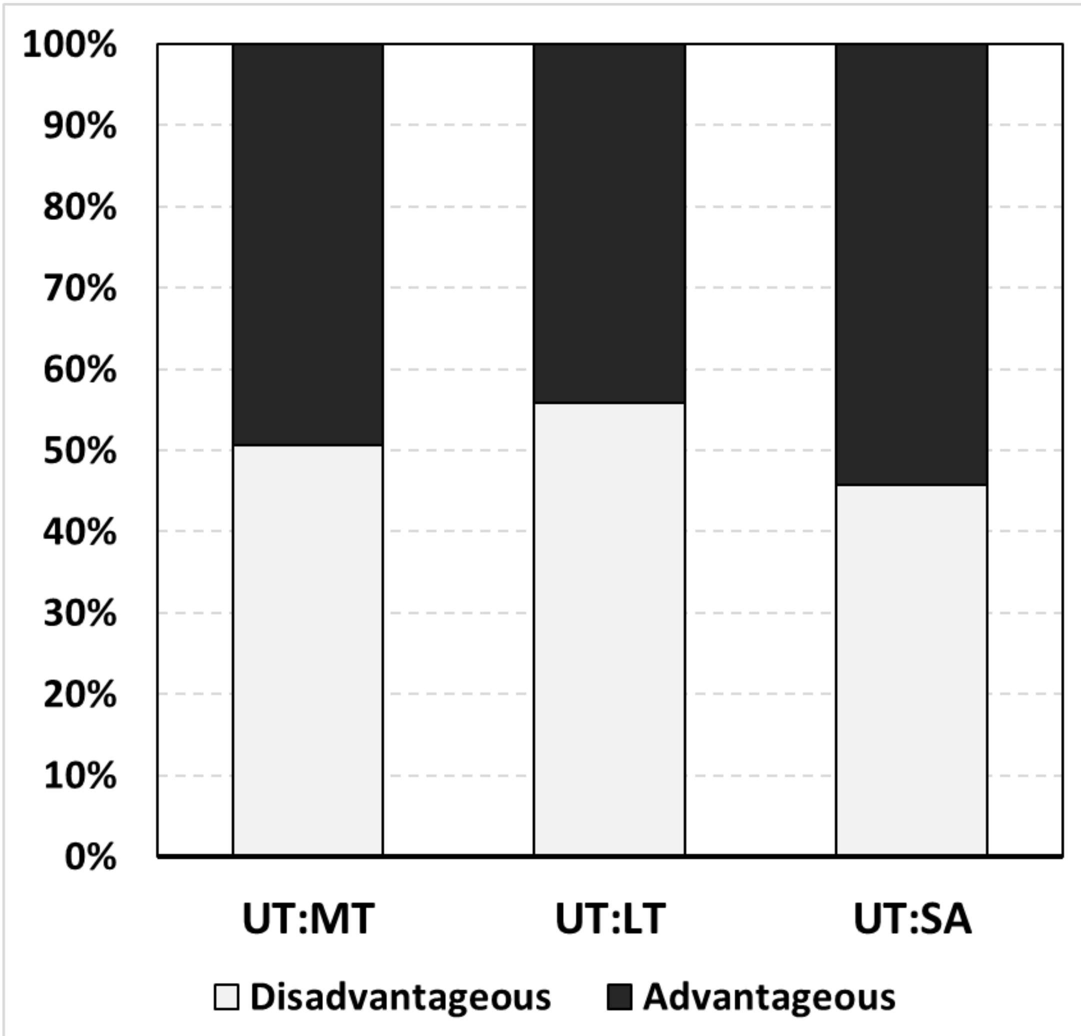

Figure 3.7. **Proportion of individual participant scapular stabilizer coactivation coefficient changes due to fatigue.** Coefficient increases are disadvantageous (white), and decreases are advantageous (black).

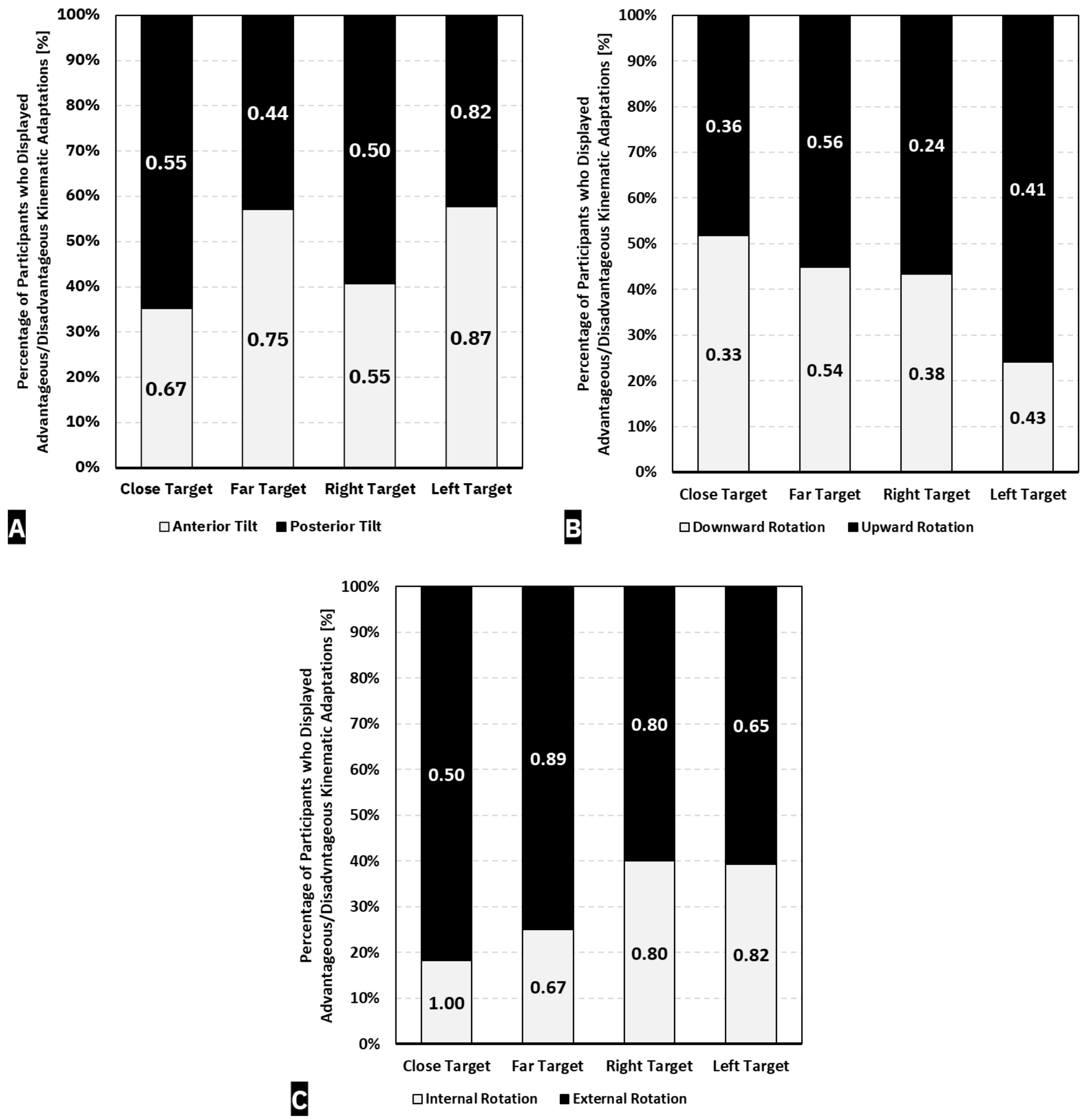

Figure 3.8. **Proportion of participants who displayed advantageous (SAS widening) (white) or disadvantageous (SAS narrowing) (black) kinematic adaptations to fatigue.** Ratios displayed within each bar indicate the proportion of participants whose kinematic changes were clinically significant ($\Delta > 5°$) [Ebaugh et al., 2005; Watson et al., 2005; McClure et al., 2012].

3.4. Discussion

This research investigated whether an occupationally-relevant muscle fatigue task targeting the shoulder would lead to muscle coactivity and kinematic responses that reflect those that have been demonstrably associated with an increased risk for SAIS and/or RC tear [Cools, et al., 2002; Ludewig, et al., 2004; Cools, et al., 2007; Myers, et al., 2009; Szucs, Navalgund, and Borstad, 2009; Michener, et al., 2016]. This study also explored whether fatigue-induced scapular co-activation changes were related to alterations in scapulothoracic joint angles. Contrary to our expectations, scapular stabilization co-activation ratios were not affected by fatigue. An effect of shoulder elevation angle on UT:LT muscle coactivity changes during shoulder adduction was observed (figure 3.5.), however, no other angle or fatigue effects for scapular stabilizer co-activity were observed. With respect to coactivity between the middle deltoid and RC musculature, while angle effects were shown, only a significant increase in MD:sIS coactivity was present following fatigue (figure 3.4.). As well, scapulothoracic upward/downward rotation, thoracohumeral elevation and plane of elevation, in addition to elbow flexion angles demonstrated fatigue-induced changes, however only for certain overhead target locations. Further, fatigue-induced relationships between scapular co-activity and kinematics were shown as hypothesized, although only for certain overhead target positions.

3.4.1. Fatigue-Induced Changes in Muscle Co-Activation and Kinematics

The overhead drilling fatigue task studied in this research did not elicit the expected fatigue responses across muscles examined; subsequently resulting in variable co-activation and kinematic responses. The large range of interindividual MPF measures of neuromechanical muscle fatigue suggest that no single muscle fatigued uniformly during overhead work, and no single muscle showed signs of fatigue in more than one third of the included participants (table 3.4.) [Öberg, Sandsjö, and Kadefors, 1991; Öberg, 1995]. Only supraspinatus (iEMG) demonstrated a mean MPF reduction of ≥8% (table 3.4.). Overhead tasks are commonly employed to elicit RC muscle fatigue while simulating occupationally relevant musculoskeletal demands [Anton, et al., 2001; Chopp, Fischer, and Dickerson, 2010; McClure, Greenberg, and Kareha, 2012; Dickerson, et al., 2015], therefore it was unexpected that fatigue-related MPF decreases in scapular stabilizer and RC muscles were not present. Since the RC muscles are often fatigued during overhead work [Cools, et al., 2004; Maciukiewicz, et al., 2016], and the scapular stabilizer muscles fatigued during loaded scapular internal rotation [Ludewig, et al., 2004; Szucs, Navalgund, and Borstad, 2009], the unconstrained postural demands of our task may have introduced sufficient musculoskeletal variability and opportunity for surrounding musculature (i.e., the humeral abductor and adductor muscles) to compensate. However, a significant increase in MD:sIS coactivation was demonstrated following fatigue.

This change in coactivation has implications for SAS reduction. A relative increase in middle deltoid EMG amplitude relative to the infraspinatus would reflect a greater discrepancy in muscle force production and impose larger superior shear forces on the humerus, which could lead to its superior translation and subsequent reduction of the SAS [Poppen and Walker, 1978; Michener, et al., 2016]. Thus, further exploration of deltoid-rotator cuff activation is needed, particularly for tasks that exhaust the RC.

The regression analyses between fatigue changes in scapular stabilizer coactivation and scapulothoracic kinematics showed a significant positive relationship between the UT:SA ratio and scapulothoracic internal rotation when approximating the left target, and between the UT:LT ratio and scapulothoracic downward rotation when approximating the far target (figure 3.6.). These regression analyses suggest that overhead drilling until failure produced an increase in scapular coactivity which was associated with potentially disadvantageous fatigue-induced kinematics for increasing SAIS risk at certain target conditions. Increases in normalized upper trapezius EMG amplitude relative to other stabilizing musculature was previously observed during tasks involving loaded scapular internal rotation [Borstad, Szucs, and Navalgund, 2009; Szucs, Navalgund, and Borstad, 2009]. Researchers have suggested that increases in upper trapezius amplitude during loaded internal rotation may have been a compensatory mechanism for shoulder muscle fatigue to provide joint stability [Alexander, et al., 2007]. Further, while scapular coactivation ratios did not show significant fatigue-mediated changes, a significant increase in scapulothoracic downward rotation was shown following fatigue when approximating the far target. This potentially disadvantageous fatigue-induced kinematic change was demonstrably related to an increase in UT:LT coactivity. Cools et al. [2007] previously suggested that resisted internal rotation of the shoulder may be an effective motion to recruit serratus anterior while specifically minimizing contributions from the lower trapezius. Thus, the far target in this study may have also prompted an increased reliance on serratus anterior Coupled with compensatory coactivity from upper trapezius to stabilize the fatigued shoulder [Ludewig, et al., 2004; Alexander, et al., 2007], while also inhibiting contributions from lower trapezius. With significant fatigue-induced changes in co-activity and kinematics were only demonstrated at far and left targets, these findings suggest that near end-range postures of scapular internal rotation may reduce the degrees of muscular freedom and kinematic variability at the shoulder, causing upper limb kinematics to be more sensitive to fatigue effects of the upper trapezius and serratus anterior. These findings also suggest that the variability in scapulothoracic responses to fatiguing stimuli may be directly consequent of the variability in muscle fatigue and muscle coactivation responses. Limitations to shoulder muscle DOF near the far and left target postures may also be responsible for decreased total time to task fatigue compared to similar protocols in previous literature which determined a median time to task fatigue of 43.7 minutes [Sood, Nussbaum, and Hager, 2007; Sood, et al., 2017].

Submaximal tests were selected for determining time-varying normalization in lieu of normalizing to maximal reference tests for the intent of minimizing fatigue due to repeated maximal muscle testing, rather than fatigue related to overhead drilling. SREs have also been shown in literature to be superior to maximal exertions for estimating submaximal efforts at, and below 50% MVE [Jull, et al., 2007]. However, intermittent, randomized SRE and SVE testing in between cycles of overhead drilling likely contributed to a complex duty-cycle that provided varying amounts of rest and fatigue for different muscles, depending on the order of SRE and SVE tests. While intermittent submaximal exertion testing likely provided periods of extended break for participants, brief (5-second) submaximal exertions were unlikely to significantly contribute to changes in EMG MPF or amplitude [Hagberg, 1981]. Therefore, we surmise that any kinematic or muscular changes in this study are consequent of fatigue garnered from overhead drilling specifically, rather than from completing SRE and SVE tests.

3.4.2. Implications of Muscular and Kinematic Variability

The negligible findings of this research pertaining to muscle-specific fatigue responses and fatigue-related changes in scapular co-activity and scapulothoracic kinematics were unexpected given the reliance on RC and scapular stabilizer muscles during overhead work [Ludewig, et al., 2004; Cools, et al., 2007; Michener, et al., 2016]. Previous work examining unconstrained shoulder fatigue tasks have similarly reported variable inter-participant responses when using EMG MPF and RMS to confirm shoulder muscle fatigue presence [Sundelin and Hagberg, 1992; Madeleine, 2010]. The high variability we observed in interindividual shoulder muscle responses to fatigue has been suggested to be attributed to the multiple degrees of kinematic and muscular freedom at the shoulder; where multiple muscles can conceivably achieve the same arm position [Looze, Bosch, and Dieën, 2009; Madeleine, 2010; Hirashima and Oya, 2016; Mulla, McDonald, and Keir, 2018]. This high intersubject variation in muscle MPF fatigue responses likely contributed to the non-significant outcomes, as standard deviations of scapular stabilizer coactivity coefficient values ranged from 123%-185% of the mean score. RC muscle MPF and MD:SS/MD:IS ratios indicated a similar degree of variability with standard deviations of coactivation coefficients ranging from 75%-160% of the mean scores. While decrements in EMG MPF exceeding the 8% threshold are considered a highly reliable technique for confirming neuromuscular fatigue, future studies investigating global shoulder fatigue may benefit form incorporating multiple EMG scores of fatigue (MPF, increase in RMS, increase in COV) [Mulla, McDonald, and Keir, 2018; Metwali, 2019], or utilizing a shoulder-specific multi-muscle fatigue score

[McDonald, et al., 2018]. Kinematic variability associated with musculoskeletal fatigue responses has been demonstrated previously with researchers similarly reporting that a significant proportion of young, healthy adults showed scapular kinematics changes which serves to reduce the SAS and increase SAIS risk in response to fatigue [Ebaugh, McClure, and Karduna, 2006; Mulla, McDonald, and Keir, 2018]. In the current study, approximately half of participants demonstrated kinematic changes indicative of SAS reduction for scapular tilt (anterior) and rotation (downward) (figure 3.8.). For scapular internal/external rotation, 20-40% of participants displayed potentially disadvantageous kinematic changes (internal). Moreover, the majority of the fatigue-mediated changes were greater than 5°, which can be considered clinically meaningful [Watson, et al., 2005; Ebaugh, McClure, and Karduna, 2006; McClure, Greenberg, and Kareha, 2012].

To construe whether the normalized EMG amplitude changes in any specific scapular muscle had a greater effect on the individual coactivation changes that were observed (equation 3.1.a.), an analysis of intersubject variability pertaining to muscle coactivation ratios was conducted to determine if numerator (upper trapezius) or denominator (middle trapezius, lower trapezius, serratus anterior) changes were more frequent following the fatigue protocol. In general, all co-activation changes were generally driven equally by both muscles. UT:MT coactivity changes were driven equally by upper trapezius (52%) and middle trapezius (48%) changes. UT:LT coactivity appeared to trend towards more participants displaying upper trapezius driven changes (60%), and UT:SA coactivity showed more participants displaying upper trapezius driven changes during adduction (55%), while abduction was split evenly (50%). Comparison of the average normalized EMG amplitude changes from pre-fatigue to post-fatigue for the scapular stabilizer muscles were similar. Specifically, upper trapezius displayed a 12% reduction in normalized EMG amplitude, while middle trapezius and lower trapezius each displayed a 10% increase in normalized EMG amplitude. Serratus anterior showed a 2% decrease (8.8 (10.6)% MVE to 8.6 (10.1)% MVE).

The relatively equal proportion of kinematic and muscular coactivity adaptations across various angles of humeral elevation and exertion directions further the ongoing narrative in research that scapular muscle and kinematic responses to fatigue – particularly global shoulder fatigue – are highly variable and therefore difficult to summarize or predict [Sundelin and Hagberg, 1992; Looze, Bosch, and Dieën, 2009; Chopp, Fischer, and Dickerson, 2010; Chopp and Dickerson, 2012; Chopp-Hurley, et al., 2016; Maciukiewicz, et al., 2016; McDonald, Tse, and Keir, 2016; Mulla, McDonald, and Keir, 2018]. The current findings suggest that the majority of coactivation coefficient changes were driven by a decrease in upper trapezius EMG amplitude and increases in middle trapezius and lower trapezius EMG amplitude, whereas group mean serratus anterior amplitude appeared to display a smaller change (figure 3.7.). The observed decreases in upper trapezius activity as a driving factor for coactivation changes has been previously hypothesized to result from the increased type-2 fiber typing and associated fatigability in this muscle compared to other scapular stabilizer muscles [Lindman, Eriksson, and Thornell, 1990; Lindman, Eriksson, and Thornell, 1991], and may suggest that upper trapezius fatigue resistance should be an important metric for restoring optimal scapular control.

3.4.3. Limitations

The overhead drilling fatigue task used in this study was developed previously and reported to be an occupationally relevant task to reliably induce volitional task failure within 45-90 minutes [Sood, Nussbaum, and Hager, 2007; Sood, et al., 2017]. While we expected all muscles to show EMG signs of fatigue (reduction in MPF), the mean fatigue results did not reflect this, despite most participants verbally and/or physically indicating they were fatigued. Failure to fatigue individual muscles, may have precluded finding important fatigue-related trends in co-activation. However, as with previous research, the extensive variability in muscle and movement patterns posed a challenge for identifying conclusive population-based fatigue responses. Sex was a variable that was grouped in this study. While equal proportions of males and females were collected, sex-based differences in strength and endurance, hormone concentration, brain blood flow, and other characteristics may contribute to the observed variability. Further, it is possible that the simulated drilling fatiguing protocol used in this study may have been too constrained for significant scapulothoracic, upper limb, and postural kinematics changes to be elicited. Thus, findings from this study may not be generalizable to workplace tasks that are unable to be anthropometrically scaled to the individual worker. Similarly, head and neck posture was unconstrained in this task, allowing participants to self-select their head orientation. This lack of head and neck constraint may not also be generalizable to workplace demands. Regarding the significant associations between fatigue-related muscle coactivation changes and scapulothoracic kinematic risk factors for SAIS, the current study suggests that work tasks which promote end range scapular internal rotation (i.e. the far and left target locations) may promote risk for impingement. In light of evidence that arm elevation angle may influence changes in UT:LT coactivity (figure 3.3.), further work may want to explore the fatigue-related muscle coactivation and kinematic risk factor relationship at different task heights. Lastly, pre-fatigue to post-fatigue changes in MPF were evaluated discretely following a pre-post repeated measures design, rather than continuously across each SRE testing session. The rationale for selecting this methodological design was to enable group-based statistical analyses between baseline resting state (pre-fatigue) and their state of volitional fatigue (post-fatigue). Conversely, had we opted to compare participants across each set, this would have likely introduced substantial variability as the range of fatigue protocol sets to failure varied widely within our sample (15-60 sets). Thus, due to the pre-post repeated measures design, we are unable to identify whether muscle-specific fatigue occurred at an earlier point in the protocol, after which kinematic adaptations may have relieved muscle stress and provided sufficient rest to return the muscle to a non-fatigued state. Future studies should consider implementing a more continuous fatigue protocol and analysis model to explore the spectrum of fatigue-related compensations that may emerge as participants approach volitional failure.

3.5. Conclusion

This study examined changes in upper limb muscle co-activation and associated kinematics from an occupationally relevant overhead drilling fatigue task. Generally, fatigue responses and associated co-activation and kinematics were considerably variable with few statistically significant fatigue effects identified. Significant associations between UT:SA and UT:LT coactivity and scapular kinematics also emerged. These findings suggest that an overhead drilling task did not conclusively yield disadvantageous muscle synergies and SAS-narrowing scapular kinematics. However, further investigation of fatigue-induced co-activation changes of scapular stabilizing and glenohumeral musculature and upper limb kinematics is needed as a considerable proportion of this young, healthy adult population demonstrated changes that would pose risk for SAIS and RC tissue damage.

Foreword to chapter 4

Findings of considerable variability in chapter 3 were expected following past work. Yet in light of the importance of serratus and lower trapezius in stabilizing the scapula which effectively stabilizes the joint reaction forces imparted by the arm, in addition to previous works highlighting the recruitment of RC muscles during overhead tasks, we were surprised to find no evidence of group-wise muscle fatigue. One potential explanation is that the cyclic or quasi-static nature of the task in chapter 3 may have allowed for more load-sharing of muscular demand. Such breadth of potential load-sharing strategies conceivably offers individuals more muscle strategies compared to a truly static task. Therefore, we posed whether participants would consolidate the many possible muscle control strategies employed during chapter 3 into a smaller subset of efficient strategies gleaned from learned experience.

These insights informed the design of the study described in chapter 4. 30 of the original 34 participants from the study in chapter 3 returned 7 days after first completing the overhead drilling task to participate in a second, identical collection. The goal for this study was to determine if fatigue effects would aggregate across a smaller set of motor patterns, and result in decreased variability upon attempting the fatigue task for a second time.

Chapter 4. Variability in Musculoskeletal Fatigue Responses Associated with Repeated Exposure to an Occupational Overhead Drilling Task Completed on Successive Days.

Matthew S. Russell, Janessa D.M. Drake, Jaclyn N. Chopp-Hurley

School of Kinesiology and Health Science, York University, Toronto, Canada

Corresponding Author:
Jaclyn Hurley, PhD
School of Kinesiology and Health Science
York University
4700 Keele Street, Toronto, Ontario, CA, M3J 1P3
Email: jnhurley@yorku.ca

Declarations of Interest: None

Funding Sources: This work was support by the Centre of Research Expertise for the Prevention of Musculoskeletal Disorders (CRE MSD) seed grant program (J.N. Chopp-Hurley) and the Ontario Graduate Scholarship program (M.S. Russell).

4.1. Introduction

The effects of muscle fatigue on kinematic changes are well documented and understood yet remain difficult to predict. Muscle fatigue produces a transient and fluctuating state of sensorimotor feedback and reductions in muscle force generating capacity [Enoka and Stuart, 1992]. Evidence suggests that as a muscle fatigues, individuals employ alternate muscular strategies in effort to maintain task performance, such that accuracy and other task parameters can be maintained [Enoka and Stuart, 1992; Forestier and Nougier, 1998; Monjo, Terrier, and Forestier, 2015; McDonald, Tse, and Keir, 2016; Tse, McDonald, and Keir, 2016]. As a result of these adaptation strategies, kinematics are also affected, altering the moment arms and orientation of the body segments [Madeleine, 2010; Bouillard, et al., 2014; Duchateau and Baudry, 2014]. On the topic of fatigue-related kinematic and muscular adaptations, the shoulder is of particular interest from a movement and motor variability perspective, as biomechanical characterizations of the shoulder are often challenged by its many DOF [Madeleine, 2010; Bouillard, et al., 2014; Mulla, McDonald and Keir, 2018].

Muscle fatigue has implications for several musculoskeletal parameters. With respect to shoulder musculature, fatigue has demonstrably led to reductions in joint position sense and accuracy [Carpenter, Blasier, and Pellizon, 1998], decrements in force generating capacity of local muscles [Vollestad, 1997; Pethick and Tallent, 2022], changes in muscle activity and co-activity [Szucs, Navalgund, and Borstad, 2008; De Looze, Bosch, and van Dieen], and kinematics changes [McQuade, Dawson, and Smidt, 1998; Chopp-Hurley et al., 2016]. However, attempts to characterize scapulothoracic and thoracohumeral shoulder motion changes due to fatigue have been challenging due to the high degree of variability reported, which has suggested both task and joint dependency [Oomen, et a., 2023; Gates and Dingwell, 2011; Ebaugh, McClure, and Karduna, 2006; Chopp-Hurley, et al., 2016; Mulla, McDonald, and Keir, 2018; McDonald, Mulla, and Keir, 2019]. This high upper limb kinematic variability demonstrated with fatigue is likely consequent of redundant motor control solutions available during shoulder and arm tasks [Scholz and Schöner, 1999; Hirashima and Oya, 2016; Sohn and Ting, 2018].

Apart from inter-participant variability, researchers have similarly demonstrated considerable intra-participant muscular and kinematic variability during overhead work, where intra-participant variability is defined as the variation in within participant responses to an identical stimulus. There are currently few studies concerned with intra-participant changes in muscular and kinematic responses. Previous work investigating shoulder kinematics changes associated with a repeated performance of a shoulder fatigue task have reported increases [Ebata, 2021] and decreases [Qin et al., 2014] in thoracohumeral elevation, along with a high degree of variability in scapulothoracic posture in particular [Mulla, McDonald, and Keir, 2018]. The authors reported that scapular kinematics revealed standard deviations in joint position of up to 14.5° between participants completing planar shoulder motions, and within-subject changes in scapulothoracic joint position ranging from a 10° to -15° difference between days [Mulla, McDonald, and Keir, 2018]. These findings are supported by Qin and colleagues who showed that participants exhibited increased variability at the shoulder, and decreased variability at the elbow and wrist [Qin, et al., 2014]. EMG measures of fatigue across repeated identical exposures have been explored minimally. Mulla and colleagues [2016] found that for the same RC fatigue task and planar shoulder motions, participants displayed varying profiles of muscle activity across days. Overall, the high degree of intrapersonal variability in muscular and kinematic responses in these studies highlight the redundancy of available muscle synergies that can conceivably achieve an end effector target position when task effort is inflated due to fatigue [Madeleine, 2010; Ebata, 2012; Mulla, McDonald, and Keir, 2018].

Overhead arm postures represent common workplace exposures and activities of daily living that may provide a useful model for exploring kinematics changes associated with arm fatigue. Tasks which are oriented above head level may often require elevation of the arm at or above 90° [Wiker, Chaffin, and Langolf, 1989; Punnett, et al., 2000; Chopp, Fischer, and Dickerson, 2010], however ergonomics literature often accepts a threshold of arm elevation greater than 60°, or work oriented above the shoulder to define overhead work [Grieve and Dickerson, 2008]. Overhead arm postures have been shown to elicit elevated muscular activity from the RC [Grieve and Dickerson, 2008; Maciukiewicz, et al., 2016], scapular stabilizer [Dickerson, et al., 2015; Maciukiewicz, et al., 2016], and humeral abductor and adductor musculature [Steenbrink, et al., 2006; Overbeek, et al., 2019], which may lead to fatigue and/or lead to discomfort more rapidly. With evidence that extensive interpersonal and intrapersonal variability of upper limb kinematics and muscle activity exists with fatigue, this suggests that there are many possible factors which may influence fatigue-related adaptations. Particularly, it is not yet known how an overhead work task, which places high demand on RC and scapular stabilizer musculature, affects upper limb motor control adaptations across subsequent sessions.

The current research explored whether (1) upper limb kinematics and static shoulder moments at baseline (pre-fatigue), (2) fatigue-related changes in upper limb muscle activity, kinematics, and kinetics, and (3) kinematic and kinetic variability, were different between repeated exposures to the same occupationally relevant overhead task designed to fatigue shoulder musculature, completed on two days that were separated one week apart. We hypothesized that upper limb kinematics and static shoulder joint moments would be different at baseline on day 2, which would reflect a potentially improved motor strategy for reducing muscle stress and static shoulder joint moment exposures. We also hypothesized that participants would display differences in which muscles reached fatigue between days [Mulla, McDonald, and Keir, 2018]. This reorganization of motor control is expected to drive an upper limb control strategy that will feature a reduction in shoulder flexion lending to a reduced static shoulder moment [Ebata, 2012]. Lastly, we also expected that interparticipant variability in kinematic and kinetic measures would be reduced on day 2 as participants converge towards a similar control strategy based on learned postural changes from their fatigue exposure on day 1 [Monjo, Terrier, and Forestier, 2015; Hirashima and Oya, 2016].

4.2. Methods

4.2.1. Participants

Thirty right-handed participants (15 male, 15 female; self-reported) were initially recruited for two identical 3-hour collections. Collections were separated by 7 days with the exception of one participant who completed their second collection after 6 days. Due to technical issues, the data from one female participant was unable to be analyzed, thus the final participant population consisted of 15 males (25.4 y ± 4.3, 24.3 kg/m^2 ± 2.7) and 14 females (22.8 y ± 3.6, 21.5 kg/m^2 ± 2.2). Participants were excluded if they self-reported any of the following: (1) working in an occupation with frequent overhead work demands within the past year, (2) pain or lifestyle factors indicative of arm or trunk disability assessed using the DASH questionnaire (cutoff score of 25) and the Oswestry Low Back Pain Disability questionnaire (cutoff score of 20), respectively [Alcántara-Bumbiedro, et al., 2006], and/or (3) psychological factors that reflect an avoidance of movement, exertion, or discomfort assessed using the FABq subscale for physical activity (cutoff score of 11) [Williamson, 2006], as well as the TSK (cutoff score of 22) [Chimenti, et al., 2021]. Additional exclusion criteria were: discomfort with needles, blood clotting disorders or currently taking blood thinning medications, HIV, Hepatitis B or C, diabetes, or respiratory conditions (Asthma, COPD, etc.), allergies to isopropyl alcohol, betadine, latex, or nickel, or were pregnant. This study received ethics approval from the York University Office of Research Ethics (#e2021-395). All participants provided written informed consent.

4.2.2. Protocol

Participants completed 64-second cycles of repetitive, overhead drilling at a 50% duty cycle (32s working, 32s resting) with their right arm (figure 4.1.). The overhead drilling task was based on previously predicted endurance times for overhead work [Sood et al., 2017], and involved pressing the tip of a 2 kg drill to four overhead targets, at 50% of the participants maximal upward push force, using their dominant right hand (figure 4.2.). Maximal upward drill press force was determined for each collection session as the peak force across two, 5-second maximal attempts with the right arm in a posture of 90° elbow flexion and 90° thoracohumeral plane of elevation (see *Centre* target location below). Maximal upward force collected in this posture was used as the target force for all overhead targets. All force output was collected using an ErgoFET push-pull force gauge (Hoggan Scientific, Salt Lake City, UT, USA) attached to the drill tip. Participants were instructed to not use their left arm and hand to support themselves or assist with the task in any way (i.e., contribute to drill force output, hold nearby structure for support, etc.). They were also not afforded any familiarization, as to not promote the consolidation of any musculoskeletal strategies prior to beginning the task which could have altered the muscular and kinematic variability observed during the baseline trials [Raviv, Lupyan, and Green, 2022; Qin et al., 2014]. During the 32-second rest portion of the duty cycle, participants were instructed to immediately place the drill on a table located at waist height, directly in front of them, and allow their arm to hang at their side until the next working cycle began (figure 4.2.). Target locations in the transverse plane were set for each participant prior to beginning of the fatigue protocol using a goniometer to define all upper limb joint angles. Target locations were set to the following four positions which approximated the listed upper limb joints angles for each position below:

1. *Center* – 70% distance from the greater trochanter to maximum overhead reach with 90° elbow flexion and 90° thoracohumeral plane of elevation.
2. *Far* – 70% distance from the greater trochanter to maximum overhead reach with 45° elbow flexion and 90° thoracohumeral plane of elevation.
3. *Left* – shoulder plane of elevation increased to 125° from *center* position.

4. *Right* – shoulder plane of elevation reduced to 45° from *center* position.

Over the 32-second task cycle, each target was presented twice in a pseudorandom order, for 4 seconds each. Five 64-second overhead working cycles at a 50% duty cycle constituted one set. The pseudorandom target order ensured that the otherwise random order of 8 targets per 64-second round of overhead work could not appear again within the same set.

Force and EMG were collected during two repetitions of isometric MVE tests which consisted of three 5-second trunk and upper limb muscle tests, completed in random order: empty can, external rotation, high flexion, [Boettcher, Ginn, and Cathers, 2008; Ginn, Halaki, and Cathers, 2011; McDonald, Sonne, and Keir, 2017]. MVE tests were selected from previously published guidelines on eliciting maximal muscle activity in the minimal number of muscle tests in effort to reduce testing time and participant effort/fatigue due to testing (figure 4.3.). At baseline, after the completion of 15, 30, 45, and 60 cycles of overhead work, or at the point of protocol termination, EMG was collected during submaximal voluntary exertions (SVE) (figure 4.1.). SVE tests were a single exertion of each MVE test scaled to 30% of the peak MVE output determined at baseline. SVE tests were used to capture muscle EMG MPF changes [McDonald, Sonne, and Keir, 2017]. All muscle testing was performed on the right side (dominant side). Protocol termination was defined when the participant met one of three completion criteria: 1) the participant reached RPE ≥

9 and indicated they were unable to continue maintaining the 50% maximal overhead force level, 2) they were unable to generate 50% of their maximal overhead force in any of the target directions within the same cycle, 3) they completed 60 cycles (12 rounds) of the overhead drilling task and maintained a stable RPE that was not increasing.

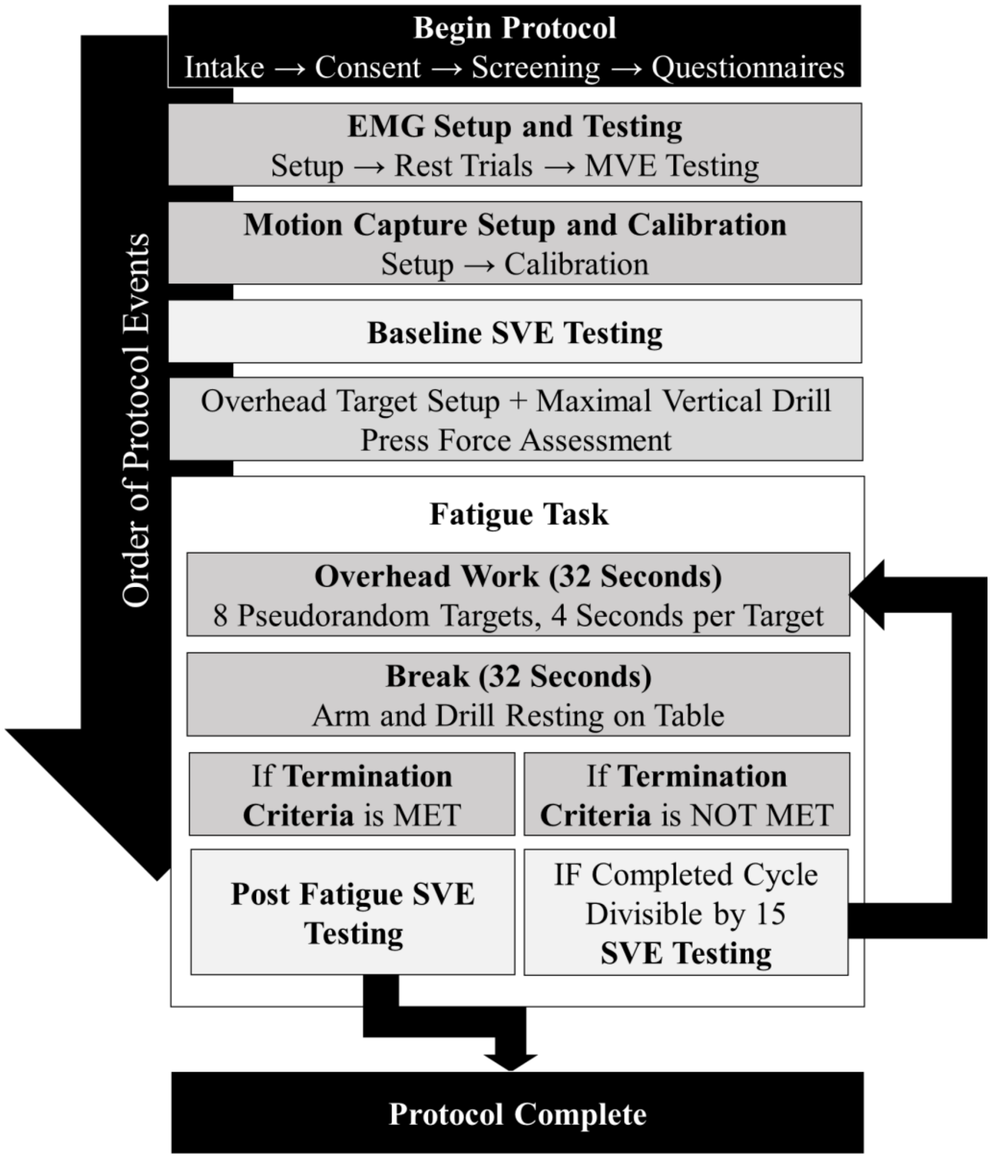

Figure 4.1. **Timeline of experimental protocol.** Order of protocol events begins at “Begin Protocol” and proceeds down the flowchart. “Protocol Complete” is only reached when participants meet one of three protocol termination criteria.

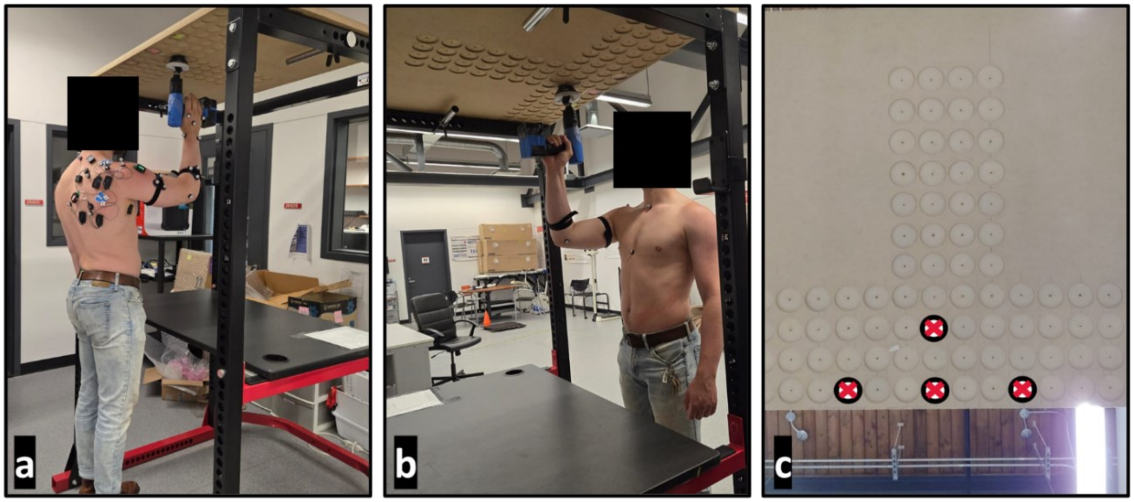

Figure 4.2. **Overhead drilling shoulder fatigue protocol target setup with kinematic markers and wireless electrodes A.** posteriolateral view **B.** anteriolateral view **C.** overhead target configuration.

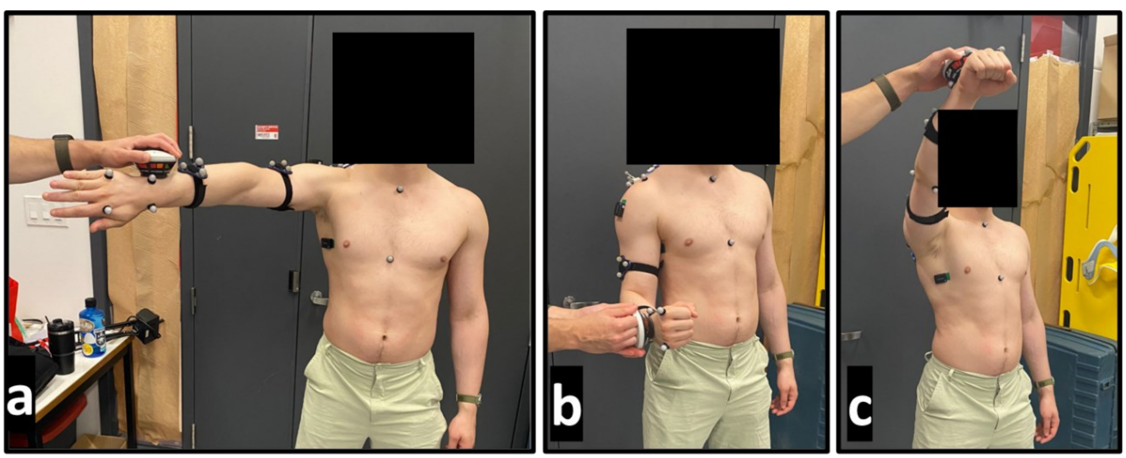

Figure 4.3. **Isometric muscle testing postures. A.** empty can **B.** external rotation **C.** high flexion. For each test, isometric resistance is applied to the participant in the direction of the handheld force transducer.

Muscle activity was collected from seven muscles of the shoulder region of the right upper limb during MVE and SVE tests. Surface electromyography (sEMG) was used to record supraspinatus (SS), infraspinatus (IS), upper trapezius (UT), middle trapezius (MT), lower trapezius (LT), serratus anterior (SA), and middle deltoid (MD). In addition, two channels of intramuscular EMG (iEMG) were collected specifically from the supraspinatus (iSS) and infraspinatus (iIS). A Delsys Trigno system (Delsys Inc., 23 Strathmore Rd, Natick, MA, USA) was utilized to collect all EMG recordings. For sEMG recordings, Trigno Avanti sensors were placed on the muscle belly of interest, following established guidelines [Perotto, 2011; Stegeman & Hermens, 2007]. These sensors featured 10 mm spaced silver (99.99%) bar electrodes aligned with the muscle fibers and recorded sEMG signals at a rate of 2148 Hz, within a bandwidth of 20-450 Hz. For intramuscular insertions, the insertion points were determined in accordance with established guidelines [Geiringer, 1999; Perotto, 2011]. Intramuscular insertions followed ultrasound guidance in addition to electromechanical confirmation from (1) muscle depolarization when the muscle is initially punctured, and (2) isolated muscle resistance testing after insertion to confirm correct placement with EMG feedback [Waite et al., 2010]. For each muscle, a 30 mm stainless surgical steel hypodermic needle housing two barbed 304 series stainless steel wires was used (0.051 mm diameter, 200 mm length, nylon coated) (Motion Lab Systems Inc., 15045 Old Hammond Way, Baton Rouge, LA, USA). iEMG sampled at 4370 Hz with a 10-2000 Hz pass band.

Kinematics were captured using a 7-MX40+ camera Vicon system (Vicon Motion Systems Ltd., 7388 S. Revere Pkwy, CO, USA) sampled at 100 Hz. 19 mm diameter reflective Vicon pearl markers were affixed to 14 bony landmarks of the trunk (7th cervical vertebrae, 8th thoracic vertebrae, suprasternal notch, xiphoid process), right scapula (trigonum spinae, inferior angle, acromion angle), right upper arm (acromion, lateral epicondyle, medial epicondyle), lower arm (radial styloid, ulnar styloid), and hand (based of the 2nd and 5th metacarpals), following the recommendations of the International Society of Biomechanics (ISB) (figure 4.4.) [Wu, et al., 2005]. Humeral and forearm tracking clusters were used, and a scapular tracking cluster was placed on the surface of the junction between the acromion and the scapular spine following the recommendations of Shaheen and colleagues [2011]. This method previously displayed error measures within 5° for all scapulothoracic DOF with scapular calibration to anatomical scapular landmarks (trigonum spinae, inferior angle, acromion angle) performed at 90° thoracohumeral abduction for overhead postures.

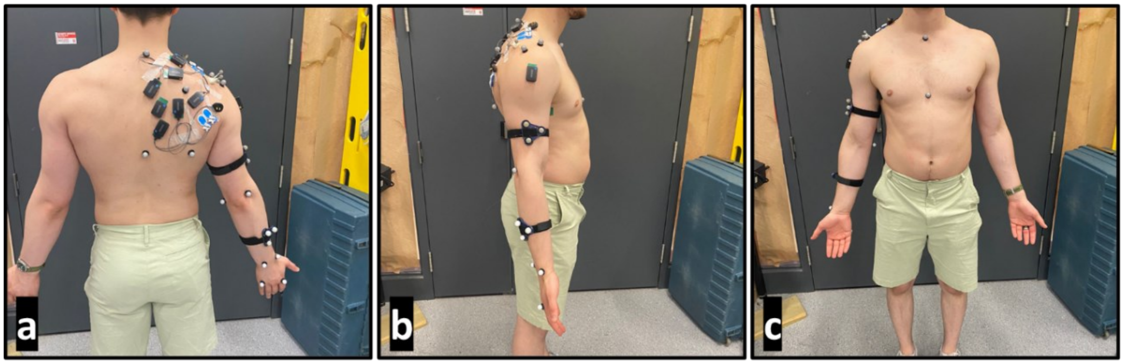

Figure 4.4. **Landmarking for motion capture. A.** posterior **B.** lateral **C.** anterior view.

4.2.3. Data Analysis

The following EMG, kinematic, and kinetic data were processed using custom MATLAB software (MATLAB 2020a, Mathworks, Natick, MA).

4.2.3.1. Neuromuscular Fatigue

To calculate EMG MPF and RMS amplitude, EMG data was analyzed from each participant's pre-fatigue (baseline SVE) and post-fatigue (their last SVE, after reaching termination criteria) trials. For each muscle, MPF and RMS was analyzed for the SVE recommended for that particular muscle (empty can: SS; external rotation: IS; high flexion: UT, MT, LT, SA, and MD) [Boettcher, Ginn, and Cathers, 2008; McDonald, et al., 2018].

4.2.3.1.1. Electromyographic Mean Power Frequency

sEMG signals were dual-band-pass Butterworth filtered at 10-500 Hz, and iEMG signals were dual-band-pass Butterworth filtered at 20-1000 Hz [Stulen and De Luca, 1981; Öberg, Sandsjö, and Kadefors, 1990; Willigenburg et al., 2012]. A discrete Fourier transform with a 0.5-second rectangular window was used to calculate MPF for the first 3-seconds of the 5-second SVE trial from which an overall mean was calculated [Hendrix, et al., 2010]. The presence of muscle-specific fatigue was defined as a reduction in MPF ≥ 8% [Öberg, Sandsjö, and Kadefors, 1990; Öberg, 1995].

4.2.3.1.2. Electromyographic Root-Mean-Squared (RMS) Amplitude

sEMG signals were dual-band-pass Butterworth filtered at 30-500 Hz, and iEMG signals were dual-band-pass Butterworth filtered at 30-1000 Hz [Stulen and De Luca, 1981; Öberg, Sandsjö, and Kadefors, 1990; Drake and Callaghan, 2006; Willigenburg et al., 2012]. Peak amplitude was sampled from the middle 3-seconds of each 5-seond SVE waveform, and amplitude was normalized to MVE.

4.2.3.2. Upper Limb Kinematics

Upper limb joint angles were evaluated by comparing the scapulothoracic, thoracohumeral, elbow, and radiocarpal joints in both the pre-fatigue and post-fatigue state. Rather than analyzing upper limb kinematics during the SVE tasks, as was done with EMG processing, kinematic joint angle comparisons were performed for each of the four overhead targets (close, far, right, left). Pre-fatigue kinematic data was captured as participants approximated each of the four overhead targets during the fifth cycle of the fatigue protocol (approximately 5 minutes of overhead work). This process allowed for four work cycles of task familiarization. Post-fatigue kinematic data was captured from the final cycle of the fatigue protocol that was successfully completed (such that the target force output was achieved for all targets) before the protocol concluded. To calculate each joint angle, three-dimensional LCS were established for the thorax, scapula, humerus, forearm, and hand [Wu et al. 2005]. LCS were also defined for each of the rigid clusters and the scapula tracking cluster. Relative rotation matrices were generated to describe the relationships between these clusters and anatomical markers. The Euler angles for the scapulothoracic, thoracohumeral, elbow, and radiocarpal joint angles were computed based on reconstructed virtual landmarks, following the recommended joint angle decomposition sequences suggested by Wu et al. [2005].

4.2.3.3. Shoulder Joint Moments

Static shoulder flexion moment exposures were calculated for the pre-fatigue and post-fatigue kinematic postures using a static inverse dynamics model. The model consisted of three body segments: hand, forearm, and upper arm. Joint center and segment center of mass (COM) locations were defined using the published guidelines by Dempster [1955] using kinematic anatomical marker positions as model input. Segment masses were calculated as percentages of total body mass, as defined in the regression equations by Churchill [1978]. Gravitational external forces were considered to be acting on the body segments at their COM. Static resistance to the upward force application of the drill was localized to be acting on the palm of the hand at the hand segment COM. Resultant shoulder joint moment was calculated from the vertical component of all loads (segment mass, drill mass, vertical drill press reaction force), multiplied by the horizontal moment arm from the shoulder, and reported in newton meters (Nm).

4.2.4. Statistical Analysis

Statistical comparisons were evaluated between day 1 and day 2 EMG, kinematic, and kinetic data. Outliers two standard deviations above or below the mean were first removed from the raw EMG, kinematic, and kinetic data. Keeping with the repeated measures design, if a data point was removed, any associated pairwise scores was removed as well [Miller, 1991].

Paired two-tailed t -tests were used to evaluate differences between day 1 and day 2 group-average baseline (pre-fatigue) measures for the following outcomes: (1) scapulothoracic (anterior/posterior tilt, upward rotation/downward rotation, internal/external rotation), thoracohumeral (plane of elevation, elevation, axial rotation), elbow (flexion/extension, axial rotation, carrying angle), and wrist (flexion/extension, ulnar/radial deviation, pronation/supination) joint angles for each target (close, far, left right) and grouped, and (2) shoulder joint moment for target grouped data.

Paired two-tailed t-tests were also used to evaluate differences in fatigue-related responses (Δ = post-fatigue – pre-fatigue) for (1) group-average percent muscle-specific MPF and RMS, (2) scapulothoracic, thoracohumeral, elbow, and wrist joint angles, and (3) shoulder moments between day 1 and day 2. Šídák correction was applied to adjust α values for multiple comparisons. Shapiro-Wilk tests assessed for normality and Wilcoxon signed-rank tests were used for non-parametric cases.

Changes in group kinematic and kinetic variability were compared between day 1 and day 2 using scores of median absolute deviation (MdAD) (Equation 1).

$$MdAD = \text{median}[|X_i - \text{median}(X)|]$$

Equation 4.1. **Median Absolute Deviation.**

Where, X_i represents each individual data point in the dataset,
median (X) is the median of the dataset, and
$|\cdot|$ denotes the absolute value.

MdAD is expressed as the median of absolute deviations of all data points from the median of the dataset, and is a more robust metric of variability when dealing with outliers compared to standard deviation (Equation 1) [Chau, Young, and Redekop, 2005; Qin, et al., 2014]. For the purpose of our analysis, MdAD was calculated from the between-participant measures of the 3-axis scapulothoracic, thoracohumeral, elbow, and wrist joints Euler angles, as well as for static shoulder joint flexion moment, and compared across day 1 and day 2.

Thus, for each degree of freedom, as well as for the static shoulder joint flexion moment dataset, the median of participant deviations from the median of that dataset was reported as the MdAD, by day. MdAD was calculated at the pre-fatigue and post-fatigue kinematic/kinetic time profiles described in section 2.3.2., as well as a "mid-fatigue" timepoint. "Mid-fatigue" data was defined as the kinematic/kinetic strategy performed during the last 32-second working cycle within the 5-cycle round of overhead work performed approximately halfway through each participant's number of rounds to volitional fatigue ([total number of rounds to fatigue]/2), rounded up to the nearest multiple of 5. Since we analyzed kinematics from the last work cycle of each 5-cycle set, the lower limit of participants cycles to fatigue limited us to only be able to sample 3 kinematic trials from each participant. Hence, we analyzed MdAD for all participants at pre-fatigue, mid-fatigue, and post-fatigue. Kinematic target data was grouped by target to constrain the number of values presented; kinetic target data was not grouped. Increases in MdAD score represent an increase in variability. Since a single MdAD value constitutes the between-participant variability for a single variable, these values could not be tested statistically. Thus, MdAD values are reported observationally only.

Statistical analyses were performed using the Statistical Package for the Social Sciences (SPSS), version 28.0 (IBM Corp. Armonk, NY, USA), and Stata/IC 18.0 (StataCorp LP, College Station, TX).

4.3. Results

4.3.1. Baseline Differences Across Days

The average of peak drill press forces recorded on day 1 was 178.7 N (± 65.1) and 188.6N (± 65.0) on day 2, and participants increased their drill press force by 10.6% on day 2, on average. With target data grouped, thoracohumeral elevation ($t_{80} = -2.79$, $p < 0.01$), elbow flexion ($t_{99} = -6.63$, $p < 0.001$), and wrist deviation ($t_{76} = -3.00$, $p < 0.01$) joint angles were significantly different across days. From day 1 baseline to day 2 baseline, thoracohumeral elevation increased by 5.0° (61.5° ± 13.2 to 66.5° ± 7.3), elbow flexion increased 8.6° (100.1° ± 12.7 to 108.7° ± 12.5), and wrist ulnar deviation decreased 5.9° (10.7° ± 13.7 to 4.8° ± 13.8) on day 2. No difference was found between pre-fatigue shoulder joint moment exposures between day 1 (37.7Nm ± 10.4) and day 2 (36.0Nm ± 12.7) ($t_{46} = 0.548$, $p = 0.707$).

4.3.2. Fatigue-related Differences Across Days

4.3.2.1. Subjective Volitional Fatigue Criteria

Subjective volitional fatigue (termination criteria 1) was achieved in 60% females on day 1, and 67% of females on day 2, and 53% of males on day 1 and 47% of males on day 2 (table 4.1.). Four participants who reached fatigue task completion due to volitions fatigue on day 1 reached fatigued task failure due to force insufficiency on day 2, and four other participants who reached fatigue task completion due to force insufficiency on day 1 reached fatigue task failure due to volitional fatigue on day 2.

Table 4.1. **Sex distribution of protocol termination criteria on day 1 and day 2.**

Day	1			2		
Termination Criteria	*RPE*[1]	*Force*[2]	*Max*[3]	*RPE*[1]	*Force*[2]	*Max*[3]
Males	8	7	0	7	8	0
Females	9	5	1	10	4	1

* *Termination criteria as follows:* 1) participant reached RPE ≥ 9 and indicated they were unable to continue maintain force level, 2) participant unable to generate 50% of their maximal overhead force in any of the target directions within the same cycle, 3) participant completed 60 cycles (12 rounds) of the overhead drilling task and maintained a stable RPE.

4.3.2.2. Neuromuscular Fatigue

Group mean EMG ΔMPF (post-fatigue – pre-fatigue) across all 7 recorded muscles (9 channels) ranged between a 12% increase and a 5% decrease on day 1, and a 6% increase and a 5% decrease on day 2 while group mean EMG ΔRMS (post-fatigue – pre-fatigue) ranged between a 31% increase and a 4% decrease on day 1, and a 19% increase and a 4% decrease on day 2. The only muscles that displayed a decrease in average MPF on both days were supraspinatus (intramuscular) (decreased by 5% on both days), and infraspinatus (surface) (decreased by 2% on day 1 and 1% on day 2), while only infraspinatus (intramuscular) showed a decrease in RMS on either day (decreased by 4% on both days). No difference in EMG ΔMPF between day 1 and day 2 was significant (figure 4.5.a), however a significant 21.0 % MVE decrease in EMG ΔRMS was observed in serratus anterior ($t_{(27)} = 2.38$, $p = 0.026$) (figure 4.5.b). 0-3 outliers were removed for all EMG channels, except for iIS which had 10 outliers removed. Removal of outliers did not change any channels average ΔMPF by more than 4.2 Hz (4.7%); 0.37 Hz on average (0.39%). Average ΔRMS did not change by more than 6.6% MVE across channels; 1.2% on average.

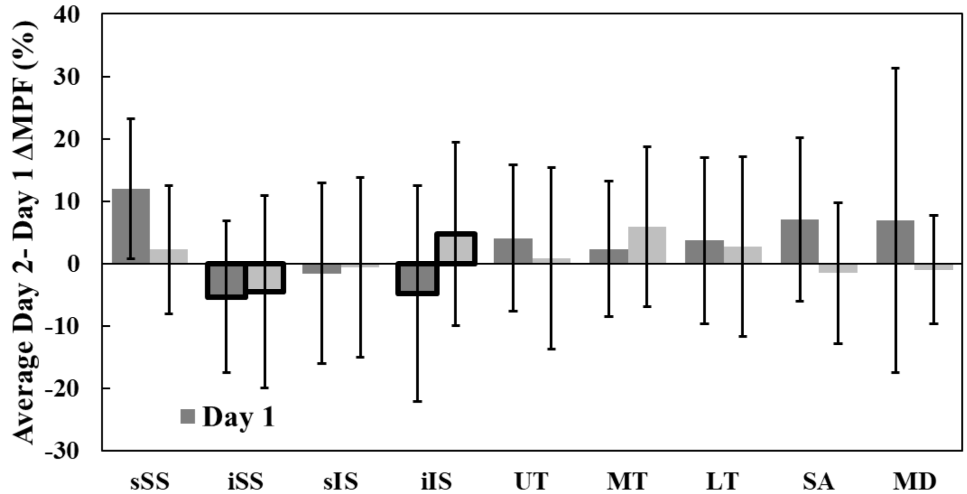

	sSS	iSS	sIS	iIS	UT	MT	LT	SA	MD
Increased D2	13	16	14	9	20	15	18	21	16
Decreased D2	16	11	16	11	10	15	12	8	13

A

EMG Channel

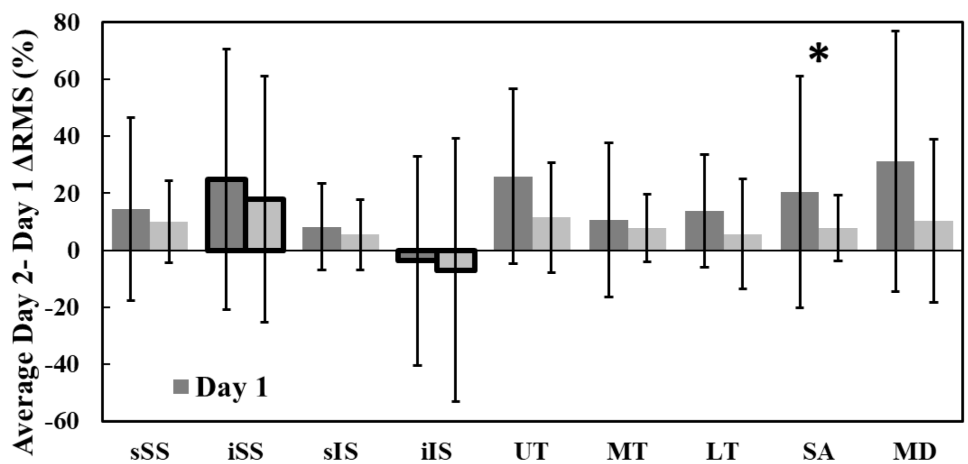

	sSS	iSS	sIS	iIS	UT	MT	LT	SA	MD
Increased D2	12	12	11	8	11	11	15	11	9
Decreased D2	17	17	19	13	19	19	15	18	20

B

EMG Channel

Figure 4.5. **Average difference between fatigue-induced (a) MPF and (b) RMS change on day 1 and day 2 (D2). A.** day 2 ΔMPF – day 1 ΔMPF **B.** day 2 ΔRMS – day 1 ΔRMS. The number of participants that displayed increased

ΔMPF/RMS and decreased ΔMPF/RMS are indicated below each respective EMG channel. The sum of the number of participants that increase and decrease for each channel constitutes the study sample size (n = 30) minus any removed outliers. Muscles monitored with both surface and intramuscular EMG are identified with lowercase "s" and "i", and intramuscular channels are outlined in black. "*" denotes $p \leq 0.05$. Error bars represent 1 standard deviation.

4.3.2.3. Joint Angle Kinematics

A significantly larger reduction in thoracohumeral elevation ($t_{(88)} = -3.55$, $p = 0.0003$; figure 4.6.) and elbow flexion ($t_{(88)} = -4.43$, $p < 0.0001$; figure 4.7.) was demonstrated on day 1 compared to day 2. With target data grouped, thoracohumeral elevation fatigue-related change decreased by 5.7° ± 12.8 on day 1 and increased by 0.4° ± 14.9 with fatigue on day 2 (table 4.2.). When separated by target, thoracohumeral elevation showed a significant decrease in fatigue-related joint angle changes between day 1 and day 2 at the *far* ($t_{(21)} = -2.20$, $p = 0.019$), *right* ($t_{(22)} = -2.51$, $p = 0.010$), and *left* ($t_{(22)} = -2.20$, $p = 0.019$) targets by 6.5°, 7.9°, and 10.3°, respectively (figure 4.6.; table 4.2.). Elbow flexion across all targets showed an increase of 6.9° ± 13.1 from pre-fatigue to post-fatigue on day 1, and an increase of 1.7° ± 7.8 from pre-fatigue to post-fatigue on day 2 (table 4.2.). When separated by target, this decrease in fatigue-induced elbow flexion for day 1 relative to day 2 was evident for the *far* ($t_{(25)} = -3.46$, $p = 0.001$) and *right* ($t_{(21)} = -2.88$, p 0.005) targets, by 8.6° and 6.2°, respectively (figure 4.7.; table 4.2.).

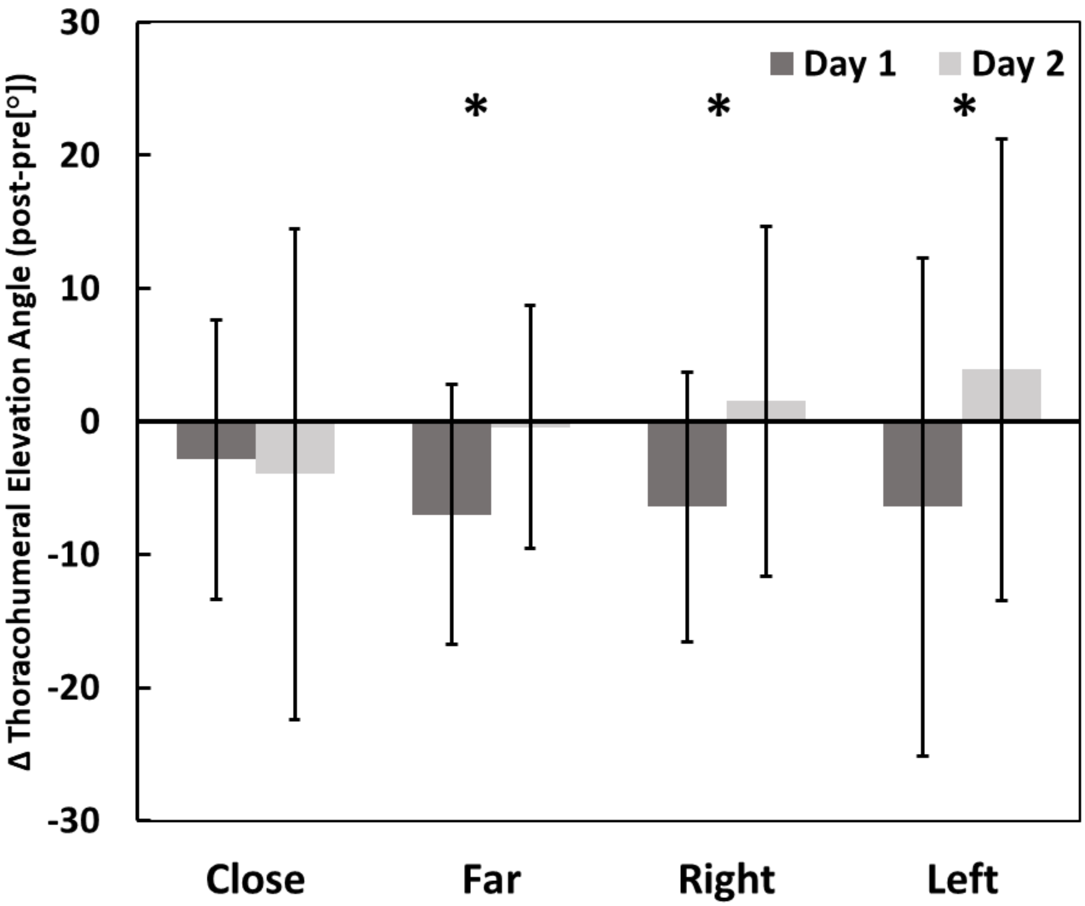

Figure 4.6. **Fatigue-induced changes in thoracohumeral elevation ($\Delta°\beta_h$) for day 1 and day 2.** * Indicates significance ($p < 0.05$). Error bars represent 1 standard deviation.

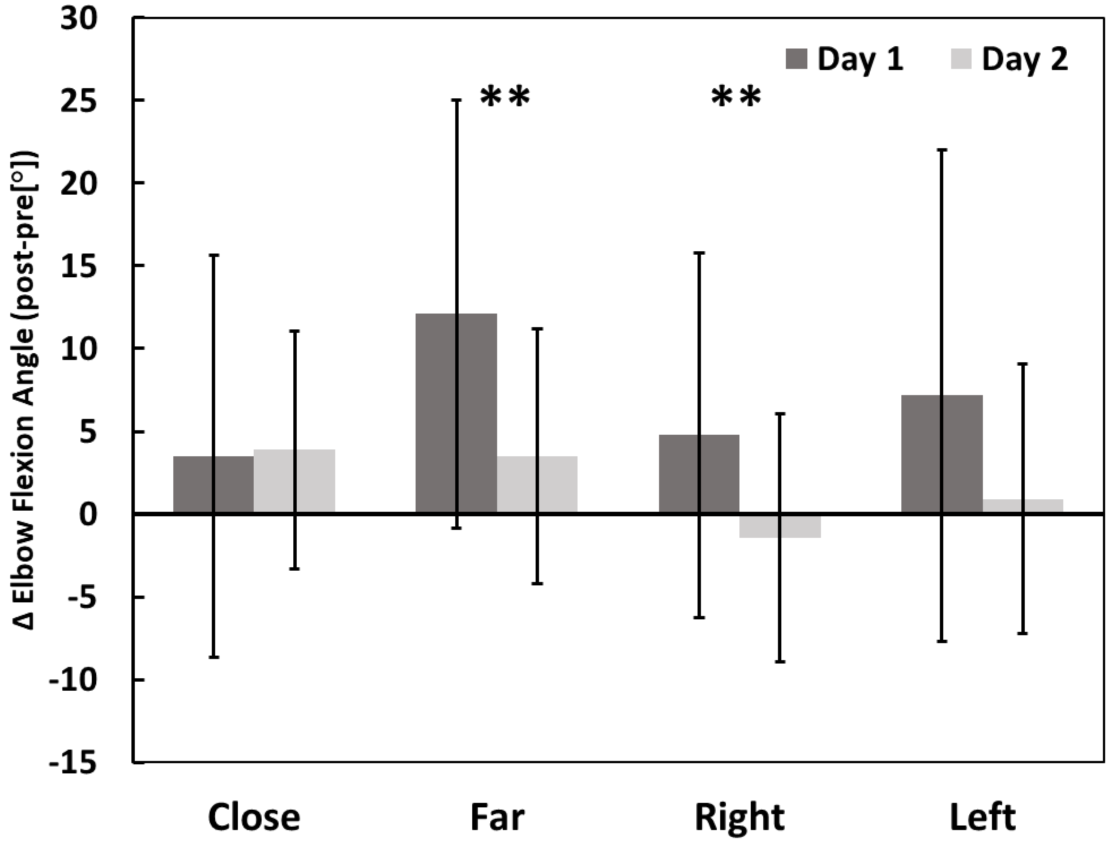

Figure 4.7. **Fatigue-induced changes in elbow flexion (Δ°α_{HF}) for day 1 and day 2.** ** Indicates significance ($p < 0.01$). Error bars represent 1 standard deviation.

Table 4.2. **Mean difference (standard deviation) and p-value (p) values for all fatigue-related kinematic joint angle degrees of freedom changes when compared across days.** Values represent Šídák corrected significance values. Shaded rows indicate Wilcoxon signed-rank test results for non-parametric distributions, all other rows are paired t-test results.

Joint	***Degree of Freedom***	***Target***				
		Overall	*Close*	*Far*	*Right*	*Left*
Scapulothoracic	Anterior/ Posterior Tilt	-10.3 (26.3) 0.918	-11.4 (25.2) 0.787	-18.8 (31.9) 0.790	3.4 (20.7) 0.382	-13.6 (26.0) 0.947
	Upward/ Downward Rotation	-4.1 (26.2) 0.874	-6.8 (29.0) 0.716	0.4 (17.6) 0.456	-3.9 (32.9) 0.720	-5.8 (21.8) 0.821
	Protraction/ Retraction	-2.7 (26.0) 0.998	-4.4 (28.5) 0.956	-0.20 (24.5) 0.981	1.8 (29.3) 0.287	-7.9 (26.9) 0.982
Thoracohumeral	Plane of Elevation (POE)	-10.2 (22.7) 0.997	-14.7 (23.3) 0.993	-7.7 (23.16) 0.959	-8.3 (22.1)0 .933	-9.9 (22.9) 0.974
	Elevation	**6.1 (14.1) 0.0003**	-1.1 (14.4) 0.452	**6.5 (9.9) 0.019**	**7.9 (12.2) 0.010**	**10.3 (18.6) 0.019**
	Axial Rotation	-0.3 (13.7) 0.38	-1.1 (12.1) 0.585	-3.1 (12.9) 0.711	0.4 (11.2)0 .328	2.5 (17.2) 0.220
Elbow	Flexion/ Extension	**5.2 (11.2) < 0.001**	-0.4 (10.1) 0.336	**8.6 (11.5) < 0.001**	**6.2 (10.0) 0.005**	6.3 (12.5) 0.054
	Carrying Angle	0.7 (9.8) 0.315	-1.4 (10.8) 0.706	1.4 (8.6) 0.215	0.9 (10.5)0 .372	1.7 (9.1) 0.281
	Pronation/	0.2	-4.9	11.6	-2.7	-4.7

	Supination	(17.9) 0.705	(15.1) 0.915	(24.7) 0.078	(13.4) 0.586	(13.5) 0.953
Wrist	Flexion/ Extension	-3.1 (10.5) 0.949	-4.4 (11.1) -.942	1.5 (9.2) 0.206	-5.5 (10.2) 0.958	-3.9 (11.6) 0.905
	Radial/ Ulnar Deviation	-1.2 (7.6) 0.805	-3.1 (10.1) 0.789	2.5 (9.3) 0.562	-0.6 (8.9) 0.515	-1.9 (7.5) 0.827
	Pronation/ Supination	-0.8 (9.2) 0.388	-0.3 (7.3) 0.304	-1.9 (7.9) 0.489	-1.9 (7.1) 0.695	-0.8 (8.1) 0.33

4.3.2.4. Shoulder Joint Moment

Shoulder joint flexion moments were largest at the *far* target for day 1 (pre-fatigue: 40.3 Nm ± 11.6, post-fatigue: 37.3 Nm ± 12.8) and day 2 (pre-fatigue: 39.3 Nm ± 14.6, post-fatigue: 37.2 Nm ± 13.0), and smallest at the *close* target for day 1 (pre-fatigue: 36.1 Nm ± 10.4, post-fatigue: 33.1 Nm ± 12.8) and day 2 (pre-fatigue: 33.8 Nm ± 12.1, post-fatigue: 33.1 Nm ± 12.2). The change in static shoulder flexion moment (ΔNm) from pre-fatigue to post-fatigue (grouped by target) revealed a significant reduction from day 1 (-3.2 ΔNm±6.4) to day 2 (-0.8 ΔNm±6.5) ($t_{(95)}$ = 02.51, p = 0.0068) (figure 4.8.; table 4.3.). When separated by target, only the *left* target showed a significant reduction in fatigued-induced static shoulder flexion moment from -3.70 ΔNm (± 5.20) on day 1 to -0.24 ΔNm (± 6.54) on day 2 ($t_{(23)}$ = -2.05, p = 0.026) (figure 4.8.; table 4.3.).

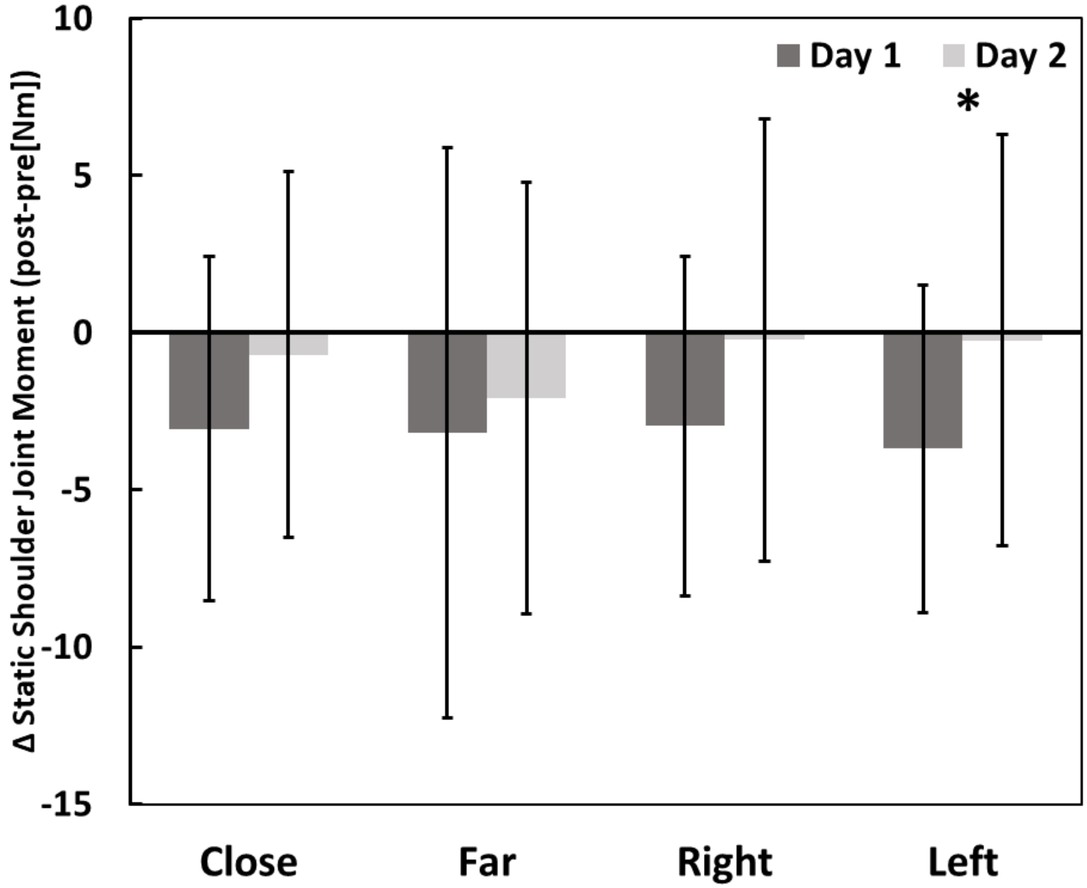

Figure 4.8. **Fatigue-induced changes in static shoulder flexion moment (ΔNm) for day 1 and day 2.** * Indicates significance ($p < 0.05$). Error bars represent 1 standard deviation.

Table 4.3. **Paired t-test mean difference (standard deviation) and significance (p) values for shoulder joint flexion moment at each overhead target, compared across days (D2-D1).** Values represent Šídák corrected significance values.

Target	***Overall***	***Close***	***Far***	***Right***	***Left***
Mean Difference	**2.3**	2.3	1.0	2.7	**3.4**
(SD)	**(12.7)**	(12.1)	(14.6)	(11.7)	**(12.4)**
p-value	**0.007**	0.086	0.334	0.066	**0.026**

4.3.3. Changes in Kinematic and Kinetic Variability Between Days

Average groupwise MdAD ranged from 12.8 to 41.3 on day 1 and 12.6 to 29.7 on day 2 at the scapulothoracic joint, 5.7 to 21.5 on day 1 and 4.5 to 16.6 on day 2 at the thoracohumeral joint, 3.4 to 24.2 on day 1 and 5.7 to 27.0 on day 2 at the elbow joint, and 4.9 to 9.9 on day 1 and 6.7 to 13.5 on day 2 at the wrist joint. Groupwise static shoulder joint flexion moment MdAD was largest at the *far* target on day 1 (10.0) and day 2 (11.2), second largest at the *left* target on day 1 (9.6) and day 2(8.3). The *right* target had the least variability on day 1 (8.0), but not on day (8.1), whereas the *close* target had the second least variability on day 1 (9.1) and the least variability on day 2 (7.8).

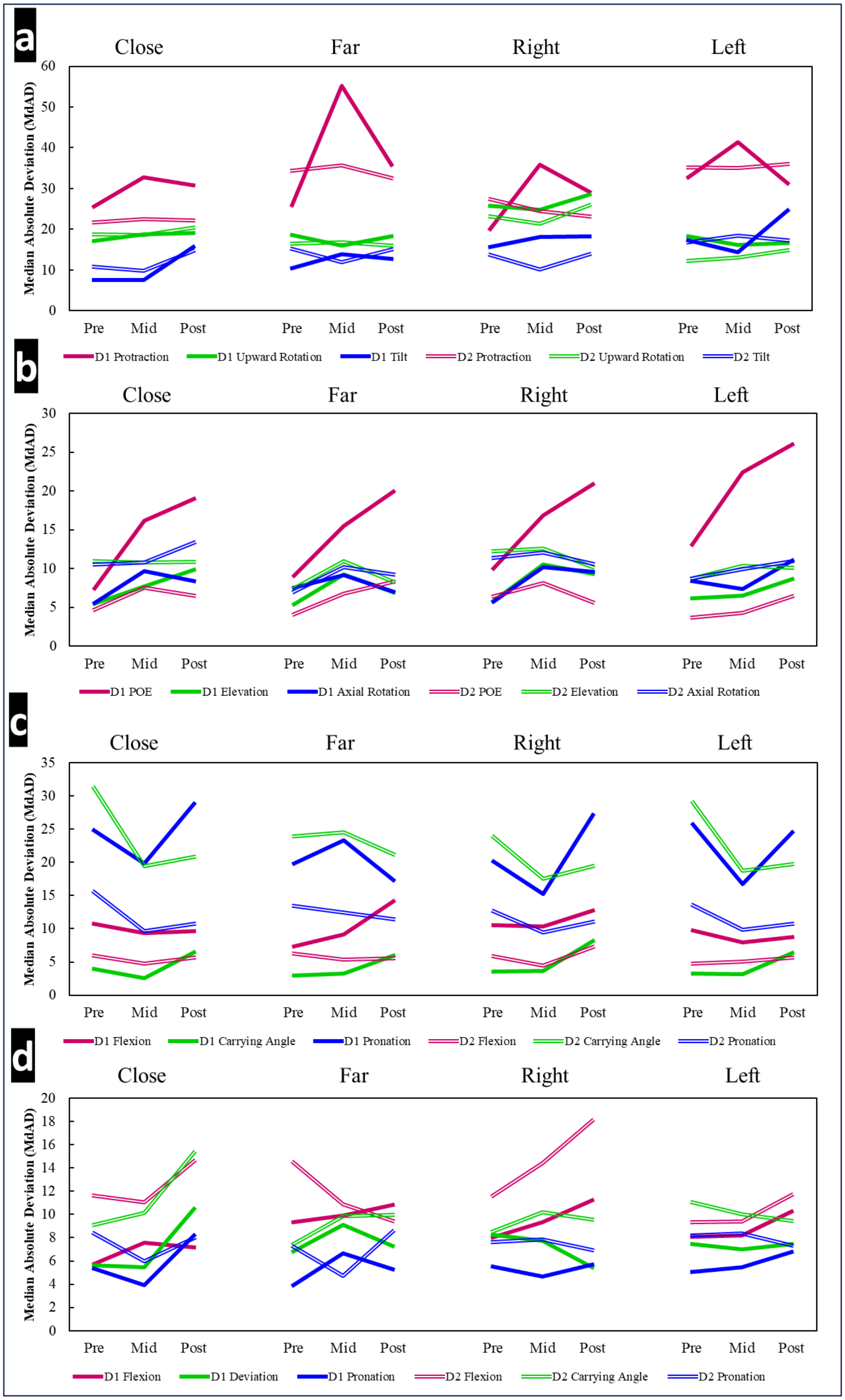
a
Close
Far
Right
Left
Median Absolute Deviation (MdAD)
60
50
40
30
20
10
0
Pre
Mid
Post
D1 Protraction
D1 Upward Rotation
D1 Tilt
D2 Protraction
D2 Upward Rotation
D2 Tilt
b
30
25
20
15
10
5
D1 POE
D1 Elevation
D1 Axial Rotation
D2 POE
D2 Elevation
D2 Axial Rotation
c
35
D1 Flexion
D1 Carrying Angle
D1 Pronation
D2 Flexion
D2 Carrying Angle
D2 Pronation
d
18
16
14
12
8
6
4
2
D1 Flexion
D1 Deviation
D1 Pronation
D2 Flexion
D2 Carrying Angle
D2 Pronation

Figure 4.9. **MdAD values for the (a) scapulothoracic, (b) thoracohumeral, (c) elbow, and (d) wrist joints on day 1 and 2.**

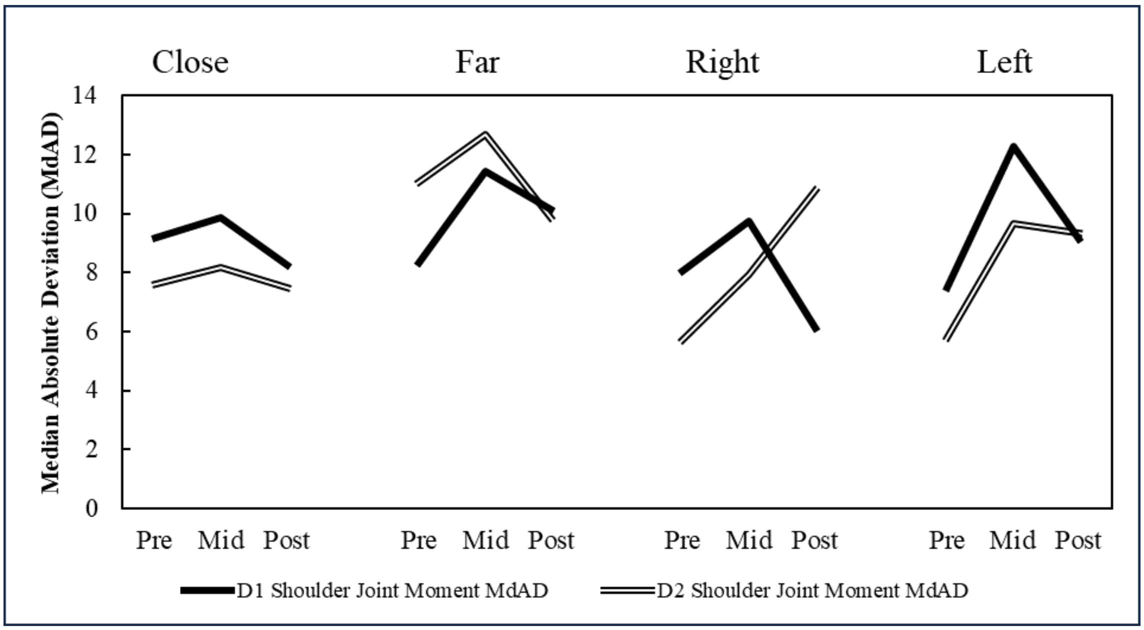

Figure 4.10. **Shoulder joint flexion moment MdAD On day 1 and day 2 at "Pre-Fatigue", "Mid-Fatigue", and "Post-Fatigue".**

Table 4.4. **Summary of baseline and fatigue-related day-to-day changes observed following repeat exposure to an overhead work task completed until fatigue.** Greyed regions indicate regions that were not examined.

		Baseline Changes	**Day-to-day fatigue-related changes**
EMG	*MPF*		• No significant differences
	RMS		• 21% decrease in serratus anterior normalized amplitude
Upper Limb Kinematics	*Group-Mean Changes*	• 5.0° increase in thoracohumeral elevation • 8.6° increase in elbow flexion • 5.9° decrease in ulnar deviation	• Thoracohumeral elevation increased 93% less due to fatigue on day 2. • Elbow flexion increased 75% less due to fatigue on day 2
	Variability		• Decreases in scapulothoracic and thoracohumeral variability • Increases in elbow and wrist variability
Static Shoulder Joint Flexion Moment	*Group-Mean Changes*	• No significant differences	• Static shoulder flexion moment exposure decreased 75% less due to fatigue on day 2
	Variability		• Variability changes between days were target-dependent

4.4. Discussion

4.4.1. Summary

This study sought to assess day-to-day muscle fatigue patterns and kinematic adaptations to an occupationally relevant overhead work task design to fatigue shoulder musculature. Specifically, musculoskeletal variability between days was assessed across three aspects: (1) between unfatigued, baseline postural states, (2) across fatigue-related changes from baseline, and (3) with respect to quantifying changes in fatigue-related kinematic and kinetic variability. While shoulder elevation, elbow flexion, and wrist deviation static joint angles were different at baseline on day 2 compared to baseline day 1, we found no significant changes in baseline static shoulder flexion moment exposures between day 1 and day 2. Thus, we partially accept our hypothesis as baseline joint angles, but not shoulder joint flexion moments, were different between days. Next, contrasting to our hypothesis, ΔMPF was highly variable and not significantly different between days, yet serratus anterior ΔRMS showed a significant reduction on day 2. Lastly, we hypothesized that on day 2, both upper limb joint angles and static shoulder flexion moments would deviate from baseline less on day 2; thereby displaying reduced variability. Thoracohumeral elevation and elbow flexion kinematics did deviate less from baseline on day 2, as did static shoulder flexion moment. We also expected a reduction in fatigue-related joint angle variability and shoulder flexion moment variability on day 2. Yet, while scapulothoracic and thoracohumeral joint kinematics demonstrated reduced variability with fatigue

(MdAD) from day 1 to day 2, elbow and wrist variability tended to increase between days. Day-to-day trends in static shoulder joint flexion moment variability increased at the *far* and *right* targets but decreased at the *close* and *left* targets.

4.4.2. Differences in Baseline Kinematic and Kinetic Between Days

Baseline upper limb kinematics and kinetics, recorded prior to completing the overhead drilling task to fatigue, were compared between the two testing sessions completed one week apart. Differences in baseline upper limb joint angles between sessions suggested that the experience of performing the specific overhead task until fatigue during the first visit may have promoted upper limb kinematic adaptations [Monjo, Terrier, and Forestier, 2015; Hirashima and Oya, 2016]. In conjunction with past research investigating the modulation of anticipatory postural adjustments under dynamic and changing conditions, these findings may contribute to the narrative that the postural system can anticipate biomechanical conditions, and update from experience [Desmurget and Grafton, 2000]. While many previous works have demonstrated the ability of the nervous system to adapt its postural responses due to immediate changes in temporal constraints [Desmurget and Grafton, 2000; Aruina, 2006] and changes in perturbation magnitude or direction [Bouisset, Richardson, and Zattara, 2000], the current study may also infer that learned postural adjustments can be maintained up to 7 days later.

Interestingly, all significant baseline kinematic changes between days were related to the joint axis most associated with end effector placement in the sagittal plane, and no kinematic changes were observed that would alter the hand position mediolaterally. An increase in thoracohumeral elevation, in particular, was unexpected, as raising the arm would act to increase the upper arm moment and the task effort [Slobounov, Hallett, and Newell, 2004] and evidence that increased arm posture is associated with increase perceived effort (relative perceived discomfort scale), although the same study found no changes in EMG measures of fatigue (including MPF) with arm height [Sood, Nussbaum, and Hager, 2007]. Interestingly, the increase in baseline thoracohumeral elevation was not associated with a change in baseline shoulder joint flexion moments between day 1 (37.7Nm) and day 2 (36.0Nm). It is likely that the expected increase in shoulder flexion moment due to thoracohumeral elevation was offset by postural reorganization at other joints in effort to not raise the total shoulder joint flexion moment. Indeed, elbow flexion and wrist deviation both displayed changes at baseline on day 2 that would reduce the shoulder moment, with an 8.6° increase in baseline elbow flexion, and a 5.9° decrease in baseline ulnar wrist deviation. Overhead working tasks are also expected to interpose the tissues of the SAS and promote rapid fatigue and discomfort which would be relieved with lowering of the humerus [Bey, et al., 2007; Graichen et al., 2001; Nakajima, et al., 1994; Lewis, Green, and Wright, 2005; Grieve and Dickerson, 2008]. However, it may be that the demands of the current work task, specifically the fixed overhead orientation of the drilling targets, may have been too incompliant as to allow significant lowering of the humerus to relieve subacromial tissue stress, thus necessitating an alternative strategy.

4.4.3. Fatigue-Related Changes Between Days

Fatigue-induced joint kinematic changes from the overhead drilling task were smaller for the second session compared to the first. These day-to-day changes in thoracohumeral elevation and elbow flexion could be motivated by a learning effect on day 2, as day 2 elbow flexion started closer to it's day 1 post-fatigue position [Monjo, Terrier, and Forestier, 2015; Hirashima and Oya, 2016]. Yet the hypothesis that day 2 kinematics converged toward a similar strategy demonstrated at post-fatigue on day 1 seems unsupported by the day-to-day changes in thoracohumeral elevation which started 5° lower at baseline on day 1 and proceeded to lower by 5.7° with fatigue, yet day 2 presented with an elevated baseline posture that changed minimally by 0.4° with fatigue. Conversely, the reduction in fatigue-induced changes in shoulder and elbow angles across successive days of the fatiguing exposure may suggest a convergence across participants from their individually diverse motor strategies on day 1, towards a more common, learned motor strategy on day 2 that may not necessarily consolidate fatigue-related postural changes featured during day 1 [Scholz and Schöner, 1999; Magill and Anderson, 2010].

The relatively small changes in shoulder and elbow joint angles on day 2 may indicate that changes in baseline kinematics were mechanically advantageous, however time to fatigue, between-day changes in ΔMPF (figure 4.5.a), and baseline shoulder joint flexion moments showed no significant changes. The only results that reflect a potential improvement in muscular and kinematic strategy is the reduction in serratus anterior ΔRMS on day 2 (figure 4.5.b), and the 10% increase in maximal drill press force on day 2. While limited literature exists on day-to-day kinematic and muscle activity changes during fatiguing manual tasks, one study [Ebata, 2012], previously investigated upper limb kinematic changes on successive attempts of an overhead drilling task and similarly showed that the humerus was 5° more elevated on the second day attempting the drilling task. Together with this study, these similar findings suggest that modest humeral elevation may permit a more efficient total arm strategy during overhead work. One potential motivation for elevating the thoracohumeral angle on day 2 posture may be to improve elbow flexor muscle length for elbow force production, which appears to be most optimally recruited at 70°-75° of humeral elevation [Moon, et al., 2013; Langenderfer, et al., 2005]. Coincidentally, overhead drilling has been previously identified as a particularly demanding task for the biceps brachii, demonstrating high myoelectric activity in overhead drilling postures that require extension of the elbow [Anton, et al., 2001]. Thoracohumeral elevation may also improve load sharing between the deltoid and RC muscles, while negligibly impacting the deltoid muscle force-length relationship [Bechtol, 1980; Breteler, Spoor, and Van der Helm, 1999].

Shoulder joint flexion moments may have also been a driving factor of upper limb postural adaptations on day 2 as, similar to kinematics, fatigue-related changes in shoulder flexion moments deviated less from baseline on day 2. Specifically, within day fatigue-related changes in shoulder flexion moment were larger on day 1 (-3.2ΔNm compared to day 2 (-0.8 ΔNm). The small decrease in baseline shoulder joint flexion moment from day 1 (37.7Nm) to day 2 (36.0Nm) together with the marginal increase in pre-fatigue to post-fatigue shoulder flexion moment on day 2 results in a post-fatigue shoulder joint demand that was similar between day 1 (34.5Nm) and day 2 (35.2Nm). This could indicate that a more efficient kinetic strategy was unable to be found on day 2. Qin et al. [2014] previously studied upper limb joint angle and joint torque changes between the first and last session of a light, below chest height, assembly work task performed by both younger and older participants and reported that shoulder, elbow, and wrist joint moments reduced due to task related fatigue. This further suggests that the reduction of shoulder joint moments is a criterion driving upper limb postural adaptations, yet further work is needed to understand how postural adaptations of manual work may differ when completed on subsequent days.

The proportion of individuals who displayed increased ΔMPF on day 2 compared to day 1 in the current study ranged between 26-54% across muscles, and those displaying increased ΔRMS on day 2 compared to day 2 ranged from 50-70% across muscles, suggesting that muscle fatigue accumulation during overhead tasks is variable within individuals. These findings of considerable intra-participant and inter-participant variability in neuromuscular fatigue responses are supported by Mulla et al. [2018], and they have been suggested to arise from many DOF and musculoskeletal redundancy of multiple muscles at the shoulder [Madeleine, 2010; Hirashima and Oya, 2016]. Findings from past research similarly suggest that muscle fatigue during overhead tasks is highly variable between individuals [Ebata, 2012; McDonald et al., 2019]. Such considerable variability both between and within individual neuromuscular fatigue responses may make group-wise differences more difficult to detect with statistical tests. Further research investigating global shoulder fatigue tasks (e.g. those which are not designed to isolate fatigue accumulation on a discrete set of muscles), should consider using multiple indicators of fatigue (MPF, RMS, COV), or utilize the shoulder-specific multi-muscle fatigue score [McDonald, Mulla, and Keir, 2018] to more confidently evaluate the presence of fatigue.

4.4.4. Kinematic and Kinetic Variability Changes Between Days

Comparisons of fatigue-related variability between days suggest that changes in fatigue-related kinematic variability on day 2 appeared joint dependent, with the scapulothoracic and thoracohumeral joints displaying decreased variability, and the elbow and wrist displaying increased variability. Scapulothoracic, thoracohumeral, and elbow joints prominently featured one degree of freedom with the most variability on day 1; those being scapulothoracic protraction, thoracohumeral POE, and elbow pronation. These same upper limb DOF showed substantial reductions in variability on day 2, with a reduced MdAD within the range of the other DOF. Interestingly, these upper limb DOF do not adjust for end effector position in the sagittal plane. While day-to-day changes in these joint angles did not reach significance, the substantial change in variability could suggest that these particular DOF of the upper limb have the most redundant kinematic solutions to this specific task. Yet on day 2 participants still converge on less variable postures despite the higher variability on day 1, suggesting that other joint angle configurations and muscle synergies exist which should achieve the same task performance [Scholz and Shoner, 1999]. This suggests that some system variable aside from target accuracy and force output would have constrained the variability observed at these DOF. Reductions in muscular and kinematic redundancy in humans are posited to arise from an optimization function that reduces the motor effort [Hirashima and Oya, 2016], which aligns with the observed reductions in shoulder flexion moments observed on day 2. Interestingly the same pattern did not emerge for the wrist joint, as there was no prominent degree of freedom with heightened variability on day 1.

This could suggest that, unlike the other joints of the upper limb, task performance (e.g. 50% upward force production) was the most sensitive to wrist kinematics and permitted the least variation. Another way to explain this finding is that the muscular or kinematic strategies available to the wrist which satisfied the task requirements of the drilling task may have featured much less redundancy than the other upper limb DOF, thereby constraining the observed kinematic variability at the wrist joint. While shoulder and scapular kinematic adaptations to fatigue have been reported to be highly variable [Chopp-Hurley, et al., 2016; Mulla, McDonald, and Keir, 2018], the current study suggests that individual adaptations to fatigue may ultimately elicit lower group variability, expressed by MdAD on a repeated session of fatiguing shoulder work.

Both the effects of fatigue and day-to-day changes appeared to have differing effects on kinetic variability which appeared to be dependent on the overhead target position, making it difficult to draw inferences (figure 4.10.). However, it is interesting to note that for all targets, kinetic variability peaked at the “mid-fatigue” time point on both days. Further, most targets showed a convergence in kinetic variability at “post-fatigue” on each day. The only instance where this was not observed was in the *right* target, where variability continued to rise after “mid-fatigue” on day 2 but dropped off at “mid-fatigue” on day 1. One possible speculation is that participants may have experienced less fatigue at the *right* target compared to the other targets on day 2, thus variability did not yet begin to drop but conceivably would have lowered if they have been able to continue the task.

4.4.5. Limitations

Certain limitations of this research should be considered. The fatigue protocol was completed in an average time of 29.3 (range: 16 to 64) minutes on day 1 and 29.5 (range: 10.7 to 64) minutes on day 2, therefore the findings of this study may not reflect that of an 8-hour workday. Due to the high degree of variability inherent with shoulder postural control, sex-based analysis would be underpowered with a sample of 29 participants. Results from this study are generalized across males and females, however sex-specific results should be investigated further as differences in muscle force-generating capacity, fatigue resistance, perfusion, hormone concentration, and many other factors are likely to contribute to the observed variability. The current study also only considered joint postures distal to, and including, the scapulothoracic joint. Future analyses may reveal more complex kinematic compensations to overhead task fatigue by employing a multivariate model that considers interactions between upper limb, trunk, and lower limb postural changes. Regarding the measurement of EMG data, RC muscle activity was recorded using both intramuscular (iEMG) and surface (sEMG) methods, in an attempt to characterize signal activity changes which may differ across recording methods due to limitations with the respective signal sensitivity and specificity [Merletti and Farina, 2009; Rainoldi et al., 1999]. Further, sEMG recordings of serratus anterior have been shown to be highly posture dependent [Hackett et al., 2014]. While we endeavoured to select a serratus anterior muscle test (high flexion) which shows good comparisons between iEMG and sEMG amplitude [Ginn, Halaki, and Cathers, 2011], variations in participant posture could introduce variability between tests. Regarding the processing of three-dimensional Euler angles, we decomposed thoracohumeral motion with a YXY sequence to maintain ISB standards, yet discontinuities associated with gimbal lock and other limitations have been noted; particularly at low levels of thoracohumeral elevation [Phadke et al., 2011]. In the current study, thoracohumeral elevation was near 90°, yet readers should be aware of bias and error associated with the Euler decomposition order for three-dimensional joint angles, with particular challenges being noted at the thoracohumeral and glenohumeral joints. Also concerning the kinematic and kinetic results presented, due to the comparison of kinematic data across day, target, and pre-fatigue to post-fatigue, pairwise removal of outliers resulted in 0-8 Δ joint angle scores being removed for each kinematic degree of freedom of the upper limb. The impact of removing these data on the results presented in this study are uncertain.

4.5. Conclusion

This study sought to identify the variability in muscle fatigue profiles and kinematic and kinetic strategies in response to an identical overhead shoulder fatigue task performed on successive days, one week apart. Upper limb kinematics showed significant changes in baseline joint angles on day 2, which also deviated less from baseline as fatigue accumulated. Baseline shoulder joint flexion moments did not change between days, yet static shoulder flexion moment exposures on day 2 showed a lower fatigue-related change compared to day 1. Kinematic variability generally increased with fatigue at all joints, yet day-to-day changes in fatigue variability were joint specific. Kinetic variability showed evidence of higher variability at mid-fatigue, and a convergence towards similar variability at post-fatigue on both days. While upper limb DOF responsible for positioning the end effector position in the sagittal plane showed significant changes in fatigue-related kinematic changes between days, DOF that do not directly motivate end effector changes in the sagittal plane displayed the greatest variability. Changes in baseline upper limb posture and decreases fatigue-related joint angle imply a learning effect aimed at sustaining a decreased shoulder joint flexion moment on day 2. However, adaptations to occupational overhead tasks require further examination, potentially focused on continuous or short-duration postural adaptations (adaptations within a work cycle, sampled over time). Future work should study trunk and lower limb kinetic and muscular strategies, as well as COM/pressure relationships, subjective factors (rate of perceived exertion/discomfort), and variability structure and entropy with overhead work tasks in order to fully understand how task variability is influenced by attempts on successive days.

Afterword to chapter 4

The study in chapter 4 sought to build on the substantial variability observed in chapter 3 by investigating how participants alter their motor strategies with task experience. This chapter found that variability did appear to be constrained when completing the fatiguing task for a second time. Specifically, comparisons to day 1 revealed that kinematic variability in the frontal plane was reduced on day 2. These findings align with models of CNS control that hypothesize that variability is only expressly controlled along dimensions that relate to task accuracy, as we observed variability changes in kinematic DOF orthogonal to the sagittal plane. These findings complemented significant kinematic changes in the sagittal plane at the shoulder, elbow, and wrist. Perhaps most interesting was the significant observed decrease in serratus anterior amplitude on day 2. This finding may be of particular significance as the dimensionality of available muscle recruitment solutions exceeds that of the available kinematic DOF. Thus, a significant decrease in muscle recruitment and potentially fatigue may reflect a higher-order optimization goal. The importance of serratus anterior as the most mechanically efficient scapular muscle for generating upward scapular rotation for sagittal plane arm tasks may suggest that repeat exposure to the fatigue task prompted muscle activity changes which sought to preserve this key muscle.

Foreword to Chapter 5

Collectively, chapters 3 and 4 demonstrate that among a relatively homogenous cohort of young, healthy adults, group-mean trends in shoulder muscle control and fatigue responses remain challenging to detect. In chapter 3, it was revealed that a bimodal distribution of scapulothoracic changes to a fatigue task may conflate this variability. In chapter 4, variability also appeared to be an important factor for task learning to determine the extent of available kinematic solutions before consolidating the most optimal solutions on day 2. These findings suggest mechanisms for both between and within individual variability.

Our approach in chapter 5 pivoted away from characterizing population-level variability present in shoulder fatigue tasks. Instead, we sought to reduce our observations from a representative population sample, down to a single comprehensive computational shoulder model. The intent was to remove the variability inherent in a population-level analysis of redundant muscle control strategies which may be too challenging to characterize without methods to constrain some variability. In chapter, we apply a deterministic approach to quantify how specific fatigue stimulus (simulated as a reduction in muscle force-generating capacity) will alter kinematics and muscle control, while avoiding potential measurement errors associated with kinematic motion tracking and EMG for quantifying muscle activity. In the following chapter, terms fatigue and weakness are synonymous due to the mechanistic nature of the model presented.

Chapter 5. Shoulder Kinematic and Muscle Activity Compensations to Scapular Stabilizer Weakness: An Optimal Control Framework.

Matthew S. Russell[1], Daanish M. Mulla[1,2], Peter J. Keir[2], Edward K. Chadwick[3], Dimitra Blana[4], Janessa D.M. Drake[1], Jaclyn N. Chopp-Hurley[1]

[1] School of Kinesiology and Health Science, York University, Toronto, Canada
[2] Department of Kinesiology, McMaster University, Hamilton, Canada
[3] School of Engineering, University of Aberdeen, Aberdeen, United Kingdom
[4] Aberdeen Centre for Health Data Science, University of Aberdeen, Aberdeen, United Kingdom

Corresponding Author:
Jaclyn Hurley, PhD
School of Kinesiology and Health Science
York University
4700 Keele Street, Toronto, Ontario, CA, M3J 1P3
Email: jnhurley@yorku.ca

Declarations of Interest: None

Funding Sources: This work was supported by the Natural Science and Engineering Council (NSERC) Discovery Grant program (J.N. Chopp-Hurley and J.D.M. Drake) and the NSERC Post-Graduate Scholarship program (M.S. Russell).

5.1. Introduction

High variability in shoulder muscle activity often precludes the ability to make clear inferences on the effects of targeted muscle stimuli on upper limb kinematics. This variability is likely consequent of the highly redundant muscular and kinematic DOF at the shoulder; a purposeful evolutionary trait in primates which offers an enhanced landscape of potential solutions to nearly every upper limb task [Bernstein, 1966; Sohn and Ting, 2018; MacLean, Langenderfer, and Dickerson, 2023; Mulla and Keir, 2023]. Scapulothoracic kinematic variability has challenged the characterization of normal/healthy, and abnormal/unhealthy scapulothoracic kinematics and muscle synergies [Phadke, Camargo, and Ludewig, 2009; Chopp and Dickerson, 2012; Chopp-Hurley, et al., 2016; McQuade, Borstad, and de Oliveira, 2016]. Recent works have even proposed a critical perspective that shoulder muscle stability and coactivation patterns which consider upper trapezius dominance and lower trapezius and serratus anterior weakness to be 'unhealthy' may in fact be a product of the morphological and anthropomorphic variability in scapular shape and muscle moment arms which promote a vast distribution of 'normal/healthy' shoulder muscle activity and kinematics [Levin, 1997; Levin, 2005; McQuade, Borstad, and de Oliveira, 2016].

A caveat of the inherent variability associated with scapulothoracic kinematics is that it can be difficult to characterize the kinematic contributions of individual shoulder muscles, which could help identify how the redundant set of shoulder joint effectors compensate for muscle weakness and fatigue. Scapulothoracic kinematics changes associated with fatiguing stimuli – stimuli that would transiently reduce the force-generating capacity of muscles which attach to the scapula - have been frequently reported in the literature [Ebaugh, McClure, and Karduna, 2006; Suzuki, et al., 2006; Szucs, Navalgund, and Borstad, 2009; Chopp-Hurley, et al., 2016; Mulla, McDonald, and Keir, 2018; Umehara, et al., 2018]. Interventions and protocols which attempt to fatigue an isolated set of one or more of the scapular stabilizer muscles (upper trapezius, middle trapezius, lower trapezius, serratus anterior) [Cools, et al., 2004; Cools, et al., 2007; Borstad, Szucs, and Navalgund, 2009; Chopp, Fischer, and Dickerson, 2011; Noguchi, et al., 2013; Chopp-Hurley, et al., 2016], RC muscles (supraspinatus, infraspinatus, subscapularis, teres minor) [Chopp, et al., 2010; Mulla, McDonald, and Keir, 2018], or tasks which focalize stress on the global shoulder musculature [Ebaugh, McClure, and Karduna, 2006; McDonald, Tse, and Keir, 2016; Tse, McDonald, and Keir, 2016; McDonald, et al., 2018; Russell, et al., 2024], are frequently reported to further augment scapulothoracic kinematic variability. Chopp-Hurley et al. previously reported highly variable changes in scapulothoracic kinematics in participants who completed a RC and scapular stabilizer muscle fatigue task [Chopp-Hurley, et al., 2016]. Fatigue induction involved lifting and lowering the arm between 60° and 120° thoracohumeral elevation in the frontal plane, while prone, with a handheld load equal to 10% of their maximal abduction force. Participants continued this task at 44 bpm, 15 seconds moving, 10 seconds resting (60% duty cycle) until they verbally indicated volitional fatigue. Results indicated that upper trapezius, lower trapezius, serratus anterior, supraspinatus, infraspinatus, and subscapularis all displayed significant decreases in EMG MPF. Importantly, scapulothoracic joint angle standard deviations ranged from 16°-27° across 5 angles of thoracohumeral elevation and the three scapulothoracic DOF [Chopp-Hurley, et al., 2016]. Such magnitudes of kinematic variability have the potential to obscure significant fatigue-related relationships by decreasing the calculated p-value of traditional hypothesis-based statistical tests. Similar levels of variability are consistent with other reports [Ebaugh, McClure, and Karduna, 2006; Borstad, Szucs, and Navalgund, 2009; Chopp, Fischer, and Dickerson, 2010], which may be considerable when the subacromial tissue thickness averages only 6 mm [Michener, et al., 2015], and changes in static scapulothoracic angle of only 5° may be clinically meaningful for injury risk [Ebaugh, McClure, and Karduna, 2005; Watson, et al., 2005; McClure, Greenberg, and Kareha, 2012]. However, no single, ubiquitous shoulder muscle fatigue protocol is used in literature. Rather, comparisons of shoulder muscle fatigue-related effects across literature are limited by the many different fatigue protocols that are exercised. Technical limitations regarding the apparent error in skin-based scapular motion tracking [Shaheen, Alexander, and Bull, 2011; Grewal, Cudlip, and Dickerson, 2017], EMG artefacts and errors due to muscle movement underneath the skin [Ekstrom, Soderberg, and Donatelli, 2005], and the difficulty to capture and characterize the full breadth of muscles which contribute to shoulder motion due to their number, many partitions [Cudlip and Dickerson, 2018; Cudlip, Kim, and Dickerson, 2020], and depth [Waite, Brookham, and Dickerson, 2010] may limit a comprehensive understanding of the kinematic-muscular relationship at the shoulder.

Computational musculoskeletal modelling tools may offer comprehensive insights into the muscular-kinematic relationship at the shoulder. Such models replace observations of empirical data from an in vivo model with simulated data which is derived from a set of biomechanical equations, constraints, and assumptions about the biomechanical system [Baker, et al., 2018; Bassani and Galbusera, 2018]. One of the most extensively cited computational shoulder models, the Delft Shoulder and Elbow Model (DSEM) [Van der Helm, 1994], is regarded for its anatomical fidelity which has been bolstered with three decades of model validation and updates [van der Helm, Chadwick, and Veeger, 2001; Nikooyan, et al., 2010; Asadi Nikooyan, et al., 2011; Chadwick, et al., 2014]. An implicit method for rapidly formulating optimal control problems harnessed with standard nonlinear program solvers [Gill, Murray, and Saunders, 2005; Wächter and Biegler, 2006] has been integrated with a current version of the DSEM to offer upper limb optimal control solutions within 6-24 hours [Chadwick, et al., 2008; Van Den Bogert, Blana, and Heinrich, 2011]. Such timeframes were previously unachievable, hindered by mechanically stiff musculoskeletal elements which required timesteps 1500 times smaller to solve using ordinary differential equations [Van Den Bogert, Blana, and Heinrich, 2011; Chadwick, et al., 2014]. These advancements in optimal control allow for more rapid tuning and validation of simulations, making optimal control predictions more accessible for exploring the muscle-kinematic relationship at the shoulder. Optimal control simulations also provide a single, deterministic set of simulation data, rather than a potentially variable distribution of empirical observations, and are not limited by technical challenges associated with motion capture and EMG method, potentially offering a comprehensive view of shoulder muscle function that was previously elusive.

The purpose of this study was to use a computational musculoskeletal model of the shoulder to predict scapulothoracic kinematics changes associated with isolated reduced force-generating capacity of the scapular stabilizer muscles. Secondary aims of this study were (1) to determine the model-predicted scapular stabilizer muscle activity compensations associated with isolated reductions in force-generating capacity of the scapular stabilizer muscles, and (2) investigate whether simultaneous reduction in lower trapezius and serratus anterior force-generating capacity will evoke upper trapezius dominance, and determine whether these compound reductions in multiple muscle force-generating capacity elicits an additive effect on muscle activity compensations.

5.2. Methods

5.2.1. Model Selection

A version of the TU Delft musculoskeletal shoulder model which contains 138 muscle elements, characterizing 25 muscles of the shoulder and elbow, was used in this research. Thoracohumeral movements were modelled as motion across the sternoclavicular, acromioclavicular, and glenohumeral anatomical joints, while scapulothoracic joint motion was consequent of motion at the sternoclavicular and acromioclavicular anatomical joints (table 5.1.; figure 5.1.).

The DSEM was previously built in SIMM (MusculoGraphics, Inc.), and later imported into OpenSim [Delp, et al., 2007] to generate polynomial approximations of muscle moment arm and length [Blana, et al., 2008]. Blana and colleagues [Blana, et al., 2008] previously used published cadaveric data [Breteler, Spoor, and Van der Helm, 1999] to characterize model joint centers, body segment inertias, the number of necessary muscle elements for each muscle, optimal fiber lengths, origins, and insertions, tendon slack lengths, physiological cross-sectional area, and element pennation angle. It is available open-source from the SimTK repository for use with OpenSim. The model-specific equations for musculoskeletal dynamics are well and thoroughly described previously [Van Den Bogert, Blana, and Heinrich, 2011], therefore the methodology will focus on describing the optimal control formulation and validation of the model performance.

Table 5.1. **Model degrees of freedom definitions and equivalent degree of freedom (DOF) notation as recommended by the International Society of Biomechanics** (Wu, Van der Helm et al. 2005).

Model Anatomical DOF	Equivalent ISB DOF	ISB DOF Definition
TH_x	$e1$: α_{GT}	Thorax flexion about the Z-axis of the global coordinate system.
TH_y	$e3$: γ_{GT}	Thorax axial rotation about the Y-axis of the global coordinate system.
TH_z	$e2$: β_{GT}	Thorax lateral flexion about the X-axis of the global coordinate system.
SC_x	$e3$: α_{SC}	Sternoclavicular axial rotation about the Z-axis of the clavicular local coordinate system.
SC_y	$e1$: γ_{SC}	Sternoclavicular protraction about the Y-axis of the proximal

		thorax local coordinate system.
SC_z	*e*2: β_{SC}	Sternoclavicular elevation about the common axis perpendicular to *e*1 and *e*3 of the sternoclavicular joint.
AC_x	*e*3: α_{AC}	Acromioclavicular tilt about the Z-axis of the scapular local coordinate system.
AC_y	*e*1: γ_{AC}	Acromioclavicular retraction about the Y-axis of the proximal clavicle.
AC_z	*e*2: β_{AC}	Acromioclavicular medial rotation about the common axis perpendicular to *e*1 and

		*e*3 of the sternoclavicular joint.
GH_y	*e*1: γ_{GH1}	Glenohumeral POE about the Y-axis of the scapular local coordinate system.
GH_z	*e*2: β_{GH}	Glenohumeral elevation about the X-axis of the humerus
GH_yy	*e*3: γ_{GH2}	Glenohumeral internal or axial rotation about the Y-Axis of the humerus.
Trunk_Hum_y	*e*1: γ_h	Thoracohumeral POE about the Y-axis of the thoracal local coordinate system.
Trunk_Hum_z	*e*2: β_h	Thoracohumeral elevation about the X-axis of the humerus.

Trunk_Hum_yy	$e3$: $(\gamma_h)_2$	Thoracohumeral internal rotation about the Y-axis of the humerus.
EL_x	$e1$: α_{HFo}	Elbow flexion about the Z-Axis of the proximal humeral local coordinate system
PS_y	$e3$: γ_{HF}	Elbow pronation or axial rotation of the forearm about the Y-axis of the forearm local coordinate system.

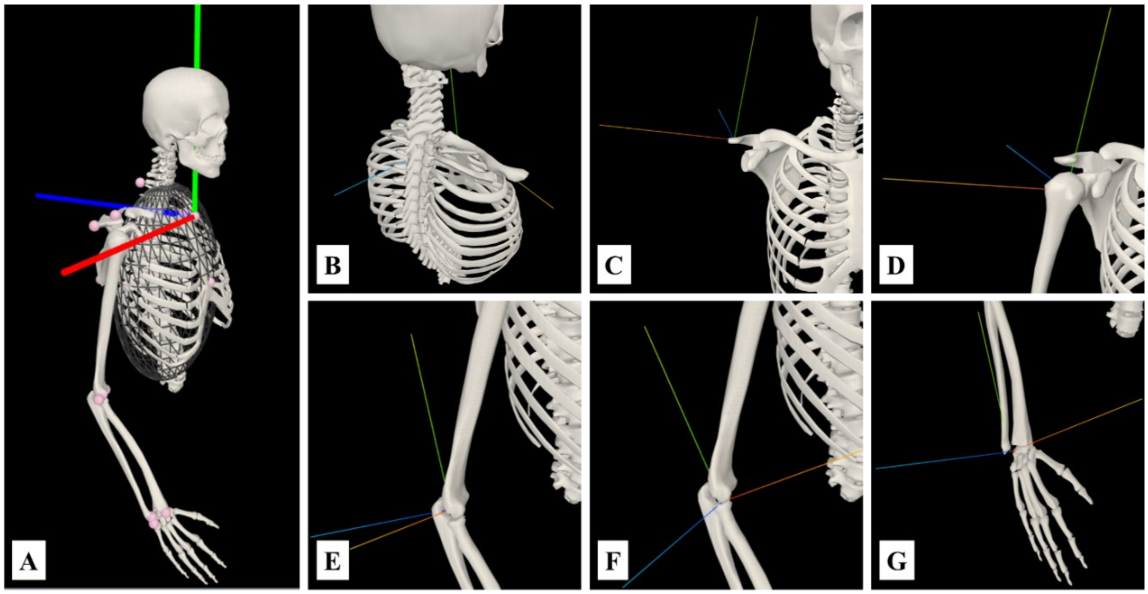

Figure 5.1. **Visualization of the model global coordinate system and the local coordinate system of each rigid body in the model.** X-axis illustrated in red, Y-Axis illustrated in green, and Z-axis illustrated in blue. A. The global coordinate system superimposed over the thorax local coordinate system – they are identical in this frame B. clavicle C. scapula D. humerus E. ulna F. radius G. hand

5.2.2. Degrees of Freedom and Optimal Control Solutions

Multibody system kinetics can be related to system kinematics using the generalized equation of motion (equation 5.1.). Within a multibody system with m number of actuators such as muscles, and n number of kinematic DOF's such as an anatomical joint, kinematic motion about the DOF can be formulated as:

$$\tau = R(q)F_0^{MT}a = M(q)\ddot{q} + C(q,\dot{q}) + G(q) + J^T\tau_{end}$$

Equation 5.1. **Generalized Equation of Motion.**

Where,

τ represents the matrix of joint forces and torques and the values,

q, $\dot{q}$, $\ddot{q}$ and represent generalized kinematic coordinates, velocities, and accelerations, respectively,

$R(q)$ stands for an n x m matrix of actuator (muscle) moment arms,

F_O^{MT} is an m x 1 matrix of maximal musculotendon forces subject to muscle length and velocity coefficients, which is multiplied by a, an m x 1 vector of muscle activations which range from 0 (no activation) to 1 (maximum),

$M(q)$ is the inertial matrix which is multiplied by $\ddot{q}$ to obtain inertial force required to generate acceleration $\ddot{q}$ and describe how the mass of a multibody system imposes joint torques which resist change in motion,

$C(q,\dot{q})$ is the vector of Coriolis forces that arise due to the interactions of the velocities on the individual bodies in the multibody system and the resulting joint forces,

$G(q)$ represents the force of gravity and the resulting torques imposed on each joint in the multibody system.

$J^T\tau_{end}$ which utilizes the transpose ^{T} of the Jacobian J to map generalized joint torques τ to the cartesian space approximation of the end effector

Since human models present a set of available muscle activation variables $a(m)$ to be solved which always exceeds the number of constrains which are the kinematic DOF n, this presents an indeterminate problem-set of solutions [Mulla and Keir, 2023]. In other words, humans have a range of possible muscle activations that they can employ to achieve a feasible solution to the imposed task constraints and requirements (equation 5.1.), presenting a problem of indeterminacy when attempting to predict how humans will actually move which is a long-identified challenge of human motor control theories [Bernstein, 1966]. Direct collocation methods can be harnessed to find an optimal solution for a set of time-varying control trajectories which satisfy muscular and kinematic requirements that optimize a set of cost-function criteria. Here the control variable u represents neural excitation supplied to the muscle. Neural excitation is proportional to muscle activation/deactivation (a) through a non-linear function which describes the electro-chemical relationship [He, Levine, and Loeb, 1989]:

$$\dot{a} = (u - a)(c_1 u + \ c_2)$$

Equation 5.2. **Mathematical model of muscle activation and deactivation time delay.**

Where c_1 and c_2 represent the rate constants of activation-deactivation and deactivation, respectively. The direct collocation methods discretize the continuous state (q) and control (u) trajectories of the system dynamics into n nodes of equal temporal spacing along the time duration of the model motion:

$$\textit{for } i = 1 \textit{ to } N\text{-}1:$$

$$C_i \equiv f\left(\frac{q_{i+1} + \ q_i}{2}, \frac{q_{i+1} - q_i}{t_{i+1} - t_i}, \frac{u_{i+1} + u_i}{2}\right) = 0$$

Equation 5.3. **Midpoint discretization method for temporal spacing of state and control variables.**

Where N is the number of nodes for direct collocation, the system dynamics constraints at time point i (C_i) are subject to approximate midpoint finite differences for the (1) the coordinates q_i and q_{i+1} $(q_{i+1}+ q_i/2)$, (2) the rate of change of q over the interval t_i to t_{i+1} $(q_{i+1}-q_i/t_{i+1} -t_i)$, and (3) the control variable (muscle activation) a_i and a_{i+1} $(a_{i+1}+a_i/2)$. These state and control variables are also subject to find solutions which satisfy the following constraints:

$$\text{[Eq. 4.1] } f(q,\dot{q},u) = 0$$

$$\text{[Eq. 4.2] } u_{Lower} \leq u \leq u_{Upper}$$

$$\text{[Eq. 4.3] } T_i\big(q(t),u(t)\big) = 0$$

Equation 5.4. **State and control variable constraints.**

where the implicit state equation f(q, q̇, u) must enforce dynamic equilibrium across the model predicted displacement (q), velocity (q̇), and muscle excitation (u) , subject to constraints on muscle activity (u_{lower}, u_{upper}), and constraints relative to the task (T_i) such as duration and workspace.

Adhering to the kinematic and muscle activation constraints listed, the optimization function employs gradient descent subject to minimize four terms: (1) mean-squared error of any input kinematic variables $\sum(qPred_i - qMeas_i)^2N$, (2) the sum of the cube of the estimated muscle activations $\sum(a_i)N^2$ [Erdemir, et al., 2007; Dickerson, Hughes, and Chaffin, 2008], (3) a constraint term representing the mean deviation of the anterior face of the scapula from the wall of the thorax $\sum(Cscap)N$, and (4) a constraint term representing the mean deviation of the head of the humerus from the centre of the glenoid cavity $\sum(Cgh)N$. Both the scapulothoracic constraint and the glenohumeral constraint have been described previously [Chadwick, et al., 2014]. Each of these terms are subject to coefficients w that weight the relative error of each term, such that the objective function appears as presented (equation 5.5):

$$Minimize\ f\big(q(N), \dot{q}(N), u(N)\big)$$
$$= \left(w_1 \cdot \sum\big(qPred(N) - qMeas(N)\big)^2\right) + \left(w_2 \cdot \sum(a_i)N^2\right) + \left(w_3 \cdot \sum(Cscap)N\right) + \left(w_4 \cdot \sum(Cgh)N\right)$$

Equation 5.5. **Algebraic cost function formulation.**

5.2.3. Prescription and Validation of Predicted Model Solutions

Prior to simulating scapulothoracic kinematics changes associated with reduced muscle force generating capacity, we first sought to validate whether the current shoulder model and optimal control framework could produce accurate scapulothoracic kinematics predictions. Empirical scapulothoracic kinematics acquired from transcortical pin placement into the scapula, tracked with electromagnetic motion sensors during full range thoracohumeral elevation trials in the frontal thoracohumeral POE were provided by Ludewig and colleagues [Ludewig, et al., 2009]. By comparison, model predicted kinematics were produced by prescribing optimal control thoracohumeral elevation trials in the frontal, scapular, and sagittal planes of thoracohumeral elevation, which were defined as 0°, 40°, and 70° thoracohumeral plane of elevation angles, respectively. Empirical elevation trials were prescribed from a resting posture with the arm hanging at the side, to a maximal elevation which differed between participants. However, all participants achieved thoracohumeral elevation of at least 120° in each POE. Thus, model-predicted simulations were also prescribed from an initial resting position with the arm hanging at the side, to a final thoracohumeral elevation of 120°. Model thoracohumeral elevation was explicitly prescribed by inputting an array of thoracohumeral joint angles at every 0.375 second interval to approximate a bell-shaped velocity profile [Ludewig, et al., 2009; Ostry, Cooke, and Munhall]. 120° thoracohumeral elevation was chosen as the target model thoracohumeral elevation as it was the lowest ROM exhibited by participants in the empirical dataset. While time-varying data was not available to infer thoracohumeral angular velocity, typical, goal-direct velocity profiles demonstrate a geometrically equivalent bell-shape Ostry, Cooke, and Munhall, 1987]. Thus, to normalize the velocity of the model predicted elevations to the average velocity of the empirical dataset, thoracohumeral velocity began and terminated at 11.73°/s, with an initial acceleration of 70.4°/s^2 that decreased by -28.16°/s^3, to return the arm to a velocity of 0°/s after 2.625 seconds at 120° elevation. Direct collocation was set to achieve a solution in 16 nodes, spanning 2.625 seconds, thus each node represented 0.175 seconds. All participants in the in vivo research started thoracohumeral elevation from an initial posture with a thoracohumeral elevation angle between 10° to 15°, thus the model was set to initiate thoracohumeral elevation from 15°. Aside from the thoracohumeral angles set as input kinematic tracking variables, sternoclavicular elevation (SC_z) was tracked as an additional input variable using the average empirical sternoclavicular elevation data [Ludewig, et al., 2009]. This decision was made in order to constrain the higher dimensional space of available model solutions, particularly for predicting scapulothoracic elevation which is most associated with scapulohumeral rhythm of arm elevation compared to other scapulothoracic DOF [McQuade, Dawson, and Smidt, 1998; Ludewig, et al., 2009]. The exact kinematic tracking terms that were input for each plane of thoracohumeral elevation are detailed in (table 5.2.).

Table 5.2.1. **Input kinematic tracking variables to prescribe model thoracohumeral elevation in the frontal plane.** Numbers provided are joint angles in degrees (°). Bolded, shaded columns indicate variables that were locked*, such that they cannot be altered in the optimal control solver.

Time (sec)	TH _x	TH _y	TH _z	Trunk_ Hum_y	Trunk_ Hum_z	Trunk_ Hum_yy	SC _z	EL _x	PS _y
0	**0**	**0**	**0**	0	15	0	11	**0**	**5**
0.375	**0**	**0**	**0**	0	23	0	14	**0**	**5**
0.75	**0**	**0**	**0**	0	38	0	16	**0**	**5**
1.125	**0**	**0**	**0**	0	57	0	17	**0**	**5**
1.5	**0**	**0**	**0**	0	78	0	17	**0**	**5**
1.875	**0**	**0**	**0**	0	97	0	18	**0**	**5**
2.25	**0**	**0**	**0**	0	112	0	19	**0**	**5**
2.625	**0**	**0**	**0**	0	120	0	20	**0**	**5**

* TH_x, TH_y, TH_z, EL_x, PS_y were locked

Table 5.2.2. **Input kinematic tracking variables to prescribe model thoracohumeral elevation in the scapular plane.** Numbers provided are joint angles in degrees (°). Bolded, shaded columns indicate variables that were locked*, such that they cannot be altered in the optimal control solver.

Time (sec)	TH_x	TH_y	TH_z	Trunk_Hum_y	Trunk_Hum_z	Trunk_Hum_yy	SC_z	EL_x	PS_y
0	**0**	**0**	**0**	40	15	0	11	**0**	**5**
0.375	**0**	**0**	**0**	40	23	0	12	**0**	**5**
0.75	**0**	**0**	**0**	40	38	0	13	**0**	**5**
1.125	**0**	**0**	**0**	40	57	0	14	**0**	**5**
1.5	**0**	**0**	**0**	40	78	0	15	**0**	**5**
1.875	**0**	**0**	**0**	40	97	0	15	**0**	**5**
2.25	**0**	**0**	**0**	40	112	0	16	**0**	**5**
2.625	**0**	**0**	**0**	40	120	0	17	**0**	**5**

* TH_x, TH_y, TH_z, EL_x, PS_y were locked

Table 5.2.3. **Input kinematic tracking variables to prescribe model thoracohumeral elevation in the sagittal plane.** Numbers provided are joint angles in degrees (°). Bolded, shaded columns indicate variables that were locked*, such that they cannot be altered in the optimal control solver.

Time (sec)	TH _x	TH _y	TH _z	Trunk_ Hum_y	Trunk_ Hum_z	Trunk_ Hum_yy	SC _z	EL _x	PS _y
0	**0**	**0**	**0**	70	15	0	10	**0**	**5**
0.375	**0**	**0**	**0**	70	23	0	10	**0**	**5**
0.75	**0**	**0**	**0**	70	38	0	11	**0**	**5**
1.125	**0**	**0**	**0**	70	57	0	12	**0**	**5**
1.5	**0**	**0**	**0**	70	78	0	13	**0**	**5**
1.875	**0**	**0**	**0**	70	97	0	13	**0**	**5**
2.25	**0**	**0**	**0**	70	112	0	14	**0**	**5**
2.625	**0**	**0**	**0**	70	120	0	14	**0**	**5**

* TH_x, TH_y, TH_z, EL_x, PS_y were locked

The initial resting position of the arm was determined from a statically optimized posture that was set to minimize muscle activity. This posture was defined by providing a range of upper and lower bound joint angle limits to ensure that the static optimization function searched for a posture that minimized muscle stress while maintaining that the arm would be hanging at the side of the body. Static optimization was used to find a posture that minimized total muscle activation within the bounds of these kinematic constraints. The final solution for the statically optimized hanging-arm posture is provided (table 5.3.; figure 5.2.). The statically optimized hanging arm posture was used as the initial guess for searching for an optimal direct collocation solution to the prescribed thoracohumeral elevation tasks in the sagittal, scapular, and frontal planes (table 5.2.). This initial state was not necessarily intended to match the empirical joint angles for a relaxed standing posture presented previously [Table 1 in Ludewig et al, 2009] as these postures were already prescribed to the model as kinematic inputs for direct collocation. The initial posture was simply intended to represent a "low-effort" initial guess to help initiate the gradient descent of the optimal control function near a globally optimal solution.

Table 5.3. **List of statically optimized model joint angles to minimize muscle effort during a static arm hang.**

Model Degree of Freedom (DOF)	Statically Optimized Joint Angle
TH_x	0°
TH_y	0°
TH_z	0°
SC_x	11.3°
SC_y	-20.4°
SC_z	21.3°
AC_x	-6.2°
AC_y	39.9°
AC_z	-10.1°
GH_y	-10.0°
GH_z	0.7°
GH_yy	-9.9°
EL_x	0.9°
PS_y	73.1°

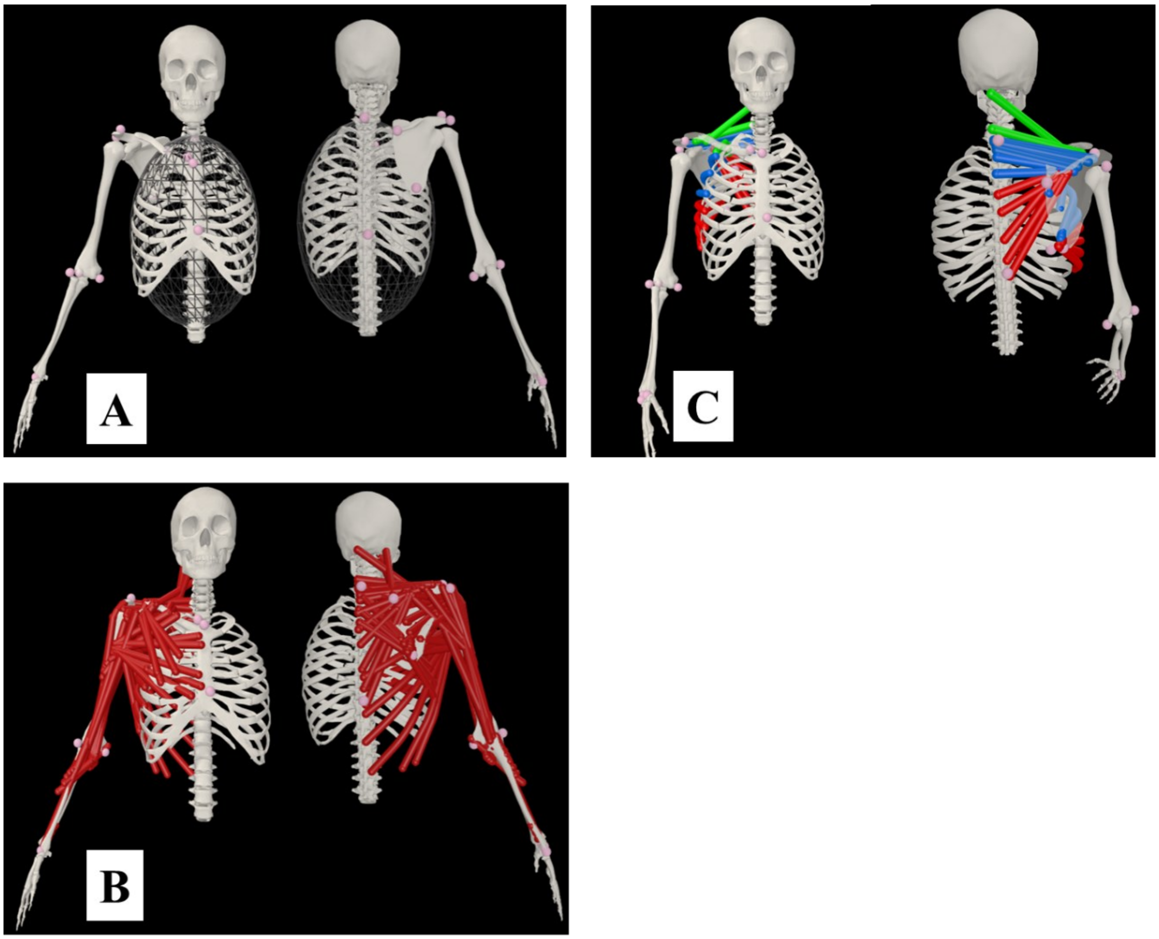

Figure 5.2. **Visualization of statically optimized “hanging arm” posture in OpenSim. A.** without and **B.** with visualization of all muscle elements. Used as initial guess for direct collocation. (c) Scapular and clavicular model geometry set to 75% opacity; muscle elements of trapezius and serratus anterior color-coded by partition: upper (green), middle (blue), lower (red).

5.2.5. Validation of Model Predictions

To validate and test the model performance, we sought to determine a set of cost function weights (equation 5.4.) that would produce an optimal control solution that falls within the range of one-dimensional continua that is non-significant from the empirical data [Ludewig, et al., 2009]. Thus, a one-dimensional statistical parametric mapping (SPM) one-sample t test [Pataky, 2010; Pataky, Robinson, and Vanrenterghem, 2016; Pataky, et al., 2019] was used to compare model predicted scapulothoracic angles to a set of 12 empirically derived scapulothoracic joint angles [Ludewig, et al., 2009] during thoracohumeral elevation trials in the frontal plane. For the following SPM models, optimal control predicted scapulothoracic angle was the independent variable, and thoracohumeral elevation angle was the one-dimensional dependent continua. As one-dimensional SPM requires a complete time-varying set of joint angles for each participant, SPM analysis could only be conducted for thoracohumeral elevation in the frontal plane as this was the only plane of motion available for the empirically derived data. Model data and empirical data was compared along a series of 5° intervals from 30° to 120° thoracohumeral elevation.

To determine a set of cost function weights that produced an optimal control solution which fell within the non-significant range of the SPM continua, we computed 18 frontal plane thoracohumeral elevation trials with all combinations of the following cost function (equation 5.4.) weights: muscle effort (w2) weights of 0.1, 1, 10, and 50 scapulothoracic constraint (w3) terms of 0.01, 0.1, and 1, and glenohumeral stability (w4) terms of 0.1 and 1. Kinematic tracking (w1), being the relative weight to which the optimal control solution can impose alterations in the input kinematic tracking variables (table 5.2.a), was set to 100 for all cost function permutations. These weights represent the unitless normalized standard deviation in humans measured for each cost function variable [Van Den Bogert, Blana, and Heinrich, 2011], such that a cost function with w1 = 100 and w2 = 10 will imply that the cost of tracking error (w1) is equal to ten times the cost of full muscle activation (w2). The terms w1 = 100 and w2 = 10 were previously found to produce reasonable predictions in an optimal controller cost function for gait prediction, and thus guided the relative weights tested for our purposes of scapulothoracic control [Van Den Bogert, Blana, and Heinrich, 2011].

Empirical scapulothoracic joint angle data during thoracohumeral elevation was unfortunately not available for the other planes of interest (scapular and sagittal plane), which limits our ability to extend a one-dimension SPM analysis to model prediction accuracy in these other planes. Therefore, the optimal control cost function weights that produced the best-matching scapulothoracic model solution for thoracohumeral elevation in the frontal plane were then used to produce scapulothoracic kinematic predictions in the scapular and sagittal planes.

5.2.6. Reducing Force Generating Capacity of Scapular Stabilizer Muscles

Following validation of the model performance in the frontal plane, and generation of model solutions in the scapular and sagittal planes, model solutions were regenerated in all three planes with maximal force generating capacity (*Fmax*) of the scapular stabilizer muscles iteratively reduced to 75%, 50%, and 25%. These model solutions were generated to simulate kinematic and muscular changes associated with upper trapezius weakness, middle trapezius weakness, lower trapezius weakness, serratus anterior weakness, and combined lower trapezius and serratus anterior weakness.

Upper trapezius partition was selected as the model muscle elements inserting on the clavicle, whereas elements attaching to the scapula were defined as middle and lower partitions [Blana et al., 2008; Klein-Breteler et al., 1999; Johnson et al., 1994] (figure 5.2.). Of the11 'scapular' trapezius elements, the 6 most superior elements were classified as representative of middle trapezius for the current simulations, and the bottom 5 were classified representative of lower trapezius (figure 5.2.). This determination was made following best practices for classifying the partitions of trapezius for EMG localization [Perotto, 2011]. Functionally, this definition characterizes the model muscle elements which insert on the scapular spine as middle trapezius, and those which insert on the trigonum spinae as lower trapezius. The 12 elements of serratus anterior were partitioned into equal thirds of 4 elements. The most superior partition consisted of elements connecting the 1st rib with the medial scapular boarder, superior to the trigonum spinae, while the lower partition elements all originated below the 4th rib, following cadaveric insights from Ekstrom et al., [2004]. The middle partition elements did not fall under either of the classifications for the upper or lower partitions (figure 5.2.).

To probe whether lower trapezius and serratus anterior weakness displayed an additive effect on muscle activity changes when weakened in combination, the model-predicted muscle activations for combined lower trapezius and serratus anterior weakness simulations were compared to the sum of the individual model-predicted muscle activations for individual lower trapezius and serratus anterior weakness simulations.

5.2.7. Post-Hoc Model Comparisons

A priori analyses were formulated to test how isolated reductions in force-generating capacity of the scapular stabilizer muscles affect the primary and secondary hypotheses of this study. The decision to focalize the analysis of this study on the scapular stabilizers was merited on substantial evidence that empirical studies on scapular muscle fatigue are particularly affected by substantial variability. However, a potential limitation of these study aims is that they insinuate that kinematics and muscle activity compensation across the scapular stabilizers muscles act as a closed system, which is indeed not the case. Thus, in cases where kinematic or muscular adaptations to limited maximal force-generating capacity did not appear to be affected, a more comprehensive set of parascapular muscle activation changes is provided in the results.

5.3. Results

5.3.1. Model Validation

Testing of all permutations of cost function weights revealed one cost function with weights $w_1 = 100$, $w_2 = 0.1$, $w_3 = 1$, and $w_4 = 1$ that was not significantly different from the empirical dataset at any point along the one-dimensional continua for scapulothoracic elevation. Each scapulothoracic degree of freedom was statistically distinct from the one-dimensional continua of the empirically derive data at a point below 60° thoracohumeral elevation, yet all three scapulothoracic DOF fit the empirical data between 60°-120° of thoracohumeral elevation. The resulting scapulothoracic kinematic solutions are illustrated in figure 5.3. and compared to the mean and standard deviation of the empirical dataset [Ludewig et al., 2009].

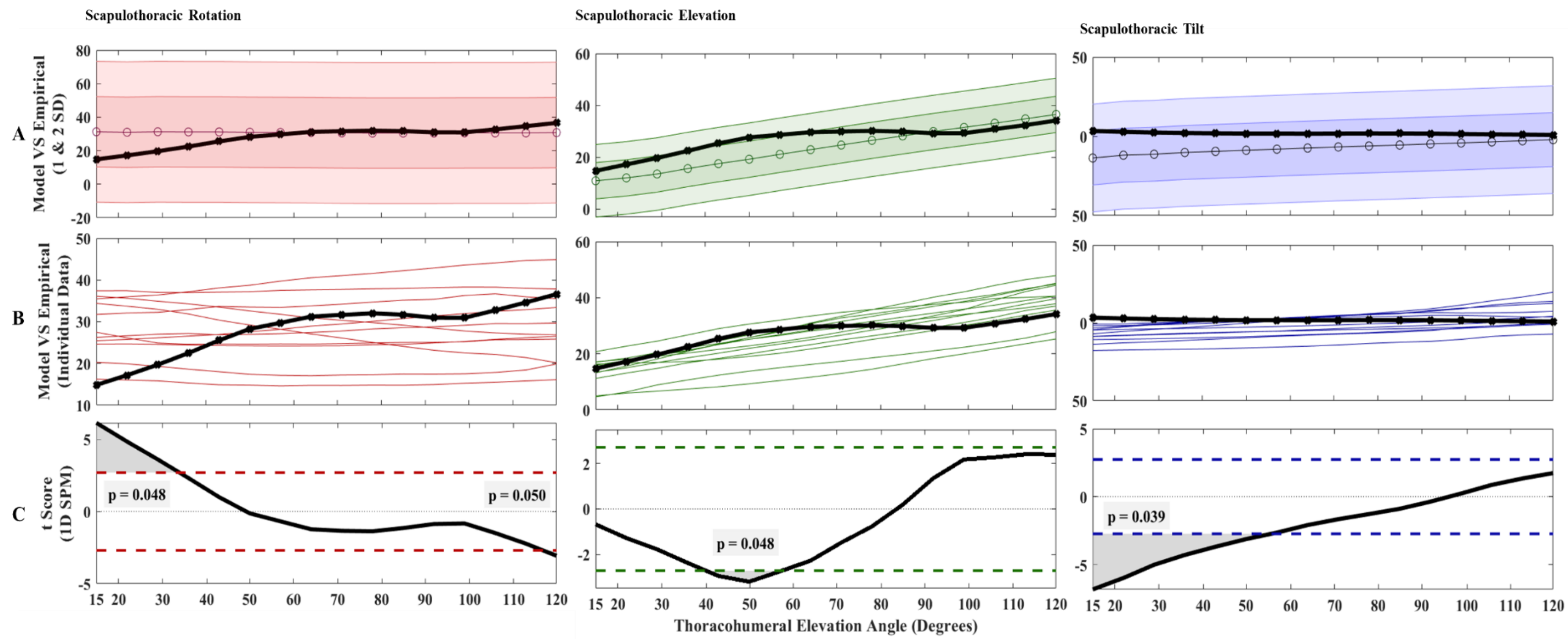

Figure 5.3. **Model-predicted scapulothoracic joint angle optimal control solution for frontal-plane thoracohumeral elevation from 15° to 120°.** Subplots **A** represent model predicted solution in black, bold, compared to empirical mean value in color. Shaded regions represent 1 standard deviation and 2 standard deviations. Subplots **B** represent model predicted solution in black, bold, compared to the twelve individual

participant scapulothoracic joint angles in color. Subplots **C** represent one-dimensional statistical parametric map t-statistic in black, bold, compared to t critical significance threshold in color, dotted.

5.3.2. Limiting Maximal Muscle Force-Generating Capacity – Kinematic Changes

Model-predicted scapulothoracic kinematics changes were typically present when scapular stabilizer muscle force-generating capacity was limited to 25% *Fmax*, yet 75% and 50% *Fmax* simulations rarely elicited an altered kinematic strategy. Thus, 25% *Fmax* simulations are illustrated for all three prescribed planes of motion, and kinematic solutions which were distinct from the 'No Weakness" state are outlined in red (figure 5.4.). 75% and 50% *Fmax* simulations are included in the appendices.

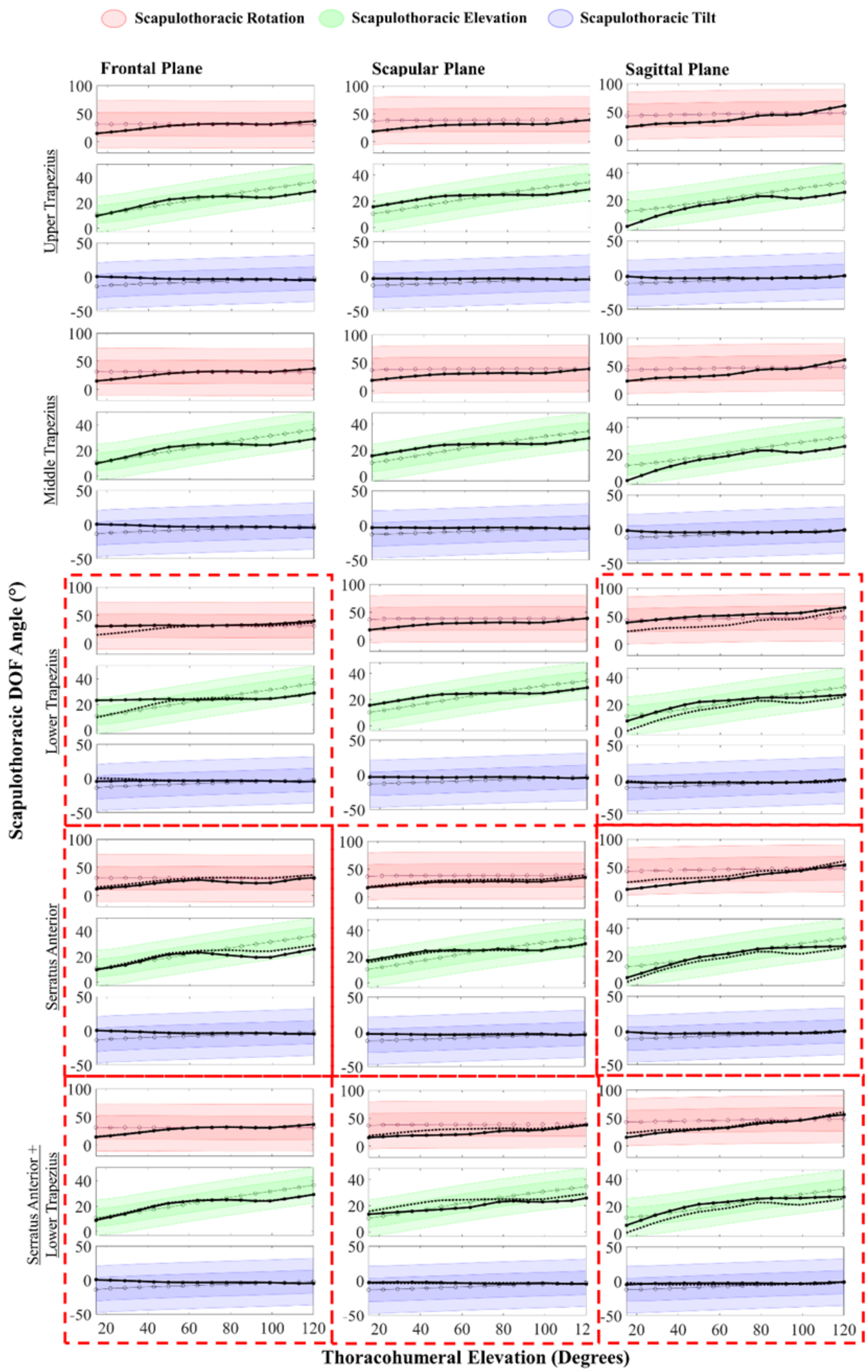
Scapulothoracic Rotation
Scapulothoracic Elevation
Scapulothoracic Tilt
Frontal Plane
Scapular Plane
Sagittal Plane
Upper Trapezius
Middle Trapezius
Lower Trapezius
Serratus Anterior
Serratus Anterior + Lower Trapezius
Scapulothoracic DOF Angle (°)
Thoracohumeral Elevation (Degrees)

Figure 5.4. **Model-predicted scapulothoracic joint angle optimal control solution for frontal-plane, scapular-plane, and sagittal-plane thoracohumeral elevation from 15° to 120°.** Subplots are organized horizontally by plane of thoracohumeral elevation displaying reduced force-generating capacity, and vertically by 25% *Fmax*-limited muscle. Solid black lines indicate the solution subject to reduced *Fmax* compared to the dotted line "no fatigue" solution. Subplots outlined in red are unique from the "no fatigue" solution.

5.3.3. Limiting Maximal Muscle Force-Generating Capacity – Scapular Stabilizer Muscle Activity Changes

Model-predicted muscle activation dynamics to account for deficits in scapular stabilizer force-generating capacity are displayed in figures 5.5.-5.7. Results illustrate predicted scapular stabilizer muscle activity compensations due to weakness while subject to model dynamics (equation 5.1.-5.4.) and kinematic constraints (table 5.2.a-c; equation 5.5.). The effects of compound deficits in force-generating capacity of lower trapezius and serratus anterior are also explored across each plane of thoracohumeral elevation (figure 5.5.-5.7.). Figure 5.8. also illustrates the summation of model-predicted lower trapezius and serratus anterior activation compared to the summation of individual lower trapezius and serratus anterior weakness simulations. Grey lines in this figure represent model-predicted scapular stabilizer muscle activity with combined lower trapezius and serratus anterior weakness, while purple lines represent the sum of model-predicted muscle activity when lower trapezius and serratus anterior are weakened individually.

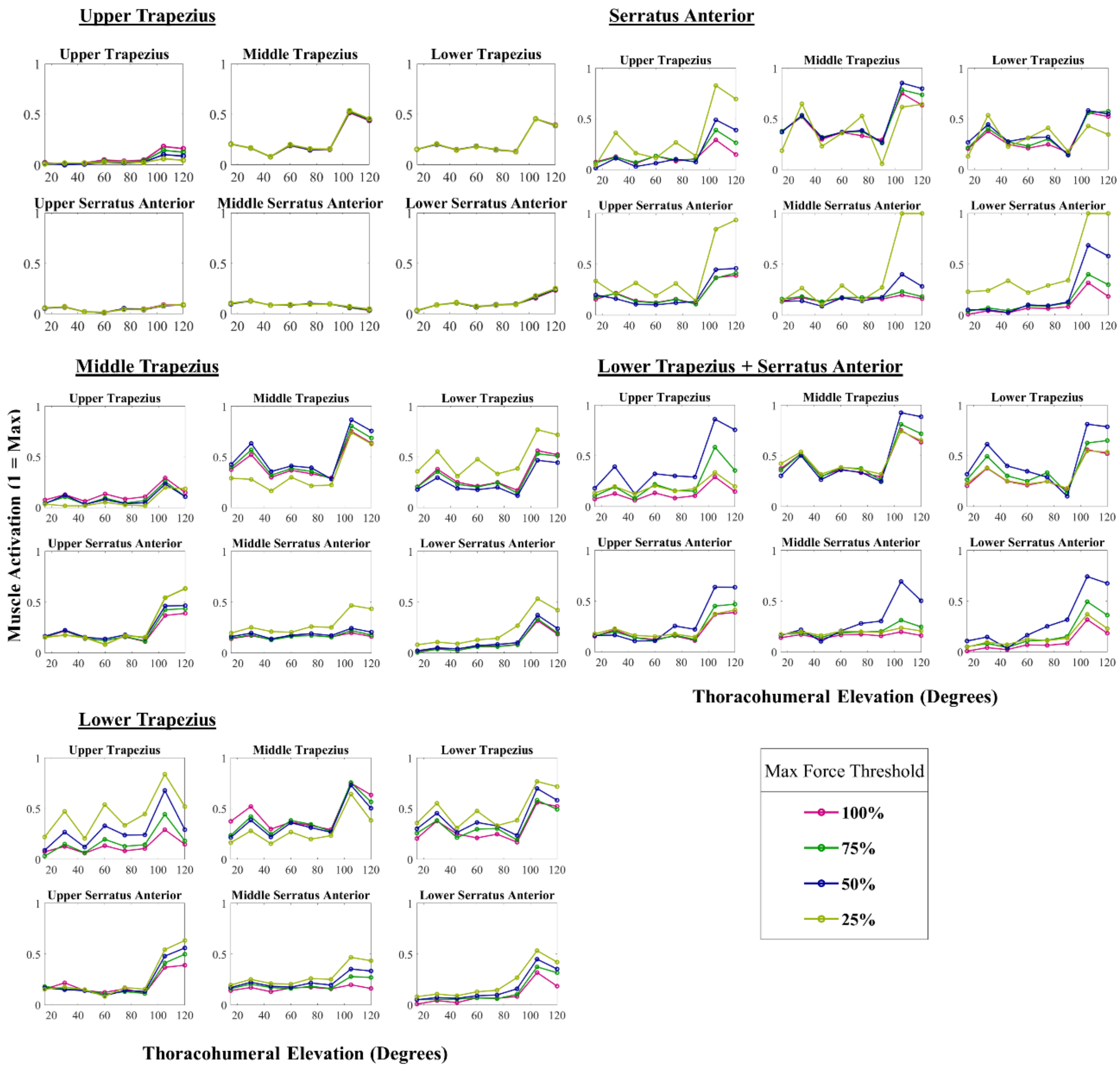

Figure 5.5. **Predicted muscle activation during thoracohumeral elevation from 15° to 120° elevation in the frontal plane while limiting maximal force-generating capacity of scapular stabilizer muscles**.

Muscles with simulated weakness are bolded and underlined above respective simulation results.

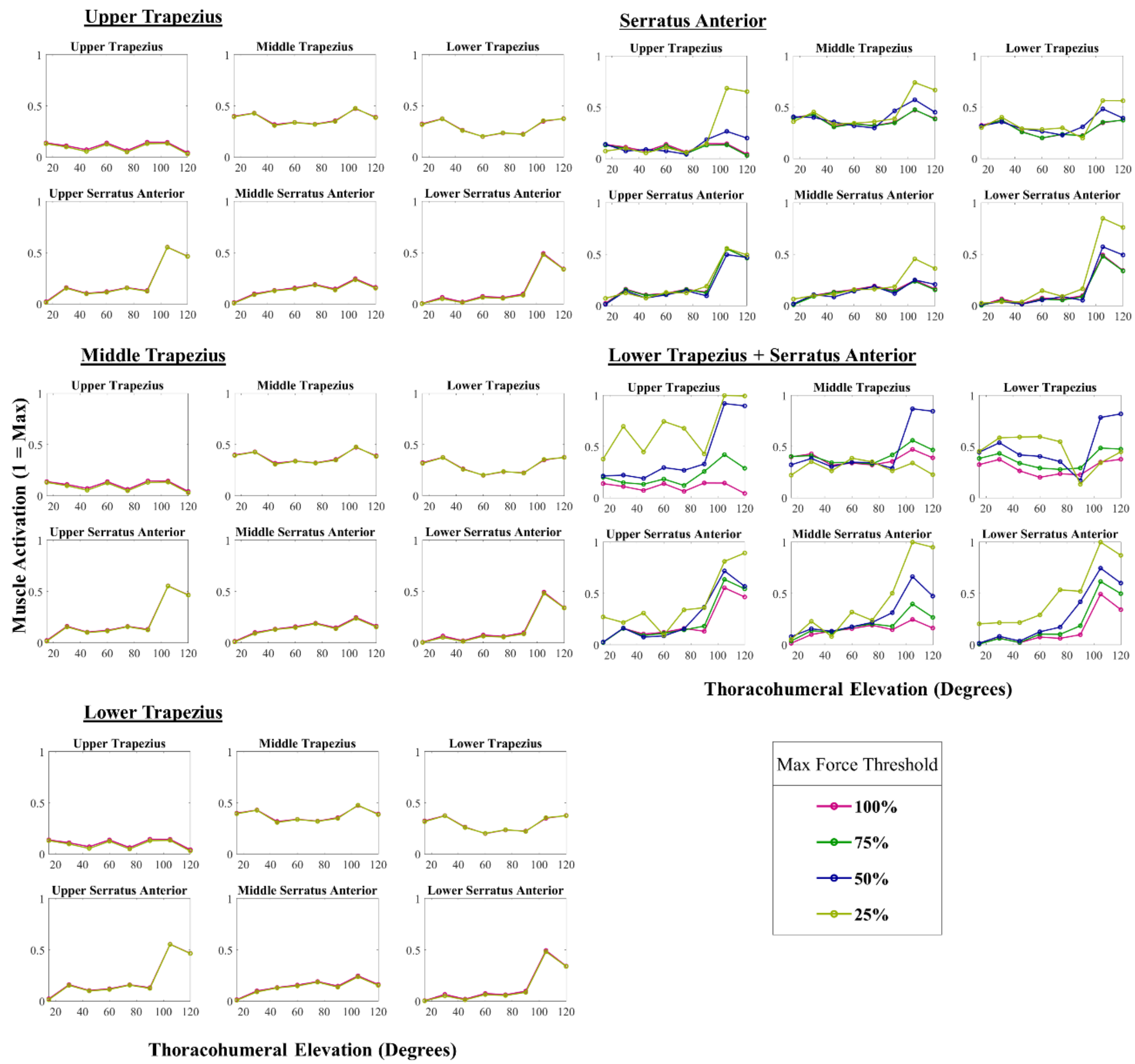

Figure 5.6. **Predicted muscle activation during thoracohumeral elevation from 15° to 120° elevation in the scapular plane while limiting maximal force-generating capacity of scapular stabilizer**

muscles. Muscles with simulated weakness are bolded and underlined above respective simulation results.

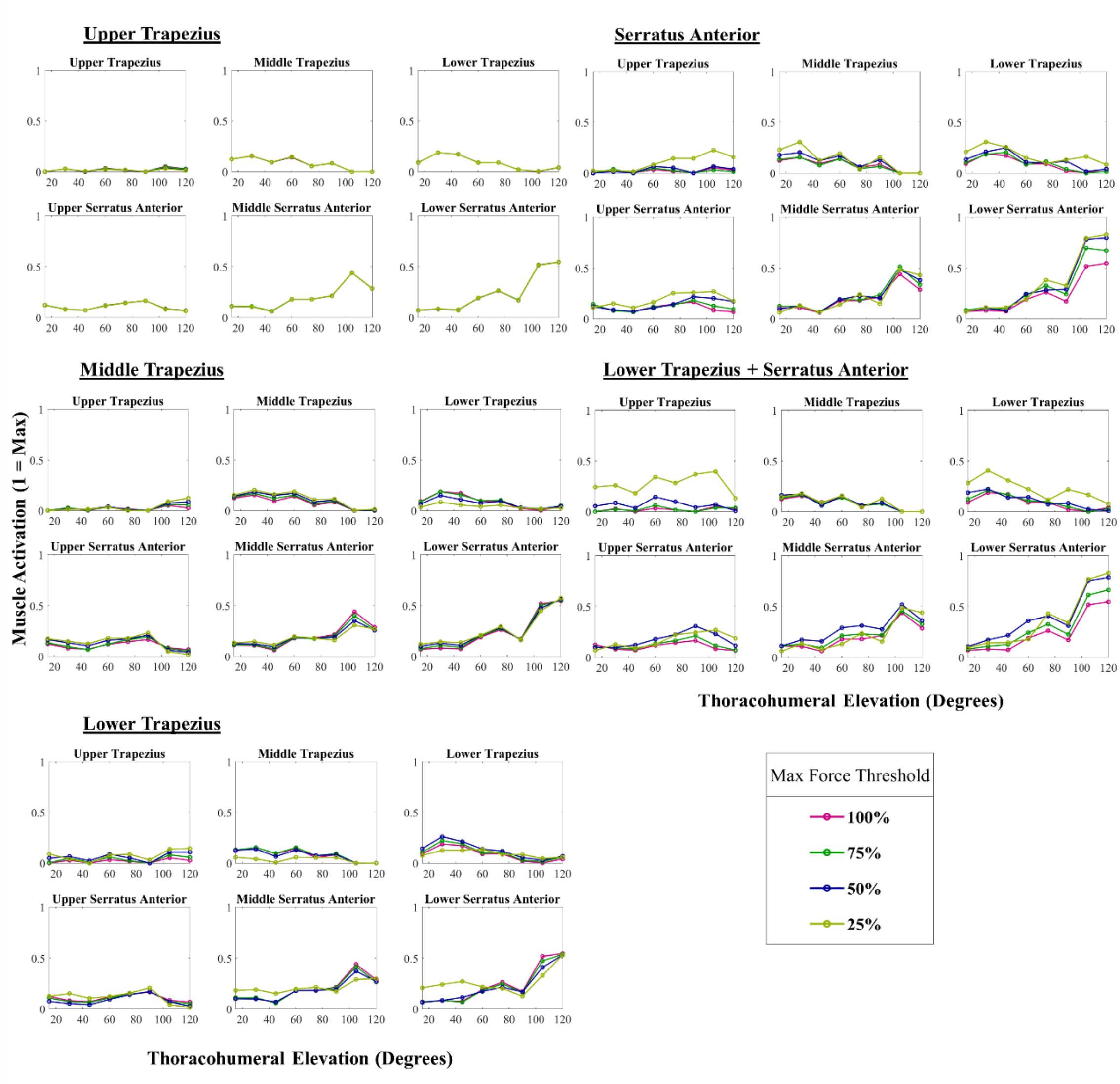

Figure 5.7. **Predicted muscle activation during thoracohumeral elevation from 15° to 120° elevation in the sagittal plane while limiting maximal force-generating capacity of scapular stabilizer muscles.**

Muscles with simulated weakness are bolded and underlined above respective simulation results.

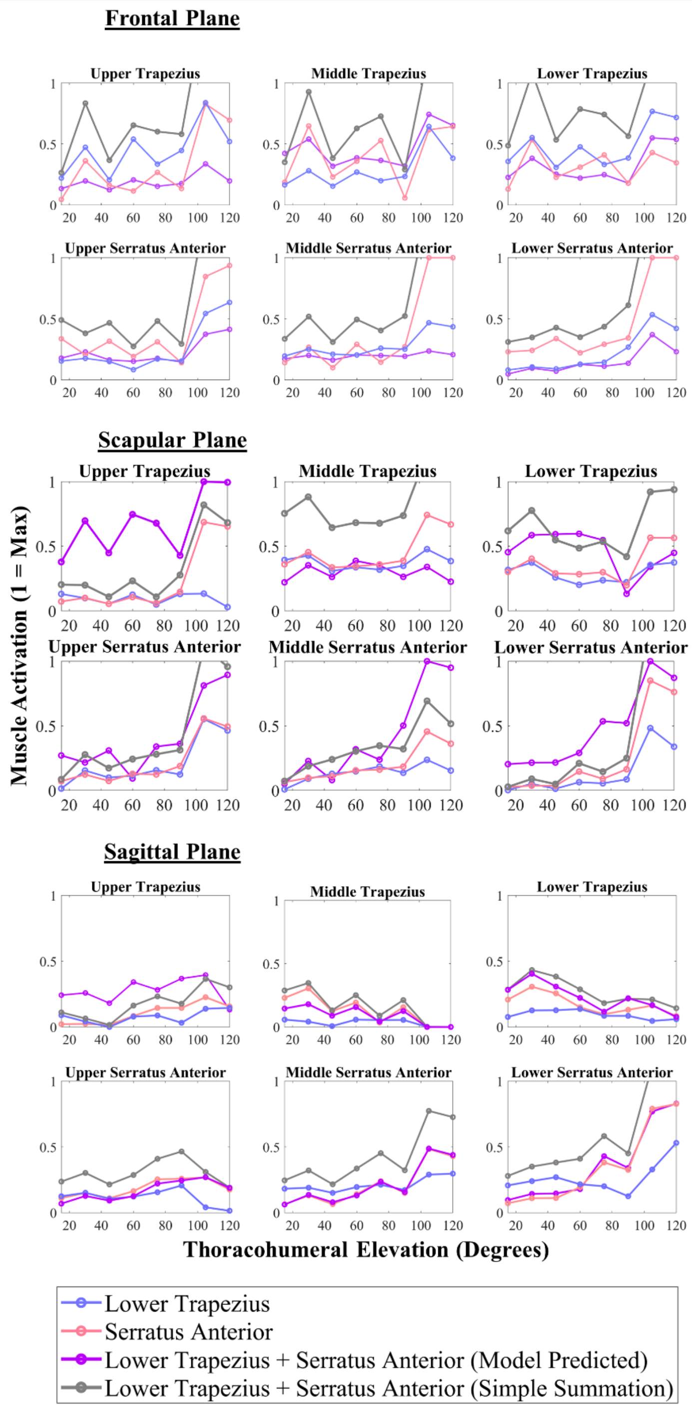
Frontal Plane
Upper Trapezius
Middle Trapezius
Lower Trapezius
Upper Serratus Anterior
Middle Serratus Anterior
Lower Serratus Anterior
Scapular Plane
Upper Trapezius
Middle Trapezius
Lower Trapezius
Upper Serratus Anterior
Middle Serratus Anterior
Lower Serratus Anterior
Sagittal Plane
Upper Trapezius
Middle Trapezius
Lower Trapezius
Upper Serratus Anterior
Middle Serratus Anterior
Lower Serratus Anterior
Muscle Activation (1 = Max)
Thoracohumeral Elevation (Degrees)
Lower Trapezius
Serratus Anterior
Lower Trapezius + Serratus Anterior (Model Predicted)
Lower Trapezius + Serratus Anterior (Simple Summation)

Figure 5.8. **Model-predicted scapular stabilizer muscle activation during thoracohumeral elevation in the frontal, scapular, and sagittal planes with simulated weakness of lower trapezius (blue), serratus anterior (red), lower trapezius and serratus anterior (grey), and the sum amplitude of the blue and red lines (purple).** *Fmax* set to 25% for all simulations.

5.3.4. Parascapular Muscle Activity Changes

Relatively stable kinematics strategies across scapular plane thoracohumeral elevation simulations in response to 25% *Fmax* limitation of the scapular stabilizers prompted a comprehensive evaluation of potential parascapular muscle activity compensations. Changes in parascapular muscle activity were only apparent when limiting maximal force-generating capacity of serratus anterior, presented in figure 5.9.

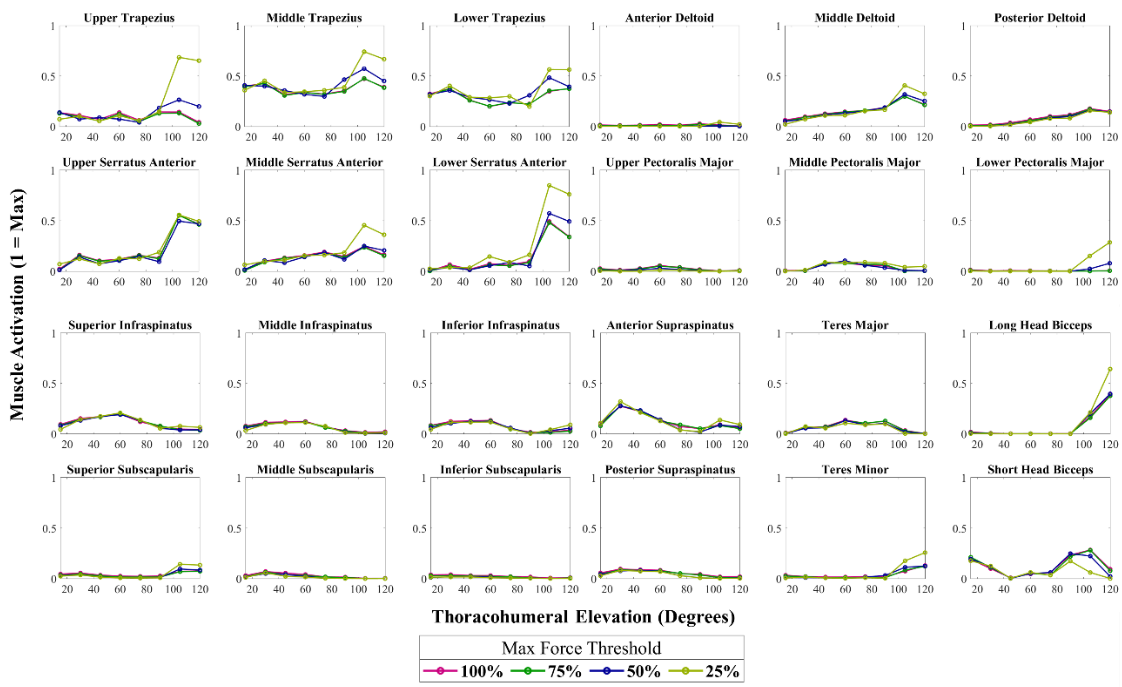

Figure 5.9. **Scapular stabilizer, rotator cuff, and accessory shoulder muscle activation during scapular plane thoracohumeral elevation with progressive serratus anterior weakness.**

5.4. Discussion

This study used a computational shoulder model to determine the scapulothoracic kinematic changes associated with reductions in force-generating capacity of isolated scapular stabilizer muscles. First, model-predicted kinematics were validated using empirical kinematics for frontal-plane thoracohumeral elevation from 15° to 120°. Results indicate three regions-of-interest that arose along the continua of comparisons between model-predicted and empirically derived scapulothoracic angles; each of these regions was at or below 55° of thoracohumeral elevation. Kinematics predictions otherwise closely matched the empirically derived scapulothoracic angles, therefore to proceed with modelling scapulothoracic kinematics changes associated with muscle weakness, subsequent kinematic solutions were produced with identical constraints and cost-function weights, while maximal force-generating capacity (Fmax) of select scapular stabilizer muscles was reduced to 75%, 50%, and 25%. Results indicated that model-predicted kinematic solutions showed changes at 25% Fmax of most scapular stabilizer when compared to the un-weakened kinematics. In some cases, the model-predicted kinematics were unaltered when Fmax was set to 25%, particularly during upper and middle trapezius weakness. Muscle activity predictions typically revealed increasing muscle activation across all scapular stabilized muscles as muscle force-generating capacity was progressively weakened. Compound reductions in lower trapezius and serratus anterior force-generating capacity prompted muscle activity compensations which appeared more efficient than the summation of muscle activity changes due to isolated lower trapezius or serratus anterior weakness.

5.4.1. Model Validation

Model-predicted kinematics revealed regions of interest between 15°-30° for scapulothoracic rotation, between 40-55° for scapulothoracic elevation, and between 15°-55° for scapulothoracic tilt. These significant regions of interest had p-values close to the alpha threshold of 0.05 however, with values of $p = 0.048$, p

= 0.048, and $p = 0.039$, respectively. The location of these significant regions of interest, near the initiation of movement, may suggest that model-predicted muscle activity is most accurate above 60°. One reason may be due to differences between model segment velocity and the segment velocities displayed by participants during thoracohumeral elevation. However, the empirical data used for model validation derived from Ludewig and colleagues [2009] reports the scapulothoracic joint angle at every 5° of thoracohumeral elevation. This information is not reported over time, making it impossible to determine segment velocity and acceleration, thus we are left to estimate the angular velocity profile. A pilot testing of thoracohumeral elevation velocities compared how bell-shaped angular velocity profiles compared to 'constant' arm velocity profiles (where elevation velocity was set to a constant 40°/s), and 'undetermined' velocity profiles (where only start and end position were prescribed). Across these three conditions kinematic solutions surpassed the one-dimensional SPM t test threshold (figure 5.3.c) below 60°, however the 'constant' and 'undetermined' velocity conditions also exceeded the SPM t test threshold above 100°, which was not observed in the bell-shaped profile. These findings align with research findings that approximate a typical bell-shaped velocity curve during goal-directed arm motion [Ostry, Cooke, and Munhall, 1987]. Further, the empirical dataset is comprised of 7 male and 5 female participants (N=12; 29.3 ± 6.8 yr; 1.74 ± 0.81m; 77.5 ± 13.8 kg), likely making any statistical comparison underpowered, as well as unlikely to capture the full range of scapulothoracic kinematics that humans can display during thoracohumeral elevation [Chopp-Hurley, et al., 2016; Mulla, McDonald, and Keir, 2018; Russell, et al., 2024]. Indeed, model-predicted kinematics that approach the boundary of one standard deviation from the mean for scapulothoracic rotation and tilt were found to be significant in the SPM analysis (figure 5.3.), although we expect that greater statistical power may have made the significance threshold less sensitive [Robinson, Vanrenterghem, and Pataky, 2015; Pataky, Robinson, and Vanrenterghem, 2016]. Despite these limitations, this empirical dataset derived from transcortical bone-pin tracking is expected to have much greater accuracy than scapulothoracic kinematics derived from tracking methods which adhere to the skin and suffer from skin motion artefact [Shaheen, Alexander, and Bull, 2011; Grewal, Cudlip, and Dickerson, 2017]. Considering the large variability observed in scapulothoracic kinematics [Ebaugh, McClure, and Karduna, 2006; Borstad, Szucs, and Navalgund, 2009; Chopp-Hurley, et al., 2016], controlling for these technological sources of variability and error with bone-pin methods offers more confidence in the validation of our model-predicted kinematics. Therefore, it should be noted that while the presently reported empirical shoulder kinematics from Ludewig and colleagues [Ludewig, et al., 2009] represent some of the most accurate scapulothoracic data available, certain limitations do exist that may explain some discrepancies between the empirical and model-predicted kinematic data.

The regions of interest during validation of model-predicted scapulothoracic kinematics during frontal-plane thoracohumeral elevation also raise considerations for the model-predicted scapulothoracic kinematics in the scapular and sagittal plane. While the full continua of scapulothoracic angle data for all 12 participants was unavailable for these planes, group mean joint angle and standard deviation was still illustrated to infer model performance (figure 5.4.). From these comparisons we can see that most solutions fluctuate within ±1 SD of the empirical data. The small region of significance observed for scapulothoracic elevation may also suggest that scapulothoracic elevation is more crucial than scapulothoracic rotation and tilt for achieving optimal thoracohumeral elevation mechanics, thus an optimal model solution could conceivably be achieved while permitting significant rotation and tilt differences compared to the empirical dataset.

5.4.2. Limiting Maximal Muscle Force-Generating Capacity – Kinematic Changes

Overall, model-predicted scapulothoracic rotation and elevation kinematic joint angle solutions for frontal plane and scapular plane thoracohumeral elevation typically remained within the threshold of ±2SD of the empirical dataset. Serratus anterior was the only muscle to alter kinematics across all three planes of motion when weakened. These kinematic changes typically demonstrated increased scapulothoracic external rotation, however changes in scapulothoracic elevation were also apparent. Scapulothoracic tilt appeared more stable and did not change in most muscle weakness simulations. Increased scapulothoracic external rotation associated with weakness of serratus anterior may be an important consideration for increased SAS width; a factor which reduces SAIS risk [Ludewig and Cook, 2000; Michener, McClure, and Karduna, 2003; Chopp, Fischer, and Dickerson, 2011]. Conversely, frontal and sagittal plane kinematics solutions with 25% Fmax limited lower trapezius displayed increases in scapulothoracic internal rotation, particularly below 60° thoracohumeral elevation, which would act to reduce SAS width and increase SAIS risk [Ludewig and Cook, 2000; Michener, McClure, and Karduna, 2003; Chopp, Fischer, and Dickerson, 2011]. However, these kinematics changes associated with weakened lower trapezius were paired with observed increases in scapulothoracic elevation, which are considered protective against SAIS and RC tears [Ludewig and Cook, 2000; Michener, McClure, and Karduna, 2003; Chopp, Fischer, and Dickerson, 2011]. Thus, while lower trapezius weakness appeared to permit kinematic changes, it is difficult to ascertain whether the net effect of these kinematic changes is more protective or harmful in nature. These findings reinforce the notion that the lower partitions of trapezius and the serratus anterior are important for maintaining scapulothoracic kinematics during dynamic motion [Mottram, 1997; Kibler, 1998; Cools, et al., 2002; Alexander, et al., 2007], and further suggest that the risk of impingement-related scapulothoracic kinematics changes associated with muscle weakness may be particularly consequent of lower trapezius weakness.

In simulations where lower trapezius and serratus anterior were both weakened, kinematic changes resembled those that appeared when only serratus anterior was weakened, particularly with respect to scapulothoracic rotation. This could suggest that weakness of serratus anterior may have the greatest effect on scapulothoracic motion of any single scapular stabilizer muscle during scapular motions in the frontal and scapular planes. Previously, the importance and unique capacity of serratus anterior has been highlighted for its ability to contribute to all three scapulothoracic DOF during thoracohumeral elevation by generating upward rotation, posterior tilting, and external rotation [Dvir and Berme, 1978; Ludewig, et al., 2004]. Serratus anterior has also been shown to have the largest moment arm of any scapular stabilizer muscle, thereby making it mechanically advantageous for recruitment amongst the redundant shoulder muscle DOF [Dvir and Berme, 1978; Ludewig, et al., 2004]. Chiefly, reductions in serratus anterior muscle activity, have been associated with abnormal and subclinical scapular motion; reported to often produce a 'shrugged' or elevated and externally rotated scapula that can present with pain [Ludewig and Cook, 2000; Cools, et al., 2002; Szucs, Navalgund, and Borstad, 2009; Michener, et al., 2016]. The current study is limited to representing a purely mechanistic model of muscle weakness, thus being indiscriminate of dynamic system changes associated with pain and somatosensory feedback that may influence motor control strategies [Riemann and Lephart, 2002; Prochazka and Ellaway, 2012; Proske, 2015; Zabihhosseinian, Holmes, and Murphy, 2015]. However, this research showed evidence that insufficiency in serratus anterior force production during dynamic motion appears to enable some of the largest changes in model-predicted kinematics.

During scapular plane thoracohumeral elevation, kinematic trends were less apparent when reducing muscle force-generating capacity, as even combined lower trapezius and serratus anterior 25% Fmax simulations appear fairly similar to the non-weakened kinematic solution (figure 5.4.). Kinematic solutions could have remained stable for two reasons: (1) weakening of scapular stabilizer muscles to 25% Fmax had not reduced the muscle forces necessary to achieve an optimal kinematic solution, or (2) compensatory activation of accessory muscles were able to supplement for weakened scapular stabilizers and maintain an optimal kinematic solution. To probe these two hypotheses, the muscle activity of the RC muscles and other accessory shoulder muscles was investigated across progressive upper trapezius, middle trapezius, lower trapezius, and serratus anterior weakness. The model-predicted muscle activity of the scapular stabilizer RC, and accessory shoulder muscles during progressive serratus anterior weakness is illustrated (figure 5.9.). These data show some progressive muscular compensations across the RC and accessory muscles due to progressive weakness, particularly middle deltoid, lower pectoralis major, and long head of biceps. However, all compensatory changes in muscle activity appear at or above 90° thoracohumeral elevation. No muscle activity changes were observed when upper trapezius, middle trapezius, or lower trapezius were weakened. These findings suggest that muscle compensations were unnecessary to maintain scapular plane thoracohumeral elevation to 90°, but have potentially important implications for overhead postures. Thorough research describes the highly fatiguing effect of sustained maintenance of overhead arm postures, which are defines as arm postures above 90°. In the scapular and sagittal planes, we see distinct rises in trapezius and serratus anterior muscle activity beyond 90°, however serratus anterior weakness appeared to generate the largest changes in muscle activity; typically resulting in increased activity across all partitions of serratus anterior. Further, the ancillary findings that rotator accessory shoulder muscles showed minimal changes in muscle activity due to trapezius and serratus anterior weakness in the scapular plane, combined with little kinematic changes observed in this plane could suggest that serratus anterior may play a particularly important role in scapular plane thoracohumeral elevation, as this position aligns the scapula with the serratus anterior and wall of the thorax, and may explain why upper serratus anterior activity was much higher in this plane compared to frontal and sagittal elevation [Bagg and Forrest, 1986; Ekstrom et al., 2004;

Phadke, Camargo, and Ludewig, 2009; Johnston, 1937]. This plane also provides an optimal alignment for the rotator cuff muscles, which may reduce the effort necessary to stabilize the glenohumeral joint and even contribute to glenohumeral joint abduction [Ekstrom et al., 2004; Phadke, Camargo, and Ludewig, 2009; Johnston, 1937]. The capacity for several RC and accessory shoulder muscles to compensate for simulated serratus anterior weakness may explain why minimal kinematic changes were observed in the model-predicted scapular plane solutions when these muscles displayed reduced Fmax capacity. Conversely, the minimal changes in scapular and accessory muscle activity when partitions of trapezius were weakened may suggest that these muscles are less integral for scapular plane thoracohumeral elevation.

5.4.3. Limiting Maximal Muscle Force-Generating Capacity – Scapular Stabilizer Muscle Activity Changes

Model-predicted scapular stabilizer muscle activity predictions were typically increased when serratus anterior was weakened. Yet upper trapezius weakness often had little to no effect on kinematic and muscle activity changes, and scapular and sagittal plane elevation also showed little kinematic and muscle activity compensations due to trapezius muscle weakness. Across the three planes of thoracohumeral elevation, frontal plane elevation typically demonstrated the greatest overall activity across the trapezius and scapular stabilizers, which appeared reduced in the sagittal plane, and further reduced in the scapular plane. These findings could be important for consolidating our understanding of scapular stabilizer muscle activity and fatigue. For instance, in the context of studies which seek to stimulate comprehensive scapular stabilizer muscle fatigue, the current study suggests that frontal plane thoracohumeral elevation tasks may be best suited for a balanced contribution of all muscles. These findings also help make sense of current trends in literature which have found some success in fatiguing the scapular stabilizers in the frontal plane [Chopp-Hurley et al., 2016; Ebaugh, McClure, and Karduna, 2006; McQuade, Dawson, and Smidt, 1998], yet fatigue stimuli in other planes appear less successful or preferentially fatigue serratus anterior [Noguchi et al., 2013; Mulla, McDonald, and Keir, 2018; McDonald, Tse, and Keir, 2015; Borstad, Szucs, and Navalgund, 2009]. Consequently, trapezius and serratus anterior weakness also appeared to prompt the largest increases in scapular stabilizer muscle activity in the frontal plane. As discussed above, scapular plane movements could be important for optimally aligning the fibres of serratus anterior and the RC muscles with the plane of movement which would improve their mechanical efficiency and potentially explain why muscle weakness had such a small effect on movements in this plane [Ekstrom et al., 2004; Phadke, Camargo, and Ludewig, 2009]. Sagittal plane motions would provide less optimal alignment for serratus anterior compared to the scapular plane, however muscle moment arm alignment for trapezius would be most diminished in this posture, as it is almost 90° off axis from its optimal alignment in the frontal plane [Inman, Sunders, and Abbott, 1944; Phadke, Camargo, and Ludewig, 2009; Johnson et al., 1994].

Considering the effects of weakening a single scapular stabilizer muscle, serratus anterior weakness appeared to prompt the greatest overall increases in scapular stabilizer muscle activity across all three planes of thoracohumeral elevation, while decreases in upper trapezius force appeared to have a negligible influence on scapular stabilizer kinematics and muscle activity. However muscular compensations to serratus anterior weakness appeared dependent on the plane of thoracohumeral elevation. Specifically, during scapular and frontal plane thoracohumeral elevation with simulated weakness of serratus anterior (figures 5.6. & 5.7.), increases in upper trapezius and middle trapezius activity were observed in addition to elevated activity in the middle and lower partitions of serratus anterior. Yet during sagittal plane thoracohumeral elevation, muscle activity only appeared to increase at serratus anterior due to limited Fmax, suggesting that recruitment of un-weakened trapezius partitions was less optimal. As discussed, previous studies have suggested that the lower fibers of serratus anterior play a particularly important role in scapulothoracic and thoracohumeral elevation, and weakness or reduced activity of serratus anterior is a common precursor of pain and suboptimal scapular kinematics [Dvir and Berme, 1978; Michener, McClure, and Karduna, 2003; Ludewig, et al., 2004; Cools, et al., 2007; Szucs, Navalgund, and Borstad, 2009; Michener, et al., 2016].

The activation or ‘coactivation’ of upper trapezius relative to lower trapezius and serratus anterior has also been identified as a possible risk factor for weakness-related and fatigue-related scapulothoracic kinematics changes associated with injury risk [Cools, et al., 2002; Ludewig, et al., 2004; Szucs, Navalgund, and Borstad, 2009; Michener, et al., 2016]. The current study generally showed model-predicted increases in upper trapezius activity when lower trapezius or serratus anterior was weakened, furthering the evidence that weakness and fatigue of these muscles may promote a more suboptimal or injurious coactivation with upper trapezius by concomitantly increasing upper trapezius activity as a compensation mechanism. Further, the middling effects of upper trapezius weakness on muscle activity changes in the other scapular stabilizers may suggest that this muscle acts primarily to compensate for scapulothoracic stability during thoracohumeral elevation when serratus anterior or lower trapezius is weakened, but weakness of upper trapezius itself may be less destabilizing to scapulothoracic joint kinetics. These model-predicted muscle activity results appear to reinforce the notion that serratus anterior plays a key role in elevated and overhead arm motions, and suggests that muscular compensations to serratus anterior weakness depends on the plane of motion and direction of loading, and may increase the risk of suboptimal muscle coactivation and injury-related kinematics.

While serratus anterior weakness appeared to produce the largest kinematic and muscular adaptations among the scapular stabilizers, the weakening of lower trapezius and serratus anterior together yielded posture-dependent changes in scapular stabilizer muscle activity (figure 5.8.). In the frontal plane, weakening of serratus anterior elicited much more scapular stabilizer muscle activity than when lower trapezius was weakened with serratus anterior. In the scapular plane, the opposite trend emerged with combined serratus anterior and lower trapezius muscle activity compensations being greater than muscle activity compensations that emerged due to individual muscle weakness. And in the sagittal plane, scapular stabilizer muscle activity compensations were often very similar whether lower trapezius, serratus anterior, or both muscles were weakened. These specific scapular stabilizers also appeared to show increased activity as scapulothoracic elevation angle increased, which may contribute to evidence that overhead tasks pose increased risk for scapular stabilizer fatigue and kinematic changes [Ekstrom, et al., 2004; Phadke, Camargo, and Ludewig, 2009; Thigpen, et al., 2010]. However, it remained unclear whether the combined weakening of lower trapezius and serratus anterior had a purely additive effect on muscle activity; whereby the increased muscle activity due to combined weakness of serratus anterior and lower trapezius would be equivalent to the summation of lower trapezius weakness-related increases in muscle activity and serratus anterior weakness-related increases in muscle activity. To probe whether lower trapezius and serratus anterior weakness displayed an additive effect on muscle activity changes when weakened in combination, the model-predicted muscle activations for combined lower trapezius and serratus anterior weakness simulations were compared to the sum of the individual model-predicted muscle activations for individual lower trapezius and serratus anterior weakness simulations (figure 5.8.). The fuchsia-colored lines in this figure represent model-predicted scapular stabilizer muscle activity with combined lower trapezius and serratus anterior weakness, while gray lines represent the sum of model-predicted muscle activity when lower trapezius and serratus anterior are weakened individually. The comparison of compound muscle weakness versus summed muscle weakness of lower trapezius and serratus anterior in figure 5.8. illustrate disparate shape and amplitude features between the grey and fuchsia lines which suggest that scapular stabilizer muscle activity with combined lower trapezius and serratus anterior weakness was not purely additive in nature. In most cases the amplitude of the purple line exceeded the grey line which may suggest that model-predicted muscle compensations strategies to weakness were more efficient than the summation of muscle activity required when each induvial muscle was weakened.

5.4.4. Limitations

As a purely mechanistic model of shoulder movement and weakness, the findings of this study are subject to several assumptions which should be considered.

Firstly, optimal weighting of terms in the cost function was tested and validated purely for frontal plane thoracohumeral elevation in a non-weakened state. The optimization function serves as an analog for the CNS's strategy to minimize several possible criteria, which literature has hypothesized to include task accuracy [Madeleine, 2010; Hirashima and Oya, 2016], muscle effort [Wada, et al., 2006], metabolic cost [Houdijk, Brown, and van Dieën, 2015], attention and cognitive load [Andersson, et al., 2002], discomfort [Marler, et al., 2009], joint stability [Cashaback and Cluff, 2015], and other variables. The present study assumes that optimization criteria remain relatively stable in the presence of muscle weakness, yet future research may improve our understanding of fatigue related kinematic and muscular compensation by investigating whether optimization criteria change in vivo due to muscle weakness or fatigue. The presently validated optimization function also produced muscle activity compensations to combined serratus anterior and lower trapezius weakness that were generally more efficient than the summation of muscle activity compensations from individual serratus anterior and lower trapezius weakness (figure 5.8.). This finding could be a product of the muscle effort minimization term in the cost function (equation 5.4.), which was set to penalize excessive muscle activity quadratically, following recommendations [Serrancolí et al., 2014]. Other muscle effort minimization exponent terms have been proposed in literature, including N^3 [Crowninshield et al., 1981; Erdemir et al., 2007]. and

$N^{5/2}$ [Wong et al., 2021] In some literature it appears that upper-limb tasks and goal-direct tasks may approximate a higher minimization exponent near N^3 [Wong et al., 2021], while ambulatory movements may be more appropriately modelled with quadratic terms. However, before validating the cost function weights in the present study, a pilot comparison between quadratic and cubic muscle weights enforced in the current model was undertaken which revealed that cubic muscle weights generally restricted scapulothoracic elevation in favor of excess glenohumeral elevation. These findings may be due to the reliance on serratus anterior that was illustrated in the present study, as a cubic muscle effort cost term would act to penalize the allocation of muscle stress on serratus anterior and this may not permit adequate scapulothoracic elevation. Crowninshield and Brand [1981] first commented that the number of model-predicted active muscles ($a > 0$) is very insensitive to changes in the muscle effort minimization term from N^2 to N^4. Altering this term appears to primarily effect the magnitude of predicted muscle forces and number of muscles recruited, whereby lower exponents permit a few muscles with optimal moment arms to drive most of the muscular effort and higher exponents may spread the effort more evenly across available effectors. Taken together with the current simulations, this may suggest that the redundancy of shoulder effectors can allow for the recruitment of many compensatory muscles at a relatively low level of activation as a more effective fatigue management strategy, yet serratus anterior in particular appears critical to stabilizing scapulothoracic elevation and compensatory muscle synergies may not be feasible. Future research may need to consider implementing a variable muscle effort term that penalizes key agonist muscles less than synergist muscles. The present study also assumes that the optimization criteria remain stable across the different planes of thoracohumeral elevation, and across alterations in muscle force producing capacity. The cost function (equation 5.5.) with weights w_1 = 100, w_2 = 0.1, w_3 = 1, and w_4 = 1 poses an optimal control problem where increases in muscle activity are weighed 1000 times less than deviations in kinematic tracking, and 10 times less than reductions in scapulothoracic adherence to the wall of the thorax and the stability of the glenohumeral joint. However scapulothoracic plane adherence and glenohumeral joint stability are both key factors that may be expected to change with muscle fatigue and muscle weakness as much research has linked shoulder muscle fatigue and muscle weakness with scapular dyskinesis and superior humeral head translation [Chopp-Hurley and Dickerson, 2015; Chopp and Dickerson, 2012; Kibler et al., 2013; Guiseppe et al., 202; Michener, McClure, and Karduna, 2003] Although the plane of motion and direction of loading was also not expected to alter the validity of the optimization function, this assumption was made based on the availability of gold-standard bone-pin scapulothoracic kinematic tracking data in the frontal plane to satisfy the requirements of SPM [Ludewig, et al., 2009]. In lieu of performing an SPM analysis between model-predicted and empirical data for scapular and sagittal plane kinematics, model-predicted data was compared to the mean joint angles from the empirical data, and typically fell within one standard deviation. Altering the weights of the optimization function terms in equation 4 also resulted in kinematic solutions with a poorer fit than those presented in figure 5.4. The statistical implications of an empirical sample size of N=12 should also be considered, as this data set likely lacks a complete characterization of the full landscape of valid empirical scapulothoracic kinematics. The DELFT shoulder and elbow model itself represents the musculoskeletal features derived from a single human cadaver [Van der Helm, 1994], thus any accurately predicted values are likely to fall somewhere within the landscape of feasible kinematic solutions but are unlikely to approximate the empirical mean. Sagittal plane model-predictions were found to be increasingly unstable beyond 75° thoracohumeral plane of elevation approaching 90°, thus sagittal plane solutions were set with thoracohumeral plane of elevation at 70°. Model instability near 90° may have arisen due to muscle-element wrapping issues and subsequent discontinuities in moment arm lengths. Finally, a version of the DELFT shoulder and elbow model with an unreduced set of 138 muscle elements was used for all simulations. This version of the model consists of 56 muscle elements connecting the thorax to the scapula, 37 muscle elements connecting the scapula to the humerus, and 14 muscle elements connecting the thorax directly to the humerus. The analysis and characterization of all model-predicted muscle activity changes is too broad to present in a single study, thus the decision was made to focus on the relationship between the scapular stabilizer muscles specifically, as weakness, fatigue, and altered activation of these muscles has shown relevance to many clinical and subclinical shoulder conditions in literature including shoulder dyskinesis, SAIS syndrome, and RC tears [Ludewig and Cook, 2000; Cools, et al., 2002; Michener, McClure, and Karduna, 2003; Szucs, Navalgund, and Borstad, 2009; Chopp, Fischer, and Dickerson, 2011; McClure, Greenberg, and Kareha, 2012; Michener, et al., 2016]. Regardless, the scapular stabilizer muscles do not operate as a closed system, and the many muscles acting on the shoulder are likely to contribute to weakness-related muscular compensations.

5.5. Conclusion

This study presents a model and optimal control framework for producing scapulothoracic kinematic solutions that closely match gold-standard empirical data. The weights of the cost function terms associated with successful scapulothoracic kinematics predictions suggest that goal-directed arm motions prioritize task accuracy, scapular adherence to the wall of the thorax, and glenohumeral joint stability over muscle effort. Reducing the maximal force generating capacity of scapular stabilizers with this modelling framework provided several insights on shoulder muscle compensation strategies to muscle weakness and fatigue. Frontal plane thoracohumeral elevation appeared the generate a more balanced recruitment of trapezius and serratus anterior and results illustrated that these muscles may compensate for isolated weakness of a single muscle. Across all planes of thoracohumeral elevation, serratus anterior weakness seems to demonstrate particular importance in maintaining scapular kinematics, and results suggest that weakness of serratus anterior may promote simultaneous increases in upper trapezius activity, which may compound the risk for suboptimal scapular stabilizer coactivation ratios. Results indicated that serratus anterior muscle recruitment may be isolated best in the scapular plane (40° anterior to the frontal plane), compare to the sagittal and frontal planes. Lower trapezius and serratus anterior also appeared to reach their highest activity above 100° of thoracohumeral elevation, which may contribute to the risks of shoulder muscle fatigue and kinematic changes associated with overhead work. Lastly, muscular activation compensations to combined muscle weakness of lower trapezius and serratus anterior appeared lesser in magnitude than the summation of muscle activation compensations to isolated lower trapezius and serratus anterior weakness which may reflect the efficiency of the muscular compensation strategies employed by the CNS. Improvements in the validity of model-predicted kinematics and muscle activity changes to weakness and fatigue would benefit from a deeper understanding of the somatosensory affects and other in vivo changes to the CNS's optimization criteria.

Afterword to chapter 5

Chapter 5 unveiled a key role for serratus anterior in stabilizing arm elevation across the frontal, scapular, and sagittal planes. In the frontal plane, trapezius and serratus weakness could be compensated for by the other shoulder musculature, but in the sagittal and scapular planes serratus anterior recruitment appeared more isolated which could have implications for fatigue protocol design. In the context of the overhead shoulder fatigue task from the previous chapters, these insights may explain why fatigue related serratus anterior amplitude change was reduced on day 2, as a learned strategy to incorporate the other shoulder musculature would have likely been an effective adaptation in this sagittal plane task. Finally, upper trapezius activity changes generally appeared to signal a compensatory mechanism for weakness at other stabilizer muscles, rather than weakness of upper trapezius itself. This could have important implications for the interpretation of scapular coactivation ratios. While chapter 3 did not find evidence of a single scapular muscle driving the observed coactivation ratio changes, simulation of muscle weakness/fatigue through reduced force-generating capacity appears to promote upper trapezius dominance as a compensatory mechanism.

Foreword to chapter 6

Thus far, chapters 3-5 largely investigate muscle fatigue as a characteristic of neuromuscular control. However, several other mechanisms contribute to muscle fatigue, as described in section 2.2. A limitation of many studies quantifying fatigue variability may be due to a reliance on EMG to fully quantify fatigue-related muscle and kinematics changes, as this tool is most commonly used in literature. Other interpretations of muscle fatigue and tools may be necessary to quantify the full scope of fatigue-relate muscle and kinematic changes, and the variability therein.

To complement the focused, mechanistic investigation of fatigue in chapter 5, chapter 6 of this dissertation steps in a new direction to investigate how muscle elasticity, a non-contractile muscle property, relates to common indices of fatigue quantification. This research approach appreciates the holistic nature of muscle fatigue, and aims to determine whether more comprehensive muscle fatigue measures are necessary to fully explain the associated variability.

Chapter 6. Congruency of Fatigue-Mediated changes in Shear Wave Velocity, Upper Limb Force, Muscle Activity, and Kinematics of the Scapular Stabilizer Muscles.

Matthew S. Russell, Janessa D.M. Drake, Jaclyn N. Chopp-Hurley

School of Kinesiology and Health Science, York University, Toronto, Canada

Corresponding Author:
Jaclyn Hurley, PhD
School of Kinesiology and Health Science
York University
4700 Keele Street, Toronto, Ontario, CA, M3J 1P3
Email: jnhurley@yorku.ca

Declarations of Interest: None

Funding Sources: This work was supported by the Natural Science and Engineering Council (NSERC) Discovery Grant program (J.N. Chopp-Hurley and J.D.M. Drake), Canadian Foundation for Innovation (CFI) (J.N. Chopp-Hurley), Ontario Research Fund (J.N. Chopp-Hurley), and the NSERC Post-Graduate Scholarship program (M.S. Russell).

6.1. Introduction

Shoulder kinematic and muscular responses to muscle fatigue are highly variable. Variability in shoulder control and response to fatigue stimuli represent how the highly redundant set of muscles in this region can resolve kinematic and kinetic task demands through a continuum of available muscular solutions [Chopp-Hurley, et al., 2016; McDonald, Mulla, and Keir, 2019; Mulla and Keir, 2023; Russell, et al., 2024]. The available muscular solutions to resolve task demands have been termed "load-sharing" strategies, which describe the relative muscle force and muscle activity contributions within the system [Bernstein, 1966; Baratta, et al., 1988; Latash, Scholz, and Schöner, 2007; Latash, 2018]. Often, these solutions minimize the muscle activity necessary to achieve a necessary kinetic task constraint by leveraging muscles with mechanically or metabolically optimal characteristics. Some muscle characteristics that improve optimality by minimizing the muscle activity required for a given task may include muscle moment arm length [Hincapie, et al., 2008; Van Den Bogert, Blana, and Heinrich, 2011; Hirashima and Oya, 2016], muscle cross-sectional area [Brand, Pedersen, and Friederich, 1986], distribution of type 1 and type 2 muscles fibers [Herzog and Leonard, 1991], fiber length [Praagman, et al., 2006], and pennation angle [Van Den Bogert, Blana, and Heinrich, 2011] while metabolic factors may include the vascular perfusion [Sjøgaard, et al., 1986; Praagman, et al., 2006] and accumulation of fatigue-related metabolites that alter cellular pH [Vatner and

Pagani, 1976; Allen, Lamb, and Westerblad, 2008]. Many of the aforementioned factors can be subject to genetic and morphological variation, and influenced further by lifestyle factors [Zhang, et al., 2003; Allen, Lamb, and Westerblad, 2008], challenging the ability to fully characterize fatigue-mediate muscular and kinematic changes.

Muscle fatigue is broadly defined as a transient state of reduced force-generating capacity [Enoka and Stuart, 1992; Enoka, 1995; Vøllestad, 1997]. This definition incorporates a holistic view of the various physiological changes that characterize muscle fatigue, including neuromuscular, mechanical, and chemical changes [Vatner and Pagani, 1976; Enoka and Stuart, 1992; Enoka, 1995; Vøllestad, 1997; Allen, Lamb, and Westerblad, 2008]. While research has spurred new techniques and technologies to characterize fatigue such as mechanomyography which quantifies acoustic muscle vibration [Beck, et al., 2004] or infrared spectroscopy which quantifies muscle oxygenation [Perrey, Quaresima, and Ferrari, 2024], EMG for quantifying neuromechanical muscle characteristics has been primarily used in research for the past 4-5 decades [de Duca and Forrest, 1973; Lindstrom and Magnusson, 1977; Hagberg, 1981; Stulen and De Luca, 1981; Christensen and Fuglsang-Frederiksen, 1988; De Luca and Merletti, 1988; De Luca, 1997]. Thusly, much research investigating load-sharing and kinematics responses to shoulder fatigue has used EMG to quantify muscle activity and muscle fatigue, and much of the variability in shoulder muscle control and fatigue-mediated changes that is yet unexplained by neuromechanical behavior may be further explored with other tools to characterize muscle fatigue.

Ultrasonographic shear wave elastography has become a prominent new technique for assessing muscle stiffness. The technique relies on a piezoelectric ultrasound transducer to impart a high amplitude, low-frequency acoustic waves relative to traditional ultrasound waves [Bercoff, Tanter, and Fink, 2004; Davis, et al., 2019]. The acoustic waves generate particle compression along the shear axis of underlying tissue [Bercoff, Tanter, and Fink, 2004], which propagates orthogonally from the point of application. Through an elastic medium, the speed of shear wave propagation will be relative to the tissue stiffness, described in Young's modulus [Nordin and Frankel, 2001; Özkaya, et al., 2012]. Muscle, a viscoelastic tissue, approximates an elastic medium over a very small timeframe due to the time-dependency characteristics of hysteresis [Nordin et al., 2001; Lynch et al., 2017; Firouzi, 2022]. Thus, ultrasonic shear wave propagation along muscle tissue can be used to directly calculate Young's modulus of elasticity, although assuming a constant density of the elastic medium (muscle) [Brandenburg, et al., 2014], the velocity of shear wave propagation (shear wave velocity; SWV) is directly proportional to Young's modulus and is often reported instead [Akagi and Kusama, 2015; Eby, et al., 2015; Agten, et al., 2017; Kelly, et al., 2018; Siracusa, et al., 2019]. Unlike traditionally used neuromechanical fatigue indices like EMG and tetanic force decrement which characterize active or contractile muscle properties [Allen, Lamb, and Westerblad, 2008], SWV assessments of muscle stiffness characterize the passive or non-contractile muscle element changes [Zimmer, et al., 2023], which is shown to viscoelastically increase compliance under consistent or repetitive loading [Andonian, et al., 2016; Siracusa, et al., 2019; Vatovec, Kozinc, and Voglar, 2022]. This viscoelastic compliance, due to mechanical creep, lengthens the time for muscle forces to transfer to bone and reduces the ability to store energy elastically [Kubo, et al., 2001; Zhang, et al., 2003]. Therefore, fatigue-mediated muscle stiffness changes due to fatigue present a hypothetical framework for disrupting muscle force through a physiological pathway that is distinct from traditional EMG based metrics.

Several studies have already explored SWV characteristics associated with contraction intensity, muscle force/joint torque, and exercise and fatigue. Specifically, SWV appears highly correlated ($r = 0.99$) to joint torque as reported in the elbow flexors [Yoshitake et al., 2014] and finger muscles ($r^2 = 0.951$-0.997), while studies reporting on the relationship between SWV and contraction intensity have found relationships of varying strength at the knee flexors ($r = 0.156$ to 0.982, $\mu = 0.740$) [Mendes et al., 2018], and shoulder muscles ($r = -0.53$ to -0.57) [Koznic et al., 2020]. The strength of SWV relationships with muscle force/joint torque may suggest that SWV relationships with muscle activity are highly dependent on the variance in muscle force generating capacity within a population, contributing to the reported variance in correlation coefficients [Yoshitake et al., 2014; Mendes et al., 2018; Kozinc et al., 2020; Cipriano et al., 2022]. Strong linear relationships between SWV and muscle force but not necessarily contraction intensity also contrast previously defined relationships between contraction intensity and EMG amplitude and frequency (Alkner, Tesch et al. 2000, Reddy, Mohr et al. 2000, Stegeman, Blok et al. 2000, Farina, Merletti et al. 2004, De Ruiter, Elzinga et al. 2005, Shenoy, Mishra et al. 2011, Lee, Min et al. 2021, Nasr, Inkol et al. 2021). Like EMG amplitude normalization techniques, the relationship between SWV and muscle force may highlight the need to normalize SWV measures as a percent change in SWV relative to 0% and 100% maximal voluntary contraction (MVC) to make comparisons between individuals more relevant as done in some previous studies (Yoshitake, Takai et al. 2014). Research investigating submaximal exertion intensity on SWV measurements have reported muscle-specific SWV responses. Kelly and colleagues [2018] previously identified significant increases in erector spinae stiffness (kPA) at 40% and 80% contraction intensity when compared to rest, yet these changes did not emerge at the infraspinatus or gastrocnemius muscle. Bouillard, Nordez and Hug [2012] previously captured shear elastic modulus changes in biceps brachii short head, biceps brachii long head, brachioradialis, brachialis, and triceps brachii long head during an elbow flexion task with ramping exertion intensity. Two important findings from this study (1) support the notion that muscle stiffness relates to joint torque with coefficient of determination values ranging from 0.85-0.93, and (2) revealed significantly higher brachialis stiffness compared to other flexor muscles ($p = 0.008$). These authors have suggested that muscles displaying increased stiffness relative to joint torque likely reflect load-sharing synergies determined by optimal muscle stiffness properties. [Bouillard et al., 2012; Yoshitake et al., 2014; Eby et al., 2015; Kelly et al., 2018]. Nordez and Hug [2012] also note that muscle stiffness changes associated with elbow flexion joint torque closely match EMG amplitude responses to joint torque from the same muscles in a previous study [2010] and surmise that EMG amplitude patterns may be a reflection of load-sharing patterns. However resting SWV measurements have also shown to be bias to passive muscle stiffness [Bouillard et al., 2012; Ewertsen et al., 2018], including studies by Alifurah et al. [2017] and Martiartu et al., [2021] who both identified that transducer positions further from the center of the muscle belly measured increased stiffness, and poorer interclass correlations. These studies highlight the importance of measuring SWV in at a consistent muscle length that is not stretched near end range. These findings mentioned also highlight the importance of studying SWV both at rest, and during submaximal exertions where the muscle is best recruited and least likely to permit load sharing. Finally, a number of studies have previously investigated SWV changes following exercise or muscle fatigue and report decrements in resting state SWV [Andonian et al., 2016; Siracusa et al., 2019; Vatovec et al., 2022], thought to be attributable to passive muscle element creep. However, thus far no analysis of fatigue-mediated scapular stabilizer muscle SWV has been reported, and the investigation of muscle stiffness changes may help to unveil load-sharing strategies associated with fatigue in a redundant muscular system.

The purpose of this study was to determine whether fatigue-mediated changes in muscle stiffness are present following a targeted fatigue task of the scapular stabilizer muscles, and whether fatigue-related changes in passive muscle element stiffness contribute significant predictive variance in determining fatigue state and subsequent kinematic changes, accounting for some of the unexplained variability in scapular kinematics. Our hypotheses are (1) muscle SWV, proportional to muscle stiffness, will decrease following a muscle fatigue protocol to reflect viscoelastic creep and hysteresis, (2) fatigue-related changes in muscle SWV will correlate with current holistic (force) and neuromuscular (EMG) indices of muscle fatigue, and (3) fatigue related changes in muscle SWV are expected to significantly improve prediction of kinematics changes.

6.2. Methods

6.2.1. Participants

Fifteen male (27.5±4.7 y; 25.3±3.1 kg/m^2) and fifteen female (23.7±2.7 y; 20.0±1.6 kg/m^2) (N = 30) participants were sampled from the local university population for a single 2-hour long collection. Participants were all self-identified as right-hand dominant although this was not an express inclusion criterion.

Participants were excluded if they self-reported a score below 25 on the DASH [Alcántara-Bumbiedro, et al., 2006], or a score below 20 on the TSK [Chimenti, et al., 2021]. This study received ethics approval from the York University Office of Research Ethics (#e2024-112). All participants provided written informed consent.

6.2.2. Protocol

6.2.2.1. Pre-Fatigue Testing

After first completing written informed consent and the self-report questionnaires to determine inclusion criteria, participants were asked to remove their shirt (male) or change into a sports bra (female) using onsite change rooms. Participants were then asked to lie on a plinth while the researcher captured resting muscle SWV of UT, MT, LT, and serratus anterior in a randomized order (figure 6.1.). Next, application of surface EMG and resting muscle activity was sampled over three 5-second trials where the participant lay prone and instructed to relax. Participants then proceeded to complete 2 bouts of maximal voluntary isometric contractions (MVIC) for 3 muscle tests presented as a random order of 6 total tests: shrug, modified prone elevation, and palm press [Ekstrom, Soderberg, and Donatelli, 2005; Boettcher, Ginn, and Cathers, 2008; Ginn, Halaki, and Cathers, 2011; McDonald, Sonne, and Keir, 2017]. The peak force across each set of dual muscle tests was used as the representative maximal force generating capacity for that muscle test. These force levels were used to scale a randomly-ordered bout of submaximal voluntary isometric contraction (SVIC) consisting of the same three muscle tests completed at 30%, 50%, and 70% MVIC force output. Due to the inability to capture two muscles simultaneously using ultrasound, all SVIC bouts for the modified prone elevation were performed twice; once to capture middle trapezius SWV and once to capture lower trapezius SWV. A total of 12 SVIC tests were performed in random order. Participants then completed static arm elevation trials by holding their arm at 30°, 60°, 90°, and 120° thoracohumeral elevation in the scapular plane (40° anterior to frontal plane) for 5 seconds while holding a 1 kg weight [Chopp, Fischer, and Dickerson, 2011]. The order of these 4 arm elevation trials was randomized.

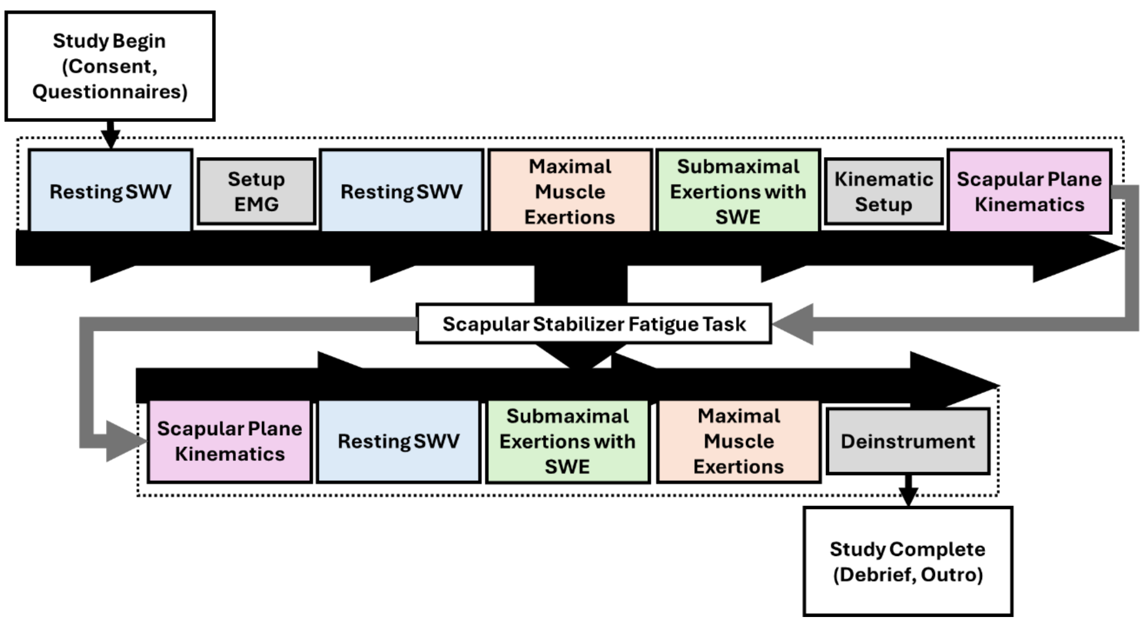

Figure 6.1. **Timeline of Study Experimental Protocol Procedures.** Identical Procedures are Color Matched.

6.2.2.2. Fatigue Protocol

Following the completion of the pre-fatigue testing protocol, participants began the scapular muscle fatigue protocol. Adapted from Suzuki and colleagues [Suzuki, et al., 2006], this protocol required participants to perform 4 muscle tests successively, for one minute each, until they failed to maintain form on 3 of the 4 tests (figure 6.2.; table 6.1.). All tests were completed at a frequency of 30 bpm (0.5 Hz). Failure criteria for each test was determined as an inability to maintain full ROM or 30 bpm after a single warning from researcher. Once a muscle test reached failure, the participant immediately proceeded to the next muscle test in the protocol. If the participant completed a full cycle without failing at least 3 muscle tests, they performed all muscle tests again until failure or for 1 minute each, whichever occurred first. An initial pilot analysis of 3 males (25.0±1 y; 26.1±1.0 kg/m^2) and 3 females (24.7±2.9 y; 20.4±1.3 kg/m^2) found that this fatigue protocol reliably induced significant group-wise increases in EMG RMS amplitude and decreases in EMG MPF of ≥ 8% across UT, MT, LT, and SA, where other fatigue protocols from literature were unsuccessful [McQuade, Dawson, and Smidt, 1998; Szucs, Navalgund, and Borstad, 2009; Noguchi, et al., 2013].

Table 6.1. **Description of Muscle Tests Used in Fatigue Protocol.** Tests are presented in Descending Order as they were Ordered for Participants.

Test	Task Description (within 2 second cadence)
Shrug	Participants were instructed to raise their shoulder to their ear and return while holding load equivalent to 70% of their maximal shrug force while seated [Suzuki, et al., 2006; Boettcher, Ginn, and Cathers, 2008].
Push-up Plus	Participants were instructed to perform max range scapular protraction and retraction while their feet were elevated 23 cm on a height-adjustable plinth [Suzuki, et al., 2006; Szucs, Navalgund, and Borstad, 2009].
Prone Row	Participants were instructed to lift a load equivalent to 20% of their maximal row force from a posture of 90° shoulder elevation and 0° elbow flexion to and posture of 0° shoulder elevation and 90° elbow flexion and return while prone [Suzuki, et al., 2006; Noguchi, et al., 2013].
Prone Elevation at 120°	Participants were instructed to raise a load equivalent to 30% of their maximal prone elevation force from a posture of 90° thoracohumeral elevation and 90°

	thoracohumeral plane of elevation to a posture of elevation force from a posture of 120° thoracohumeral elevation and 0° thoracohumeral plane of elevation and return while maintaining a straight elbow [Suzuki, et al., 2006; Boettcher, Ginn, and Cathers, 2008].

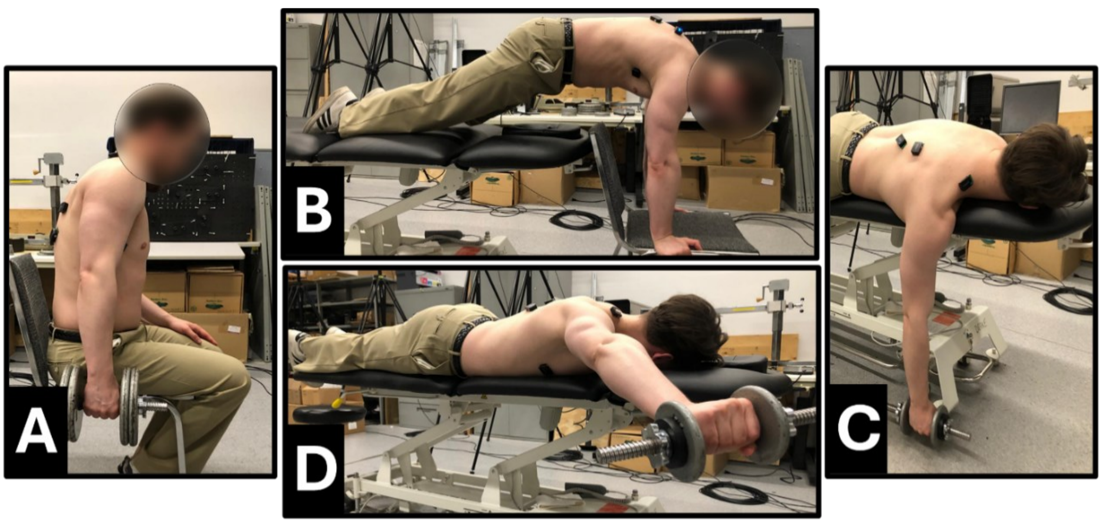

Figure 6.2. **Illustration of Fatigue Protocol Tasks. A.** Shrug. **B.** Push-up Plus. **C.** Row. **D.** Prone Elevation.

6.2.2.3. Post-Fatigue Tests

After completing the muscle fatigue protocol, participants immediately reperformed the 4 static thoracohumeral elevation tasks with a 1kg hand load. Participants then proceeded to have their resting SWV assessed for UT, MT, LT, and serratus anterior again. Finally, participants completed 15 isometric muscle tests consisting of the 12 SVIC tests and 3 MVIC tests. Following completion of these post-fatigue muscle tests, the study protocol was completed and participants were unequipped of all electrodes, promptly changed back into their shirt, and reimbursed for their time.

6.2.3. Data Acquisition and Analysis

6.2.3.1. Surface Electromyography

Muscle activity of UT, MT, LT, and serratus anterior was collected from the dominant right side of all participants using a Delsys Trigno system (Delsys Inc., 23 Strathmore Rd, Natick, MA, USA) and surface Avanti electrodes. Sensors featured 10mm spaced silver (99.99%) bar electrodes aligned with the muscle fibre orientation and record at 2148 Hz within a passband of 20-450 Hz. Electrode placement was standardized to the middle one-third of the muscle belly, oriented in the direction of the muscle fibres [Stegeman and Hermens, 2007; Besomi, et al., 2019] (figure 6.3.).

EMG signal was decomposed into two metrics of muscle fatigue: RMS amplitude, and MPF. To characterize RMS amplitude, all raw signals were first dual-band-pass filtered at 30-500 Hz [Stulen and De Luca, 1981; Öberg, 1995; Willigenburg, et al., 2012]. Peak amplitude was acquired from the middle 3-seconds of each 5-second MVIC and SVIC contraction, from which all amplitudes were subtracted by the average resting muscle EMG RMS amplitude, and normalized to MVIC EMG RMS amplitude for statistical analysis. To decompose

EMG signals into MPF, all raw signals were first dual-band-pass filtered at 10-500 Hz [Stulen and De Luca, 1981; Öberg, 1995; Willigenburg, et al., 2012]. Signal were subsequently divided into 0.5-second epochs and filtered with a discrete Fourier transform to calculate the MPF across the first 3-seconds of all MVIC and SVIC trials [Hendrix, et al., 2010]. Muscle-specific fatigue was defined as a MPF reduction of 8% or more [Öberg, 1995].

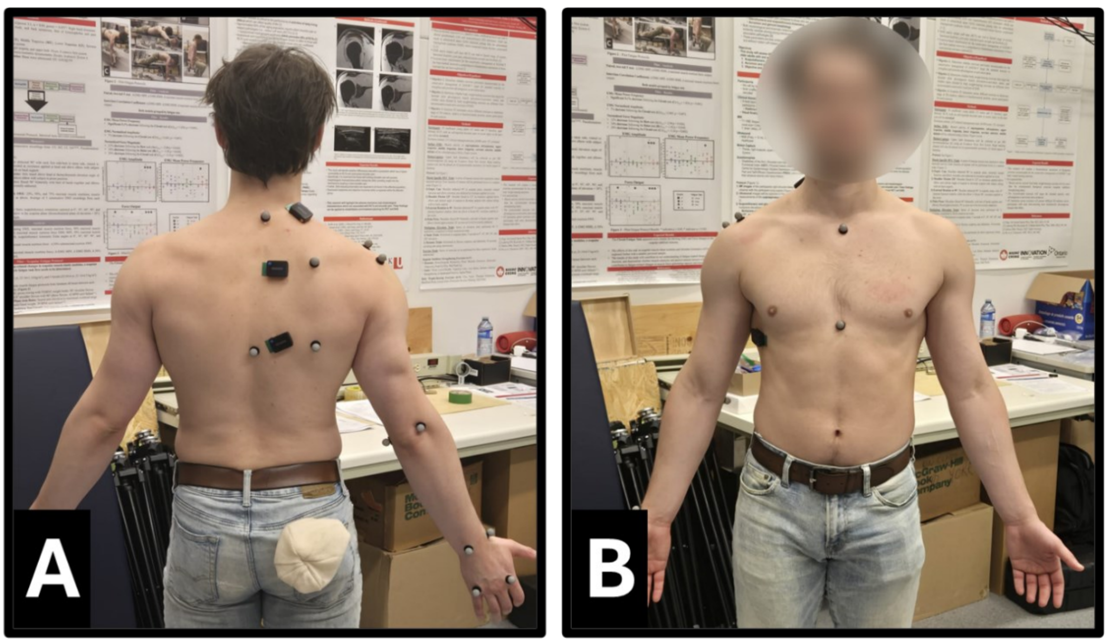

Figure 6.3. **Electrode and Reflective Marker Placement. A.** Posterior, and **B.** Anterior View.

6.2.3.2. Ultrasonographic Shear Wave Velocity

Ultrasonographic SWV measurements were captured with a Logic E10 unit (General Electric HealthCare, Mississauga, On, Canada) from UT, MT, LT, and SA. Several previous studies have described optimal ultrasound transducer placement in parallel with muscle fibre orientation, approximated to the middle one-third of the muscle belly [Eby, et al., 2015; Kelly, et al., 2018; Koppenhaver, et al., 2018]. These locations conflate with recommended surface EMG sensor placement locations [Stegeman and Hermens, 2007; Besomi, et al., 2019] presenting a equivocal dilemma. In the present study EMG sensor placement was prioritized to the recommended area, while ultrasound transducer location was localized 2 cm superior to the recommended area, such that it was directly overlaying the EMG electrode (figure 6.4.). Upper and lower bounds of the ultrasound SWV function ROI window were set to the superficial and deep aponeuroses of the target muscle, from which a 0.25 cm radii measurement region was automatically rectified in the centre of the ROI (Figure 6.5.) similar to previous methods [Kelly, et al., 2018; Siracusa, et al., 2019]. A pilot study involving 5 male (27.2±4.0 y; 25.5±1.5 kg/m^2) and 5 female (24.8±2.2 y; 20.0±1.6 kg/m^2) participants who went on to participate in the full study were used to assess the minimum ROI bounds representative of the participant sample of interest. From this pilot study, a minimum ROI depth of 0.25cm was determined, from which the 0.25cm radii measurement region size was determined and standardized across all participants for the current study.

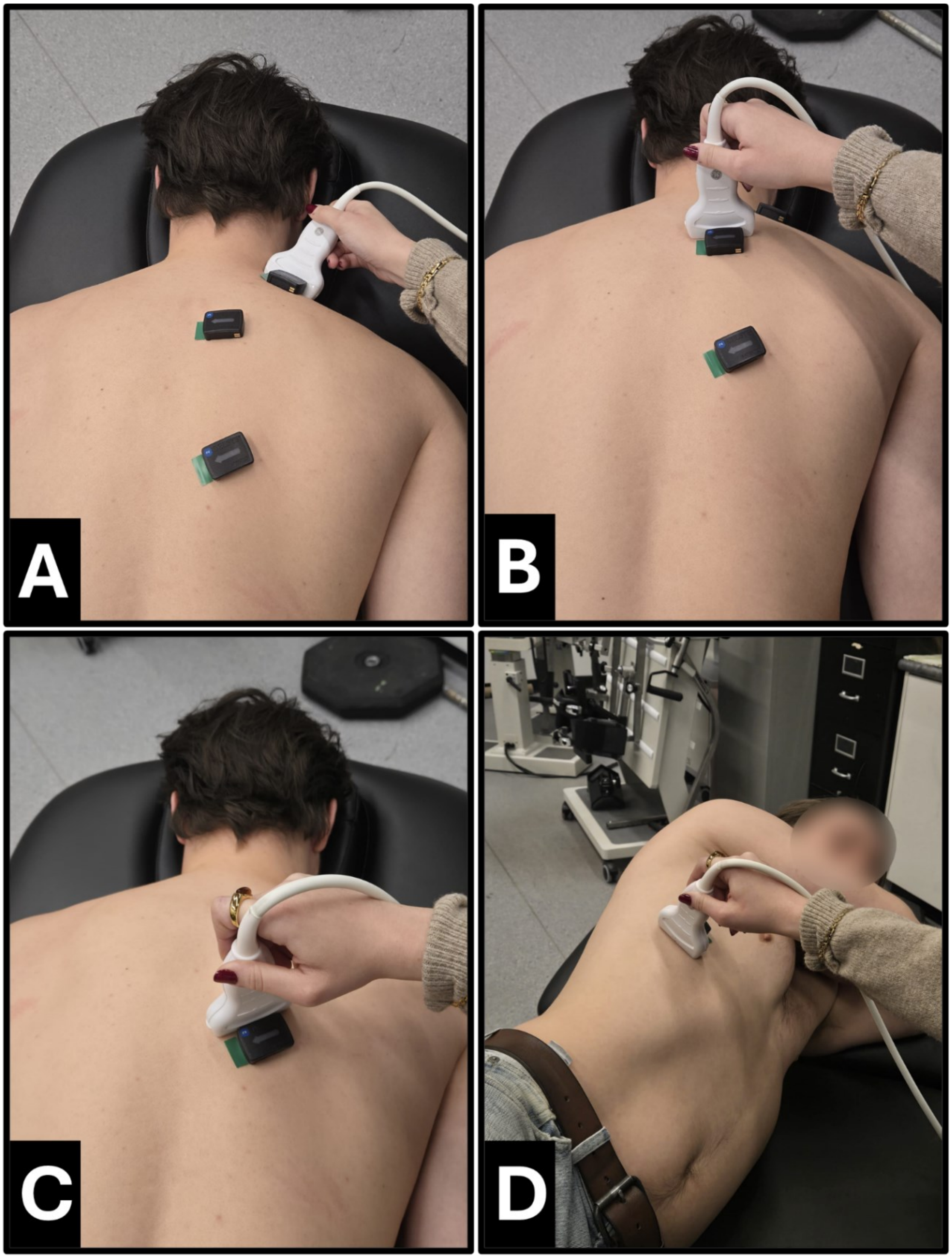
A
B
C
D

Figure 6.4. **Resting Ultrasonographic Shear Wave Velocity Testing Postures. A.** Upper Trapezius **B.** Middle Trapezius **C.** Lower Trapezius and **D.** Serratus Anterior.

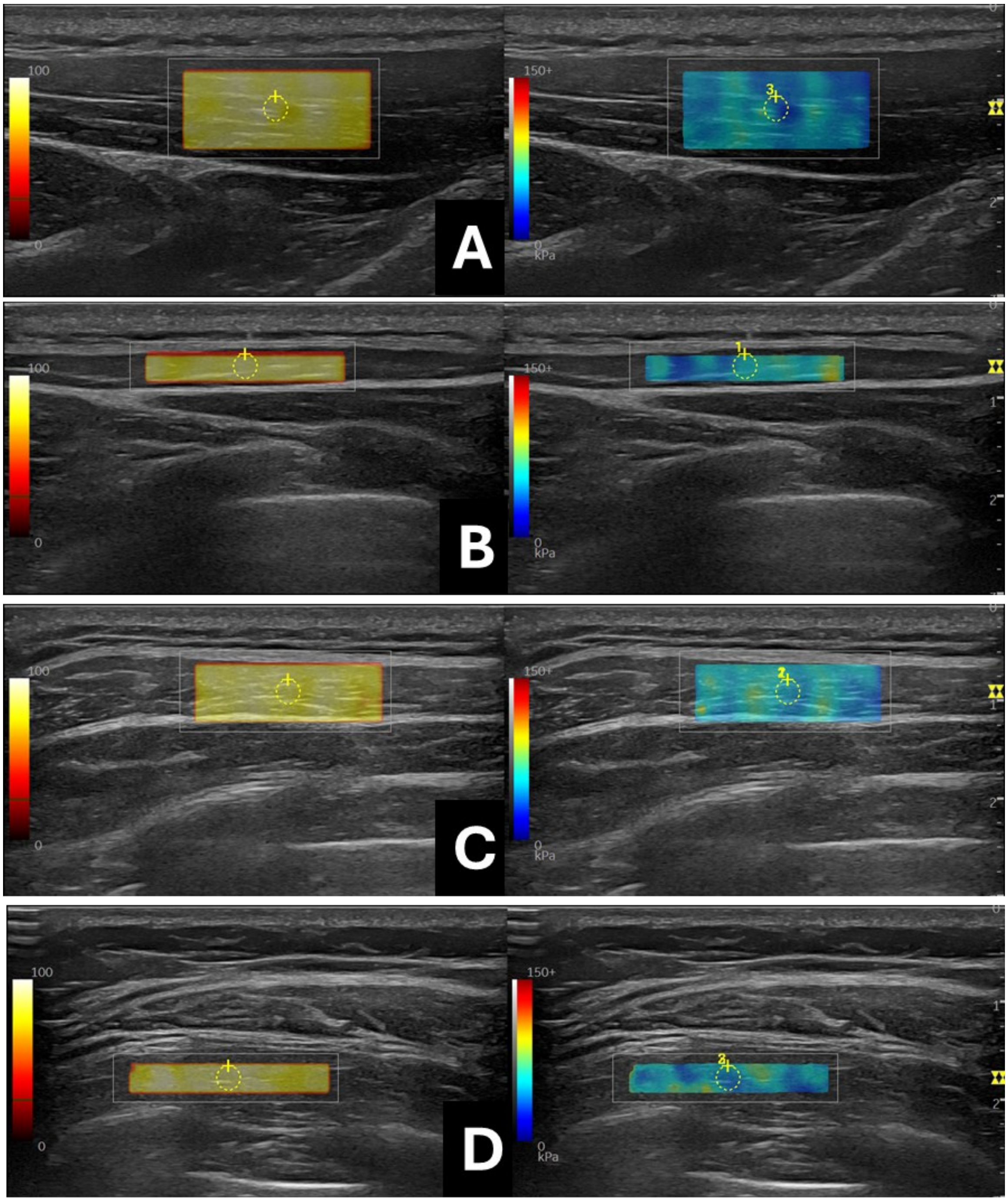

Figure 6.5. **Ultrasonographic Shear Wave Elastogram Visualization. A.**

Upper Trapezius **B.** Middle Trapezius **C.** Lower Trapezius and **D.** Serratus Anterior.

During pre-fatigue and post-fatigue resting SWV trials, SWV was calculated as the median measure captured across 7 successive SWV scans [Hatta, et al., 2014; Siracusa, et al., 2019; Vanhaezebrouck, 2021; Vatovec, Kozinc, and Voglar, 2022]. During pre-fatigue and post-fatigue SVIC muscle testing, the 5 second contraction window permitted 2 full SWV scans, from which the average was taken. SVIC SWV values were normalized as a ratio of each participants resting SWV for each muscle to account for interindividual differences in SWV which may be considerable and are likely to influence between-participant comparisons of SWV measures.

6.2.3.3. Manual Muscle Force Testing

Muscle force for all MVIC and SVIC tests (figure 6.6.; table 6.2.) was captured using a Biodex System 4 Quickset isokinetic dynamometer. All muscle test configurations were set to isometric resistance, and testing postures were identical across all contraction intensities (30%, 50%, 70%, 100%). For statistical analysis purposes, only the change in 100% (MVIC) force was recorded to be compared from pre-fatigue to post-fatigue. SVIC force output levels were only used to standardized force output while obtaining EMG and SWV measures.

Table 6.2. **Description of MVIC and SVIC Muscle Tests.** For all Tests, The Contralateral Hand was Instructed to be Used to Stabilize the Exertion by Holding a Handle at Seat Height.

Test	Muscle	Description
Shrug	Upper Trapezius; UT	Dynamometer handle was aligned to participant with their dominant/right hand/arm hanging at their side while seated. Participant was instructed to attempt to bring their shoulder to their ear against immovable resistance [Ekstrom, Soderberg, and Donatelli, 2005; Boettcher, Ginn, and Cathers, 2008].
Modified Prone Elevation	Middle Trapezius; MT Lower Trapezius; LT	Dynamometer arm was aligned with the participant's arm while seated with their dominant/right arm in a posture of 120° thoracohumeral elevation, 0° thoracohumeral elevation, palm facing forward. Participants were

		instructed to push their arm backwards into the dynamometer handle supplying immovable resistance. This test was shown to be highly reliable for both middle trapezius and lower trapezius muscle recruitment [Ekstrom, Soderberg, and Donatelli, 2005].
Palm Press	Serratus Anterior; SA	Dynamometer handle was oriented at the height of the participants navel, inline with their sagittal plane, 20cm in front of them. The participant, seated, was instructed to press the handle towards the left side of their body against immovable resistance [Boettcher, Ginn, and Cathers, 2008; Ginn, Halaki, and Cathers, 2011; McDonald, Sonne, and Keir, 2017].

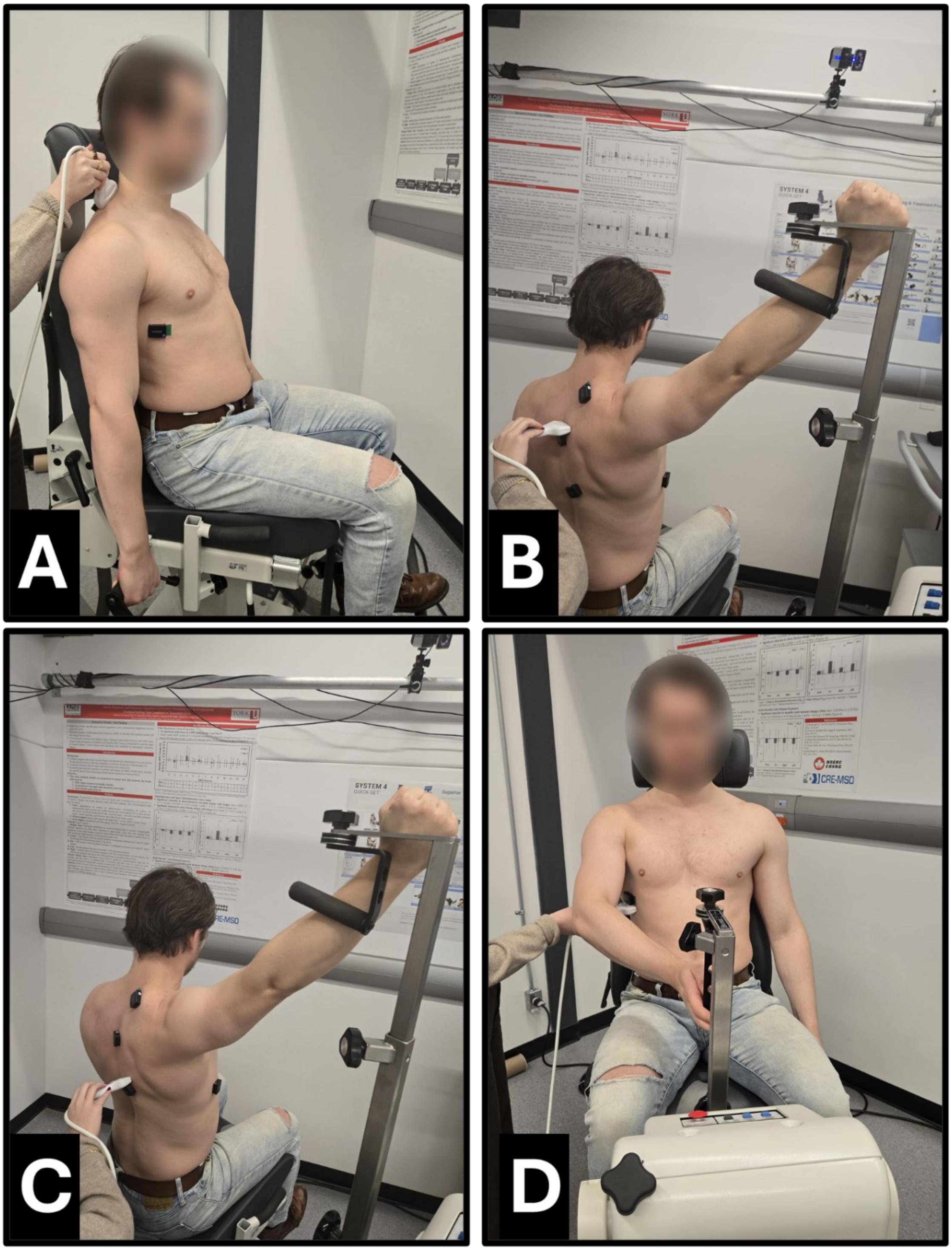
A
B
C
D

Figure 6.6. **MVIC and SVIC Testing Postures**. **A.** Shrug Test (Upper Trapezius) **B.** Modified Prone Elevation Test (Middle Trapezius) **C.** Modified Prone Elevation Test (Lower Trapezius) and **D.** Palm Press Test (Serratus Anterior). Ultrasound Transducer Placements during SVIC Testing are Illustrated.

6.2.3.4. Kinematic Motion Capture

Fourteen 19mm diameter reflective Vicon pearl markers were affixed across participants upper limb (acromion, lateral epicondyle, medial epicondyle, radial styloid, ulnar styloid, base of 2nd metacarpal, base of 5th metacarpal), scapula (inferior angle, acromion angle, trigonum spinae) and thorax (7th cervical vertebrae, 8th thoracic vertebrae, suprasternal notch, xiphoid process) following recommendations by the ISB Standards and Terminology Committee (STC) [Wu, et al., 2005] (figure 6.3.). For each static thoracohumeral elevation trial (4 pre-fatigue, 4post-fatigue) participants were instructed to hold a pole with their hand height measured in advance to produce the desired thoracohumeral elevation angle (30°, 60°, 90°, 120°). While holding the desired height, the researcher manually palpated all three scapular landmarks (inferior angle, acromion angle, trigonum spinae) and affixed 19mm Vicon pearl markers. This process was repeated before each static arm elevation trial to attempt to control for scapular movement artefact below the skin [Shaheen, Alexander, and Bull, 2011; Grewal, Cudlip, and Dickerson, 2017].

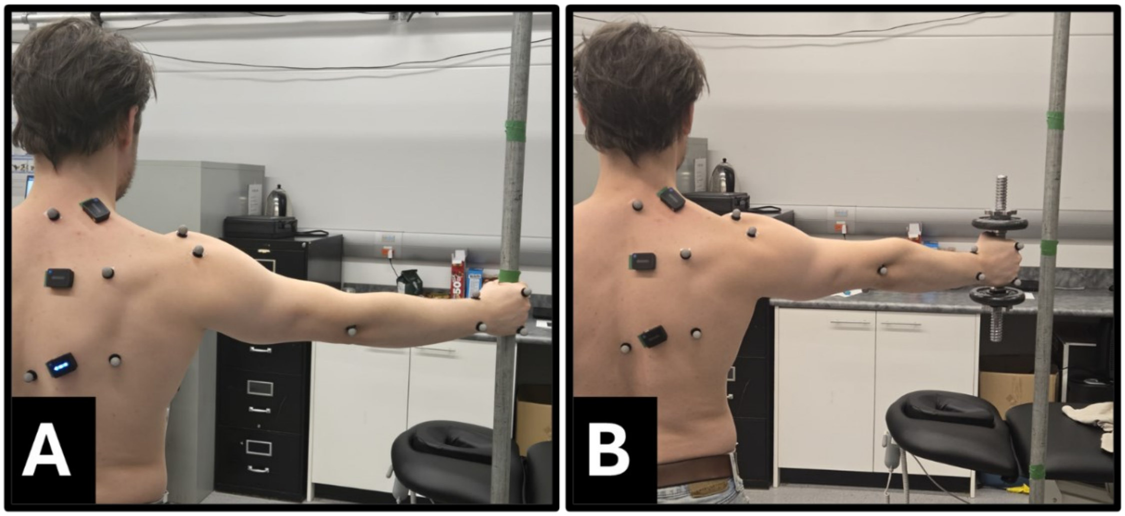

Figure 6.7. **Static Arm Elevation Trial. A.** Static Pole Hold at 90° Thoracohumeral Elevation. **B.** Static Arm Elevation with 1kg Manual Load at 90° Thoracohumeral Elevation.

Scapulothoracic joint angles were decomposed from marker positions following the defined axes of rotation suggested by the STC [Wu and Cavanagh, 1995; Wu, et al., 2005]. Average scapulothoracic joint angle for each axis of motion was reported for each static elevation trial height and compared from pre-fatigue to post-fatigue.

6.2.4. Statistical Analysis

For all statistical modelling, EMG RMS and MPF, force output, SWV, and kinematic joint angle factors had all outliers beyond 2 standard deviations removed before analysis. For all pairwise comparisons, if an outlier was removed from analysis, the comparative pairwise scores were not entered into analysis.

To determine the effect of fatigue on maximal and submaximal SWV changes, two-way repeated measures ANOVA models compared the change in relative SWV from pre-fatigue to post-fatigue (post-fatigue minus pre-fatigue) as the dependent variable across muscle (upper trapezius, middle trapezius, lower trapezius, serratus anterior) and intensity (0% rest, 30%, 50%, and 70% factors). Two additional two-way repeated measures ANOVA models were also computed to compare the change in relative EMG RMS from pre-fatigue to post-fatigue (post minus pre), and relative EMG MPF ([post/pre]*100). MPF was presented as a ratio from baseline to easily identify post-fatigue changes which exceed a decrease of 8% used to identify myoelectric fatigue [Öberg, 1995]. (Öberg 1995). To easily identify contraction intensities that elicited significant pre-fatigue to post-fatigue changes in SVW, EMG RMS amplitude, or EMG MPF, 95% confidence intervals were reported when interaction factors were significant. Lastly, 3 paired t tests compared groupwise changes in MVIC force output as the dependent variable by muscle test (shrug, modified prone elevation, and palm press). For all ANOVA models, pairwise comparisons were computed with Sidak adjustments. In the event that muscle and contraction intensity factors revealed an interaction effect for any model, pairwise comparisons were only reported by muscle, and comparisons across muscles were not reported.

To test the linear relationship between SWV and EMG/force based indications of muscle fatigue, a multiple regression was computed post hoc by comparing fatigue-related SWV changes (dependent variable) to fatigue-related EMG RMS, EMG MPF, and force decrement changes (predictor variables). To control for model overfitting and multicollinearity, only the contraction intensity deemed most sensitive to fatigue-related changes for the dependent variable and each predictor variable was selected for regression model input. These contraction intensities were 100% MVIC for EMG MPF and EMF RMS variables, and 30% SVIC for SWV. Force decrement was only captured at MVIC. Variance inflation factor diagnostics (VIF) were reviewed to determine risk of multicollinearity among the selected predictor variables.

Lastly, to determine fatigue-related neuromuscular and viscoelastic muscle tissue changes that predict scapulothoracic kinematics changes, 48 multiple regression models were computed using fatigue-related changes in EMG RMS, EMG MPF, SWV of each muscle (UT, MT, LT, SA), and force as predictor variables. For each model, the dependent variable was one scapulothoracic DOF (posterior tilt, medial rotation, protraction) at one angle of thoracohumeral elevation (30°, 60°, 90°, 120°). To control for model overfitting and multicollinearity, the contraction intensity deemed most sensitive to fatigue-related changes for each predictor variable was determined post hoc and selected for assignment to the regression.

6.3. Results

6.3.1. Fatigue-Related Changes

ANOVA revealed significant changes in SWV associated with muscle ($F_{(3,44)}$ = 4.76, p ≤ 0.001) and contraction intensity ($F_{(3,44)}$ = 58.91, p ≤ 0.001) variables, with no interaction effect. Pairwise comparisons (figure 6.8.) revealed a significantly greater increase in serratus anterior SWV compared to lower trapezius (p ≤ 0.001), middle trapezius (p = 0.007), and upper trapezius (p = 0.015) across all trials. Contraction intensity indicated significantly greater increases in SWV at 30% MVIC compared to all other intensities (p ≤ 0.001) (figure 6.8.). 50% MVIC was also significantly different from all other contraction intensities (p ≤ 0.001). 95% confidence interval margins for muscle contraction intensity were 0% = [-11.66 6.64], 30% = [82.74 110.93], 50% = [38.91 57.11], and 70% = [-10.42 7.87].

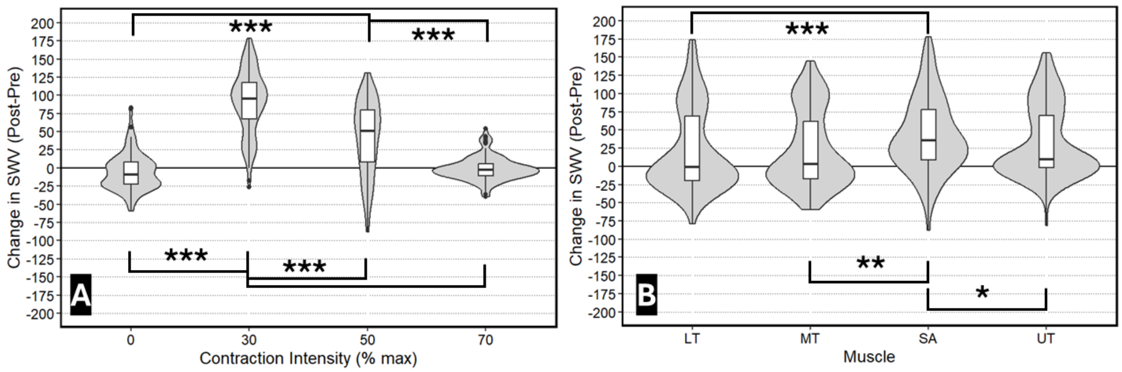

Figure 6.8. **Fatigue-Related Change in Ultrasonic Shear Wave Velocity.** Grouped by Muscle, Separated by Contraction Intensity (Panel **A**), and Grouped by Contraction Intensity, Separated by Muscle (Panel **B**). * Indicates Significance at p ≤ 0.05, ** Indicates Significance at p ≤ 0.01, *** Indicates Significance at p ≤ 0.001.

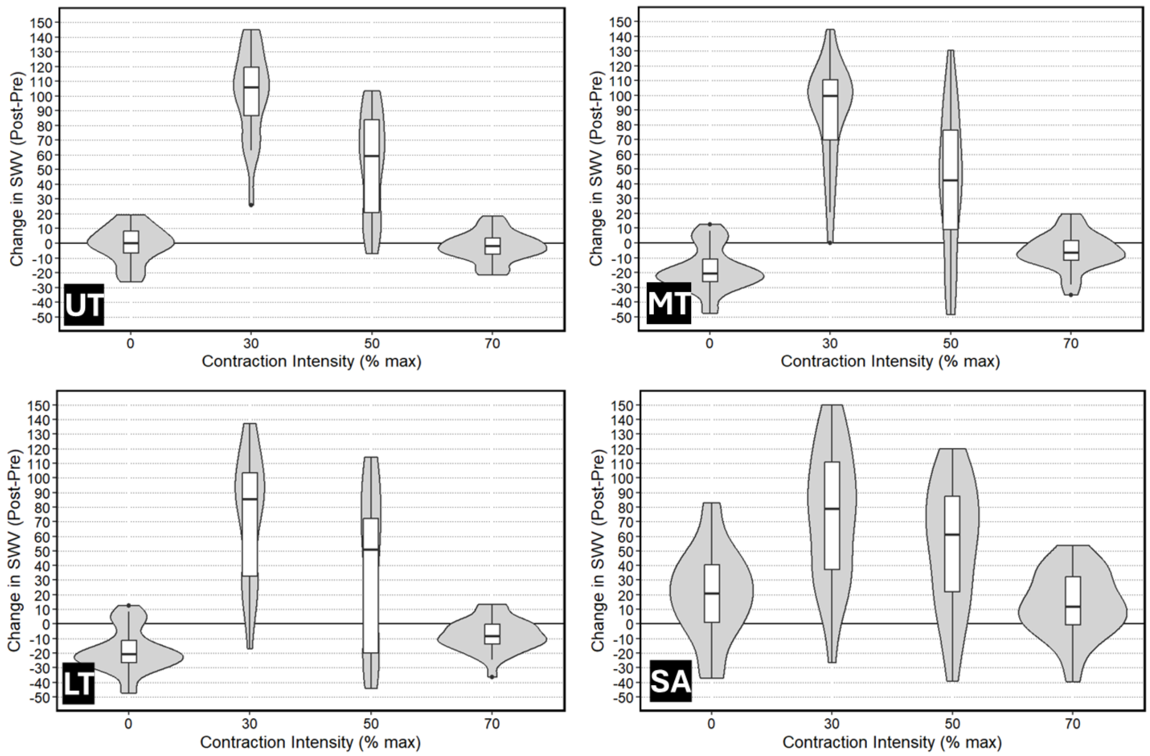

Figure 6.9. **Fatigue-Related Change in Ultrasonic Shear Wave Velocity.** Separated by Muscle (Panel) and Contraction Intensity (Abscissa). Illustrative Purposes Only; Significant Relationships Plotted in **Figure 6.8.**

ANOVA of EMG RMS amplitude change from pre-fatigue to post-fatigue indicated a significant main effect of contraction intensity ($F_{(3,43)} = 34.92$, $p \leq 0.001$) while comparisons by muscle neared the designated significant alpha threshold of $p \leq 0.05$ ($F_{(3,43)} = 2.55$, $p = 0.055$) (figure 6.10.). Pairwise comparisons between contraction intensity thresholds revealed that 100% MIVC EMG RMS amplitude changes post-fatigue were significantly greater than those at submaximal intensities ($p \leq 0.001$). However, 70% contraction intensity was still more sensitive at identifying EMG RMS amplitude increases post-fatigue than 50% (p = 0.027) or 30% (p = 0.001) MVIC. 95% confidence interval margins by contraction intensity were 30% = [-10.40 9.31], 50% = [0.88 20.24], 70% = [6.35 35.22], 100% = [41.10 60.25].

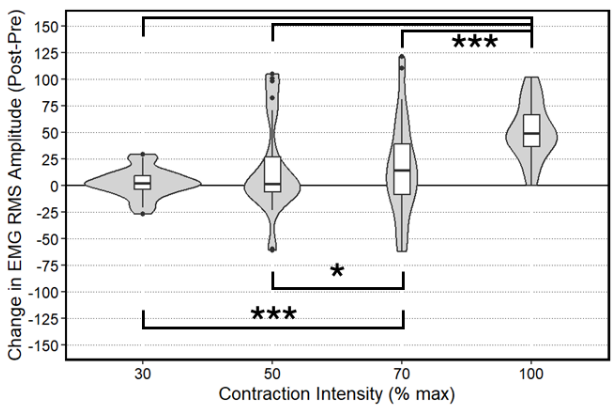

Figure 6.10. **Fatigue-Related Change in Electromyographic Root-Mean-Squared Amplitude.** Grouped by Contraction Intensity (Abscissa). Muscle Factor Grouped. * Indicates Significance at $p \leq 0.05$, *** Indicates Significance at $p \leq 0.001$.

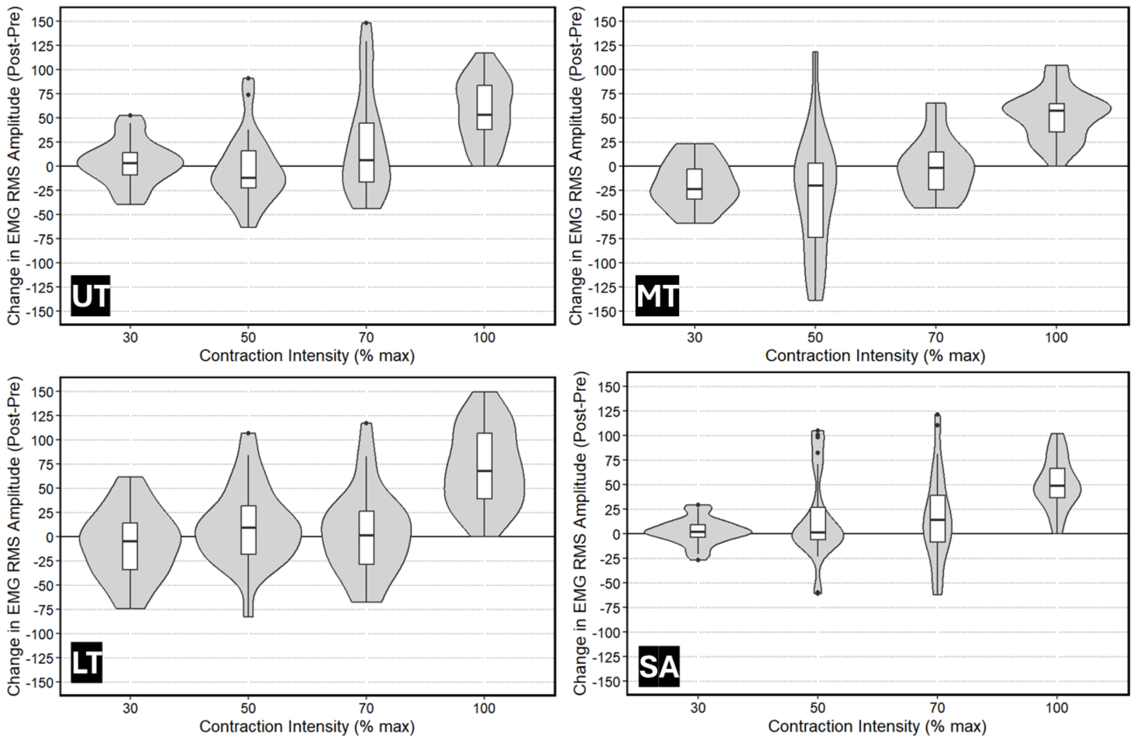

Figure 6.11. **Fatigue-Related Change in Electromyographic Root-Mean-Squared Amplitude.** Separated by Muscle (Panel) and Contraction Intensity (Abscissa). Illustrative Purposes Only; Significant Relationships Plotted in **Figure 6.10.**

ANOVA modelling of EMG MPF changes revealed a significant muscle by contraction intensity interaction effect ($F_{(9,42)} = 4.99$, $p \leq 0.001$), therefore, pairwise comparisons were reported by muscle. Comparisons revealed that MPF only showed meaningful post-fatigue decreases in serratus anterior at 100% MVIC compared to 70% ($p = 0.045$), 50% ($p = 0.015$), and 30% ($p \leq 0.001$) (figure 6.12.). Post-fatigue MPF at 100% MVIC was the only group-wise fatigue-related change in MPF to decrease, and to surpass a threshold of 8% decrease (9.6 ± 14.2%; 95% CI = [-11.19 -1.30]).

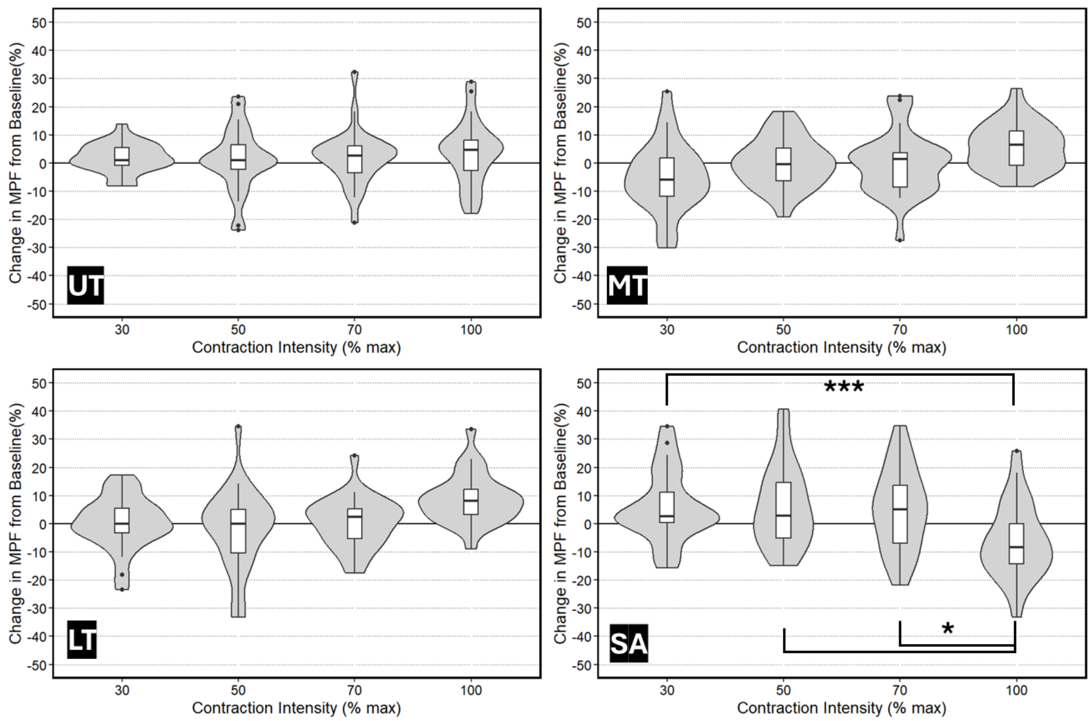

Figure 6.12. **Fatigue-Related Change in Electromyographic Mean-Power-Frequency.** Separated by Muscle (Panel) and Contraction Intensity (Abscissa). * Indicates Significance at $p \leq 0.05$, *** Indicates Significance at $p \leq 0.001$.

Lastly, paired t test revealed significant post-fatigue decreases in MVIC force output for the modified prone elevation task ($t_{(59)} = 4.941$, $p \leq 0.001$), and a significant post-fatigue increase in MVIC force output for the palm press task ($t_{(29)} = -2.963$, $p = 0.030$) (figure 6.13.).

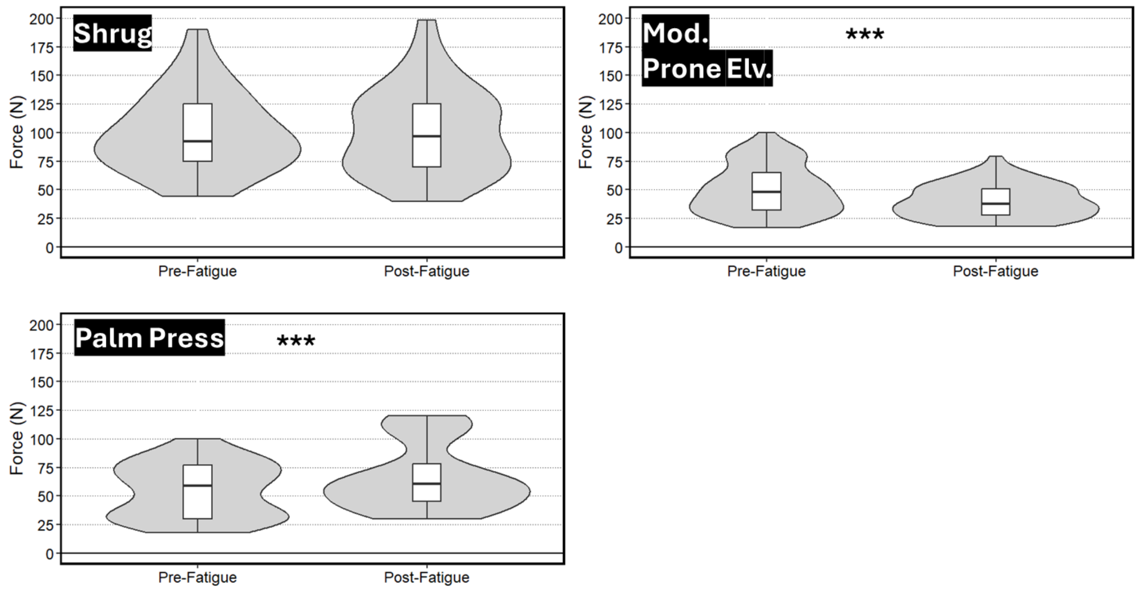

Figure 6.13. **Fatigue-Related Change in Maximal Voluntary Isometric Contraction Force Generating Capacity.** Separated by Muscle (Panel). *** Indicates Significance at $p \leq 0.001$.

6.3.2. Predictor Correlations with Ultrasonographic Shear Wave Velocity

Multiple regression between fatigue-related change in SWV (dependent variable) and fatigue-related change in EMG RMS amplitude, EMG MPF, and MVIC force production (predictor variables) ($F_{(3,78)} = 3.40$, $p = 0.0219$, Ajd R-squared = 0.0816) revealed a significant negative relationship between SWV and EMG RMS amplitude across all muscles ($t_{(82)} = -3.08$, $p = 0.003$) (figure 6.14.). When grouped by muscle, these relationships appeared to persist at upper trapzius($t_{(20)}$

= -2.12, p = 0.048) and serratus anterior ($t_{(20)}$ = -2.13, p = 0.048)(figure 6.15.). Variance inflation factors (table 6.3.) indicate magnitudes approximate to 1, indicating no correlation between predictors.

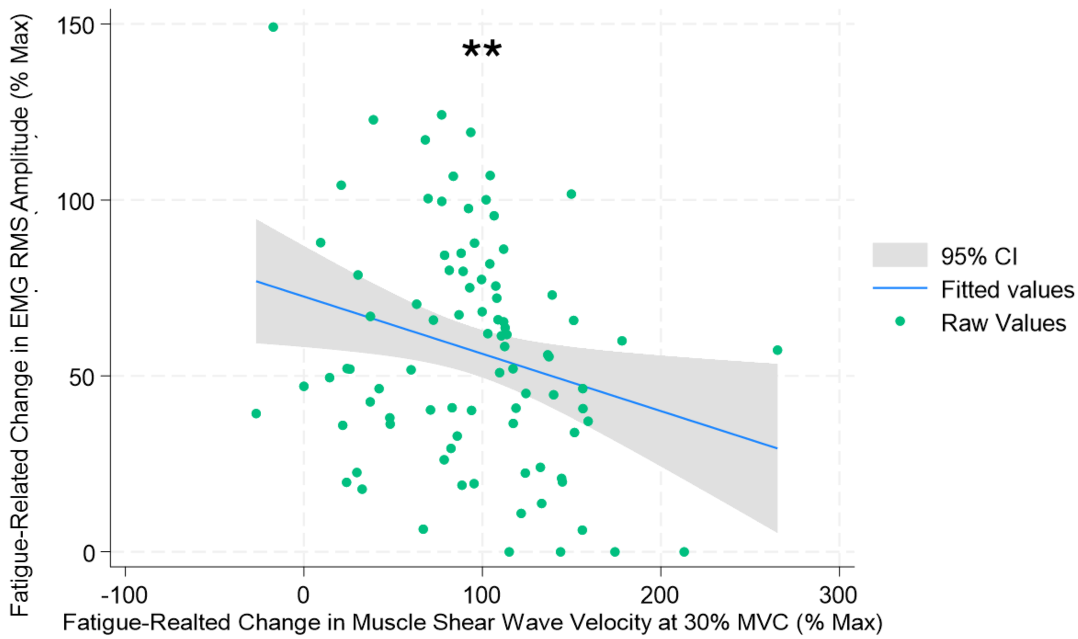

Figure 6.14. **Bivariate Regression between Fatigue-Related Change in EMG RMS Amplitude (Ordinate) and Fatigue-Related Change in Ultrasonographic Shear Wave Velocity (Abscissa).** ** Indicates Significance at $p \leq 0.01$.

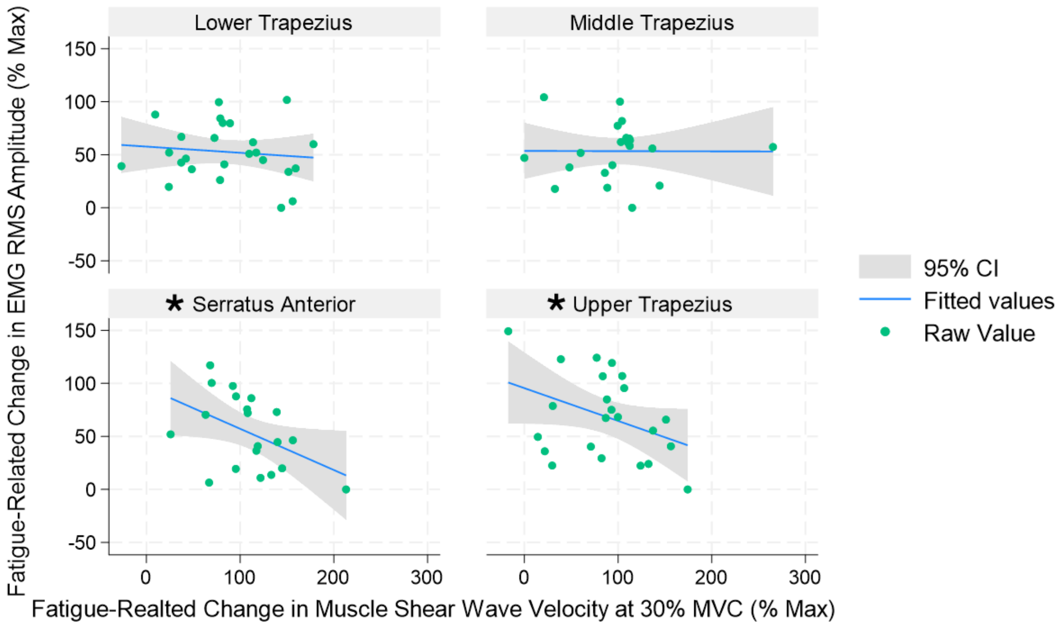

Figure 6.15. **Bivariate Regression between Fatigue-Related Change in EMG RMS Amplitude (Ordinate) and Fatigue-Related Change in Ultrasonographic Shear Wave Velocity (Abscissa).** Grouped by Muscle. * Indicates Significance at $p \leq 0.05$.

Table 6.3. **Variance Inflation Factor (VIF) Diagnostics for All Predictor Variables Regressed to Ultrasonographic Shear Wave Velocity.**

Predictor Variable	**VIF**
Force	1.13
Mean Power Frequency	1.12
Root-Mean-Squared Amplitude	1.02
Mean VIF	**1.09**

6.3.3. Predictor Relationships with Scapulothoracic Kinematics

Two significant regression models were apparent at 90° thoracohumeral elevation and 3 models were apparent at 120°. Across all 5 significant models, EMG MPF was always a significant predictor variable (Table 6.4.).

Table 6.4. **Significant Predictor Variables Regressed to Fatigue-Related Scapulothoracic Kinematics Changes.** Greyed Boxes Indicated Non-Significant Regression Models. 30° and 60° Thoracohumeral Elevation Angle Not Reported (No Significant Models).

Thoracohumeral Elevation Angle	**90**	**120**
Posterior Tilt		
Upper Trapezius	RMS: $t_{(4,20)} = 3.48$, $p = 0.002$ MPF: $t_{(4,20)} = -2.10$, $p = 0.049$ SWV: $t_{(4,20)} = 2.95$, $p = 0.008$	
Middle Trapezius		MPF: $t_{(4,17)} = 3.56$, $p = 0.002$ SWV: $t_{(4,17)} = -3.06$, $p = 0.007$
Lower Trapezius		
Serratus Anterior		
Medial Rotation		
Upper Trapezius		
Middle Trapezius		MPF: $t_{(4,17)} = -2.19$, $p = 0.042$ Force: $t_{(4,17)} = -2.97$, $p = 0.007$ SWV: $t_{(4,17)} = 2.15$, $p = 0.046$
Lower Trapezius		RMS: $t_{(4,16)} = 2.20$, $p = 0.041$

		MPF: $t_{(4,16)} = -2.82$, $p = 0.012$ Force: $t_{(4,16)} = -3.37$, $p = 0.004$
Serratus Anterior		
Protraction		
Upper Trapezius	MPF: $t_{(4,20)} = -2.11$, $p = 0.048$	
Middle Trapezius		
Lower Trapezius		
Serratus Anterior		

6.4. Discussion

The purpose of this study was to determine changes whether changes in muscle stiffness would be spurred by a muscle fatigue task, and if stiffness changes and other common indices of fatigue (EMG RMS, EMG MPF, force) would explain scapulothoracic kinematics changes. First, we hypothesized that passive muscle element properties responsible for passive muscle stiffness would experience creep and hysteresis following repetitive loading from a fatigue task and display subsequent reductions in resting muscle SWV. Contrary to these expectations, increases in muscle SWV were identified at submaximal (≥ 50% SVIC) contraction intensities which can be identified by the lower bound 95% confidence intervals at 30% [82.74 110.93] and 50% [38.91 57.11] contraction which surpass a threshold of 0. 0% resting SWV and 70% were significantly different from 30% and 50%, and these 95% confidence intervals did not surpass a threshold of 0, indicating no fatigue-mediated change. Second, we hypothesized that muscle SWV would correlate with other classical indices of muscle fatigue, yet only fatigue-related changes in EMG RMS amplitude showed a significant relationship. Further, EMG RMS amplitude, EMG MPF, and MVIC force reduction did not display multicollinearity. Finally, we hypothesized that SWV would be a significant predictor of fatigue-related kinematics changes by uniquely characterizing muscle stiffness changes associated with fatigue, for which classical fatigue metrics do not capture. Overall EMG MPF appeared to be the strongest predictor of fatigue-related kinematics changes, yet SWV appeared to significantly predict kinematics changes in 3 of the 5 significant models, while RMS and force only found significance in two models. However, kinematics changes were only apparent at 90° and 120° of thoracohumeral elevation.

6.4.1. Fatigue Measures: Ultrasonographic Shear Wave Velocity

Identifying SWV increases at 30% and 50% submaximal contraction intensities rejected our initial hypothesis as we expected to see decreases in SWV apparent at muscle rest. These observed increases in stiffness, rather than the decreases we expected, may point towards exercise-induced muscle edema as an underlying physiological mechanism to explain our findings. Previously, Agten and colleagues reported increases in SWV of the elbow flexor muscle group apparent as early as 15 minutes following targeted eccentric resistance exercise, and SWV increases appeared to last up to 72 hours before returning to baseline values, with SWV being measured in a relaxed, mid-length posture [Agten, et al., 2017]. This study presents evidence that increases in SWV lasting up to 72 hours post exercise had a strong correlation with Apparent Diffusion Coefficient (ADC) ($r = 0.92$, $p = 0.028$), a measure of post-exercise edema [Hincapie, et al., 2008]. Similarly, Vanhaezebrouck reported increases in hamstring stiffness ($p \leq 0.05$) 48 hours after strenuous hamstring muscle exercise, yet unlike the study by Agten et al. they did not see stiffness changes immediately after exercise completion [Vanhaezebrouck, 2021]. Most other previous SWV literature involving an exercise or fatigue-related intervention report decreases in SWV when measured in a rest position [Andonian, et al., 2016; Siracusa, et al., 2019; Vatovec, Kozinc, and Voglar, 2022]. Taken together with this study, it appears that all SWV responses to exercise are not equivalent, and exercise characteristics may be attributable to the SWV response. Chiefly, the present study utilized a fatigue task consisting of alternating concentric and eccentric contractions based on previously recommended tasks in literature [McQuade, Dawson, and Smidt, 1998; Suzuki, et al., 2006; Szucs, Navalgund, and Borstad, 2009; Noguchi, et al., 2013] similar to the methods reported by Vanhaezebrouck [Vanhaezebrouck, 2021], while the study by Agten et al. utilized an eccentric exercise protocol [Agten, et al., 2017]. Conversely, Vatovec and colleagues previously used an isometric lumbar extension fatigue protocol and Siracusa and colleagues used repeated bouts of 5-second isometric knee extension contractions. Both the studies by Vatovec and Siracusa identified post-exercise decreases in shear elastic modulus; directly proportional to SWV [Siracusa, et al., 2019; Vatovec, Kozinc, and Voglar, 2022]. Collectively, these findings may suggest that isometric exercises are likely to induce muscle elasticity reductions. Isometric reductions in muscle elasticity could be due to the time-dependent characteristics associated with hysteresis characterized in mathematical models of linear hysteresis [Nordin and Frankel, 2001; Özkaya, et al., 2012; Lynch, Ramos, and Jones, 2017]. Concentric and eccentric exercise may resist hysteresis since the muscle is not subjected to a consistent length, producing very short time-dependent loading characteristics compared to isometric contractions. Such short loading frequencies may greatly reduce the amount of energy that is expelled thermally, thus the stress/strain rate of the muscle tissue is minimally impacted, where stress/strain is equivalent to stiffness [Nordin and Frankel, 2001].

A second unexpected fatigue-mediate response to muscle stiffness in our study is the presentation of significant increases in SWV at 30% and 50% SVIC, but not at 0% or 70%. This phenomenon may further support previous evidence that muscle stiffness increases following concentric or eccentric exercise are mediated by muscle fluid diffusion and edema. Literature has long established an apparent muscle force threshold of approximately 50% MVE, above which muscle circulation collapses under the force of muscle contraction [Barcroft and

Millen, 1939; Sjøgaard, et al., 1986; Allen, Lamb, and Westerblad, 2008]. This supports the hypothesis that post-exercise increases in muscle stiffness are due to muscle edema, as any additional muscle stiffness supplied by inward diffusion would be obstructed beyond 50% MVE, explaining why no change in muscle stiffness was observed at 70% SVIC. It remains less clear why muscle stiffness at 0% MVE (rest) appeared unaffected due to muscle edema, however competing changes in underlying viscoelastic muscle stiffness due to exercise may have obscured any additional stiffness supplied by edema. Specifically, middle trapezius and lower trapezius SWV changes at 0% MVE (rest) in figure 5.9. appear to trend towards stiffness decreases, in line with our original hypothesis on fatigue-related stiffness changes as well as other studies that have observed stiffness decreases at rest [Andonian, et al., 2016; Siracusa, et al., 2019; Vatovec, Kozinc, and Voglar, 2022]. Overall, the results of this study regarding muscle SWV changes due to exercise add to the growing literature suggesting that resting decreases in muscle stiffness and increases in ≥50% submaximal contraction stiffness can emerge due to muscle tissue creep and muscle edema, respectively. These muscle stiffness responses appear dependent on exercise type (isometric/concentric/eccentric).

6.4.2. Fatigue Measures: Force and EMG

Classical neuromuscular fatigue measures (EMG RMS, EMG MPF) and force decline trended as hypothesized, with EMG RMS specifically suggesting the presence of fatigue for all muscles due to increases in MVIC amplitude. Upon initial inspection, force decline only appears to support fatigue of the middle trapezius and lower trapezius muscle through overall decrease in modified prone elevation force, while shrug force appeared unchanged and palm press force increased. However, cross-refencing the significant decreases in EMG MPF for serratus anterior MVIC (figure 6.12.) would suggest that serratus anterior did in fact fatigue, and increases in palm press force are likely a product of fatigue-mediated load-sharing to recruit synergists such as pectoralis or anterior deltoid which this muscle test can also be sensitive to [Enoka, 1995; Boettcher, Ginn, and Cathers, 2008; Ginn, Halaki, and Cathers, 2011; McDonald, Sonne, and Keir, 2017]. To date no study has comprehensively assessed muscle recruitment strategies to multi-muscle recruitment tests such as the palm press following fatigue-mediated load sharing and kinematics changes. Without this information available, we can surmise that substantial muscle fatigue is likely to motivate load-sharing strategies which reduce muscle stress on the fatigued serratus anterior [Dul, et al., 1984; Weir, et al., 1998; Bouillard, et al., 2012; Duchateau and Baudry, 2014]. Overall, these findings suggest that serratus anterior was the most reliably fatigued muscle across the participant pool while upper trapziusmay be the least reliably fatigued, evidence by non-significant force and EMG MPF changes.

6.4.3. Fatigue Metrics Regressed to Ultrasonographic Shear Wave Velocity

Multiple regression between SWV at 30% SVIC (dependent variable) and EMG RMS amplitude, EMG MPF, and force decrement during MVIC suggest that RMS and SWV changes may be correlated. Despite the apparent correlation between EMG RMS amplitude and SWV, both metrics appear to capture unique information, as fatigue-mediated RMS changes reflected a statistically significant increase in serratus anterior RMS amplitude compared to other muscles, while SWV did not reflect significant differences between muscles. RMS differences at serratus anterior may reflect significant EMG MPF changes observed at this muscle. Overall, similar muscle-specific changes between MVIC EMG RMS amplitude and MVIC MPF, combined with significant correlations between MVIC EMG RMS amplitude and 30% SVIC SWV, may point towards EMG RMS being highly sensitive to both fatigue-mediated viscoelastic and neuromuscular changes. While EMG amplitude and SWV measures are both associated with sustained exercise and muscle fatigue, the physiological pathways that precipitate EMG amplitude changes and muscle stiffness changes are assuredly distinct [Mendes, et al., 2018; Kozinc and Šarabon, 2020]. Particularly. Nordez and Hug [2010] reported similar increases in both EMG amplitude and muscle stiffness during ramped intensity elbow flexor contractions. The authors suggest that the apparent relationship between EMG amplitude and muscle stiffness is likely a strategy by the CNS to optimize muscle recruitment based on mechanically efficient muscle elasticity characteristics, yet more research may be necessary to fully unveil this potential relationship at more complex or redundant joints. Fatigue-mediated changes in EMG RMS and MPF however do share some common neurophysiological bases to support their relationship. Both characteristics of EMG signal are sensitive to changes in MU conduction velocity which is decreased during sustained muscle contraction due to a constant efflux of intracellular potassium [Lindstrom and Magnusson, 1977; Stulen and De Luca, 1981; Arendt-Nielsen and Mills, 1985]. However, these time-dependent, fatigue-mediated reductions in cellular ion concentration result in decreased EMG amplitude and MPF [Arendt-Nielsen and Mills, 1985; Bigland-Ritchie, et al., 1986], therefore fatigue-mediated increases in amplitude are more likely to be an immediate response to fatigue through centrally-mediated adjustments to spatial and temporal MU summation [Adam and De Luca, 2003; Contessa, De Luca, and Kline, 2016]. Thus, fatigue-mediated RMS changes may be more sensitive to initial muscle stress, while EMG MPF may represent a progression of neuromuscular responses to sustained fatigue stimuli. Force changes due to fatigue are considered holistically attributable to the combined fatigue-mediated changes in passive muscle stiffness, neuromuscular control, metabolic state, and other factors [Enoka and Stuart, 1992; Enoka, 1995; Enoka and Duchateau, 2008]. Thus, the physiological differences between EMG RMS amplitude, EMG MPF, and muscle force may support the unique variance observed across these predictor variables (table 6.3.) and point towards the importance of utilizing multiple measures of muscle fatigue.

6.4.4. Fatigue-Mediated Scapulothoracic Kinematics Changes

Significant indices of fatigue-mediate kinematics changes were dependent on muscle and axis of scapulothoracic motion (Table 5.4.). Fatigue-related increases in scapulothoracic posterior tilt at 90° appeared mediated by RMS amplitude and SWV increases, and EMG MPF decreases in upper trapezius. However, for middle trapezius, fatigue mediated increases SWV and decreases in EMG MPF permitted increased anterior tilting at 120°. Fatigue-related increases in medial rotation at 120° appeared related to decreased EMG MPF and force of middle trapezius and lower trapezius, while increased SWV was also significant for middle trapezius and increased RMS was also significant for lower trapezius. Finally, decreases in upper trapezius EMG MPF appeared to permit increased scapulothoracic retraction at 90°. Overall, these findings show that increased EMG RMS amplitude and SWV, and decreased EMG MPF and muscle force were related to scapulothoracic kinematics changes. However these changes only appear sensitive to specific arm elevations which suggest that fatigue-mediated changes in dynamic scapulothoracic motion could be challenging to detect.

EMG MPF appeared to be the most significant variable for predicting fatigue-mediated scapulothoracic kinematics changes, being a significant predictor in all significant multivariable regression models. The relationship between EMG and altered kinematics could reinforce the discussion presented in section 4.2. that serratus anterior MPF reductions prompted load sharing changes during the palm press, resulting in increased force at post fatigue. Such evidence that kinematics changes are sensitive to EMG MPF may also provide important context to the discussion in section 6.4.3. that fatigue-mediated RMS amplitude increases are more immediate and precipitate EMG MPF changes, as MPF appears to more reliably prompt kinematics changes that would adjust the load-sharing strategy and redistribute the muscle stress across available synergists. Taken together, the evidence that EMG MPF changes may occur later than EMG amplitude changes in the cascade of fatigue accumulation, and that MPF changes promoting kinematics adjustments may provide a rationale for why so much variability is attributable to fatigue-mediated shoulder kinematics [Chopp-Hurley, et al., 2016; Russell, et al., 2024]. As MPF changes prompt kinematic adjustments that redistribute muscle stress to less fatigued synergist muscles, this adjustment potentially supports MPF recovery from fatigue. We propose here that in a highly redundant muscular system such as the shoulder complex, the availability of numerous equivalent load-sharing strategies may make it challenging to maintain sustained contraction from a single muscle long enough to accumulate MPF changes associated with intracellular potassium efflux before kinematics adjustments are ultimately prompted to mitigate muscle stress. The greater sensitivity of EMG amplitude to muscle fatigue and muscle stress may explain why many studies in literature have reported more reliable fatigue-mediated changes in amplitude compared to MPF.

6.4.5. Limitations

A number of limitations present in the current study are a result of decisions made to follow published guidelines for EMG and SWV data collection as best as possible when competing interests were presented. Firstly, as mentioned the recommended ultrasound transducer placement and electrode placement locations in literature both suggest the middle one-third of the muscle belly [Stegeman and Hermens, 2007; Kelly, et al., 2018; Koppenhaver, et al., 2018; Besomi, et al., 2019; Cipriano, et al., 2022], in line with the fiber orientation. Since EMG measures represent a highly validated metric of fatigue confirmation, and the sensitivity of EMG placement on signal characteristics is well established [Barbero, Merletti, and Rainoldi, 2012; Besomi, et al., 2019], the decision was made to prioritize correct EMG placement over ultrasound probe location. This resulted in transducer placements tangential to EMG electrode placement, offset from the recommended localization by approximately 2 cm but still in line with fiber orientation. Across large muscles like trapezius and serratus anterior, we do not expect this difference to have a meaningful effect on SWV measurements, however more research is required to determine the significance of these decisions. Secondly, the order of data collection procedures during the study protocol (figure 6.1.) prioritized kinematic and SWV data collection immediately following the fatigue protocol, opting to collect post-fatigue force and EMG changes last. As fatigue is a transient condition that resolves with rest [Enoka and Stuart, 1992; Enoka, 1995; Enoka and Duchateau, 2008], post-fatigue EMG and force measurements may have been influenced by the 15-20 minute window where kinematic and resting SWV measurements were acquired. In a pilot collection involving 6 participants who proceeded to participate in the present study, force, EMG RMS amplitude and EMG MPF changes were collected using the same 100% MVE reference contractions as this study (table 6.2.) immediately after completion of an identical fatigue protocol, and all three metrics showed significant differences. In light of evidence that SWV increases due to edema may last up to 72 hours [Agten, et al., 2017], future studies may opt to prioritize post-fatigue/post-exercise EMG acquisition ahead of SWV acquisition. The 15-20 minute window between completion of the fatigue protocol and assessment of post-fatigue EMG signal characteristics may explain why significant fatigue-related changes were only apparent at MVIC and not SVIC, and may suggest that additional significant fatigue-related neuromuscular changes could have emerged if these data were collected sooner. Further, the present fatigue protocol was modified from a comprehensive shoulder fatigue protocol by Suzuki and colleagues [Suzuki, et al., 2006], that incorporated other published fatigue protocol stimuli for the trapezius [Noguchi, et al., 2013], serratus anterior [Szucs, Navalgund, and Borstad, 2009], and general scapular stabilizers [McQuade, Dawson, and Smidt, 1998]. Our intent was to consolidate some of the most promising scapular stabilizer muscle fatigue protocols in literature, however upper trapezius in particular appeared potentially resistant to fatigue. Future studies may wish to modify the current protocol with a different upper trapezius fatigue stimuli. However, it remains unclear if non-significant fatigue-mediated changes in upper trapezius force were due to failure to fatigue this muscle, load-sharing to sustain post-fatigue force output, or whether upper trapezius recovered from fatigue before post-fatigue force and EMG were captured. Lastly, a difference of 5.3 kg/m^2 was observed between sexes, which may contribute to variability in the current dataset.

6.5. Conclusion

This study sought whether fatigue-mediated changes in muscle stiffness, measured using ultrasonographic SWV, can be utilized to assess fatigue state and predict fatigue-mediate kinematics changes prompted by load-sharing. Unexpectedly, SWV measures reliably increased during 30% and 50% submaximal contractions, indicating that SWV responses to exercise appear dependent on the type of muscle contraction stimulus (e.g. isometric, concentric, eccentric). Regression modelling between metrics of muscle fatigue (force, EMG amplitude, EMG MPF) and SWV suggest that EMG amplitude and SWV changes may both be highly sensitive to muscle stress, where as EMG MPF may signal a threshold of sustained fatigue accumulation that prompts load-sharing changes and subsequent kinematics changes. Future research may wish to find more direct methods for testing the hypothesis that kinematics changes are prompted by fatigue-mediate changes in MPF, such as evaluating kinematics changes during a sustained contraction in a redundant muscular system with time-synchronized EMG amplitude and EMG MPF comparisons.

Chapter 7. General Discussion and Conclusion of Dissertation

Matthew S. Russell, Janessa D.M. Drake, Jaclyn N. Chopp-Hurley

School of Kinesiology and Health Science, York University, Toronto, Canada

Declarations of Interest: None

Funding Sources: This work was supported by the Natural Science and Engineering Council (NSERC) Discovery Grant program (J.N. Chopp-Hurley & J.D.M. Drake), and the NSERC Post-Graduate Scholarship program (M.S. Russell).

7.1. Summary of Dissertation

Chapter specific objectives and hypotheses will not be revisited in this section. Rather, this section of the dissertation will summarize consistent and novel findings across chapters 3-6 as they pertain to the primary aims of this dissertation outlined in section 1.2.

7.1.1. Muscle Control and Kinematic Variability

The primary goal of this dissertation was to quantify factors that explain some of the yet unexplained variability associated with shoulder muscle and kinematic control changes due to muscle fatigue. Due to the intersection of these themes with many occupational tasks, chapters 3 and 4 of this dissertation sought to investigate how occupationally relevant task variables like task orientation affect fatigue-mediated muscle control adaptations. The approach in chapter 3 was to determine whether such factors modulate coactivation of the scapular stabilizer muscles and present coactivation changes that characterize increased SAIS and RC tear risk. Chapter 4 concentrated on muscle activity, kinematic, and kinetic variability changes between days to determine how participants repeating an occupational task designed to focalize stress on the scapular stabilizers and RC muscles might adapt or 'learn'. Chapters 5 and 6 complement this dissertation by presenting novel methods and models for understanding shoulder muscle-fatigue adaptations. In chapter 5, a mechanistic computational shoulder model is harnessed to examine how simulated fatigue or muscle weakness will spur muscle activity and kinematics compensations in an optimal control solver. In chapter 6, fatigue-mediated muscle elasticity changes, characterized with ultrasonographic SWV, was investigated to determine how non-contractile muscle element changes may contribute to muscle control adaptations.

Throughout the chapters of this dissertation, fatigue-mediated muscle activity changes among the shoulder complex consistently indicate a key importance of the serratus anterior muscle. Chapters 4 and 5 provided evidence that central control schemes may respond to serratus anterior muscle fatigue stimuli by recruiting other shoulder muscles depending on the plane of arm elevation, while chapters 3, 5, and 6 all link serratus anterior muscle fatigue with kinematics changes. The mechanical efficiency of serratus anterior for stabilizing scapulothoracic all three planes of scapulothoracic motion has been reported, and taken together with current evidence this suggests that the CNS may aim to supplement the stress on this muscle with load sharing strategies [Ekstrom, et al., 2004; Ludewig, et al., 2004; Phadke, Camargo, and Ludewig, 2009]. This may be because while other shoulder muscles can effectively compensate for serratus anterior weakness in some planes of arm elevation, the mechanical advantage of this muscles moment arm and fibre alignment make is a desirable effector from among the available motor strategies; and this fact appears to be appreciated by the CNS [Ekstrom, et al., 2004]. From a muscle coactivation lens, serratus anterior weakness appears to drive increases in upper trapezius activity as a compensatory mechanism that may implicate mechanical risk factors for SAIS and RC injury. Results from chapter 5 also indicate that other accessory shoulder muscles like deltoid, pectoralis, and long head of biceps may help compensate for serratus weakness, and these mechanics may have important implications for the rationale underlying upper trapezius dominance. Viewing the shoulder musculature as a comprehensive system provides a new vantage that upper trapezius dominance in response to serratus anterior weakness may in fact also be acting to stabilize the scapula against the pull of pectoralis and deltoid. This function of upper trapezius would help explain the high relative activity amongst the scapular stabilizers, likely due to its unique insertion on the lateral clavicle and its ability to retract the clavicle [Johnson et al., 1994].

Variability of muscle activity and kinematics appears to be more than a product of redundancy, as chapter 4 points towards the importance of variability in consolidating optimal motor strategies [Corcos, et al., 1993; Magill and Anderson, 2010; Raviv, Lupyan, and Green, 2022]. Kinematic variability may also be associated with muscle MPF, such that centrally mediated load sharing changes may be sensitive to muscle fiber conduction velocity [Lindstrom and Magnusson, 1977; Stulen and De Luca, 1981; Arendt-Nielsen and Mills, 1985; Öberg, Sandsjö, and Kadefors, 1991]. Challenges persist in identifying a ubiquitous methodology for comprehensively fatiguing the scapular stabilizer muscles, yet insights from this dissertation confer that (1) frontal plane thoracohumeral motions promote more balanced recruitment of scapular stabilizers, (2) arm motions near the extent of the reach profile may also exist near a boundary of muscular degrees of freedom and limit motor compensation strategies, and (3) shear wave muscle velocity and stiffness changes appear dependent on the mode of contraction (concentric, eccentric, isometric) but evidence suggests these factors are related to kinematics changes. Future muscle fatigue protocols for the shoulder may be recommended to use frontal plane exercises to target comprehensive scapular stabilizer fatigue or use the scapular or sagittal plane to target serratus anterior.

The hypothesis that central-control scheme changes to compensate for fatigue may be signaled by MPF over other factors like EMG amplitude or SWV, may explain why MPF changes have been elusive in unconstrained shoulder endurance and fatigue tasks [Anton, et al., 2001; Fuller, et al., 2009; Looze, Bosch, and Dieën, 2009; Chopp, et al., 2010; Emery and Côté, 2012; Tse, McDonald, and Keir, 2016; Mulla, McDonald, and Keir, 2018; Umehara, et al., 2018; McDonald, Mulla, and Keir, 2019]. End-range postures may reduce the variation in available strategies as reported in chapter 3. Studies which successfully identify kinematic changes due to scapular stabilizer muscle fatigue all appear to all employ a very similar fatigue protocol that involves resisted arm abduction with the arm maximally outstretched [McQuade, Dawson, and Smidt, 1998; Ebaugh, McClure, and Karduna, 2006; Chopp-Hurley, et al., 2016]. Tasks in this plane appear to stimulate recruitment from trapezius and serratus anterior and may exist near a boundary of the available motor control landscape making clear inferences between muscle coactivation and kinematics changes possible. Future studies should test this hypothesis more directly by investigating time-varying amplitude, MPF, and kinematics changes near end-range postures within the reach envelope.

7.1.2. Secondary Aims of Dissertation

Three secondary overarching aims of this dissertation were presented, which were either directly or indirectly addressed throughout multiple chapters of this dissertation:

7.1.2.1. Fatigue-Related Factors Associated with Chronic Shoulder Joint Injury.

Fatigue-related factors associated with chronic shoulder injury were primarily addressed through scapular stabilizer coactivation ratios and scapulothoracic joint angle changes in chapter 3. Although group-wise trends in muscle coactivation and scapulothoracic kinematics were difficult to detect in this study, two key findings emerged. First, muscle coactivation changes indicated that upper trapezius dominance with fatigue did show evidence of kinematic changes, but this relationship emerged near end ranges of the reach envelope. Second, within the variable spectrum of scapulothoracic kinematic responses to fatigue, approximately 20-40% of participants demonstrated uniaxial kinematic changes that would implicate a clinically significant reduction of the SAS

[Watson, et al., 2005; Ebaugh, McClure, and Karduna, 2006; McClure, Greenberg, and Kareha, 2012]. These changes primarily occurred for scapulothoracic anterior tilt and downward rotation. However, it remains unclear how the combined tri-axial scapulothoracic adaptations to fatigue would interact to alter the SAS width, as direct measurement of the SAS requires imaging techniques that have only been featured in a few studies [Chopp, et al., 2010; Chopp and Dickerson, 2012]. Future works may benefit from a model to approximate SAS width from three-dimensional scapulothoracic position. Results from chapter 3 did not provide conclusive evidence of fatigue-mediated upper trapezius dominance being driven by muscle activity changes from a specific scapular stabilizer. However, optimal control predictions in chapter 5 suggest that in a purely mechanistic model, upper trapezius dominance may be driven as a compensation for lower trapezius and serratus anterior weakness. In an in vivo muscle model, sensory feedback and non-contractile muscle properties may also contribute to how fatigue-mediated upper trapezius dominance is signaled.

7.1.2.2. How Familiarity to a Muscle Fatigue Task Adjusts Kinematic and Muscular Control Strategies.

Chapter 4 represents one of the first comprehensive studies on fatigue-mediated shoulder muscle activity, kinematic, and kinetic changes across repeat exposure to a goal-direct fatigue task. Key to this research is the hypothesis that task familiarity would influence a more optimal strategy on day 2. Key findings in this study were (1) a reduction in fatigue-mediated EMG amplitude changes was apparent for serratus anterior between days, and (2) kinematic changes indicate that some degree of task improvement was consolidated across our participant sample, while kinetics changes indicated that reduced shoulder joint torque was more consistently achieve on day 2.

Results that serratus anterior muscle activity responses to fatigue were altered on day 2 may be contextual to additional results in chapters 5 and 6 which suggest that this muscle is key for stabilizing sagittal plane arm elevation. However, load sharing strategies in this plane appear to have the potential to supplement kinematic requirements, albeit the muscle activity and descending neural drive to achieve this strategy may be elevated through the coordination of multiple muscles with less mechanical efficiency. Through the lens of chapter 6, muscle strategies on day 2 may have helped minimize the increase in serratus anterior amplitude on day 2 as a sophisticated strategy to avoid reaching a fatigue threshold which would promote kinematics changes. This may help to explain why kinematic variability was reduced on day 2.

7.1.2.3. Fatigue-Related Viscoelastic Muscle Change Influences on Neuromechanical and Kinematic Adaptation Strategies.

A unique focus of chapter 6 was the influence of quantifying muscle stiffness changes to help control for some of the variability associated with muscle-fatigue-mediated changes. However, the link between fatigue-mediated SWV and kinematic changes was not clear from this study, and EMG MPF appeared to be a preeminent predictor of kinematics changes. SWV did appear to correlate with EMG amplitude changes, suggesting that these distinct etiologies share a similar sensitivity to fatigue stimuli. However, SWV changes trended opposite from what we hypothesized, which is likely due to a dependency of viscoelastic changes on the method of fatigue/exercise stimulus. Our findings suggest that concentric and eccentric muscle stimuli may be more likely to promote transient increases in stiffness due to muscle edema, while isometric loading likely permits creep and hysteresis prompting stiffness decreases. Therefore, future studies should still seek to identify whether isometric muscle loading prompts muscle stiffness decreases that correlate with kinematics and muscle control changes. Interestingly, many occupational tasks associated with chronic shoulder injury involve static and quasi-static postures (hairdressing, overhead work, dentistry) [Sood, Nussbaum, and Hager, 2007; Grieve and Dickerson, 2008; De Smet, Germeys, and De Smet, 2009; Van Rijn, et al., 2010], similar to prolonged low back loads associated with low back injury [Norman, et al., 1998; Howarth, et al., 2016]. Therefore, muscle stiffness and SWV assessments of static, overhead tasks may be an important next step to investigate.

7.2. Conclusion

This dissertation sought to advance our understanding of kinematic and muscle activity changes due to shoulder muscle fatigue by quantifying several factors which are expected to explain this highly variable relationship, including task orientation, task familiarity, muscle fatigue stimulus, and muscle stiffness. Key findings across the chapters of this dissertation advance our understanding of scapular stabilizer muscle control. Plane of thoracohumeral elevation appears key for determining which scapular stabilizer muscles are recruited, and this appears to have important implications for explaining some of the variability associated with shoulder fatigue. In particular, tasks oriented in the frontal plane may spread the muscular demand across the scapular stabilizers while scapular plane tasks may be more dependent on serratus anterior. These findings are important with regards to the variation in shoulder muscle fatigue tasks across literature. To constraint approaches for future research and make research more comparable, tasks which seek to promote a balanced fatigue of the scapular stabilizer muscles are advised to design a fatigue task in the front plane, while tasks oriented in the scapular and frontal planes may be useful for targeting serratus anterior. Regardless, serratus anterior seems to be an integral muscle for scapular stability across all planes of arm motion, highlighting the importance of healthy serratus anterior muscle coordination, control, and strength. EMG MPF appears to signal kinematics changes in the shoulder and may present a model for signalling load sharing changes in highly redundant musculoskeletal system. The hypothesis that muscle MPF changes instigate load sharing changes should be tested more thoroughly and directly and may have implications for other redundant muscle systems like postural control. Constraint of posture and task were two variables that were explored in chapters 3 and 4, where evidence suggests that these factors may influence the amount of processing required to consolidate an 'optimized' or learned strategy. Even across a redundant complex like the shoulder, the convergence of muscular and kinematic strategies in chapter 4 suggest a similar criteria is driving learned improvements across our target population. Regarding these findings, more research on how muscle fatigue impacts learned strategies, and central and peripheral fatigue affects in particular may help to identify what variables the CNS is attempting to optimize.

References

Ackland, D.C., Pak, P., Richardson, M., and Pandy, M.G. (2008). Moment arms of the muscles crossing the anatomical shoulder. Journal of anatomy, 213(4):383-390.

Ackland, D.C. and Pandy, M.G. (2011). Moment arms of the shoulder muscles during axial rotation. Journal of Orthopaedic Research, 29(5):658-667.

Adam, A. and De Luca, C.J. (2003). Recruitment order of motor units in human vastus lateralis muscle is maintained during fatiguing contractions. Journal of neurophysiology, 90(5):2919-2927.

Agten, C. A., Buck, F. M., Dyer, L., Flück, M., Pfirrmann, C. W. and Rosskopf, A. B. (2017). Delayed-onset muscle soreness: temporal assessment with quantitative MRI and shear-wave ultrasound elastography. American Journal of Roentgenology, 208(2), 402-412.

Akagi, R. and Kusama, S. (2015). Comparison between neck and shoulder stiffness determined by shear wave ultrasound elastography and a muscle hardness meter. Ultrasound in medicine & biology, 41(8), 2266-2271.

Alcántara-Bumbiedro, S., Flórez-García, M., Echávarri-Pérez, C. and García-Pérez, F. (2006). Oswestry low back pain disability questionnaire. Rehabilitacion Madrid, 40(3), 150.

Alexander, C., Miley, R., Stynes, S. and Harrison, P. (2007). Differential control of the scapulothoracic muscles in humans. The Journal of physiology, 580(3), 777-786.

Alkner, B. A., Tesch, P. A. and Berg, H. E. (2000). Quadriceps EMG/force relationship in knee extension and leg press. Medicine and science in sports and exercise, 32(2), 459-463.

Allen, D.G., Lamb, G.D., Westerblad, H. (2008). Skeletal muscle fatigue: cellular mechanisms. Physiological reviews, 88(1), 287-332.

Allen, T.R., Brookham, R.L., Cudlip, A.C., Dickerson, C.R. (2013). Comparing surface and indwelling electromyographic signals of the supraspinatus and infraspinatus muscles during submaximal axial humeral rotation. Journal of Electromyography and Kinesiology, 23(6):1343-1349.

Amann, M. (2011). Central and peripheral fatigue: interaction during cycling exercise in humans. Medicine & Science in Sports & Exercise, 43(11):2039-2045.

Amann, M. (2012). Significance of Group III and IV muscle afferents for the endurance exercising human. Clinical and Experimental Pharmacology and Physiology, 39(9):831-835.

Amasay, T., Karduna, A.R. (2009). Scapular kinematics in constrained and functional upper extremity movements. Journal of Orthopaedic & Sports Physical Therapy, 39(8):618-627.

Anderson, F.C., Pandy, M.G. (2001). Dynamic optimization of human walking. Journal of Biomechanical Engineering, 123(5):381-390.

Andersson, J.A., Gillis, J., Horn, G., Rawlings, J.B., Diehl, M. (2019). CasADi: a software framework for nonlinear optimization and optimal control. Mathematical Programming Computation, 11(1):1-36.

Andersson, G., Hagman, J., Talianzadeh, R., Svedberg, A. and Larsen, H. C. (2002). Effect of cognitive load on postural control. Brain research bulletin, 58(1), 135-139.

Andonian, P., Viallon, M., Le Goff, C., de Bourguignon, C., Tourel, C., Morel, J., Giardini, G., Gergele, L., Millet, G. P. and Croisille, P. (2016). Shear-wave elastography assessments of quadriceps stiffness changes prior to, during and after prolonged exercise: a longitudinal study during an extreme mountain ultra-marathon. PLoS One, 11(8), e0161855.

Angel, R., Eppler, W., Iannone, A. (1965). Silent period produced by unloading of muscle during voluntary contraction. The Journal of physiology, 180(4):864.

Anton, D., Shibley, L. D., Fethke, N. B., Hess, J., Cook, T. M. and Rosecrance, J. (2001). The effect of overhead drilling position on shoulder moment and electromyography. Ergonomics, 44(5), 489-501.

Arendt-Nielsen, L. and Mills, K. (1985). The relationship between mean power frequency of the EMG spectrum and muscle fibre conduction velocity. Electroencephalography and clinical Neurophysiology, 60(2), 130-134.

Aruin, A. S. (2006). The effect of asymmetry of posture on anticipatory postural adjustments. Neuroscience Letters, 401(1-2), 150-153.

Asadi Nikooyan, A., Veeger, H., Chadwick, E., Praagman, M. and van der Helm, F. C. (2011). Development of a comprehensive musculoskeletal model of the shoulder and elbow. Medical & biological engineering & computing, 49, 1425-1435.

Bagg, S.D., Forrest, W.J. (1986). Electromyographic study of the scapular rotators during arm abduction in the scapular plane. American Journal of Physical Medicine & Rehabilitation, 65(3):111-124.

Baker, R. E., Pena, J.-M., Jayamohan, J. and Jérusalem, A. (2018). Mechanistic models versus machine learning, a fight worth fighting for the biological community? Biology letters, 14(5), 20170660.

Bang, M.D., Deyle, G.D. (2000). Comparison of supervised exercise with and without manual physical therapy for patients with shoulder impingement syndrome. Journal of Orthopaedic & Sports Physical Therapy, 30(3):126-137.

Baratta, R., Solomonow, M., Zhou, B., Letson, D., Chuinard, R. and D'ambrosia, R. (1988). Muscular coactivation: the role of the antagonist musculature in maintaining knee stability. The American journal of sports medicine, 16(2), 113-122.

Barbero, M., Merletti, R. and Rainoldi, A. (2012). Atlas of muscle innervation zones: understanding surface electromyography and its applications, Springer Science & Business Media.
Barcroft, H. and Millen, J. (1939). The blood flow through muscle during sustained contraction. The Journal of physiology, 97(1), 17.
Barnes, C. J., Van Steyn, S. J. and Fischer, R. A. (2001). The effects of age, sex, and shoulder dominance on range of motion of the shoulder. Journal of Shoulder and Elbow Surgery, 10(3), 242-246.
Bassani, T. and Galbusera, F. (2018). Musculoskeletal modeling. Biomechanics of the Spine, Elsevier: 257-277.
Bechtol, C.O. (1980). Biomechanics of the shoulder. Clinical Orthopaedics and Related Research, 146:37-41.
Beck, T. W., Housh, T. J., Johnson, G. O., Weir, J. P., Cramer, J. T., Coburn, J. W. and Malek, M. H. (2004). Mechanomyographic and electromyographic time and frequency domain responses during submaximal to maximal isokinetic muscle actions of the biceps brachii. European journal of applied physiology, 92, 352-359.
Bercoff, J., Tanter, M. and Fink, M. (2004). Supersonic shear imaging: a new technique for soft tissue elasticity mapping. IEEE transactions on ultrasonics, ferroelectrics, and frequency control, 51(4), 396-409.
Bernstein, N. (1966). The co-ordination and regulation of movements. The co-ordination and regulation of movements.
Besomi, M., Hodges, P. W., Van Dieën, J., Carson, R. G., Clancy, E. A., Disselhorst-Klug, C., Holobar, A., Hug, F., Kiernan, M. C. and Lowery, M. (2019). Consensus for experimental design in electromyography (CEDE) project: Electrode selection matrix. Journal of Electromyography and Kinesiology, 48, 128-144.
Bey, M. J., Brock, S. K., Beierwaltes, W. N., Zauel, R., Kolowich, P. A., Lock, T. R. (2007). In vivo measurement of subacromial space width during shoulder elevation: technique and preliminary results in patients following unilateral rotator cuff repair. Clinical Biomechanics, 22(7), 767-773.
Bigland-Ritchie, B., Dawson, N., Johansson, R. and Lippold, O. (1986). Reflex origin for the slowing of motoneurone firing rates in fatigue of human voluntary contractions. The Journal of physiology, 379(1), 451-459.
Blana, D., Hincapie, J. G., Chadwick, E. K. and Kirsch, R. F. (2008). A musculoskeletal model of the upper extremity for use in the development of neuroprosthetic systems. Journal of biomechanics, 41(8), 1714-1721.
Boettcher, C. E., Ginn, K. A. and Cathers, I. (2008). Standard maximum isometric voluntary contraction tests for normalizing shoulder muscle EMG. Journal of Orthopaedic Research, 26(12), 1591-1597.
Borg, G.A. (1982). Psychophysical bases of perceived exertion. Medicine & science in sports & exercise, 14(5), 377-381.

Borstad, J. D., Szucs, K. and Navalgund, A. (2009). Scapula kinematic alterations following a modified push-up plus task. Human movement science, 28(6), 738-751.

Bortolotto, S.K., Cellini, M., Stephenson, D.G., Stephenson, G.M. (2000). MHC isoform composition and Ca2+-or Sr2+-activation properties of rat skeletal muscle fibers. American Journal of Physiology-Cell Physiology, 279(5):C1564-C1577.

Bouillard K, Nordez A, Hodges PW, Cornu C, Hug F. Evidence of changes in load sharing during isometric elbow flexion with ramped torque. Journal of biomechanics 2012;45(8):1424-1429.

Bouillard, K., Jubeau, M., Nordez, A. and Hug, F. (2014). Effect of vastus lateralis fatigue on load sharing between quadriceps femoris muscles during isometric knee extensions. Journal of neurophysiology, 111(4), 768-776.

Bouillard, K., Nordez, A., Hodges, P. W., Cornu, C. and Hug, F. (2012). Evidence of changes in load sharing during isometric elbow flexion with ramped torque. Journal of biomechanics, 45(8), 1424-1429.

Bouisset, S., Richardson, J., & Zattara, M. (2000). Are amplitude and duration of anticipatory postural adjustments identically scaled to focal movement parameters in humans?. Neuroscience Letters, 278(3), 153-156.

Bradley, J.P., Tibone, J.E. (1991). Electromyographic analysis of muscle action about the shoulder. Clinics in sports medicine, 10(4):789-805.

Brand, R. A., Pedersen, D. R. and Friederich, J. A. (1986). The sensitivity of muscle force predictions to changes in physiologic cross-sectional area. Journal of biomechanics, 19(8), 589-596.

Brandenburg, J. E., Eby, S. F., Song, P., Zhao, H., Brault, J. S., Chen, S. and An, K.-N. (2014). Ultrasound elastography: the new frontier in direct measurement of muscle stiffness. Archives of physical medicine and rehabilitation, 95(11), 2207-2219.

Breteler, M. D. K., Spoor, C. W., Van der Helm, F. C. T. (1999). Measuring muscle and joint geometry parameters of a shoulder for modeling purposes. Journal of Biomechanics, 32(11), 1191-1197.

Buchanan, T. S., Lloyd, D. G., Manal, K. and Besier, T. F. (2004). Neuromusculoskeletal modeling: estimation of muscle forces and joint moments and movements from measurements of neural command. Journal of applied biomechanics, 20(4), 367-395.

Cairns, S.P., Knicker, A.J., Thompson, M.W., Sjøgaard, G. (2005). Evaluation of models used to study neuromuscular fatigue. Exercise and sport sciences reviews, 33(1):9-16.

Caler, W.E., Carter, D.R. (1989). Bone creep-fatigue damage accumulation. Journal of biomechanics, 22(6-7):625-635.

Carpenter, J.E., Blasier, R.B., and Pellizzon, G.G. (1998). The effects of muscle fatigue on shoulder joint position sense. The American Journal of Sports Medicine, 26(2), 262-265

Carroll, T.J., Taylor, J.L., Gandevia, S.C. (2017). Recovery of central and peripheral neuromuscular fatigue after exercise. Journal of Applied Physiology, 122(5):1068-1076.

Cashaback, J. G. and Cluff, T. (2015). Increase in joint stability at the expense of energy efficiency correlates with force variability during a fatiguing task. Journal of biomechanics, 48(4), 621-626.

Chadwick, E. K., Blana, D., Kirsch, R. F. and van den Bogert, A. J. (2014). Real-Time Simulation of Three-Dimensional Shoulder Girdle and Arm Dynamics. IEEE Transactions on Biomedical Engineering, 61(7), 1947-1956. 10.1109/TBME.2014.2309727.

Chadwick, E. K., Blana, D., van den Bogert, A. J. and Kirsch, R. F. (2008). A real-time, 3-D musculoskeletal model for dynamic simulation of arm movements. IEEE Transactions on Biomedical Engineering, 56(4), 941-948.

Chau, T., Young, S. and Redekop, S. (2005). Managing variability in the summary and comparison of gait data. Journal of Neuroengineering and Rehabilitation, 2(1), 1-20.

Chen, W.H., Ballance, D.J., Gawthrop, P.J. (2003). Optimal control of nonlinear systems: a predictive control approach. Automatica, 39(4):633-641.

Chimenti, R. L., Post, A. A., Silbernagel, K. G., Hadlandsmyth, K., Sluka, K. A., Moseley, G. L. and Rio, E. (2021). Kinesiophobia Severity Categories and Clinically Meaningful Symptom Change in Persons With Achilles Tendinopathy in a Cross-Sectional Study: Implications for Assessment and Willingness to Exercise. Frontiers in Pain

Chopp, J. N. and Dickerson, C. R. (2012). Resolving the contributions of fatigue-induced migration and scapular reorientation on the subacromial space: an orthopaedic geometric simulation analysis. Human movement science, 31(2), 448-460.

Chopp, J. N., Fischer, S. L. and Dickerson, C. R. (2010). The impact of work configuration, target angle and hand force direction on upper extremity muscle activity during sub-maximal overhead work. Ergonomics, 53(1), 83-91.

Chopp, J. N., Fischer, S. L. and Dickerson, C. R. (2011). The specificity of fatiguing protocols affects scapular orientation: Implications for subacromial impingement. Clinical Biomechanics, 26(1), 40-45.

Chopp, J. N., O'Neill, J. M., Hurley, K. and Dickerson, C. R. (2010). Superior humeral head migration occurs after a protocol designed to fatigue the rotator cuff: a radiographic analysis. Journal of shoulder and elbow surgery, 19(8), 1137-1144.

Chopp-Hurley, J.N., Dickerson, C.R. (2015). The potential role of upper extremity muscle fatigue in the generation of extrinsic subacromial impingement syndrome: a kinematic perspective. Physical Therapy Reviews, 20(3):201-209.

Chopp-Hurley, J.N., Langenderfer, J.E., Dickerson, C.R. (2016). A probabilistic orthopaedic population model to predict fatigue-related subacromial geometric variability. Journal of biomechanics, 49(4):543-549.

Chopp-Hurley, J. N. and Dickerson, C. R. (2015). The potential role of upper extremity muscle fatigue in the generation of extrinsic subacromial impingement syndrome: a kinematic perspective. Physical Therapy Reviews, 20(3), 201-209.

Chopp-Hurley, J. N., O'Neill, J. M., McDonald, A. C., Maciukiewicz, J. M. and Dickerson, C. R. (2016). Fatigue-induced glenohumeral and scapulothoracic kinematic variability: implications for subacromial space reduction. Journal of Electromyography and Kinesiology, 29, 55-63.

Christensen, H. and Fuglsang-Frederiksen, A. (1988). Quantitative surface EMG during sustained and intermittent submaximal contractions. Electroencephalography and clinical Neurophysiology, 70(3), 239-247.

Christou, E. A. (2011). Aging and variability of voluntary contractions. Exercise Sport Science Review, 39, 77-84.

Cipriano, K. J., Wickstrom, J., Glicksman, M., Hirth, L., Farrell, M., Livinski, A. A., Esfahani, S. A., Maldonado, R. J., Astrow, J. and Berrigan, W. A. (2022). A scoping review of methods used in musculoskeletal soft tissue and nerve shear wave elastography studies. Clinical Neurophysiology, 140, 181-195.

Collinsworth, A.M., Zhang, S., Kraus, W.E., Truskey, G.A. (2002). Apparent elastic modulus and hysteresis of skeletal muscle cells throughout differentiation. American Journal of Physiology Cell Physiology,283(4):C1219-1227.

Contessa, P., De Luca, C. J. and Kline, J. C. (2016). The compensatory interaction between motor unit firing behavior and muscle force during fatigue. Journal of neurophysiology, 116(4), 1579-1585.

Cools, A. M., Dewitte, V., Lanszweert, F., Notebaert, D., Roets, A., Soetens, B., Cagnie, B. and Witvrouw, E. E. (2007). Rehabilitation of scapular muscle balance: which exercises to prescribe? The American journal of sports medicine, 35(10), 1744-1751.

Cools, A. M., Witvrouw, E. E., De Clercq, G. A., Danneels, L. A., Willems, T. M., Cambier, D. C. and Voight, M. L. (2002). Scapular muscle recruitment pattern: electromyographic response of the trapezius muscle to sudden shoulder movement before and after a fatiguing exercise. Journal of Orthopaedic & Sports Physical Therapy, 32(5), 221-229.

Cools, A., Witvrouw, E., Declercq, G., Vanderstraeten, G. and Cambier, D. (2004). Evaluation of isokinetic force production and associated muscle activity in the scapular rotators during a protraction-retraction movement in overhead athletes with impingement symptoms. British journal of sports medicine, 38(1), 64-68.
Cooper, J., Karduna, A. (2022) Submaximal contractions can serve as a reliable technique for shoulder electromyography normalization. Journal of Biomechanics, 134:111014.
Corcos, D. M., Jaric, S., Agarwal, G. C. and Gottlieb, G. L. (1993). Principles for learning single-joint movements. I. Enhanced performance by practice. Exp Brain Res, 94(3), 499-513. 10.1007/bf00230208.
Cudlip, A. C. and Dickerson, C. R. (2018). Regional activation of anterior and posterior supraspinatus differs by plane of elevation, hand load and elevation angle. Journal of Electromyography and Kinesiology, 43, 14-20.
Cudlip, A. C., Kim, S. Y. and Dickerson, C. R. (2020). The ability of surface electromyography to represent supraspinatus anterior and posterior partition activity depends on elevation angle, hand load and plane of elevation. Journal of biomechanics, 99, 109526.
Davis, L. C., Baumer, T. G., Bey, M. J. and Van Holsbeeck, M. (2019). Clinical utilization of shear wave elastography in the musculoskeletal system. Ultrasonography, 38(1), 2.
de Duca, C. J. and Forrest, W. J. (1973). Force analysis of individual muscles acting simultaneously on the shoulder joint during isometric abduction. Journal of biomechanics, 6(4), 385-393.
De Groot, J., and Brand, R. (2001). A three-dimensional regression model of the shoulder rhythm. Clinical Biomechanics, 16(9):735-743.
De Groot, J. H. (1997). The variability of shoulder motions recorded by means of palpation. Clinical Biomechanics, 12(7-8), 461-472.
De Groote, F., Kinney, A.L., Rao, A.V., Fregly, B.J. (2016). Evaluation of direct collocation optimal control problem formulations for solving the muscle redundancy problem. Annals of biomedical engineering, 44(10):2922-2936.
De Looze, M., Bosch, T., and Van Dieen. (2009). Manifestations of shoulder fatigue in prolonged activities involving low-force contractions. Ergonomics, 52(4), 428-437.
De Luca, C. J. (1997). The use of surface electromyography in biomechanics. Journal of applied biomechanics, 13(2), 135-163.
De Luca, C. J. and Merletti, R. (1988). Surface myoelectric signal cross-talk among muscles of the leg. Electroencephalography and clinical neurophysiology, 69(6), 568-575.
De Ruiter, C., Elzinga, M., Verdijk, P., Van Mechelen, W. and De Haan, A. (2005). Changes in force, surface and motor unit EMG during post-exercise

development of low frequency fatigue in vastus lateralis muscle. European journal of applied physiology, 94(5), 659-669.

De Smet, E., Germeys, F. and De Smet, L. (2009). Prevalence of work related upper limb disorders in hairdressers: a cross sectional study on the influence of working conditions and psychological, ergonomic and physical factors. Work, 34(3), 325-330.

de Witte, P.B., van der Zwaal, P., Visch, W., Schut, J., Nagels, J., Nelissen, R., de Groot, J.H. (2012). Arm Adductor with arm Abduction in rotator cuff tear patients vs. healthy–Design of a new measuring instrument. Human movement science, 31(2):461-471.

de Witte, P., Henseler, J., Van Zwet, E., Nagels, J., Nelissen, R. and De Groot, J. (2014). Cranial humerus translation, deltoid activation, adductor co-activation and rotator cuff disease—different patterns in rotator cuff tears, subacromial impingement and controls. Clinical Biomechanics, 29(1), 26-32.

Delp, S. L., Anderson, F. C., Arnold, A. S., Loan, P., Habib, A., John, C. T., Guendelman, E. and Thelen, D. G. (2007). OpenSim: open-source software to create and analyze dynamic simulations of movement. IEEE transactions on biomedical engineering, 54(11), 1940-1950.

Desmurget, M., and Grafton, S. (2000). Forward modeling allows feedback control for fast reaching movements. Trends in Cognitive Sciences, 4(11), 423-431.

Dickerson, C.R., McDonald, A.C., Chopp-Hurley, J.N. (2020). Between two rocks and in a hard place: Reflecting on the biomechanical basis of shoulder occupational musculoskeletal disorders. Human Factors, 0018720819896191.

Dickerson, C. R., Hughes, R. E. and Chaffin, D. B. (2008). Experimental evaluation of a computational shoulder musculoskeletal model. Clinical Biomechanics, 23(7), 886-894.

Dickerson, C. R., Meszaros, K. A., Cudlip, A. C., Chopp-Hurley, J. N. and Langenderfer, J. E. (2015). The influence of cycle time on shoulder fatigue responses for a fixed total overhead workload. Journal of Biomechanics, 48(11), 2911-2918.

Drake, J. D. and Callaghan, J. P. (2006). Elimination of electrocardiogram contamination from electromyogram signals: An evaluation of currently used removal techniques. Journal of Electromyography and Kinesiology, 16(2), 175-187.

Duchateau, J. and Baudry, S. (2014). The neural control of coactivation during fatiguing contractions revisited. Journal of Electromyography and Kinesiology, 24(6), 780-788.

Dul, J., Johnson, G., Shiavi, R. and Townsend, M. (1984). Muscular synergism—II. A minimum-fatigue criterion for load sharing between synergistic muscles. Journal of biomechanics, 17(9), 675-684.
Dupuis, F., Sole, G., Wassinger, C., Bielmann, M., Bouyer, L. J. and Roy, J.-S. (2021). Fatigue, induced via repetitive upper-limb motor tasks, influences trunk and shoulder kinematics during an upper limb reaching task in a virtual reality environment. PloS one, 16(4), e0249403.
Dvir, Z. and Berme, N. (1978). The shoulder complex in elevation of the arm: a mechanism approach. Journal of biomechanics, 11(5), 219-225.
Ebata, S. E. (2012). Postural and muscular adaptations to repetitive simulated assembly line work. McMaster University.
Ebaugh, D. D., McClure, P. W. and Karduna, A. R. (2005). Three-dimensional scapulothoracic motion during active and passive arm elevation. Clinical Biomechanics, 20(7), 700-709.
Ebaugh, D. D., McClure, P. W. and Karduna, A. R. (2006). Effects of shoulder muscle fatigue caused by repetitive overhead activities on scapulothoracic and glenohumeral kinematics. Journal of Electromyography and Kinesiology, 16(3), 224-235.
Eby, S. F., Cloud, B. A., Brandenburg, J. E., Giambini, H., Song, P., Chen, S., LeBrasseur, N. K. and An, K.-N. (2015). Shear wave elastography of passive skeletal muscle stiffness: influences of sex and age throughout adulthood. Clinical biomechanics, 30(1), 22-27.
Ekstrom, R. A., Bifulco, K. M., Lopau, C. J., Andersen, C. F. and Gough, J. R. (2004). Comparing the function of the upper and lower parts of the serratus anterior muscle using surface electromyography. Journal of Orthopaedic & Sports Physical Therapy, 34(5), 235-243.
Ekstrom, R. A., Soderberg, G. L. and Donatelli, R. A. (2005). Normalization procedures using maximum voluntary isometric contractions for the serratus anterior and trapezius muscles during surface EMG analysis. Journal of Electromyography and Kinesiology, 15(4), 418-428.
Emery, K. and Côté, J. N. (2012). Repetitive arm motion-induced fatigue affects shoulder but not endpoint position sense. Experimental brain research, 216(4), 553-564.
Enoka, R. M. (1995). Mechanisms of muscle fatigue: central factors and task dependency. Journal of Electromyography and Kinesiology, 5(3), 141-149.
Enoka, R. M. and Duchateau, J. (2008). Muscle fatigue: what, why and how it influences muscle function. The Journal of physiology, 586(1), 11-23.
Enoka, R. M. and Stuart, D. G. (1992). Neurobiology of muscle fatigue. Journal of applied physiology, 72(5), 1631-1648.
Erdemir, A., McLean, S., Herzog, W. and van den Bogert, A. J. (2007). Model-based estimation of muscle forces exerted during movements. Clinical biomechanics, 22(2), 131-154.

Escamilla, R.F., Andrews, J.R. (2009). Shoulder muscle recruitment patterns and related biomechanics during upper extremity sports. Sports medicine, 39:569-590.
Ewertsen, C., Carlsen, J., Perveez, M. A. and Schytz, H. (2018). Reference values for shear wave elastography of neck and shoulder muscles in healthy individuals. Ultrasound international open, 4(01), E23-E29.
Farina, D., Blanchietti, A., Pozzo, M., Merletti, R. (2004). M-wave properties during progressive motor unit activation by transcutaneous stimulation. Journal of Applied Physiology, 97(2):545-555.
Farina, D., Merletti, R. and Enoka, R. M. (2004). The extraction of neural strategies from the surface EMG. Journal of applied physiology, 96(4), 1486-1495.
Fewster, K.M., Dickerson, C.R. (2021). Overhead Work–Reduce the Injury Risk.
Forestier, N. and Nougier, V. (1998). The effects of muscular fatigue on the coordination of a multijoint movement in human. Neuroscience Letters, 252(3), 187-190.
Frey-Law, L.A., Avin, K.G. (2013). Muscle coactivation: a generalized or localized motor control strategy? Muscle & nerve, 48(4):578-585.
Fuller, J. R., Lomond, K. V., Fung, J. and Côté, J. N. (2009). Posture-movement changes following repetitive motion-induced shoulder muscle fatigue. Journal of Electromyography and Kinesiology, 19(6), 1043-1052.
Gandevia, S., Allen, G.M., Butler, J.E., Taylor, J.L. (1996). Supraspinal factors in human muscle fatigue: evidence for suboptimal output from the motor cortex. The Journal of physiology, 490(2):529-536.
Gandevia, S. (1998). Neural control in human muscle fatigue: changes in muscle afferents, moto neurones and moto cortical drive. Acta physiologica Scandinavica, 162(3):275-283.
Gates, D. H. and Dingwell, J. B. (2008). The effects of neuromuscular fatigue on task performance during repetitive goal-directed movements. Experimental Brain Research, 187(4), 573-585.
Gates, D. H., & Dingwell, J. B. (2011). The effects of muscle fatigue and movement height on movement stability and variability. Experimental brain research, 209, 525-536.
Geiringer, S.R. (1999). Anatomic localization for needle electromyography, Hanley & Belfus.
Gill, P. E., Murray, W. and Saunders, M. A. (2005). SNOPT: An SQP algorithm for large-scale constrained optimization. SIAM review, 47(1), 99-131.
Ginn, K., Halaki, M. and Cathers, I. (2011). Revision of the shoulder normalization tests is required to include rhomboid major and teres major. Journal of Orthopaedic Research, 29(12), 1846-1849.

Giszter, S., Patil, V., Hart, C. (2007). Primitives, premotor drives, and pattern generation: a combined computational and neuroethological perspective. Progress in brain research, 165:323-346.

Giuseppe, L.U., Laura, R.A., Berton, A., Candela, V., Massaroni, C., Carnevale, A., Stelitano, G., Schena, E., Nazarian, A., DeAngelis, J. (2020). Scapular dyskinesis: from basic science to ultimate treatment. International journal of environmental research and public health, 17(8):2974.

Graichen, H., Stammberger, T., Bonel, H., Englmeier, K-H., Reiser, M., Eckstein, F. (2000). Glenohumeral translation during active and passive elevation of the shoulder—a 3D open-MRI study. Journal of biomechanics, 33(5):609-613.

Graichen, H., Bonel, H., Stammberger, T., Englmeier, K-H., Reiser, M., Eckstein, F. (2001). Sex-specific differences of subacromial space width during abduction, with and without muscular activity, and correlation with anthropometric variables. Journal of Shoulder and Elbow Surgery, 10(2), 129-135.

Grewal, T.-J., Cudlip, A. and Dickerson, C. (2017). Comparing non-invasive scapular tracking methods across elevation angles, planes of elevation and humeral axial rotations. Journal of Electromyography and Kinesiology, 37, 101-107.

Grieve, J. R. and Dickerson, C. R. (2008). Overhead work: Identification of evidence-based exposure guidelines. Occupational Ergonomics, 8(1), 53-66.

Groot, J. (1998). The variance of the shoulder motions recorded by means of palpation. The shoulder kinematics and dynamic analysis of motion and loading. Delft: Delft University of Technology, 23-37.

Guney-Deniz, H., Harput, G., Toprak, U. and Duzgun, I. (2019). Relationship between middle trapezius muscle activation and acromiohumeral distance change during shoulder elevation with scapular retraction. Journal of sport rehabilitation, 28(3), 266-271.

Guo, K., Zhao, S., Liu, B., Liu, Y., Zhang, Y., Yang, H. (2020). Research on Lower Extremity Exoskeleton System Based on Elastic Energy Storage Components. IOP Conference Series: Materials Science and Engineering, IOP Publishing.

Hagberg, M. (1981). Muscular endurance and surface electromyogram in isometric and dynamic exercise. Journal of Applied Physiology, 51(1), 1-7.

Halder, A. M., Itoi, E. and An, K.-N. (2000). Anatomy and biomechanics of the shoulder. Orthopedic Clinics, 31(2), 159-176.

Hatta, T., Yamamoto, N., Sano, H. and Itoi, E. (2014). In vivo measurement of rotator cuff tendon strain with ultrasound elastography: an investigation using a porcine model. Journal of ultrasound in medicine, 33(9), 1641-1646.

He, J., Levine, W. S. and Loeb, G. E. (1989). Feedback gains for correcting small perturbations to standing posture. Proceedings of the 28th IEEE Conference on Decision and Control, IEEE.

Hendrix, C. R., Housh, T., Johnson, G., Mielke, M., Zuniga, J., Camic, C. and Schmidt, R. (2010). The effect of epoch length on the electromyographic mean power frequency and amplitude versus time relationships. Electromyography and Clinical Neurophysiology, 50(5), 219-227.

Herberts, P., Kadefors, R., Broman, H. (1980). Arm positioning in manual tasks an electromyographic study of localized muscle fatigue. Ergonomics, 23(7):655-665.

Herberts, P., Kadefors, R., Högfors, C., Sigholm, G. (1984). Shoulder pain and heavy manual labor. Clinical orthopaedics and related research, (191):166-178.

Herzog, W. (2019). The problem with skeletal muscle series elasticity. BMC biomedical engineering, 1(1):1-14.

Herzog, W. and Leonard, T. (1991). Validation of optimization models that estimate the forces exerted by synergistic muscles. Journal of biomechanics, 24, 31-39.

Hik, F., Ackland, D.C. (2019). The moment arms of the muscles spanning the glenohumeral joint: a systematic review. Journal of anatomy, 234(1):1-15.

Hincapie, J. G., Blana, D., Chadwick, E. K. and Kirsch, R. F. (2008). Musculoskeletal model-guided, customizable selection of shoulder and elbow muscles for a C5 SCI neuroprosthesis. IEEE Transactions on Neural Systems and Rehabilitation Engineering, 16(3), 255-263.

Hirashima, M. and Oya, T. (2016). How does the brain solve muscle redundancy? Filling the gap between optimization and muscle synergy hypotheses. Neuroscience Research, 104, 80-87.

Hodges, P.W., Bui, B.H. (1996). A comparison of computer-based methods for the determination of onset of muscle contraction using electromyography. Electroencephalography and Clinical Neurophysiology/Electromyography and Motor Control, 101(6):511-519.

Hoffmann, M., Begon, M., Lafon, Y., Duprey, S. (2020). Influence of glenohumeral joint muscle insertion on moment arms using a finite element model. Computer Methods in Biomechanics and Biomedical Engineering, 23(14):1117-1126.

Houdijk, H., Brown, S. E. and van Dieën, J. H. (2015). Relation between postural sway magnitude and metabolic energy cost during upright standing on a compliant surface. Journal of Applied Physiology, 119(6), 696-703.

Howarth, S.J., Kingston, D.C., Brown, S.H., Graham, R.B. (2013). Viscoelastic creep induced by repetitive spine flexion and its relationship to dynamic spine stability. Journal of Electromyography and Kinesiology, 23(4):794-800.

Howarth, S. J., Grondin, D. E., La Delfa, N. J., Cox, J. and Potvin, J. R. (2016). Working position influences the biomechanical demands on the lower back during dental hygiene. Ergonomics, 59(4), 545-555.
Huisstede, B.M., Bierma-Zeinstra, S.M., Koes, B.W., Verhaar, J.A. (2006). Incidence and prevalence of upper-extremity musculoskeletal disorders. A systematic appraisal of the literature. BMC musculoskeletal disorders, 7(1):1-7.
Humphrey. D., Reed, D., Desmedt, J. (1983). Motor control mechanisms in health and disease.
Inman, V.T., Saunders, J.M., Abbott, L.C. (1944). Observations on the function of the shoulder joint. Journal of Bone and Joint Surgery, 26(1):1-30.
Inouye, J.M., Valero-Cuevas, F.J. (2016). Muscle synergies heavily influence the neural control of arm endpoint stiffness and energy consumption. PLoS computational biology, 12(2):e1004737.
Janwantanakul, P., Magarey, M. E., Jones, M. A. and Dansie, B. R. (2001). Variation in shoulder position sense at mid and extreme range of motion. Archives of physical medicine and rehabilitation, 82(6), 840-844.
Johnson, G., Bogduk, N., Nowitzke, A. and House, D. (1994). Anatomy and actions of the trapezius muscle. Clinical biomechanics, 9(1), 44-50.
Johnston, H. A. and Drake, J. D. (2021). Multivariate shoulder and spine relationship using planar range of motion assessment. Musculoskeletal Science and Practice, 54, 102398.
Jull, G., Falla, D., Treleaven, J., Hodges, P., Vicenzino, B. (2007). Retraining cervical joint position sense: the effect of two exercise regimes. Journal of orthopaedic research, 25(3):404-412.
Kelly, J. P., Koppenhaver, S. L., Michener, L. A., Proulx, L., Bisagni, F. and Cleland, J. A. (2018). Characterization of tissue stiffness of the infraspinatus, erector spinae, and gastrocnemius muscle using ultrasound shear wave elastography and superficial mechanical deformation. Journal of Electromyography and Kinesiology, 38, 73-80.
Kelly, M. (2017). An introduction to trajectory optimization: How to do your own direct collocation. SIAM Review, 59(4), 849-904.
Kibler, W.B., Ludewig, P.M., McClure, P.W., Michener, L.A., Bak, K., Sciascia, A.D. (2013). Clinical implications of scapular dyskinesis in shoulder injury: the 2013 consensus statement from the 'Scapular Summit'. British journal of sports medicine, 47(14):877-885.
Kibler, W. (1998). The role of the scapula in athletic shoulder function. The American journal of sports medicine, 26(2), 325-337.
Koo, T.K., Guo, J-Y., Cohen, J.H., Parker, K.J. (2013). Relationship between shear elastic modulus and passive muscle force: an ex-vivo study. Journal of biomechanics, 46(12):2053-2059.

Koppenhaver, S., Kniss, J., Lilley, D., Oates, M., Fernández-de-Las-Peñas, C., Maher, R., Croy, T. and Shinohara, M. (2018). Reliability of ultrasound shear-wave elastography in assessing low back musculature elasticity in asymptomatic individuals. Journal of Electromyography and Kinesiology, 39, 49-57.

Kozinc, Ž. and Šarabon, N. (2020). Shear-wave elastography for assessment of trapezius muscle stiffness: Reliability and association with low-level muscle activity. PLoS One, 15(6), e0234359.

Kubo, K., Kanehisa, H., Kawakami, Y. and Fukunaga, T. (2001). Influences of repetitive muscle contractions with different modes on tendon elasticity in vivo. Journal of applied physiology, 91(1), 277-282.

Langenderfer, J., LaScalza, S., Mell, A., Carpenter., J. E., Kuhn, J. E., Hughes, R. E. (2005). An EMG-driven model of the upper extremity and estimation of long head biceps force. Computers in Biology and Medicine, 35(1), 25-39.

Latash, M. L. (2018). Muscle coactivation: definitions, mechanisms, and functions. Journal of neurophysiology, 120(1), 88-104.

Latash, M. L., Scholz, J. P. and Schöner, G. (2002). Motor control strategies revealed in the structure of motor variability. Exercise and sport sciences reviews, 30(1), 26-31.

Latash, M. L., Scholz, J. P. and Schöner, G. (2007). Toward a new theory of motor synergies. Motor control, 11(3), 276-308.

Lee, K. H., Min, J. Y. and Byun, S. (2021). Electromyogram-Based Classification of Hand and Finger Gestures Using Artificial Neural Networks. Sensors, 22(1), 225.

Levin, S. M. (1997). Putting the shoulder to the wheel: a new biomechanical model for the shoulder girdle. Biomedical sciences instrumentation, 33, 412-417.

Levin, S. M. (2005). The scapula is a sesamoid bone. Journal of biomechanics, 38(8), 1733-1733.

Lewis, J. S., Green, A. and Wright, C. (2005). Subacromial impingement syndrome: the role of posture and muscle imbalance. Journal of shoulder and elbow surgery, 14(4), 385-392.

Lindman, R., Eriksson, A., Thornell, L.E. (1991). Fiber type composition of the human female trapezius muscle: Enzyme-histochemical characteristics. American Journal of Anatomy, 190(4):385-392.

Lindman, R., Eriksson, A., Thornell, L.E. (1990). Fiber type composition of the human male trapezius muscle: Enzyme-histochemical characteristics. American Journal of anatomy, 189(3):236-244.

Lindstrom, L. H. and Magnusson, R. I. (1977). Interpretation of myoelectric power spectra: a model and its applications. Proceedings of the IEEE, 65(5), 653-662.

Looze, M. d., Bosch, T. and Dieën, J. v. (2009). Manifestations of shoulder fatigue in prolonged activities involving low-force contractions. Ergonomics, 52(4), 428-437.

Ludewig, P.M., Cook, T.M. (2002). Translations of the humerus in persons with shoulder impingement symptoms. Journal of Orthopaedic & Sports Physical Therapy, 32(6):248-259.

Ludewig, P. M. and Cook, T. M. (2000). Alterations in shoulder kinematics and associated muscle activity in people with symptoms of shoulder impingement. Physical therapy, 80(3), 276-291.

Ludewig, P. M., Hoff, M. S., Osowski, E. E., Meschke, S. A. and Rundquist, P. J. (2004). Relative balance of serratus anterior and upper trapezius muscle activity during push-up exercises. The American journal of sports medicine, 32(2), 484-493.

Ludewig, P. M., Phadke, V., Braman, J. P., Hassett, D. R., Cieminski, C. J. and LaPrade, R. F. (2009). Motion of the shoulder complex during multiplanar humeral elevation. The Journal of Bone and Joint Surgery. American volume., 91(2), 378.

Lynch, S., Ramos, J. and Jones, D. (2017). Hysteresis in muscle. International Journal of Bifurcation and Chaos, 27(1), 1730003.

Maas, R. (2014). Biomechanics and optimal control simulations of the human upper extremity, Friedrich-Alexander-Universität Erlangen-Nürnberg (FAU).

Maciukiewicz, J. M., Cudlip, A. C., Chopp-Hurley, J. N. and Dickerson, C. R. (2016). Effects of overhead work configuration on muscle activity during a simulated drilling task. Applied Ergonomics, 53, 10-16.

MacLean, K. F., Langenderfer, J. E. and Dickerson, C. R. (2023). A comparative probabilistic analysis of human and chimpanzee rotator cuff functional capacity. Journal of Anatomy, 243(3), 431-447.

Madeleine, P. (2010). On functional motor adaptations: from the quantification of motor strategies to the prevention of musculoskeletal disorders in the neck–shoulder region. Acta Physiologica, 199, 1-46.

Magill, R. and Anderson, D. I. (2010). Motor learning and control, McGraw-Hill Publishing New York.

Marler, R. T., Arora, J. S., Yang, J., Kim, H.-J. and Abdel-Malek, K. (2009). Use of multi-objective optimization for digital human posture prediction. Engineering Optimization, 41(10), 925-943.

McClure, P., Greenberg, E. and Kareha, S. (2012). Evaluation and management of scapular dysfunction. Sports medicine and arthroscopy review, 20(1), 39-48.

McDonald, A.C., Savoie, S.M., Mulla, D.M., Keir, P.J. (2018); Dynamic and static shoulder strength relationship and predictive model. Applied Ergonomics, 67:162-169.

McDonald, A. C., Mulla, D. M. and Keir, P. J. (2019). Muscular and kinematic adaptations to fatiguing repetitive upper extremity work. Applied ergonomics, 75, 250-256.
McDonald, A. C., Mulla, D. M., Stratford, P. W. and Keir, P. J. (2018). Submaximal normalizing methods to evaluate load sharing changes in the shoulder during repetitive work. Journal of Electromyography and Kinesiology, 39, 58-69.
McDonald, A. C., Sonne, M. W. and Keir, P. J. (2017). Optimized maximum voluntary exertion protocol for normalizing shoulder muscle activity. International Biomechanics, 4(1), 9-16.
McDonald, A. C., Tse, C. and Keir, P. J. (2016). Adaptations to isolated shoulder fatigue during simulated repetitive work. Part II: Recovery. Journal of Electromyography and Kinesiology, 29, 42-49.
McQuade, K. J., Borstad, J. and de Oliveira, A. S. (2016). Critical and theoretical perspective on scapular stabilization: what does it really mean, and are we on the right track? Physical therapy, 96(8), 1162-1169.
McQuade, K. J., Dawson, J. and Smidt, G. L. (1998). Scapulothoracic muscle fatigue associated with alterations in scapulohumeral rhythm kinematics during maximum resistive shoulder elevation. Journal of Orthopaedic & Sports Physical Therapy, 28(2), 74-80.
McQuade, K., Wei, S. H. and Smidt, G. (1995). Effects of local muscle fatigue on three-dimensional scapulohumeral rhythm. Clinical Biomechanics, 10(3), 144-148.
McQuade, K.J., Dawson, J., and Smidt, G.L. (1998). Scapulothoracic muscle fatigue associated with alterations in scapulohumeral rhythm kinematics during maximum resistive shoulder elevation. Journal of Orthopaedic and Sports Physical Therapy, 28(2), 74-80.
Mendes, B., Firmino, T., Oliveira, R., Neto, T., Infante, J., Vaz, J. R. and Freitas, S. R. (2018). Hamstring stiffness pattern during contraction in healthy individuals: analysis by ultrasound-based shear wave elastography. European Journal of Applied Physiology, 118, 2403-2415.
Menegaldo, L.L., de Toledo, F.A., Weber, H.I. (2003). Biomechanical modeling and optimal control of human posture. Journal of biomechanics, 36(11):1701-1712.
Merletti, R., Farina, D. (2009). Analysis of intramuscular electromyogram signals. Philosophical Transactions of the Royal Society A: Mathematical, Physical and Engineering Sciences, 367(1887):357-368.
Metwali, M. (2019). Motor Variablity, Task Performance, and Muscle Fatigue during Training of a Repetitive Lifting Task: Adapting Motor Learning Topics to Occupational Ergonomics Research, The University of Iowa.

Michener LA, McClure PW, Karduna AR. Anatomical and biomechanical mechanisms of subacromial impingement syndrome. Clinical biomechanics 2003;18(5):369-379.
Michener, L. A., McClure, P. W. and Karduna, A. R. (2003). Anatomical and biomechanical mechanisms of subacromial impingement syndrome. Clinical biomechanics, 18(5), 369-379.
Michener, L. A., McClure, P. W. and Karduna, A. R. (2003). Anatomical and biomechanical mechanisms of subacromial impingement syndrome. Clinical biomechanics, 18(5), 369-379.
Michener, L. A., Sharma, S., Cools, A. M. and Timmons, M. K. (2016). Relative scapular muscle activity ratios are altered in subacromial pain syndrome. Journal of Shoulder and Elbow Surgery, 25(11), 1861-1867.
Michener, L. A., Subasi Yesilyaprak, S. S., Seitz, A. L., Timmons, M. K. and Walsworth, M. K. (2015). Supraspinatus tendon and subacromial space parameters measured on ultrasonographic imaging in subacromial impingement syndrome. Knee Surgery, Sports Traumatology, Arthroscopy, 23, 363-369.
Miller, J. (1991). Reaction time analysis with outlier exclusion: Bias varies with sample size. The Quarterly Journal of Experimental psychology, 43(4), 907-912.
Minajeva, A., Kulke, M., Fernandez, J.M., Linke, W.A. (2001). Unfolding of titin domains explains the viscoelastic behavior of skeletal myofibrils. Biophysical journal, 80(3):1442-1451.
Monjo, F., Terrier, R. and Forestier, N. (2015). Muscle fatigue as an investigative tool in motor control: A review with new insights on internal models and posture–movement coordination. Human Movement Science, 44, 225-233.
Moon, J., Shin, I., Kang, M., Kim, Y., Lee, K., Park, J., Kim, K., Hong, D., Koo, D. and O'Sullivan, D. (2013). The Effect of Shoulder Flexion Angles on the Recruitment of Upper-extremity Muscles during Isometric Contraction. Journal of Physical Therapy Science, 25(10), 1299-1301. .
Mottram, S. (1997). Dynamic stability of the scapula. Man ther, 2(3), 123-131.
Mulla, D.M., Hodder, J.N., Maly, M.R., Lyons, J.L., Keir, P.J. (2019). Modeling the effects of musculoskeletal geometry on scapulohumeral muscle moment arms and lines of action. Computer Methods in Biomechanics and Biomedical Engineering, 22(16):1311-1322.
RMulla, D. M. and Keir, P. J. (2023). Neuromuscular control: from a biomechanist's perspective. Frontiers in Sports and Active Living, 5, 1217009.
Mulla, D. M., McDonald, A. C. and Keir, P. J. (2018). Upper body kinematic and muscular variability in response to targeted rotator cuff fatigue. Human Movement Science, 59, 121-133.

Myers, J.B., Hwang, J-H., Pasquale, M.R., Blackburn, J.T., Lephart, S.M. (2009). Rotator cuff coactivation ratios in participants with subacromial impingement syndrome. Journal of science and medicine in sport, 12(6):603-608.
Myers, J. B., Guskiewicz, K. M., Schneider, R. A. and Prentice, W. E. (1999). Proprioception and neuromuscular control of the shoulder after muscle fatigue. Journal of athletic training, 34(4), 362.
Nakajima, T., Rokuuma, N., Hamada, K., Tomatsu, T. and Fukuda, H. (1994). Histologic and biomechanical characteristics of the supraspinatus tendon: reference to rotator cuff tearing. Journal of Shoulder and Elbow Surgery, 3(2), 79-87.
Nasr, A., Inkol, K. A., Bell, S. and McPhee, J. (2021). InverseMuscleNET: Alternative Machine Learning Solution to Static Optimization and Inverse Muscle Modeling. Front Comput Neurosci, 15, 759489. 10.3389/fncom.2021.759489.
Nikooyan, A. A., Veeger, H., Westerhoff, P., Graichen, F., Bergmann, G. and Van Der Helm, F. (2010). Validation of the Delft Shoulder and Elbow Model using in-vivo glenohumeral joint contact forces. Journal of biomechanics, 43(15), 3007-3014.
Noguchi, M., Chopp, J. N., Borgs, S. P. and Dickerson, C. R. (2013). Scapular orientation following repetitive prone rowing: implications for potential subacromial impingement mechanisms. Journal of Electromyography and Kinesiology, 23(6), 1356-1361.
Nordin, M. and Frankel, V. H. (2001). Basic biomechanics of the musculoskeletal system, Lippincott Williams & Wilkins.
Norman, R., Wells, R., Neumann, P., Frank, J., Shannon, H., Kerr, M. and Study, T. O. U. B. P. (1998). A comparison of peak vs cumulative physical work exposure risk factors for the reporting of low back pain in the automotive industry. Clinical biomechanics, 13(8), 561-573.
Öberg, T., Sandsjö, L., Kadefors, R. (1994). EMG mean power frequency: obtaining a reference value. Clinical Biomechanics, 9(4):253-257.
Öberg, T. (1995). Muscle fatigue and calibration of EMG measurements. Journal of Electromyography and Kinesiology, 5(4), 239-243.
Öberg, T., Sandsjö, L. and Kadefors, R. (1990). Electromyogram mean power frequency in non-fatigued trapezius muscle. European Journal of Applied Physiology and Occupational Physiology, 61(5), 362-369.
Öberg, T., Sandsjö, L. and Kadefors, R. (1991). Variability of the EMG mean power frequency: a study on the trapezius muscle. Journal of Electromyography and Kinesiology, 1(4), 237-243.
Oomen, N. M., Graham, R. B., & Fischer, S. L. (2023). Exploring the relationship between kinematic variability and fatigue development during repetitive lifting. Applied Ergonomics, 107, 103922.Overbeek, C. L., Kolk, A., de

Groot, J. H., de Witte, P. B., Gademan, M. G., Nelissen, R. G. and Nagels, J. (2019). Middle-aged adults cocontract with arm ADductors during arm ABduction, while young adults do not. Adaptations to preserve pain-free function? Journal of Electromyography and Kinesiology, 49, 102351.
Ostry, D. J., Cooke, J. D. and Munhall, K. G. (1987). Velocity curves of human arm and speech movements. Experimental Brain Research, 68, 37-46.
Overbeek, C.L., Kolk, A., Nagels, J., de Witte, P.B., van der Zwaal, P., Visser, C.P., Fiocco, M., Nelissen, R.G., de Groot, J.H. (2018). Increased co-contraction of arm adductors is associated with a favorable course in subacromial pain syndrome. Journal of Shoulder and Elbow Surgery, 27(11):1925-1931.
Özkaya, N., Nordin, M., Goldsheyder, D. and Leger, D. (2012). Fundamentals of biomechanics, Springer.
Page, P. (2011). Shoulder muscle imbalance and subacromial impingement syndrome in overhead athletes. International Journal of Sports Physical Therapy, 6(1):51-58.
Pataky, T. C. (2010). Generalized n-dimensional biomechanical field analysis using statistical parametric mapping. Journal of biomechanics, 43(10), 1976-1982.
Pataky, T. C., Robinson, M. A. and Vanrenterghem, J. (2016). Region-of-interest analyses of one-dimensional biomechanical trajectories: bridging 0D and 1D theory, augmenting statistical power. PeerJ, 4, e2652.
Pataky, T. C., Vanrenterghem, J., Robinson, M. A. and Liebl, D. (2019). On the validity of statistical parametric mapping for nonuniformly and heterogeneously smooth one-dimensional biomechanical data. Journal of biomechanics, 91, 114-123.
Perotto, A.O. (2011). Anatomical guide for the electromyographer: the limbs and trunk, Charles C Thomas Publisher.
Perrey, S., Quaresima, V. and Ferrari, M. (2024). Muscle oximetry in sports science: An updated systematic review. Sports Medicine, 54(4), 975-996.
Pethick, J., & Tallent, J. (2022). The Neuromuscular Fatigue-Induced Loss of Muscle Force Control. Sports, 10(11), 184.
Phadke, V., Camargo, P. and Ludewig, P. (2009). Scapular and rotator cuff muscle activity during arm elevation: a review of normal function and alterations with shoulder impingement. Brazilian Journal of Physical Therapy, 13, 1-9.
Poppen, N., Walker, P. (1978). Forces at the glenohumeral joint in abduction. Clinical Orthopaedics and Related Research, 135:165-170.
Potvin, J.R., Fuglevand, A.J. (2017). A motor unit-based model of muscle fatigue. PLoS computational biology, 13(6):e1005581.
Praagman, M., Chadwick, E., Van Der Helm, F. and Veeger, H. (2006). The relationship between two different mechanical cost functions and muscle oxygen consumption. Journal of biomechanics, 39(4), 758-765.

Prescher, A. (2000). Anatomical basics, variations, and degenerative changes of the shoulder joint and shoulder girdle. European journal of radiology, 35(2), 88-102.

Prochazka, A. and Ellaway, P. (2012). Sensory systems in the control of movement. Comprehensive Physiology, 2(4), 2615-2627.

Proske, U. (2015). The role of muscle proprioceptors in human limb position sense: a hypothesis. Journal of anatomy, 227(2), 178-183.

Punnett, L., Fine, L. J., Keyserling, W. M., Herrin, G. D. and Chaffin, D. B. (2000). Shoulder disorders and postural stress in automobile assembly work. Scandinavian Journal of Work, Environment & Health, 283-291.

Qin, J., Lin, J.-H., Faber, G. S., Buchholz, B. and Xu, X. (2014). Upper extremity kinematic and kinetic adaptations during a fatiguing repetitive task. Journal of Electromyography and Kinesiology, 24(3), 404-411.

Rathelot, J-A., Strick, P.L. (2009). Subdivisions of primary motor cortex based on cortico-motoneuronal cells. Proceedings of the National Academy of Sciences of the United States of America, 106(3):918-923.

Raviv, L., Lupyan, G. and Green, S. C. (2022). How variability shapes learning and generalization. Trends in cognitive sciences, 26(6), 462-483.

Reddy, A. S., Mohr, K. J., Pink, M. M. and Jobe, F. W. (2000). Electromyographic analysis of the deltoid and rotator cuff muscles in persons with subacromial impingement. Journal of shoulder and elbow surgery, 9(6), 519-523.

Reinold, M.M., Escamilla, R., Wilk, K.E. (2009). Current concepts in the scientific and clinical rationale behind exercises for glenohumeral and scapulothoracic musculature. journal of orthopaedic & sports physical therapy, 39(2):105-117.

Riemann, B. L. and Lephart, S. M. (2002). The sensorimotor system, part I: the physiologic basis of functional joint stability. Journal of athletic training, 37(1), 71.

Robinson, M. A., Vanrenterghem, J. and Pataky, T. C. (2015). Statistical Parametric Mapping (SPM) for alpha-based statistical analyses of multi-muscle EMG time-series. Journal of Electromyography and Kinesiology, 25(1), 14-19.

Rosenbaum, D. A., Loukopoulos, L. D., Meulenbroek, R. G., Vaughan, J. and Engelbrecht, S. E. (1995). Planning reaches by evaluating stored postures. Psychological Review, 102(1), 28.

Russell, M. S., Vasilounis, S. S., Lefebvre, E., Drake, J. D. and Chopp-Hurley, J. N. (2024). Variability in musculoskeletal fatigue responses associated with repeated exposure to an occupational overhead drilling task completed on successive days. Human Movement Science, 97, 103276.

Russell, M.S., Vasilounis, S.S., Lefebvre, E., Drake, J.D.M., Chopp-Hurley, J.N. (2024). Muscle coactivation changes following a fatiguing overhead

drilling task: Implications for Subacromial Impingement Syndrome. Applied Ergonomics, Submitted.
Saldana, R., Smith, D. (1991). Four aspects of creep phenomena in striated muscle. Journal of Muscle Research & Cell Motility, 12(6):517-531.
Sangwan, S., Green, R.A., Taylor, N.F. (2015). Stabilizing characteristics of rotator cuff muscles: a systematic review. Disability and rehabilitation, 37(12):1033-1043.
Scholz, J. P. and Schöner, G. (1999). The uncontrolled manifold concept: identifying control variables for a functional task. Experimental Brain Research, 126(3), 289-306.
Schouten, A. C., de Vlugt, E., van der Helm, F. C. and Brouwn, G. G. (2001). Optimal posture control of a musculo-skeletal arm model. Biological Cybernetics, 84, 143-152.
Selvan, K. E. and Sen, D. (2020). Estimating functional reach envelopes for standing postures using digital human model. Theoretical Issues in Ergonomics Science, 21(2), 153-182.
Shaheen, A., Alexander, C. and Bull, A. (2011). Effects of attachment position and shoulder orientation during calibration on the accuracy of the acromial tracker. Journal of biomechanics, 44(7), 1410-1413.
Shenoy, S., Mishra, P. and Sandhu, J. (2011). Peak torque and IEMG activity of quadriceps femoris muscle at three different knee angles in a collegiate population. Journal of Exercise Science & Fitness, 9(1), 40-45.
Siracusa, J., Charlot, K., Malgoyre, A., Conort, S., Tardo-Dino, P.-E., Bourrilhon, C. and Garcia-Vicencio, S. (2019). Resting muscle shear modulus measured with ultrasound shear-wave elastography as an alternative tool to assess muscle fatigue in humans. Frontiers in physiology, 10, 626.
Sjøgaard, G., Kiens, B., Jørgensen, K. and Saltin, B. (1986). Intramuscular pressure, EMG and blood flow during low-level prolonged static contraction in man. Acta Physiologica Scandinavica, 128(3), 475-484.
Slobounov, S., Hallet, M., Newell, K. M. (2004). Perceived effort in force production as reflected in motor-related cortical potentials. Clinical Neurophysiology, 115(10), 2391-2402.
Sohn, M. H. and Ting, L. H. (2018). The cost of being stable: Trade-offs between effort and stability across a landscape of redundant motor solutions. bioRxiv, 477083.
Sood, D., Nussbaum, M. A. and Hager, K. (2007). Fatigue during prolonged intermittent overhead work: reliability of measures and effects of working height. Ergonomics, 50(4), 497-513.
Sood, D., Nussbaum, M. A., Hager, K. and Nogueira, H. C. (2017). Predicted endurance times during overhead work: influences of duty cycle and tool mass estimated using perceived discomfort. Ergonomics, 60(10), 1405-1414.

Sparto, P. J., Parnianpour, M., Reinsel, T. E. and Simon, S. (1997). The effect of fatigue on multijoint kinematics and load sharing during a repetitive lifting test. Spine, 22(22), 2647-2654.

Steenbrink, F., de Groot, J. H., Veeger, H., Meskers, C. G., van de Sande, M. A. and Rozing, P. M. (2006). Pathological muscle activation patterns in patients with massive rotator cuff tears, with and without subacromial anaesthetics. Manual therapy, 11(3), 231-237.

Stegeman, D. and Hermens, H. (2007). Standards for surface electromyography: The European project Surface EMG for non-invasive assessment of muscles (SENIAM). Enschede: Roessingh Research and Development, 10, 8-12.

Stegeman, D. F., Blok, J. H., Hermens, H. J. and Roeleveld, K. (2000). Surface EMG models: properties and applications. Journal of Electromyography and Kinesiology, 10(5), 313-326.

Stulen, F. B. and De Luca, C. J. (1981). Frequency parameters of the myoelectric signal as a measure of muscle conduction velocity. IEEE Transactions on Biomedical Engineering, (7), 515-523.

Sundelin, G., Hagberg, M. (1992). Effects of exposure to excessive drafts on myoelectric activity in shoulder muscles. Journal of Electromyography and Kinesiology, 2(1):36-41.

Suzuki, H., Swanik, K. A., Huxel, K. C., Kelly, J. D. and Swanik, C. B. (2006). Alterations in upper extremity motion after scapular-muscle fatigue. Journal of Sport Rehabilitation, 15(1), 71-88.

Suzuki, H., Swanik, K. A., Huxel, K. C., Kelly, J. D. and Swanik, C. B. (2006). Alterations in upper extremity motion after scapular-muscle fatigue. Journal of Sport Rehabilitation, 15(1), 71-88.

Szucs, K., Navalgund, A. and Borstad, J. D. (2009). Scapular muscle activation and co-activation following a fatigue task. Medical & biological engineering & computing, 47(5), 487-495.

Szucs, K., Navalgund, A. and Borstad, J. D. (2009). Scapular muscle activation and co-activation following a fatigue task. Medical & biological engineering & computing, 47(5), 487-495.

Terrier, R. and Forestier, N. (2009). Cognitive cost of motor reorganizations associated with muscular fatigue during a repetitive pointing task. Journal of Electromyography and Kinesiology, 19(6), e487-e493.

Thigpen, C. A., Padua, D. A., Michener, L. A., Guskiewicz, K., Giuliani, C., Keener, J. D. and Stergiou, N. (2010). Head and shoulder posture affect scapular mechanics and muscle activity in overhead tasks. Journal of Electromyography and Kinesiology, 20(4), 701-709.

Thigpen, C. A., Padua, D. A., Michener, L. A., Guskiewicz, K., Giuliani, C., Keener, J. D. and Stergiou, N. (2010). Head and shoulder posture affect scapular

mechanics and muscle activity in overhead tasks. Journal of Electromyography and kinesiology, 20(4), 701-709.
Todorov, E. (2004). Optimality principles in sensorimotor control. Nature Neuroscience, 7(9), 907-915. 10.1038/nn1309.
Tse, C., McDonald, A. C. and Keir, P. J. (2016). Adaptations to isolated shoulder fatigue during simulated repetitive work. Part I: Fatigue. Journal of Electromyography and Kinesiology, 29, 34-41.
Tskhovrebova, L., Trinick, J. (2003). Titin: properties and family relationships. Nature reviews Molecular cell biology, 4(9):679-689.
Umehara, J., Kusano, K., Nakamura, M., Morishita, K., Nishishita, S., Tanaka, H., Shimizu, I. and Ichihashi, N. (2018). Scapular kinematic and shoulder muscle activity alterations after serratus anterior muscle fatigue. Journal of Shoulder and Elbow Surgery, 27(7), 1205-1213.
van Boxtel, A., Schomaker, L. (1984). Influence of motor unit firing statistics on the median frequency of the EMG power spectrum. European journal of applied physiology and occupational physiology, 52(2):207-213.
Van den Bogert, A., Schamhardt, H. (1993). Multi-body modelling and simulation of animal locomotion. Cells Tissues Organs,146(2-3):95-102.
Van Den Bogert, A. J., Blana, D. and Heinrich, D. (2011). Implicit methods for efficient musculoskeletal simulation and optimal control. Procedia Iutam, 2, 297-316.
Van der Helm, F. C. (1994). A finite element musculoskeletal model of the shoulder mechanism. Journal of biomechanics, 27(5), 551-569.
van der Helm, F., Chadwick, E. and Veeger, H. (2001). A large-scale musculoskeletal model of the shoulder and elbow: The Delft Shoulder (and elbow) Model. Proceedings of the XVIIIth Conference of the International Society of Biomechanics, Zurich.
Van der Windt, D., Koes, B.W., De Jong, B.A., Bouter, L.M. (1995). Shoulder disorders in general practice: incidence, patient characteristics, and management. Annals of the rheumatic diseases, 54(12):959-964.
Van Rijn, R. M., Huisstede, B. M., Koes, B. W. and Burdorf, A. (2010). Associations between work-related factors and specific disorders of the shoulder—a systematic review of the literature. Scandinavian journal of work, environment & health, 189-201.
Vanhaezebrouck, E. (2021). The influence of fatigue on the hamstring muscle stiffness in adult athletes, using shear wave elastography, Ghent University.
Vatner, S. F. and Pagani, M. (1976). Cardiovascular adjustments to exercise: hemodynamics and mechanisms. Progress in cardiovascular diseases, 19(2), 91-108.

Vatovec, R., Kozinc, Ž. and Voglar, M. (2022). The Effects of Isometric Fatigue on Trunk Muscle Stiffness: Implications for Shear-Wave Elastography Measurements. Sensors, 22(23), 9476.
Veeger, H. and Van Der Helm, F. (2007). Shoulder function: the perfect compromise between mobility and stability. Journal of biomechanics, 40(10), 2119-2129.
Vøllestad, N. K. (1997). Measurement of human muscle fatigue. Journal of neuroscience methods, 74(2), 219-227.
Wächter, A. and Biegler, L. T. (2006). On the implementation of an interior-point filter line-search algorithm for large-scale nonlinear programming. Mathematical programming, 106, 25-57.
Wada, Y., Yamanaka, K., Soga, Y., Tsuyuki, K. and Kawato, M. (2006). Can a kinetic optimization criterion predict both arm trajectory and final arm posture? 2006 International Conference of the IEEE Engineering in Medicine and Biology Society, IEEE.
Waite, D. L., Brookham, R. L., & Dickerson, C. R. (2010). On the suitability of using surface electrode placements to estimate muscle activity of the rotator cuff as recorded by intramuscular electrodes. Journal of Electromyography and Kinesiology, 20(5), 903-911.
Watson, L., Balster, S., Finch, C. and Dalziel, R. (2005). Measurement of scapula upward rotation: a reliable clinical procedure. British Journal of Sports Medicine, 39(9), 599-603.
Webb, J.D., Blemker, S.S., Delp, S.L. (2014). 3D finite element models of shoulder muscles for computing lines of actions and moment arms. Computer Methods in Biomechanics and Biomedical Engineering, 17(8):829-837.
Weir, J. P., Keefe, D. A., Eaton, J. F., Augustine, R. T. and Tobin, D. M. (1998). Effect of fatigue on hamstring coactivation during isokinetic knee extensions. European journal of applied physiology and occupational physiology, 78(6), 555-559.
Wiedenbauer, M., Mortensen, O. (1952). An electromyographic study of the trapezius muscle. American Journal of Physical Medicine & Rehabilitation, 31(5):363-372.
Wiker, S. F., Chaffin, D. B. and Langolf, G. D. (1989). Shoulder posture and localized muscle fatigue and discomfort. Ergonomics, 32(2), 211-237.
Williamson, E. (2006). Fear avoidance beliefs questionnaire (FABQ). Australian Journal of Physiotherapy, 52(2):149.
Williamson, E. (2006). Fear avoidance beliefs questionnaire (FABQ). Australian Journal of Physiotherapy, 52(2), 149.
Willigenburg, N. W., Daffertshofer, A., Kingma, I., & Van Dieën, J. H. (2012). Removing ECG contamination from EMG recordings: A comparison of

ICA-based and other filtering procedures. Journal of Electromyography and Kinesiology, 22(3), 485-493.
Wren, T.A., Lindsey, D.P., Beaupré, G.S., Carter, D.R. (2003). Effects of creep and cyclic loading on the mechanical properties and failure of human Achilles tendons. Annals of biomedical engineering, 31(6):710-717.
Wu, G. and Cavanagh, P. R. (1995). ISB recommendations for standardization in the reporting of kinematic data. Journal of biomechanics, 28(10), 1257-1262.
Wu, G., Van der Helm, F. C., Veeger, H. D., Makhsous, M., Van Roy, P., Anglin, C., Nagels, J., Karduna, A. R., McQuade, K. and Wang, X. (2005). ISB recommendation on definitions of joint coordinate systems of various joints for the reporting of human joint motion—Part II: shoulder, elbow, wrist and hand. Journal of Biomechanics, 38(5), 981-992.
Yoshitake, Y., Takai, Y., Kanehisa, H. and Shinohara, M. (2014). Muscle shear modulus measured with ultrasound shear-wave elastography across a wide range of contraction intensity. Muscle & nerve, 50(1), 103-113.
Zabihhosseinian, M., Yielder, P., Holmes, M.W., Murphy, B. (2019). Neck muscle fatigue affects performance of an eye-hand tracking task. Journal of Electromyography and Kinesiology, 47:1-9.
Zabihhosseinian, M., Holmes, M. W. and Murphy, B. (2015). Neck muscle fatigue alters upper limb proprioception. Experimental brain research, 233, 1663-1675.
Zhang, L. Q., Wang, G., Nuber, G. W., Press, J. M. and Koh, J. L. (2003). In vivo load sharing among the quadriceps components. Journal of Orthopaedic Research, 21(3), 565-571.
Zimmer, M., Kleiser, B., Marquetand, J. and Ateş, F. (2023). Shear wave elastography characterizes passive and active mechanical properties of biceps brachii muscle in vivo. Journal of the Mechanical Behavior of Biomedical Materials, 137, 105543.

Appendix A: Model-Predicted Scapulothoracic Joint Angle Solutions at 75%, 50%, and 25% limited Fmax.

Figure A.1. **Model-predicted scapulothoracic joint angle optimal control solution for frontal-plane thoracohumeral elevation from 15° to 120°.** Subplots are organized vertically by Fmax limited muscle, and horizontally by magnitude of Fmax. Solid black lines indicate the solution subject to reduced Fmax compared to the dotted line "no fatigue" solution. Subplots outlined in red are unique from the "no fatigue" solution.

Figure A.2. **Model-predicted scapulothoracic joint angle optimal control solution for scapular-plane thoracohumeral elevation from 15° to 120°.** Subplots are organized vertically by Fmax limited muscle, and horizontally by magnitude of Fmax. Solid black lines indicate the solution subject to reduced Fmax compared to the dotted line "no fatigue" solution. Subplots outlined in red are unique from the "no fatigue" solution.

Figure A.3. **Model-predicted scapulothoracic joint angle optimal control solution for sagittal-plane thoracohumeral elevation from 15° to 120°.** Subplots are organized vertically by Fmax limited muscle, and horizontally by magnitude of Fmax. Solid black lines indicate the solution subject to reduced Fmax compared to the dotted line "no fatigue" solution. Subplots outlined in red are unique from the "no fatigue" solution.

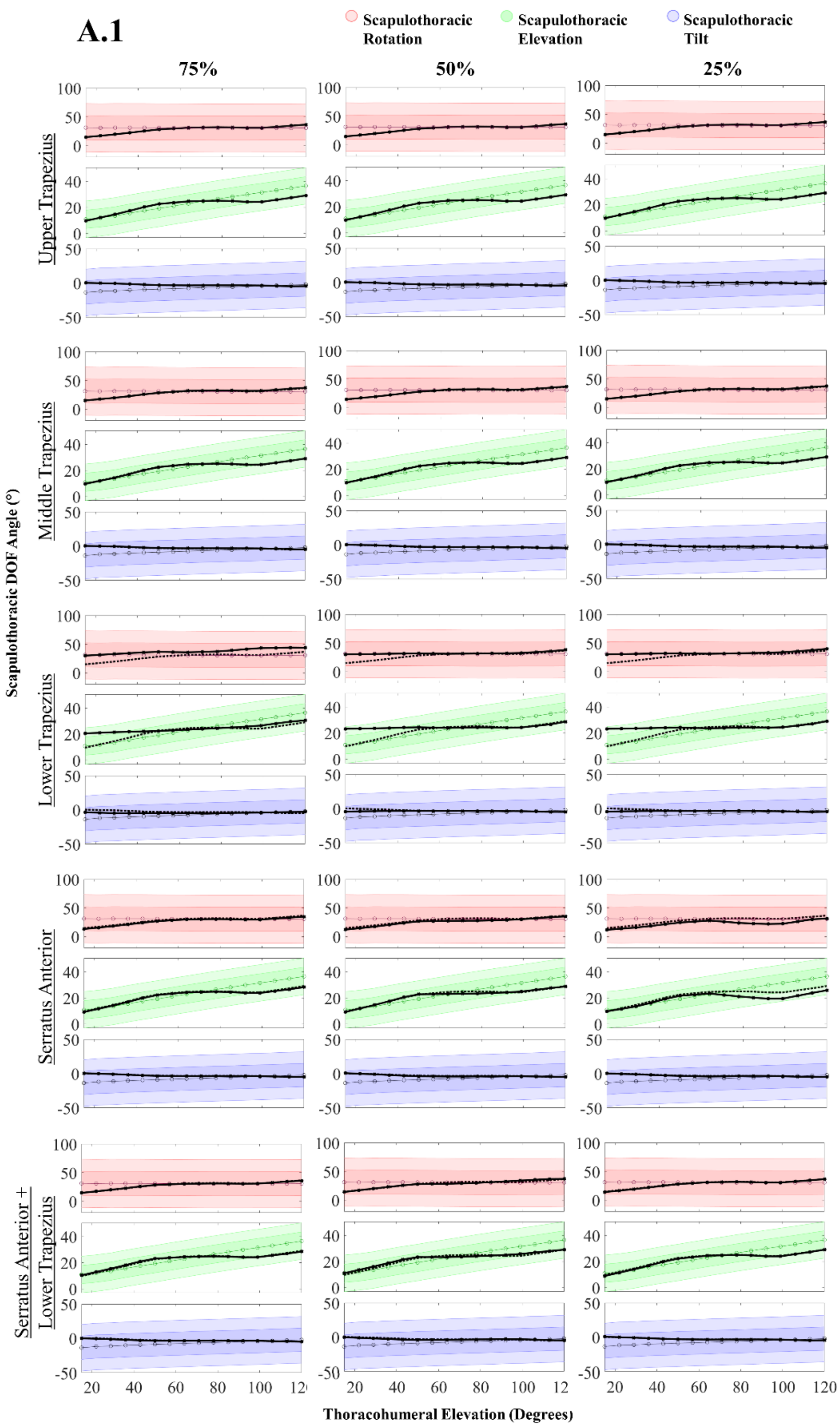
A.1
Scapulothoracic Rotation
Scapulothoracic Elevation
Scapulothoracic Tilt
75%
50%
25%
Upper Trapezius
Middle Trapezius
Lower Trapezius
Serratus Anterior
Serratus Anterior + Lower Trapezius
Scapulothoracic DOF Angle (°)
Thoracohumeral Elevation (Degrees)

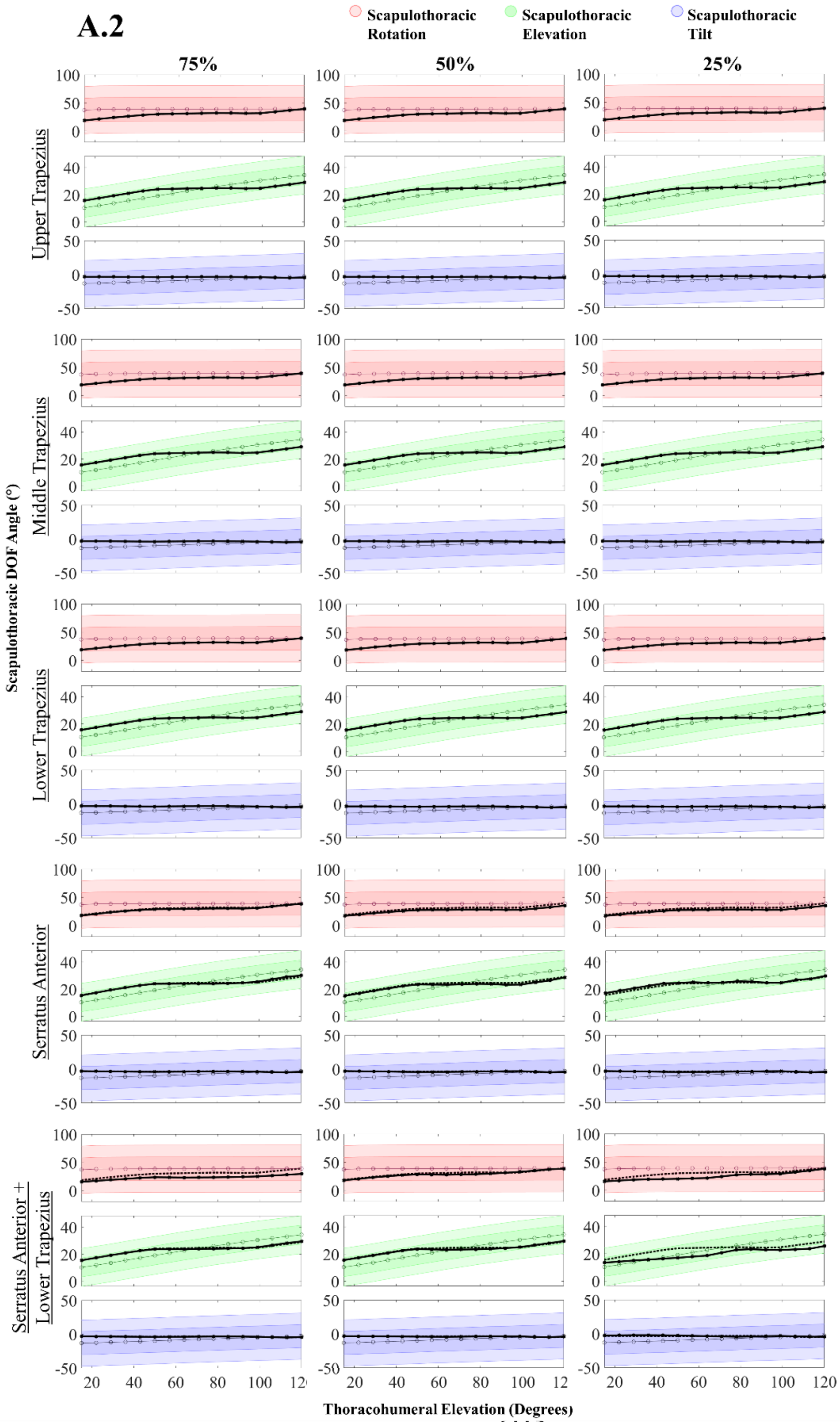

A.2
Scapulothoracic Rotation
Scapulothoracic Elevation
Scapulothoracic Tilt
75%
50%
25%
Upper Trapezius
Middle Trapezius
Lower Trapezius
Serratus Anterior
Serratus Anterior + Lower Trapezius
Scapulothoracic DOF Angle (°)
Thoracohumeral Elevation (Degrees)

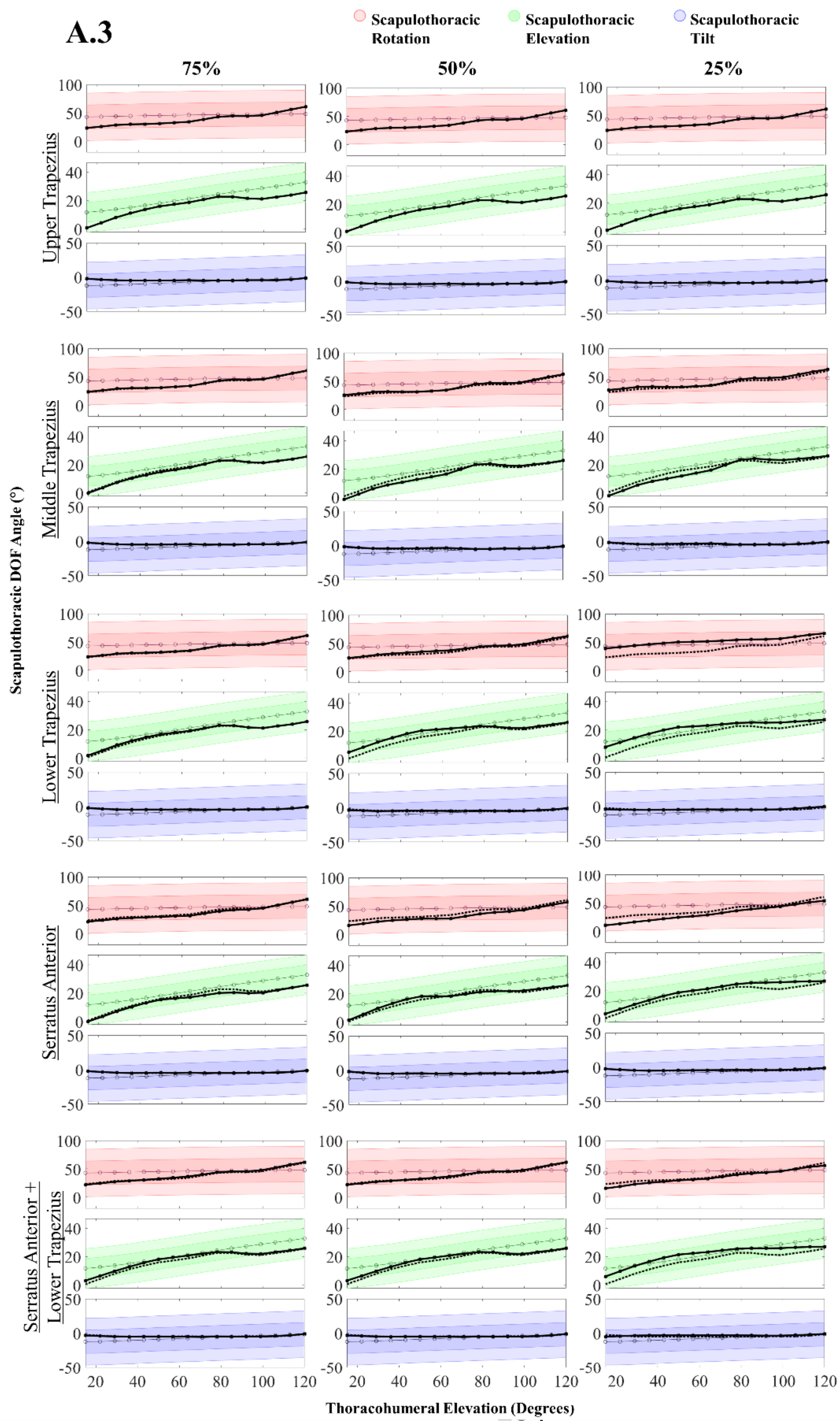
A.3
Scapulothoracic Rotation
Scapulothoracic Elevation
Scapulothoracic Tilt
75%
50%
25%
Upper Trapezius
Middle Trapezius
Lower Trapezius
Serratus Anterior
Serratus Anterior + Lower Trapezius
Scapulothoracic DOF Angle (°)
Thoracohumeral Elevation (Degrees)